# Using Mixture Design Data and Existing Prediction Models to Evaluate the Potential Performance of Asphalt Pavements

by

Jolina Joseph Karam

A Thesis Presented in Partial Fulfillment
of the Requirements for the Degree
Master of Science

Approved April 2020 by the
Graduate Supervisory Committee:

Kamil Kaloush, Co-Chair
Michael Mamlouk, Co-Chair
Hasan Ozer

ARIZONA STATE UNIVERSITY

May 2020

# ABSTRACT

Several ways exist to improve pavement performance over time. One suggestion is to tailor the asphalt pavement mix design according to certain specified specifications, set up by each state agency. Another option suggests the addition of modifiers that are known to improve pavement performance, such as crumb rubber and fibers. Nowadays, improving asphalt pavement structures to meet specific climate conditions is a must. In addition, time and cost are two crucial settings and are very important to consider; these factors sometimes play a huge role in modifying the asphalt mix design needed to be set into place, and therefore alter the desired pavement performance over the expected life span of the structure. In recent studies, some methods refer to predicting pavement performance based on the asphalt mixtures volumetric properties.

In this research, an effort was undertaken to gather and collect most recent asphalt mixtures' design data and compare it to historical data such as those available in the Long-Term Pavement Performance (LTPP), maintained by the Federal Highway Administration (FHWA). The new asphalt mixture design data was collected from 25 states within the United States and separated according to the four suggested climatic regions. The previously designed asphalt mixture designs in the 1960's present in the LTPP Database implemented for the test sections were compared with the recently designed pavement mixtures gathered, and pavement performance was assessed using predictive models.

Three predictive models were studied in this research. The models were related to three major asphalt pavement distresses: Rutting, Fatigue Cracking and Thermal

Cracking. Once the performance of the asphalt mixtures was assessed, four ranking criteria were developed to support the assessment of the mix designs quality at hand; namely, Low, Satisfactory, Good or Excellent. The evaluation results were reasonable and deemed acceptable. Out of the 48 asphalt mixtures design evaluated, the majority were between Satisfactory and Good.

The evaluation methodology and criteria developed are helpful tools in determining the quality of asphalt mixtures produced by the different agencies. They provide a quick insight on the needed improvement/modification against the potential development of distress during the lifespan of the pavement structure.

# DEDICATION

I would like to dedicate this thesis to my joy, pride and love, my sister Joana, my mother Lina and father Joe. Thank you for always believing in me, pushing me to go further and achieve greater. Thank you for your infinite support, I am eternally grateful.

ACKNOWLEDGMENTS

I would like to sincerely thank my advisor, Dr Kamil Kaloush, for his unlimited support, guidance and inspiration. Dr Kaloush has been one of the main reasons why I chose to come to the U.S. and pursue my graduate studies. I am very grateful that I was able to learn, work and expand my background and knowledge under his supervision and advice. As he is one of the co-chairs of my committee, he initially inspired me to direct my studies towards pavements, where I discovered my passion. Above all, he was a patient and supportive mentor and friend.

I would like to thank Dr Michael Mamlouk for always providing valuable advice and support throughout my graduate studies. Dr Mamlouk is continuously available for recommendations, and advice not only for research purposes, but also for future plans in life. As the other co-chair of my committee, he drove my curiosity about several topics and gave me several important ideas to tackle and consider.

I would also like to thank Dr Hasan Ozer, for being on my committee and always offering his help, comments and suggestions to improve and enhance my skills. He is always willing to share his knowledge and his experience.

Special thanks go to all of my colleagues at the Advanced Pavement Laboratory, for the great time we have spent together. With their presence, I was able to learn from their experiences and share valuable experiences. As they were always ready to help, I was able to adapt to the new environment at ASU in no time.

I would also like to personally thank my friends, who accompanied me through my journey. Special thanks go to the new friends I made in Arizona. Without them, I would not have been able to accomplish the things I am mostly proud of. They provided me with tireless help, support, cheer and mostly fun and care. The countless hours spent studying together finally paid off. I also want to thank my friends in Canada and Lebanon, who have watched me grow ever since I was little and provided their interminable encouragements and joyfulness. Having them in my life is a blessing that I am very lucky to have.

Last but not least, I would like to take the chance to thank personally and deeply my family, both in Arizona and Lebanon, for always being there for me. I am grateful for their endless care, patience, love and support. My family always had my back, and without their involvement and contribution in my life, nothing is possible.

Finally, many thanks to FORTA Corporation for partially funding my studies towards my thesis.

TABLE OF CONTENTS

CHAPTER Page

CHAPTER Page

CHAPTER Page

CHAPTER Page

CHAPTER Page

LIST OF TABLES

Table Page

Table Page

Table Page

Table Page

LIST OF FIGURES

Figure Page

Figure Page

Figure Page

Figure Page

Figure Page

NOMENCLATURE

***Rutting Section:***

| | |
|---|---|
| $V_a$ | air voids (%) |
| AC | asphalt content (%) |
| Vbeff or $V_{be}$ | effective binder content (%) |
| VMA | voids in the mineral aggregate (%) |
| VFA | voids filled with asphalt (%) |
| p | normal stress (psi) |
| q | maximum shear stress (psi) |
| σ1 | major principal stress at failure (psi) |
| σ3 | minor principal stress at failure (psi) |
| V1 | binder viscosity at testing temperature (poise) |
| V2 | binder viscosity at 70oF (poise) |
| % R34 | percentage retained in 3/4" sieve |
| % R38 | percentage retained in 3/8" sieve |
| % R04 | percentage retained in #4 sieve |
| % P200 | percentage passing #200 sieve |
| c | cohesion (psi) |
| φ | friction (degrees) |
| Teff | effective temperature (°F) |
| Freq or f | frequency loading (Hz) |
| z | desired pavement depth (in) |

| | |
|---|---|
| MAAT | Mean Annual Air Temperature (°F) |
| σMMAT | Standard deviation, Mean Monthly Air Temperature (°F) |
| Wind | mean annual wind speed (mph) |
| Sunshine | mean annual sunshine (%) |
| Rain | cumulative annual rainfall depth (in) |
| RD | rut depth, in |
| ESAL | number of 80 KN (18 kip) ESAL corresponding to the rut depth |
| $T_{avg}$ | average annual temperature, °F |
| $h_{AC}$ | equivalent thickness of base material, in |
| $E_{base}$ | effective resilient modulus of base materials, psi (effective means it is influenced by the freezing index and seasonal variations) |
| $\delta_0$ | surface deflection, in |
| $M_R$ | effective resilient modulus of subgrade, psi 40 |
| $\varepsilon_v$ | compressive strain at the bottom of the asphalt mix layer, in./in |
| $\eta_k$ | kinematic viscosity of the asphalt binder at 135 °C (275 °F), cSt |
| Y | design year |
| Tl | accumulated average annual daily truck traffic |
| SN | structural Number |
| $H_{AC}$ | thickness of asphalt layer, in. |
| $T_{max}$ | maximum temperature in the year, °F |
| $F_{ave}$ | annual freezing index |
| $H_{base}$ | thickness of the base, in. |

| | |
|---|---|
| $P_{ave}$ | average annual precipitation |
| $\tau_{ff}$ | shear stress at failure on failure plane |
| $\sigma_{ff}$ | normal stress at failure on failure plane |
| c | intercept of the failure envelope, cohesion13 |
| tan φ | slope of the failure envelope (φ is the angle of internal friction) |
| $\varepsilon_p$ | the permanent strain |
| $\varepsilon_{ps}$ | permanent strain related to the beginning of the secondary stage |
| $\varepsilon_{st}$ | permanent strain related to the beginning of the tertiary stage |
| N | number of load cycles |
| $N_{ps}$ | number of load repetitions related to the beginning of the secondary stage |
| $N_{st}$ | number of load repetitions related to the beginning of the tertiary stage |
| a, b, c, d, e, f | material constants |
| FN | flow number |
| T | test temperature, $^oF$ |
| S | deviatory stress level, psi |
| Visc | the viscosity of the binder at $70^oF$, $10^6$ Poise |
| Vbeff | the effective binder content in % volume |
| PD | pavement permanent deformation |
| nsublayers | number of sublayers |
| $\varepsilon_p^i$ | total plastic strain in sublayer i |
| $h^i$ | thickness of sublayer i |
| I | the initial pseudostiffness |

| | |
|---|---|
| $\varepsilon_e^R$ | effective pseudostrain |

***Fatigue Section:***

| | |
|---|---|
| $N_{fwithoutRP}$ | the number of cycles from a fatigue test without a rest period |
| $\Delta N_{f,i}$ | the increase in $N_f$ due to the $i^{th}$ rest period |
| E* | dynamic modulus in function of frequency and temperature |
| $\varepsilon^a$ | critical strain and a is the slope of the fatigue curve |
| h, L and A | the beam dimensions (mm) |
| $F_0$ | Load (N), |
| $V_{max}$ | maximum deflection at the center of the beam (mm) |
| $\sigma_{max}$, $\varepsilon_{max}$ | maximum bending stress and the maximum tensile strain |
| K | ratio of the stress to the strain |
| $N_f$-50% | failure criterion as a 50% reduction of the initial stiffness measured after 50 applied load cycles |
| $N_f$ | the load repetitions to failure |
| $\varepsilon_t$ | initial strain at the $200^{th}$ load repetition |
| $E_t$ | elastic modulus of the HMA (psi) |
| $N_{f\text{-}HMA}$ | allowable number of axle-load applications for HMA |
| $E_{HMA}$ | dynamic modulus of the HMA in compression |
| $K_{f1}$, $k_{f2}$, $k_{f3}$ | global field parameters taken to be equal to 0.007566, -3.9492 and -1.281 |
| $\beta_{f1}$, $\beta_{f2}$, $\beta_{f3}$ | local or mixture specific field calibration constants, set to be equal to 1.0 |

| | |
|---|---|
| $\Delta DI$ | the incremental damage indices throughout the HMA layers |
| n | actual number of axle-load applications within a certain time |
| j | axle-load interval |
| m | axle load type (Single, tandem, tridem, etc.) |
| l | truck type using the truck classification groups within the MEPDG |
| p | the month period |
| T | median temperature for the five temperature intervals used to subdivide each month |
| $FC_{Bottom}$ | area of the alligator cracking initiated at the bottom of the HMA layer, in % of the total lane area |
| $DI_{Bottom}$ | cumulative damage index at the bottom of the HMA layers |
| $C_{1,2,4}$ | transfer function regression constants having values of 1, 1 and 6 respectively |
| $DI_{Top}$ | Cumulative Damage Index near the top of the HMA surface |
| $C_{1,2,4}$ | transfer regression constants equal to 7, 3.5 and 1,000 respectively |
| FSC | binder fatigue strain capacity, in % |
| $K_1$ | fatigue exponent coefficient |
| $\delta$ | binder phase angle, in degrees |
| $G^*_b$ | dynamic shear modulus of the asphalt binder |
| $T_R$ | effective temperature in Rankine (fatigue or rutting) |
| FFPR | fracture/fatigue performance ratio |
| S(T,t) | initial stiffness of the material at a certain temperature |

| | |
|---|---|
| FSC* | typical failure envelope |

***Thermal Cracking Section:***

| | |
|---|---|
| $N_{cf}$ | number of thermal cycles to failure |
| $\sigma_t$ | tensile stress |
| $\varepsilon_t$ | tensile strain |
| $\beta$ | volumetric coefficient of thermal contraction |
| $V_0$ | volume at the reference temperature |
| $\Delta V$ | change of volume due to the temperature change from the reference temperature to the other temperature considered ($\Delta T$) |
| $\alpha$ | linear coefficient of thermal contraction |
| $L_0$ | length at the reference temperature |
| $\Delta L$ | change of length due to the change in temperature from the reference temperature to the one considered ($\Delta T$) |
| $T_g$ | Glassy Temperature |
| $\sigma(\xi)$ | stress at reduced time $\xi$ |
| $E(\xi - \xi')$ | relaxation modulus at reduced time $\xi - \xi'$ |
| $\varepsilon$ | strain at the reduced timed $\xi$, equal to $\alpha T(\xi') - T_0)$ |
| $\alpha$ | linear coefficient for thermal contraction |
| $T(\xi')$ | pavement temperature at reduced time $\xi'$ |
| $T_0$ | pavement temperature when the stress is equal to 0 |
| $\xi'$ | variable of integration |

| | |
|---|---|
| t | real and actual time |
| $a_T$ | temperature shift factor |
| $E_i$ and $\lambda_i$ | Prony series parameters |
| $D(\xi)$ | creep compliance at the reduced time $\xi$ |
| $\xi$ | reduced time at $t=a_T$ |
| $a_T$ | temperature shift factor |
| $D(0)$, $D_i$ | Prony series parameters |
| $\tau_I$, $\eta_V$ | Prony series parameters |
| $\Delta C$ | change in crack depth due to a cooling cycle |
| $\Delta K$ | change in the stress intensity factor due to the same cooling cycle |
| A and n | fracture parameters |
| E | mixture stiffness in psi |
| $\sigma_m$ | mixture strength in psi |
| σ | stress from the pavement response model at the depth of the crack tip |
| $C_0$ | current crack length |
| AC | observed amount of thermal cracking |
| $\beta_1$ | regression coefficient equal to 381.4 |
| P() | probability that [logC>logD] |
| N() | standard normal distribution evaluated at [log(C/D)/σ] |

| | |
|---|---|
| $\sigma$ | standard deviation of the log of the depth cracks in the pavement, equal to 0.654 |
| C | crack depth determined from the fracture model |
| D | thickness of the surface layer |
| $\varepsilon_t$ | Total Strain |
| $\varepsilon_e$ | elastic strain, recoverable and time independent |
| $\varepsilon_p$ | plastic strain, irrecoverable and time independent |
| $\varepsilon_{ve}$ | viscoelastic strain, recoverable and time dependent |
| $\varepsilon_{vp}$ | visco-plastic strain, irrecoverable and time-dependent |
| D(t) | total compliance at any time |
| t | loading time |
| $D_1$ and m | material regression coefficients |
| $H_M(t)$ | measured horizontal deflection at time t |
| GL | gage length |
| P | creep load |
| t | specimen thickness |
| D | specimen diameter |
| $\mu$, v | Poisson's Ratio |
| $D(\xi)$ | creep compliance at reduced time $\xi$ |
| $D_0$, $D_1$ and m | power model parameters |
| $P_f$ | failure load |
| $C_{sx}$ | correction factors |

| | |
|---|---|
| D | specimen diameter |
| $Pen_{77}$ | Penetration at 77 °F = $10^{290.5013\sqrt{8.1177.288+257.0694*10^{A+2.72973*VTS}}}$ |
| $S_t$ | Tensile Strength in psi |

# CHAPTER 1

# 1 INTRODUCTION

## 1.1 Background

Pavement performance is the most important criteria when designing a pavement mixture. It is defined as the ability of the pavement to hold traffic loads in a safely manner. Although progress has been made in improving the overall condition of the pavement structures, a huge need still exist to continue improve the overall quality of the materials against pavement distresses.

Generally, pavement structures suffer from the development of distresses due to different factors. These factors are mainly the following: traffic loading, subgrade support, materials used for construction, structural characteristics, maintenance variation and rehabilitation programs, and environment (temperature and moisture).

There are several indicators that show how well the pavement is performing; on top of this list are safety and the smoothness of the road for the users. The pavement performance is also measured by distresses (based on the type, severity and extent), the structural response, surface friction and roughness.

For Hot Mix Asphalt (HMA) pavements, distresses refer to the different deterioration types that the pavement structure will encounter during its life span while being exposed to traffic and the environment. The types include longitudinal and transverse cracking, alligator cracking, block cracking, raveling and rutting.

As for the structural response, it refers to the response recorded by the structure with respect to the application of a wheel load. For surface friction, the concern is the skid

resistance during wet seasons while the pavement's surface is subjected to traffic and surface wear. Roughness and serviceability are the measurement of ride quality of the pavement structure.

Each layer of the pavement structure has a specific and important role. Beginning with the surface layer, it is exposed to the traffic volume and must resist the distortion, as well as provide a smooth surface. It also needs to able to resist water penetration or shed the water to the roadside. It protects the entire pavement structure and avoid the excessive wetting of the subgrade soil. Underneath this layer, the base (bound or unbound) along with the subbase, add to the structural support of the pavement. The load distribution on the subgrade depends on those two layers. They must be constructed with material of quality, as they improve the load distribution, structure capacity and moisture susceptibility. Finally, the natural soil, or subgrade, provide the platform for which the pavement structure is built on, but it is, generally, the weakest in strength and most susceptible for moisture effects.

Rutting, fatigue cracking, and thermal cracking are the major distresses classically observed on the asphalt pavement structures. While rutting and fatigue are both caused by traffic loading, thermal cracking depends on the environment and temperature fluctuation. All those three distresses affect the pavement performance and the safety of the pavement structure. Assessing the potential development and severity of these distresses will provide insights on improving materials quality, pavement design and will greatly improve the overall pavement performance with less need for frequent maintenance and rehabilitation programs.

## 1.2 Study Objective

The main objective of this study is to outline a process to assess the potential performance of HMA pavement structures in terms of Rutting, Fatigue and Thermal cracking using only the asphalt mix design information and volumetric data. This assessment will provide insight on the quality of the asphalt mixture and suggest the need for further adjustment or modification. In this process, three predictive models were investigated, and their reliability was assessed based on existing pavement structures performance using LTPP (Long Term Pavement Performance) data. These models were also used to assess the quality of the asphalt mixtures for 48 current asphalt mixture designs collected from 25 States.

## 1.3 Scope of Work

In order to carry on this study, a plan was proposed and implemented. A literature review concerning the three asphalt pavement distresses was conducted, followed by an extensive study of the three pavement performance predictive models proposed. Asphalt mixtures designs were gathered from 25 States within the United States,; these asphalt mixture designs were the latest implemented by highway agencies in their respective location, and sometimes in various climate zones within the State itself.

Three pavement performance predictive models were evaluated for their use of basic asphalt mixtures design and volumetric data; the pavement performance of interest were: rutting depth, fatigue life as well as tensile strength and effective fracture energy for thermal cracking evaluation. In order to be able to assess the reliability of the predictive models used, asphalt mixtures and pavement performance data were also collected from

the LTPP Database for the same States under consideration. Each state was assessed with respect to the mix design used in the past, and pavement performance (distresses) measured from various test sections. Therefore, the mix design volumetric data of the previous mix designs were gathered, and the predictive models were tested against pavement performance data. The results are compared, and thus giving us how reliable the models are. Having the measured and the predicted distresses at hand, the models were validated based on their accuracy and reliability.

Next, the predictive models were used on the new gathered asphalt mix designs to provide insight on how the States are addressing the potential development of these distresses. This approach resulted in general criteria categorizing each asphalt mixture, and how most likely it will perform in the future in terms of Rutting, Fatigue and Thermal Cracking.

The following flow chart outlines the work process included in this thesis:

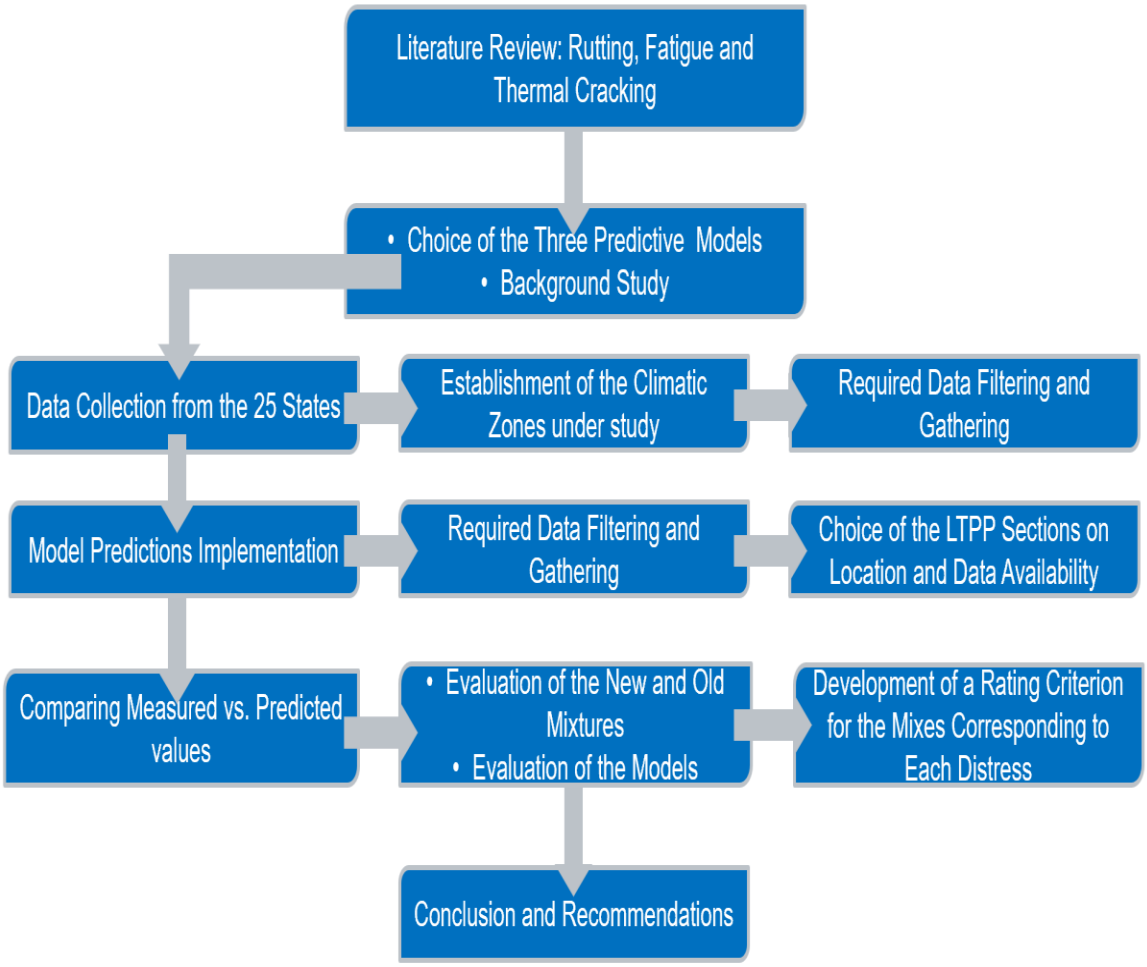


*Figure 1- Outline flowchart*

## 1.4 Organization of the Thesis

This thesis is divided into 7 chapters. The first chapter includes the background, the study objective and the scope of work. The second chapter provides the literature review on asphalt pavement distresses and pavement performance models. The third chapter contains the background information and application of the pavement performance predictive models chosen, as well as a sensitivity and statistical analysis. The fourth chapter includes information on the sections chosen from the LTPP Database and the application of the models for these sections. The fifth chapter provides a description of the data collected from the 25 States, as well as the application of the predictive models on the data gathered. The sixth chapter presents the analysis and comparison of the results, the final assessment concerning the reliability and accuracy of the models, and the final criteria assessed based on the analysis. The seventh and final chapter includes a summary of the work, conclusions and final recommendations of this study.

# CHAPTER 2

# 2 LITERATURE REVIEW

## 2.1 Distress Types

The distresses considered in this study are Rutting, Fatigue and Thermal Cracking. In this section, they are described extensively to understand their importance as well as their effects on pavement performance. Moreover, each distress is affected by different factors. These factors are emphasized in the section that follow.

### 2.1.a Rutting

Rutting, also referred as Permanent Deformation, refers to the accumulation of deformation due to wheel load repetition. The permanent deformation happening in one or more layer will lead in a significant depression in the surface layer of the pavement. It happens essentially in the wheel paths of the roadway. This permanent deformation is related to the Flow Number (FN), which is the number of repetitions of the wheel load until failure (or permanent deformation). The main problem associated with rutting happens during wet seasons: the presence of water in the ruts will cause hydroplaning. It is mainly defined as a thin water film building between the surface layer and the wheel of the vehicle. It will lead to a loss of traction and will cause the vehicle to lose control. Rutting occurring in the surface layer may be due to multiple factors: overloading of the surface layer, extreme loading during a hot weather where the HMA layer could have softened, instability of the pavement mixture and finally temperature susceptibility of the asphalt binder used.

In other terms, permanent deformation is mainly a densification of the layer. It is also caused by the settlement of some materials.

If rutting happens in other layers, such as base/subbase, it may be due to a too thin surface layer, as well as an inadequate mix design and poor construction methods. Moisture can also be a factor inducing rutting in these layers.

Finally, if rutting occurs within the entire pavement structure, this means that the structure is weak (too thin) for the loads applied, or that the natural soil beneath it is too weak (can also be possibly contaminated by moisture).

In the following Figure 2 (2), are the main stresses/strains that may cause the permanent deformation in the pavement structure. Noticeably, 1,3 and 4 are the vertical compressive stresses on the HMA Surface, Base and Subgrade. Number 2 represents the tensile stresses at the bottom of the HMA Layer to be discussed in the following sections. It should be noted that to reduce the effect of rutting, a stiffer asphalt binder should be chosen when designing, to reduce the softening effect at high temperatures or hot climates.

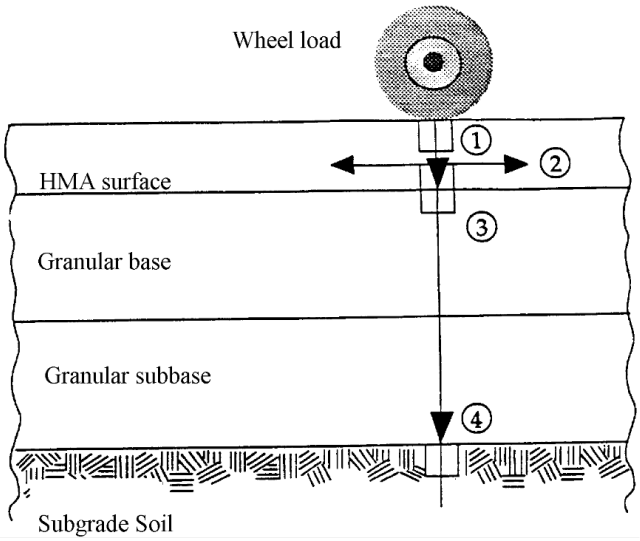


*Figure 2- Stresses and Strains within the HMA Structure causing Rutting (46)*

The amount of rutting is influenced by other factors, such as Temperature, Traffic Volume, Tire Pressure, Environmental conditions as well as Mixture Properties. The mixture

properties include the type of binder and its consistency, the binder content as well as the air void level within the mixture.

Many studies have taken the initiative of studying the mechanisms behind the rutting distress. Also, several predictive models have been developed for the sole purpose of estimating the rutting behavior of a pavement structure, based on several inputs.

2.1.a.1 Rutting Depth Calculation

In 1975, Akili (1) studied the strength properties of asphalt mixtures using the conventional triaxial setup. He found out that asphalt content and confining pressures affect the dynamic modulus and the shear strength of the mixture greatly. A decrease in the asphalt content following with an increase in confinement will lead to an increase in the modulus and shear strength.

In 2015, an ASU research associate studied the effect of maximum temperature change on asphalt pavement using LTPP sections. Also, the rutting behavior due to the temperature change was studied. It was found that rutting is generally affected by the increasing maximum temperature. However, the layer thicknesses of the asphalt layers played a great deal in the analysis. As thicker layers are observed in some states (i.e., Arizona), the rutting values with increase of temperature remained the same.

In addition, the asphalt film thickness plays a great deal in terms of durability of the mix. The film thickness is commonly known as the interface of the aggregates coated by the asphalt. A thick film thickness is characterized by a high fine aggregate content covered by asphalt. This theory resulting from the gradation of the mix may justify the performance levels of each section.

A rutting depth model was also developed, in terms of the pavement structure's characteristics as follows by Baker et al (2011) (2):

$$Log\ RD = -1.6 + 0.06 * V_a - 1.4 * \log(h_{AC}) + 0.07 * T_{avg} - 0.000434 * \eta_k + 0.15$$
$$* \log(ESAL) - 0.4 * \log(M_R) - 0.50 * log(E_{Base}) + 0.1 * \log(\delta_0)$$
$$+ 0.01 * \log(\varepsilon_v) - 0.7 * \log(h) + 0.09 * \log(50 - h_{AC} + h_{EC})$$

Where,

RD is the rut depth, in

ESAL is the number of 80 KN (18 kip) ESAL corresponding to the rut depth

$T_{avg}$ is the average annual temperature, °F

$h_{AC}$ is the equivalent thickness of base material, in

$E_{base}$ is the effective resilient modulus of base materials, psi (effective means it is influenced by the freezing index and seasonal variations)

$\delta_0$ is the surface deflection, in

$V_a$ are the air voids (% in mix)

$M_R$ is the effective resilient modulus of subgrade, psi 40

$\varepsilon_v$ is the compressive strain at the bottom of the asphalt mix layer, in./in.

$\eta_k$ is the kinematic viscosity of the asphalt binder at 135 °C (275 °F), cSt

Based on this model, a rutting predictive model based on the LTPP input has been developed:

$$\begin{aligned} RD = {} & 5.211835 + (-0.0453 \times Y) + (0.000323 \times Tl) + (6.872935 \times SN) \\ & + (-1.3E-5\,06 \times |E*|) + (-3.90563 \times HAC) \\ & + (3.400868 \times Tmax) + (0.001749 \times Fave.) \\ & + 6\,(-1.25546 \times Hbase) + (-0.00438 \times Pave.) \end{aligned}$$

Where,

RD is the rut depth,

Y is the design year

Tl is the accumulated average annual daily truck traffic

SN is the structural Number

$H_{AC}$ is the thickness of asphalt layer, in.

$T_{max}$ is the maximum temperature in the year, °F

$F_{ave}$ is the annual freezing index

$H_{base}$ is the thickness of the base, in.

$P_{ave}$ is the average annual precipitation

This model is based on a linear regression model. It was determined that the rutting depth increases with an increase of the dynamic modulus, traffic loads, and precipitation levels. It was also depicted that the rutting depth is greatly affected by the base layer thickness, which suggests that at high temperature, having a thicker base would potentially provide more resistance to rutting.

Another study was conducted by Fwa et al in 2004 (3) used the c and φ parameters, which are co-related with the strength of a mix obtained during the triaxial testing, in a rutting prediction model. This model is a power-based model that considers the accumulated rutting with the number of load repetitions. All in all, the suggested model depends on the duration of each load application, the load bearing capacity (the maximum load applied that an asphalt layer can withstand before shear failure), the c and φ parameters, as well as the Ep (Elastic Modulus) of the underlying layers.

Having introduced the c and φ parameters, it is important to understand the nature of the Mohr-Coulomb failure criterion. This criterion states that the shear stress is a function of the normal stress on the plane of failure.

The plane of failure is determined by the following equation:

$$\tau_{ff} = c + \sigma_{ff} * tan\varphi$$

Where,

$\tau_{ff}$ = shear stress at failure on failure plane

$\sigma_{ff}$ = normal stress at failure on failure plane

c = intercept of the failure envelope, cohesion13

tan φ = slope of the failure envelope (φ is the angle of internal friction)

This is represented graphically, by plotting several Mohr's Circles together. These circles represent the different stress states applied under different confinement levels during triaxial testing. The tangent line to those circles is called the Mohr-Coulomb failure envelope and is shown in the Figure 3 below.

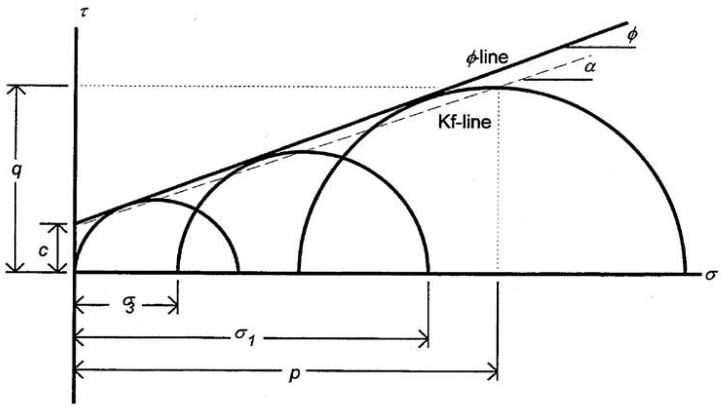


*Figure 3- Mohr-Coulomb Failure Criterion (46)*

This notion is important in order to understand the stress state that the pavement structure is subjected to whenever a wheel load is applied to it.

This theory is represented mathematically in the equation below:

$$\sigma_1 = \sigma_3 * \tan^2\left(45^o + \frac{\varphi}{2}\right) + 2 * c * \tan\left(45^o + \frac{\varphi}{2}\right)$$

Where

$\sigma_1$ is the major principal stress applied

$\sigma_3$ is the minor principal stress applied and confinement level

c is the cohesion and intercept of the failure envelope

$\phi$ is the internal angle of friction

Referring to this figure, p and q, which are the coordinates of the maximum shear stress, represent the average normal stress and maximum shear stress applied respectively.

This concept is shown in the following formulas:

$$p = \frac{\sigma_1+\sigma_3}{2} \text{ and } q = \frac{\sigma_1-\sigma_3}{2}$$

Now that the stress conditions can be determined and evaluated theoretically and experimentally, this concept can be implemented in the Flow Number analysis, explained in the following section 2.1.a.2

2.1.a.2 Repeated Load Permanent Deformation Test

This test, also known as the flow number test, consists of the application of a dynamic load for several repetitions. The accumulated permanent deformation caused by the load repetition is recorded in terms of the number of cycles. The load is characterized by a 0.1s loading time followed by 0.9s of resting period.

The cumulative permanent strain versus the number of cycles denotes three different and major zones. As shown in the following Figure 4, the three zones are represented as primary, secondary and tertiary.

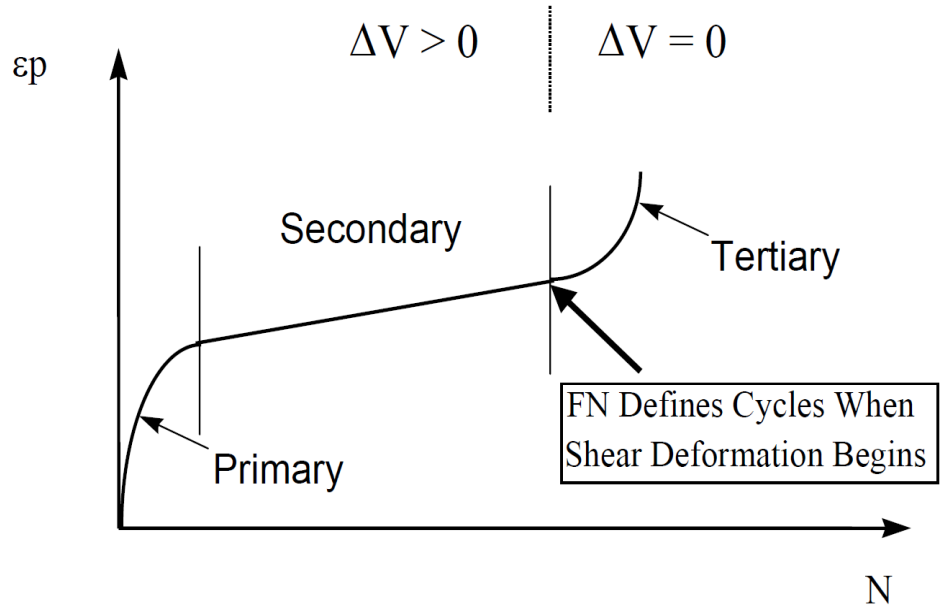


*Figure 4- Flow Number according to (46)*

In the primary zone, the strain rate decreases. As the secondary zones follows, the permanent strain rate remains constant. Finally, in the tertiary zone, the permanent strain

rate increases rapidly, ending the material rupture or failure. The beginning of this zone is denoted by the Flow Number, or the number of repetitions until failure of the sample is reached.

At low stress levels, the material will exhibit the primary and secondary permanent strain. The strain rate approaches zero as total strain reaches a certain value. However, this indicates that the tertiary flow/zone may never appear before a considerably large amount of time. It also refers to the value when shear deformation, under constant volume, begins.

Many studies have reported the flow number with respect to the permanent strain accumulated. These studies included material characterization, traffic distribution, temperature within the pavement and many others.

Several models have been developed to predict permanent deformation. However, they are mostly empirical. Fully mechanistic models are almost non-existent. These models are not accepted universally, and must be tailored to each state's climatic condition, history, construction techniques as well as materials used.

A model developed by Brown and Bell (4), compared predicted rutting theoretically used a layer-strain approach with measured values. The model has shown good assessment, as the predicted and measure values agree. The model is terms of permanent strain, deviator stress, number of load applications, and two regression constants.

$$\varepsilon_p = \left(\frac{q}{a}\right)^b * N$$

Where

$\varepsilon_p$ is the permanent strain

q is the deviator stress

N is the number of load applications

And a and b are the constants

Another rutting model was developed by Francken in 1977 (5) based on the triaxial repeated load test. This test is run for different temperatures, load frequencies and stress levels. The model goes as follows:

$$\varepsilon_p(t) = At^B + C\,(e^{Dt} - 1)$$

Where

$\varepsilon_p(t)$ = relative permanent deformation

t = time (t=N/f) expressed in 1000 seconds time units, and where

N = the number of loading cycles and f is the loading frequency

A, B, C, D = constants adjust to the specific material. The constant C defines if tertiary failure would occur or not. Therefore, it is very significant for this model.

The Francken Model has been recommended since it considers all the three stages of permanent deformation. These stages are characterized by a power model for the primary and secondary stages, as well as an exponential model for the tertiary stage (Biligiri et al) (6).

Khedr (7) from Ohio State University developed a relationship to calculate the permanent strain in terms of Number of Load Cycles and Material Properties function of Resilient Modulus and Applied stress. The mode goes as follows:

$$\frac{\varepsilon_p}{N} = A_a * N^{-m}$$

Where

$\varepsilon_p$ is the permanent strain

N is the number of load cycles

$A_a$ reflects the material properties in function of the resilient modulus and applied stresses

And m is a material parameter.

Similar to this study, the most common model that relates permanent strain to the number of load repetition is the one evaluating the secondary phase of the permanent deformation curved, developed by Witczak et al. (8) It is a power model in the following form:

$$\varepsilon_p(N) = a * N^b$$

Where

$\varepsilon_p$ is the permanent strain

N is the number of load cycles

And a and b are regression coefficients based on the material test conditions.

This model, not representing the three stages, was further modified by Zhou et al. (9). It was separated into three parts, where each stage has its own respective model:

For the Primary Stage, considering $N<N_{ps}$

$$\varepsilon_p = a * N^b$$

For the Secondary stage, for $N_{ps} \leq N<N_{st}$

$$\varepsilon_p = \varepsilon_{ps} + c * \left(N - N_{ps}\right)$$

Finally, for the Tertiary stage, where $N \geq N_{st}$

$$\varepsilon_p = \varepsilon_{st} + d * (e^{f(N-N_{st})} - 1)$$

Where

$\varepsilon_p$ is the permanent strain

$\varepsilon_{ps}$ is the permanent strain related to the beginning of the secondary stage

$\varepsilon_{st}$ is the permanent strain related to the beginning of the tertiary stage

N is the number of load cycles

$N_{ps}$ is the number of load repetitions related to the beginning of the secondary stage

$N_{st}$ is the number of load repetitions related to the beginning of the tertiary stage

And a, b, c, d, e and f are material constants.

An algorithm is presented for identifying the transition points between the stages, especially the flow number, that indicates the beginning of the tertiary flow.

A conceptual relationship was developed by Kaloush (10), relating the flow number to the measured rut depth in field based on different traffic levels. The number of repetitions till failure ($N_{required}$) is determined in the lab, compared to the $N_{mix}$, the number of cycles to repetition to failure for the mix. The criteria are set in such a way that if $N_{mix}$ is greater than $N_{required}$, the mixture is accepted and will behave good in terms of rutting.

Other studies, such as the NCHRP Report 580 (11), explored the relationship between FN and rutting measured in the field at different traffic levels.

The measured flow number in the lab was used to predict the field rutting depth ($R_d$) following this model, where $i_1$, $m_2$, $m_1$ and $l_o$ are constants.

$$R_d = i_1 * N^{-m2} * FN^{m_1 * \log(N) - l_o}$$

However, this model was used to predict the field rutting depth for a certain traffic load and reduced flow number, using shift factors for each individual site.

2.1.a.3 Flow Number Prediction

Several attempts have been carried in order to predict the Flow Number values, based on solely volumetric values from the different mix designs. Kaloush (10) first attempted to predict the flow number based on the equation below.

$$FN = (20408400) * T^{-2.0799} * S^{0.368} * Visc^{0.368} * Vbeff^{-2.7175} * Va^{-0.1658}$$

Where

FN is the flow number

T is the test temperature, $^{o}$F

S is the deviatory stress level, psi

Visc is the viscosity of the binder at 70$^{o}$F, $10^6$ Poise

Vbeff is the effective binder content in % volume

And Va is the air void %

However, since the stress level was not rational, it showed an increase in the flow number value whenever it increased. Therefore, another attempt was made with regards to this model. The newer version is the following:

$$FN = (432367000) * T^{-2.215} * Visc^{0.321} * Vbeff^{-2.6604} * Va^{-0.1525}$$

This time, this model only worked for a certain range for each of the input variables:

- Test Temperatures, T: 100-130°F
- Confined Stress Level, S: 20 psi
- Binder Viscosity, Visc: $0.92x10^6$-$26.7x10^6$ poise at 70°F
- Effective Asphalt Content, Vbeff: 7.4-14%
- Air Voids, Va: 2.5-12%

- Nominal Aggregate Size: 12.5-37.5mm

Kvasnak et al. (12) presented a flow number predictive model using the aggregate gradation, volumetrics and binder properties. The model had constant deviatory stress testing conditions of 87 psi, and having the following ranges for the input variables:

- Binder Viscosity: $0.020x10^6$-$0.286x10^6$ Poise at testing temperature
- Asphalt content, 4.2-6%
- Nominal maximum aggregate size: 12.5-19mm
- Voids in the mineral aggregate: 12.4-21.4%
- Percentage passing sieve
- No.4: 52.7- 76.5
- No.16: 29.1- 47.9
- No.200: 3.0- 6.0
- PG Grading: PG-58-34- PG64-28

The suggested model is the following:

$$logFN = 2.866 + 0.00613 * Gyr + 3.86 * Visc - 0.072 * VMA + 0.0282 * P_4 - 0.051 * P_{16} + 0.075P_{200}$$

However, this model was specifically made for dense graded mixtures only, and for certain ranges taking into consideration that the number of gyrations has the higher impact on the model.

2.1.a.4 MEPDG Rutting Depth Analysis and Prediction

One main objective of this study is to show what additional contribution it provides to the world of asphalt pavement distresses and predictions.

Studying how the MEPDG predicts permanent deformation is an important step to understand the whole purpose of the study.

The MEPDG models study both the primary and secondary stages of permanent deformation. An extrapolation of the secondary stage trend is used in the modeling of the primary stage. Finally, the third and tertiary stage is not considered.

The main concept behind the MEPDG predictions is based on Incremental Damage. The rutting is estimated at the mid-depth of each sub-layer within the pavement structure.

The system verifies the type of layer and applies the respective model based on the material type of the layer and calculates the plastic strain at the end of the sub-season. Finally, the permanent deformation is the sum of all the permanent deformations of each layer:

$$PD = \sum_{i=1}^{n,sublayers} \varepsilon_p^i \times h^i$$

Where:

PD =pavement permanent deformation

nsublayers =number of sublayers

$\varepsilon_p{}^i$ =total plastic strain in sublayer i

$h^i$=thickness of sublayer i

The process is then repeated for each load level selected, sub-season, and month of the analysis period.

### 2.1.b Fatigue

Fatigue is generally defined as the phenomenon of fracture caused by load repetition or stress having a value less than the tensile strength of the material. The HMA Pavement structure undergoes many road repetitions, leading to its cracking. The tensile strength of the layer is not reached at once, but the stress accumulation over time is enough to cause fatigue. The stress in question is nothing but the tensile stress accumulated at the bottom of the HMA Surface layer. The repeated application of this stress will cause initial cracks in the pavement, at the bottom of the surface layer. Continued repetition will cause the crack to evolve and reach the surface (the top) of the layer. This phenomenon indicates a loss of structural capacity (or load carrying capacity). Once the cracks are initiated, the amount of fatigue cracks will increase at an exponential rate. It should be noted that fatigue cracking is not always generated within the HMA surface layer; if a stabilized base course is present, its stiffness may be large enough that the tensile strains at the bottom of this layer generate the cracks. In order to avoid fatigue cracking from happening, choosing a flexible asphalt binder is recommended, as it will be more convenient for a higher number of repetitions to failure. The stiffness is defined as the ratio between the stress and strain amplitudes and is greatly affected by the speed of loading and temperature: High temperature indicates a lower stiffness.

Also, pavement performance under traffic depends not only on the characteristics of the layers' materials, but also on the interaction between the layers. Fatigue life is influenced by various factors; considerable amount of crack propagation will have to occur on a wide area of pavement.

The factors affecting the fatigue life of the pavement mainly includes load application, environment and specimen characteristics such as changes in the ambient temperatures, moisture conditions and varying loading (compound/load pulses, varying in size and duration).

Fatigue characterization of asphalt mixtures is an important part of performance-based mix design. Accurate prediction of the fatigue life of asphalt concrete is rather difficult due to the complex nature of the fatigue phenomenon under varying circumstances. These are defined by the material type, loading and environmental conditions. Over the years, significant efforts have focused on developing reliable fatigue prediction models, falling into two main categories: phenomenological and mechanistic approaches. The most commonly used phenomenological fatigue modeling approach considers the initial response or tensile strain of the mixture to the fatigue life. This however do not consider how damage evolves throughout the fatigue life and therefore is only valid for a given loading condition without accurately predicting the complex damage evolution under realistic conditions. Concerning the mechanistic approach, fracture mechanics or damage mechanics with or without viscoelasticity are adopted. They describe the fatigue damage growth in the asphalt. It is a way more complex approach but is applicable to broader ranges of loading and environmental conditions. The fatigue life of a new pavement or remaining life of existing pavement is better and more accurately assessed. Stress-strain relationships form the basis of the mechanistic approach and therefore inherently includes the material properties. For this reason, the mechanistic

approach provides a relationship between the material properties and fatigue performance, that could be effectively used for the selection of more fatigue-resistant binders.

Currently the most current fatigue models developed in the lab underpredict the actual fatigue life of asphalt in the field. This is attributed to the different loading conditions (loading, rest) and environmental conditions (aging, temperature variations) between the lab and the field.

Resting periods affect significantly the fatigue life of the material, as the stresses are released during this period from the asphalt structure.

2.1.b.1 Fatigue Life Predictive Models

According to Hyun-Jong Lee et al. (2001) (13), a uniaxial constitutive model of nonaging asphalt mixture have been developed by Kim et al. in 1997 (15) and (16). This model includes the elastic-viscoelastic correspondence principle and Schapery's work potential theory to model the mechanical behavior of asphalt under cyclic loading. A simplified fatigue prediction model is developed from the constitutive model. It predicts the stress-strain behavior of asphalt under different loading histories as well as rates of loading, stress-stain amplitudes and random rest periods.

2.1.b.2 The Constitutive Fatigue Model

In 1990, Schapery (17) applied the method of thermodynamics of irreversible processes to develop a work potential theory applicable to the mechanical behavior of elastic medias, with growing damage and structural changes. It considers the internal states that account for the effects of damage and dissipated energy due to microstructural changes. The word damage in continuum damage is defined as any structural change in a system including a

reduction of its stiffness or strength during loading. Concerning microdamage healing, it is defined to include all mechanisms except linear viscoelastic relaxation contributing to the recovery of stiffness or strength during rest periods. The constitutive model is represented by the formula below:

$$\sigma = I \times \varepsilon_e^R [F + G + H]$$

Where I is the initial pseudostiffness,

$\varepsilon_e^R$ is the effective pseudostrain

F and H are two functions to characterize the change in pseudostiffness, due to the damage growth and microdamage healing

G is the function that accounts for the difference in stress values between the loading and unloading conditions.

Referring to the previous section, the simplified predictive model developed in 2001 (13) has the following form:

$$C_1 + H = 0.5$$

This fatigue prediction model is based on the assumption of the strain-controlled mode of testing. Also, prediction of the fatigue performance requires accurate modeling of the change in $S^R$ (pseudostiffness which is used to represent the change of the stress-strain slopes) as a function of loading cycles. Only F and H are required to predict the number of cycles to failure ($N_f$) of a mixture. The left-hand side of the model ($C_1$+H) can help to identify the elapsed loading time to failure corresponding to a value of 0.5. The number of cycles to failure $N_f$ is then determined by multiplying the time elapsed to failure (t) by the loading frequency (f).

$$N_{ftotal} = N_{fwithoutRP} + \sum_{i=1}^{M} \Delta N_{f,i}$$

Where $N_{fwithoutRP}$ is the number of cycles from a fatigue test without a rest period, and $\Delta N_{f,i}$ is the increase in $N_f$ due to the $i^{th}$ rest period.

Following this study, a simplified fatigue model that can predict the fatigue life of asphalt mixes using only the viscoelastic properties is presented by Lee and Kim in 2003 (14). It was reduced to a simpler version based on observations from experimental data. The findings of this study included that the fatigue behavior is affected by both the viscoelastic properties (|E*| and me) and fatigue characteristics. Also, the coefficient $\alpha_1$ in the damage evolution law was found to be related to the m-value using the following relationship: $\alpha_1 = 0.5 + \frac{1}{m}$

Also, the coefficients $k_1$ and $k_2$ from the conventional fatigue model ($N_f = k_1 * \varepsilon^{-(k_2)}$) were represented as follows:

$$k_1 = \frac{4f}{\sqrt{\pi}} a(\alpha_1)^{0.5+b} |E*|^{-2\alpha_1} \text{ and } k_2 = 2\alpha_1 = 1 + \frac{2}{m}$$

The model in this paper can accurately predict the change in the fatigue life of an HMA mix due to the changes in asphalt content and air voids. However, further levels of ageing and temperature variations should be studied in the future since only isothermal and nonageing conditions were considered for the development of the model. The final and simplified version of the model is the following:

$$N_f = \frac{4f}{\sqrt{\pi}} a(\alpha_1)^{0.5+b} |E*|^{-2\alpha_1} * \epsilon_0^{-2\alpha_1}$$

The parameters are defined as follows:

The constants a and b are regression constants

E* is the dynamic modulus in function of frequency and temperature, but is constant due to the isothermal and single-loading frequency used for the testing

$\epsilon_0$ and f are loading conditions parameters

E* and $\alpha_1$ are the material's viscoelastic properties parameters

And the m values were obtained from creep and dynamic modulus data.

Another study states that four ship factors, which can be used with the laboratory-derived fatigue life prediction equations to estimate the in-service fatigue life of HMA have been identified. These four factors are: stress state, traffic wander, HMA healing and material properties. These derived factors utilize the measured stresses and strains at the Virginia Smart Road, to determine the stress state and traffic wander shift factors based on appropriate pavement and loading modeling.

According to Vanelstraete et al in 2000 (18) , the number of cycles of a specific load that a pavement can withstand before it cracks may be related to the critical strain using a classical fatigue law:

$$N = C \times \varepsilon^a$$

Where N is the number of cycles before crack initiation,

$\varepsilon^a$ is the critical strain and a is the slope of the fatigue curve

And C is the constant of the fatigue life.

To address the differences between the measured and calculated strains, a different approach had to be considered by introducing the real field conditions by Al Qadi et al (2003)(19). It has been found that the multi-layer elastic theory deviates by almost 65% of real measured pavement responses. To adjust for this difference, shift factors were used as follows:

$$SHF_{overall} = SHF_{stress-state} \times SHF_{traffic-wander} \times SHF_{material} \times SHF_{healing}$$

Where $SHF_{overall}$ is the overall shift factor, $SHF_{stress-state}$ is the shift factor to account for the difference in stress state, $SHF_{traffic-wander}$ is the one to account for traffic wander, $SHF_{material}$ is the shift factor to account for the difference in materials in the lab and placed in the field. Finally, the last shift factor accounts for the HMA healing during the rest periods.

These adjustments have shown a variation of 15% instead of 65%, which is a great deal in terms of fatigue prediction.

In 1996, Monismith and Deacon (20) defined a fatigue failure criterion of 50% loss of the initial flexural stiffness under a cyclic loading condition, as an allowable load repetition for fatigue damage. This conventional fatigue analysis assumes that the damage is accumulated during cycle loadings to a predefined fatigue failure criterion. This approach focuses on modelling a fatigue life transfer function, that correlates between the number of cycles to failure. This number of cycles is governed by a pre-defined failure criterion and strain amplitude, as well as an initial stiffness or dissipated energy.

2.1.b.3 Four-Point Bending Beam and Fatigue Cracking

Fatigue cracking was generally thought to be the greatest at the bottom of the HMA, where the critical tensile strain exists. However, it is often hard to measure these tensile strains at the bottom of the HMA at the lab. Therefore, the four-point bending beam fixture is usually employed to characterize the fatigue behavior under displacement-controlled mode, at the middle of the specimen by Pronk, in 2006 (21). The maximum bending stress is given by the following formula:

$$\sigma_{max} = \frac{3A}{bh^2} F_0$$

And the maximum tensile strain is given by:

$$\varepsilon_{max} = \frac{12h}{3L^2 - 4A^2} V_{max}$$

Where h, L and A are the beam dimensions (mm),

$F_0$ is the Load (N),

$V_{max}$ is the maximum deflection at the center of the beam (mm)

And $\sigma_{max}$ and $\varepsilon_{max}$ are the maximum bending stress and the maximum tensile strain respectively.

The stiffness Modulus K is simply the ratio of the stress to the strain, in MPa. The specimen is repeatedly loaded in stress or strain controlled, until the predefined failure occurs (tertiary flow is reached or $N_f$-50%). The test runs until visible cracks occur and propagate from the near end of the secondary stage to the end of the tertiary stage.

The number of cycles to reach this failure is measured. As it takes a relatively long time to reach the failure criterion at low strain levels, SHRP M-009 and AASHTO TP8-94 (22)set a new failure criterion as a 50% reduction of the initial stiffness measured after 50 applied load cycles.

As the maximum tensile strains at the bottom the HMA layer are used to determine the fatigue damage in the pavement design process, they are used to predict the fatigue life in several models. One model uses the extreme strain at the 200$^{th}$ loading cycle of the 3$^{rd}$ point loading as follows by Monismith and Deacon 1969, Monismith et al., 1972 (23)

$$N_f = K_1 \left(\frac{1}{\varepsilon_t}\right)^{K2}$$

Where $N_f$ is the load repetitions to failure,

$\varepsilon_t$ is the initial strain at the 200$^{th}$ load repetition,

And K1 and K2 are regression coefficients.

If the tensile strain at the bottom of the HMA is utilized, then the fatigue damage function is generally described as:

$$N_f = f_1 * \varepsilon_t^{-(f_2)} * E_t^{-f_3}$$

Where $N_f$ is the allowable load repetitions,

$\varepsilon_t$ is the horizontal tensile strain at the bottom of the HMA

$E_t$ is the elastic modulus of the HMA (psi)

And $f_1$, $f_2$ and $f_3$ are constants determined from fatigue testing at the lab.

In 1982, the Asphalt Institute developed a fatigue damage model for the 20% of cracked area as (Finn et al., 1986) (25):

$$N_f = 0.0796 * \varepsilon_t^{-3.291} * E_t^{-0.854}$$

It is to be noted that most of the conventional fatigue damage criteria are based on the $N_f$-50% failure criterion (50% reduction in the initial stiffness of the HMA). However, no approach considers a process to classify the behavior of the HMA as brittle or ductile based on fatigue parameters.

2.1.b.4 New Fatigue Prediction Threshold

In 2010, Yoo and Al-Quadi (26) proposed a promising fatigue life prediction threshold, $N_f$, as a transition point where the stable fatigue behavior evolves into the fatigue failed. It is an allowable loading repetition reaching the crack initiation and propagation. This method uses the ratio of the dissipated energy change instead of the conventional $N_f$-50%.

The $N_f$ threshold was used, and a transfer function for the number of loading cycles to fatigue failure was constructed. Four fatigue parameters were needed for the mix used (13-mm dense graded HMA) as $\frac{\sigma_f}{E}, \varepsilon_f', b$ and c. There are the intercepts of the fitting lines at failure, evaluated at $N_f$=0.5 and b and c are the slopes of the log-log plot for the elastic and plastic strains respectively.

As the accumulated fatigue damage may result in micro and macro cracks on the 4PD specimens, it means that the fatigue cracks may be developed in two strain-controlled

modes, LCF (by high strain amplitudes) and HCF (by low strain amplitudes). The LCF failure occurs at fewer than 5000 loading cycles, at strain levels in the range of 800 to 1200 με. The HCF failure occurs at more than 300,000 loading cycles and at strain ranges from 100 to 300 με. This may be due to the presence of a transition area, separating the LCF and HCF into the elastic region that considers the limit strain amplitude without any noticeable damage to the sample (referring to the Coffin-Manson formulation of the transfer function). The final form of the total strain amplitude to the loading cycles to failure for the 13-mm dense graded HMA is given as follows:

$$\varepsilon_a = \frac{\sigma_f'}{E}\left(2N_f\right)^b + \varepsilon_f'\left(2N_f\right)^c$$

This equation assumes that the specimen fails at the highest point of the half cycle of a reversed strain amplitude ($\varepsilon_a$) at a very high strain input.

In addition, this method classifies the HMA as either brittle or ductile. However, it still depends on the mixture, temperature and loading conditions. Therefore, further testing is still required at different conditions.

2.1.b.5 MEPDG Fatigue Life Prediction and Analysis

According to the AASHTO Mechanistic-Empirical Pavement Design Guide, the MEPDG can predict two types of cracking: Alligator cracking and Longitudinal Cracking. It is assumed that the alligator or area cracks are initiated at the bottom of the HMA layer and propagate to the surface with traffic. As for longitudinal cracks, they are assumed to originate from the surface.

Since these cracks are load related, the allowable number of load repetitions is predicted based on certain inputs related to the mixture. This number is corrected based on the type

of cracking endured. This number of allowable axel-load applications is based on the dynamic modulus, field calibrated parameters, as well as the Effective asphalt content by volume ($V_{BE}$), and the percent of air void in the mixture.

The predictive model goes as follows:

$$N_{f-HMA} = k_{f1}(C)(C_H)(\beta_{f1})(\varepsilon_t)^{k_{f2}\beta_{f2}}(E_{HMA})^{k_{f3}\beta_{f3}}$$

Where the $N_{f\text{-}HMA}$ is the allowable number of axle-load applications for HMA

$\varepsilon_t$ is the tensile strain at critical locations

$E_{HMA}$ is the dynamic modulus of the HMA in compression

$K_{f1}$, $k_{f2}$, $k_{f3}$ are the global field parameters taken to be equal to 0.007566, -3.9492 and -1.281 respectively

$\beta_{f1}$, $\beta_{f2}$, $\beta_{f3}$ are local or mixture specific field calibration constants, set to be equal to 1.0

$C=10^M$ where $M = 4.84 * (\frac{V_{be}}{V_a+V_{be}} - 0.69)$

And $V_{beff}$ is the effective asphalt content by volume and $V_a$ is the percent of air voids

$C_H$ is the thickness correction term, depending on the type of cracking under study.

This correction term is solely based on the total thickness of the HMA layer and has two different equations depending if it reflects the alligator cracking or the longitudinal cracking.

For alligator cracking:

$$C_H = \frac{1}{0.000398 + \left(\frac{0.003602}{1 + e^{11.02-3.49*H_{HMA}}}\right)}$$

For top down longitudinal cracking:

$$C_H = \frac{1}{0.01 + \left(\frac{12}{1 + e^{15.676 - 2.8186 H_{HMA}}}\right)}$$

Based on this number, the MEPDG calculates the incremental damage indices throughout the HMA layers (ΔDI). It is found by diving the actual number of axle-loads by the allowable number of axle loads just defined previously. The incremental damage indices over time are summed up in order to find the cumulative damage index DI for each critical location. After this term is found, it is used to predict the amount of cracking on an area basis.

$$DI = \sum (\Delta DI)_{j,m,l,p,T} = \sum \left(\frac{n}{N_{f-HMA}}\right)_{j,m,l,p,T}$$

Where n is the actual number of axle-load applications within a certain time

j is the axle-load interval

m is the axle load type (Single, tandem, tridem, etc.)

l is the truck type using the truck classification groups within the MEPDG

p is the month period

And T is the median temperature for the five temperature intervals used to subdivide each month.

This parameter is then used to estimate the amount of alligator and longitudinal cracking according to these two formulas respectively:

$$FC_{Bottom} = (\frac{1}{60})(\frac{C_4}{1 + e^{C_1 C_1^* + C_2 C_2^* Log(DI_{Bottom} * 100)}}$$

$FC_{Bottom}$ is the area of the alligator cracking initiated at the bottom of the HMA layer, in % of the total lane area

$DI_{Bottom}$ is the cumulative damage index at the bottom of the HMA layers

$C_{1,2,4}$ are the transfer function regression constants having values of 1, 1 and 6 respectively

$$C_1^* = -2C_2^* \; and \; C_2^* = -2.40874 - 39.748 * (1 + H_{HMA}) - 2.856$$

The same procedure is done in order to get the length of the longitudinal cracks at the top of the HMA layer. Noting:

$$FC_{Top} = 10.56\left(\frac{C_4}{1 + e^{C_1 - C_2 \log(DI_{Top})}}\right)$$

Where $DI_{Top}$ is the Cumulative Damage Index near the top of the HMA surface

$C_{1,2,4}$ are the transfer regression constants equal to 7, 3.5 and 1,000 respectively.

### 2.1.c Thermal Cracking

#### 2.1.c.1 Mechanism of Thermal Cracking

Concerning HMA pavements, thermal cracking is mainly associated with the change in temperature. Thermal cracking is also referred to as Transverse Cracking. It occurs in the asphalt surface layers as the temperature fluctuates in certain areas. The more the temperature fluctuates, the more the asphalt structure will be subjected to contraction and expansion phenomena. In addition, the more the structure is exposed to temperature cycles, the higher the formation and propagation of this type of cracks. Further on, the surface layer is subjected daily to contraction. With a higher temperature drop, the surface layer will contract even more. However, some constraints will prevent this layer to contract, including the friction at the bottom of the HMA layer and the continuity of the layer itself

(referring to Figure 5). Tensile stresses are going to build up in this layer, and eventually lead to the formation of cracks. These cracks are the result of the accumulation of stresses gathered on each temperature change cycle.

With time and continuous temperature cycles, the cracks will develop, interact with load related forces and increase in severity. A high severity and expanded version of this type of cracking is called Block Cracking, which is a series of interconnecting cracks that form in a roughly rectangular pattern on surface layer.

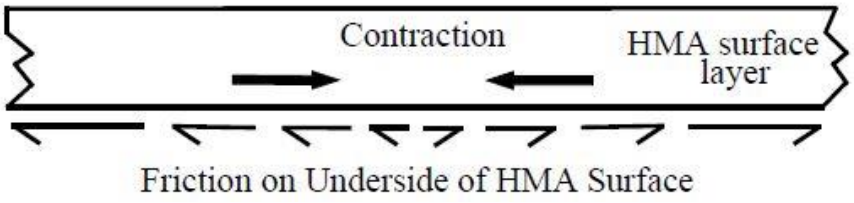


*Figure 5- Contraction Constraints (31)*

This phenomenon happens if a material is unrestrained. In other words, it will shorten as the temperature drops. If the material restrained, it would result in the development of thermal stresses. This concept is referred to the tensile stress to tensile strength relationship shown in the Figure 6 below:

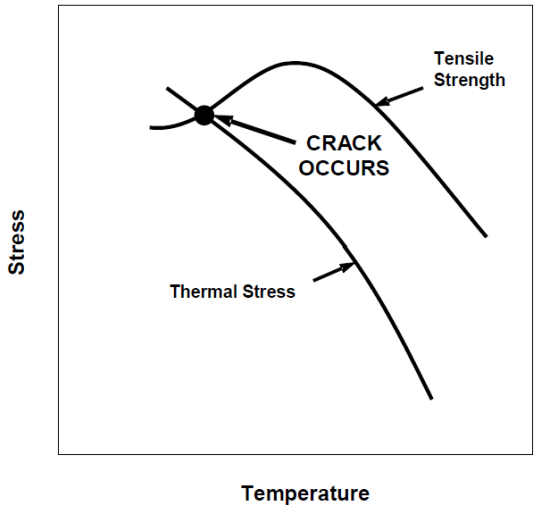


*Figure 6- Relationship between Tensile Strength and Tensile Stress (31)*

This figure shows the concept that when the material is subjected to a tensile stress equal or greater than the tensile strength of the material, cracking will be developed. In terms of viscoelasticity, in the case of the asphalt material, thermal stresses will develop when the temperature drops. The stresses are dissipated through stress relaxation. However, at lower temperatures, the asphalt cannot relax the stresses and therefore the stresses cannot be relaxed as fast as for higher temperature. For this reason, the stresses that are not released are dissipated. The more the stresses are stored, the most likely a crack will occur.

According to Vinson and Janoo (1989) **Error! Reference source not found.** , it is to be n oted that the temperature at which the failure occurs, or in other words the crack occurs, is referred as the fracture temperature.

Thermal cracking is observed to appear at a constant pattern and spacing, approximately 100 feet apart or more. As the pavement ages, with temperature fluctuations, the spacing of thermal cracking gets lower and cracks are more frequent.

Two types of temperature cracking are known so far: Low Temperature Cracking and Thermal Fatigue Cracking. These two types are further discussed in the following sections.

2.1.c.2 Low Temperature Cracking

As mentioned previously, the tensile stresses developed in the HMA pavement as temperature drops are associated to the low temperature cracking. At first, micro-cracks will develop at the surface of the pavement and will propagate through the depth of the layer as thermal cycles occur. Low temperature cracking is characterized by being

transverse to the direction of the traffic, and are spaced from 3 ft up to 300 ft. Transverse cracking that are spaced less than the width of the pavement are most likely to cause longitudinal thermal cracking. This behavior leads to a block pattern, referring to the Block Cracking distress.

2.1.c.3 Thermal Fatigue Cracking

In general, the daily temperature cycling occurs at higher temperatures than the one required for low temperature cracking. Also, the stresses in the pavement is far below the strength of the mixture for these temperatures. For this reason, failure does not happen immediately and develops over time. This is quite similar to fatigue cracking associated with traffic load induced strains in asphalt concrete.

In order to show the difference in temperatures for both low temperature cracking and thermal fatigue cracking, the Figure 7 below illustrates the importance of the temperature ranges.

Fatigue failure occurs when the ratio of the applied strength to stress is closer to 1. The higher the ratio, the faster the damage accumulates.

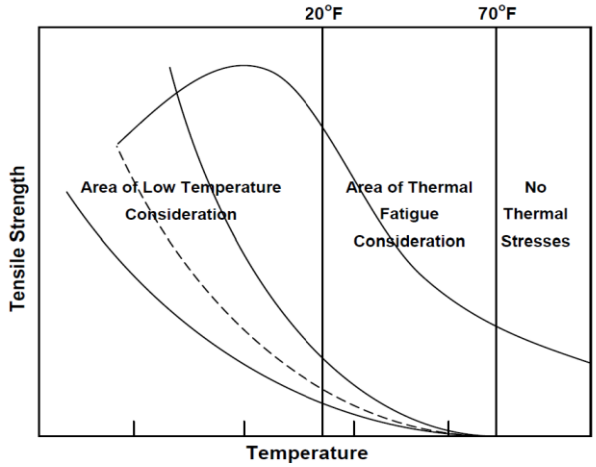


*Figure 7- Temperature Ranges Associated with Different Thermal Cracking (31)*

In 1984, Sugawara and Mariyoshi (34) studied when mixtures were subjected to thermal cycling until failure was reached. It was determined that fatigue failures occurred when the minimum temperature was close to the fracture temperature (explained in section 2.1.c.2).

In addition, fatigue failures were observed with stiffer binders. In other words, a lower number of cycles to failure was observed for harder and stiffer binders. The number of thermal cycles to failure was assessed by the equation stated below. Several tests were conducted at different temperatures and different cycle magnitudes. The relationship derived is close to the one identified for the load-related cycles to failure:

$$N_{cf} = c * \left(\frac{1}{\sigma} \; or \frac{1}{\varepsilon}\right)^{m}$$

Where

$N_f$ is the number of thermal cycles to failure

$\sigma_t$ is the tensile stress

$\varepsilon_t$ is the tensile strain

c and m are factors depending on the material composition and mix properties.

In 1974, Shahin and McCullough (35) have presented a damage model to predict temperature cracking in flexible pavements. However, there method was highly criticized as it doesn't account for crack initiation and propagation as well as redistribution of the stresses in a multi-layered system.

In 1985, Mahboub and Little Mahboub (37) highlighted the importance of crack initiation and propagation. According to those two researchers, these phenomena are greatly related to estimating the thermal fatigue life of asphalt pavements.

If the asphalt pavements behave in a brittle manner, as they would normally do at lower temperatures or high loading frequencies, the time required to initiate the crack will be a great factor contributing to the fatigue life, and crack initiation will be faster. However, if the asphalt pavement has a ductile behavior, the time needed for crack propagation will be grater, and delaying the fatigue life of the pavement.

In 1976, Majidzadeh et al. (38), developed a linear elastic fracture describing the fatigue life of asphalt pavement. It represents the process of crack initiation, propagation and fracture.

In August 2013, Dave and Buttlar (50) developed a new version of the TCMODEL, called IlliTC. It is a software that uses a user-friendly graphical interface with a stand-alone finite-element-based simulation program. It includes a pre-analyzer and data input generator module that develops a 2-D finite element pavement stress simulation algorithm. Cooling events are identified as critical and are rigorously simulated using a viscoelastic analysis engine coupled with a fracture-energy-based cohesive zone fracture model.

2.1.c.4 Coefficient of Thermal Contraction

The volume of asphalt concrete decreases as temperature decreases. The relative change in volume for this case is expressed by the coefficient of thermal contraction. The average value of the volumetric thermal coefficient of contraction over a temperature change interval is defined by the following formula:

$$\beta = \frac{\Delta V}{\Delta T * V_0}$$

Where β is the volumetric coefficient of thermal contraction

$V_0$ is the volume at the reference temperature

ΔV is the change of volume due to the temperature change from the reference temperature to the other temperature considered (ΔT)

The linear thermal coefficient of contraction reflecting the relative change in length of the material due to temperature change is given by the following formula:

$$\alpha = \frac{\Delta L}{\Delta T * L_0}$$

Where

α is the linear coefficient of thermal contraction

$L_0$ is the length at the reference temperature

ΔL is the change of length due to the change in temperature from the reference temperature to the one considered (ΔT)

If the material exhibits the same thermal expansion/contraction in every direction, it is said to be isotropic:

$$\alpha = \frac{1}{3}\beta$$

2.1.c.5 Glassy Transition Temperature

This concept is important to mention, as viscoelastic materials exhibit two coefficients of thermal contraction: the glassy and fluid coefficients.

When the change of thermal coefficient happens, the temperature defining this change is called the Glassy Transition Temperature "$T_g$". For temperatures greater than $T_g$, the

asphalt binder exhibits its fluid coefficient of contraction. For temperature lower than $T_g$, the binder is defined by its glassy coefficient of contraction.

These two modes greatly differ in terms of physical properties, between glassy and fluid behaviors.

The glassy behavior is reflected by testing the specific volume change over a wide range of temperatures. At the glassy temperature, the volume-temperature curve has a sudden change in slope. In 1966, Schmidt and Santucci (39) has investigated the glassy temperature of multiple asphalt binders and found that the $T_g$ ranges from -36 to -15$^o$C. In addition, in 1984, Sugawara and Moriyoshi (40) noted that if the temperature is maintained to be higher than $T_g$, the sress would relax without fracture under thermal stresses. However, if the temperature is lower than $T_g$, failure will occur.

2.1.c.6 Superpave Thermal Cracking Predictive Model

Several models have been developed over the years to predict the thermal cracking behavior of the HMA pavements.

Hiltunen and Roque (41) have proposed a model consisting of three major components: the first model is a pavement response model used to calculate the stress due to cooling, the second module is a mechanics-based model used to determine the progression of a virtual crack at one crack site having average material properties, and the third component is a probabilistic models determining the whole amount of thermal cracking visible on the pavement surface.

This model is also known as the “Superpave TC Model” or “Superpave Thermal Cracking Model”. The final output of this model is the amount of thermal cracks per unit length of the pavement.

The first module, which is the pavement response model, predicts the thermal stresses within the pavement using the material properties and structural information as well as the temperature predictions. The Thermal Response Model is based on a one-dimensional constitutive equation to model the two-dimensional stress distribution within the asphalt later. The thermal stress predictions within the asphalt layer are based on Boltzmann’s Superposition Principle for Linear Viscoelastic Materials:

$$\sigma(\xi) = \int_0^{\xi} E(\xi - \xi') \left(\frac{d\varepsilon}{d\xi}\right) d\xi'$$

Where

$\sigma(\xi)$ is the stress at reduced time ξ

E(ξ- ξ’) is the relaxation modulus at reduced time ξ- ξ’

ε is the strain at the reduced timed ξ, equal to $\alpha T(\xi') - T_0)$

with α as the linear coefficient for thermal contraction

T(ξ’) the pavement temperature at reduced time ξ’

$T_0$ is the pavement temperature when the stress is equal to 0

ξ' the variable of integration

The viscoelastic properties of the asphalt mixture were represented using a generalized Maxwell Model expressed as follows:

$$E(\xi) = \sum_{i=1}^{N+1} E_i e^{-\frac{\xi}{\lambda_i}}$$

Where

$\xi$ is the reduced time, and is equal to $t/a_T$

$E(\xi)$ is the relaxation modulus at the reduced time

t is the real and actual time

$a_T$ is the temperature shift factor

and $E_i$ and $\lambda_i$ are the Prony series parameters

The relaxation modulus function is obtained by the interconversion principle. It consists of transforming the creep compliance function that is determined by multiple creep tests at multiple temperatures. The creep compliance formula goes as follows:

$$D(\xi) = D(0) + \sum_{i=1}^{N} D_i(1 - e^{-\frac{\xi}{\tau_i}}) + \frac{\xi}{\eta_v}$$

Where $D(\xi)$ is the creep compliance at the reduced time $\xi$

$\xi$ is the reduced time at $t=a_T$

$a_T$ is the temperature shift factor

and $D(0)$, $D_i$, $\tau_I$, $\eta_V$ are Prony series parameters

The second model, which is the Crack Depth Fracture Model, is based on the Paris Law for crack propagation. It is used to predict the change in depth of a crack subjected to a cooling cycle as follows by Paris and Erdogan:

$$\Delta C = A\,(\Delta K)^n$$

Where:

$\Delta C$ is the change in crack depth due to a cooling cycle

$\Delta K$ is the change in the stress intensity factor due to the same cooling cycle

A and n are fracture parameters

The following figure represents this model:

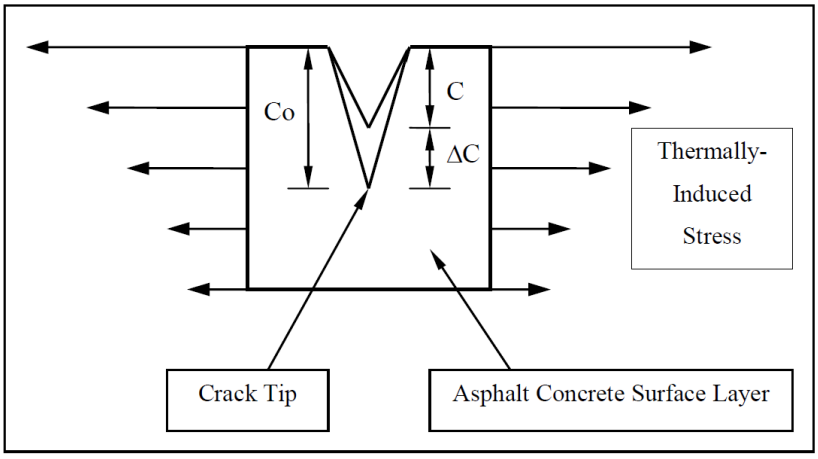


*Figure 8- Representation of the Crack Depth Fracture Model (30)*

The change in crack depth is accumulated on a daily basis to determine the total crack depth in function of time. It is related to the total amount of cracking according to a crack depth distribution function. As the material changes along the length of the pavement section, different crack depths will be resulting for the same exposure conditions.

The fracture parameters A and n must be determined based on the material properties. According to Schapery's theory of crack propagation in the nonlinear viscoelastic materials, the parameters A and n are theoretically related to the slope of the linear portion of the compliance vs time relationship obtained from creep tests, the fracture energy measured when released by crack propagation and the maximum strength of the material determined after the creep test.

According to Molenaar, A and n chould be estimated based on experimental results, such as the m-value and maximum stress at failure of the material:

$$logA = 4.389 - 2.52 * \log(E * \sigma_m * n)$$

Where

E is the mixture stiffness in psi

$\sigma_m$ is the mixture strength in psi

And $n = 0.8 * \left(1 + \frac{1}{m}\right)$, suggested to Lytton et al. in 1993 (42)

Both the mixture strength and the m-value are determined from laboratory tensile creep and failure tests.

Concerning ΔK, which reflects the stress intensity, another model is involved. It predicts essentially the stress at the tip of the local crack. The software CRACKTIP was used by Hitunen and Roque (41) to model a single vertical crack. Using the software, an estimate of the stress intensity factors was developed to model the software in a simplified way:

$$K = \sigma(0.45 + 1.99 * C_0^{0.56})$$

K is the stress intensity factor

σ is the stress from the pavement response model at the depth of the crack tip and $C_0$ is the current crack length.

The last and third component of the TCMODEL reflects the Crack Amount based on probability. It uses the crack depths calculated by the second component (Crack Depth Fracture Model). According to Shahin and McCullough in 1974 (35), this model is associated to the following assumptions:

- There is a maximum number of thermal cracks that can occur and they are uniformly distributed throughout the sections
- A crack is not considered to be a thermal crack until it has propagated through the depth of the entire asphalt later
- The distribution of the crack depths is normally distributed.

This model is represented by the following equation, as a function of the probability that the crack depth is greater than or equal to the thickness of the surface layer:

$$AC = \beta_1 * N\left[\left(\frac{\log\left(\frac{C}{D}\right)}{\sigma}\right)\right]$$

Where

AC is the observed amount of thermal cracking

$\beta_1$ is the regression coefficient equal to 381.4

P() is the probability that [logC>logD]

N() is the standard normal distribution evaluated at [log(C/D)/σ]

σ is the standard deviation of the log of the depth cracks in the pavement, equal to 0.654

C is the crack depth determined from the fracture model

D is the thickness of the surface layer

This concept is also shown by the following figure:

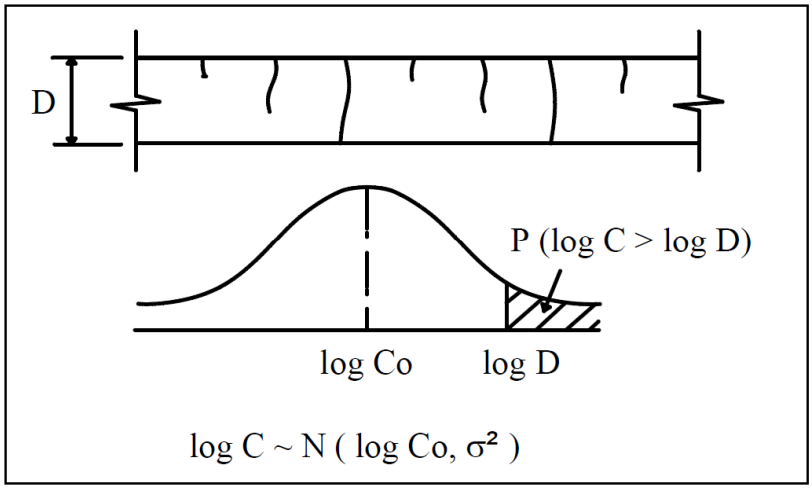


*Figure 9- Crack Amount Model (30)*

The initial SuperPave study on modeling thermal cracking utilized Schapery's theory of crack propagation in nonlinear viscoelastic materials. Schapery justified the use of the Paris' law for the description of the crack growth process in viscoelastic materials. He presented the following relationship:

$$A = \frac{\pi}{6 * \sigma_m^2 I_1^2}\left[\frac{(1-v^2)D_1}{2\Gamma}\right]^{\frac{1}{m}} * [\int_0^{\Delta t} w(t)^n dt]$$

Where $n = 2 * \left[1 + \frac{1}{m}\right]$ for stress-controlled tests and $n = \frac{2}{m}$ for strain-controlled tests

$\sigma_m$= the tensile strength of the material

$I_1$= value of the integral of the dimensionless stress-strain curve of the material having an average value between 1 and 2.

D1 = the compliance coefficient D1, in the power-law creep compliance

m = slope of the log compliance versus log time graph

Γ = fracture energy, defined as work (applied force times resulting displacement) done on a material to increase the fractured surface with a unit area

w(t) = the normalized waveform of the applied load with time. Its values range between 0 and 1.

Δt = period of the loading to complete one cycle of loading

Zborowski et al. in 2007 (31) suggested a modified TCMODEL, comparing to the MEPDG at a $R^2$ value of 0.995. he developed a new and modified Schapery parameter "A". The only modification done to this model was to assume a value 0.12 for the Poisson's Ratio. The second part of Schapery's model is assumed to be equal to one, since in the case of the thermal cracking analysis using the IDT methodology, cyclic loading doesn't occur. The tensile strength and total fracture energy are using the calculating "A" and were interpolated from three laboratory measured values at the temperature of the maximum stress occurrence. The new "A" is not a constant material property anymore, and is temperature-depending with every new cooling cycle:

$$A = \frac{\pi}{6 * \sigma_m^2 I_1^2}\left[\frac{(1 - 0.12^2)D_1}{2\Gamma}\right]^{\frac{1}{m}}$$

The old "A" values were higher and were indicating higher potential for thermal cracking for softer mixtures when compared to the new "A" model.

Twenty-three mixtures including conventional and asphalt rubber were used in the four different climatic regions to conduct a preliminary calibration and check the rationality of the new thermal cracking model. The results obtained were improved and more rational in terms of predicted thermal cracking with the new model. Also, lower predictions were found for the asphalt rubber mixtures whereas using the older model, higher predicted cracking was found in colder regions and unreasonable results for the warmer climates.

### 2.1.c.7 Factors Affecting Thermal Cracking

Vinson et al. **Error! Reference source not found.** describe and discuss the i nfluence of multiple factors on how HMA resist low temperatures and thermal fatigue cracking. The factors that influence of low temperature and thermal fatigue cracking of pavements are categorized under 3 main titles: Main properties, Environmental Conditions and Pavement Structure Geometry.

Under the first category, the main properties of an asphalt mixture have a great effect on the thermal behavior of the structure. The Asphalt binder plays a big deal with regards to low temperature cracking in HMA. Since the Temperature-Stiffness relationship of the binder is a very important concept to consider, mainly as the consistency of the binder and temperature susceptibility at low temperature. A softer binder will have a lower rate of increase of stiffness when the temperature decreases, and therefore reduces the potential for low temperature cracking. Concerning the Aggregate type and gradation, the resistance to transverse cracking is related to the aggregates that have a high abrasion

resistance, low absorption and low freeze and thaw losses. However, it was found to have little influence on the low temperature strength.

The asphalt binder content also doesn't have a significant influence on the low temperature cracking. As the asphalt content increases the thermal contraction coefficient, it lowers the stiffness. Finally, the air void content and the degree of compaction do not significantly influence the low temperature cracking of the mix as well.

Now concerning the Environmental Factors and Conditions, the Temperature has a high impact as the colder the pavement surface, the greater the occurrence of thermal cracking. Most of the thermal cracks are initiated when the temperature decreases to a level below the glassy temperature, as explained in the section 2.1.c.5. Second, the rate of the cooling is also a major factor, whereas the greater the rate of cooling, the greater is the tendency for thermal cracking. Finally, the pavement age plays a big role as well. As the pavement gets older, the greater the occurrence of thermal cracking. As the pavement ages, its stiffness increases. Also, the air void content influences the ageing characteristics of the mix.

Concerning the pavement geometry factors, several ones affect the thermal cracking response. The first one concerns the pavement width, as thermal cracks are more closely spaced for narrow pavements. The initial crack spacing for secondary roads is of 24ft, whereas for general aviation airports, the spacing is greater than 150ft. In addition, as the pavement ages, secondary and tertiary cracks develop. Second, the pavement thickness affects thermal cracking as the thicker the asphalt layer is, the lower the

occurrence of thermal cracking. The friction coefficient in the asphalt layer and the base course also have an impact on the thermal performance of the asphalt pavement structure. It has been shown that using a prime coat on an untreated base reduces the occurrence of low temperature cracking. This may be due to the fact that the asphalt binder layer is bonded perfectly to the underlying granular based having a reduced coefficient of thermal contraction. The subgrade type also plays a role in the thermal performance, as the low-temperature cracking shrinkage cracking occurs more for pavements having sand subgrades than with cohesive soils. Finally, the construction flaws affect the asphalt layers at high temperature and having low mix stiffness. It creates transverse flows as the pavement cools, cracks may be initiated.

2.1.c.8 Thermal Cracking Testing Methods

Several testing methods are defined and used to measure the thermal cracking performance of asphalt mixtures, notable the Direct Tension Test (DTT) , the Indirect Tension Test (IDT) and the Thermal Stress Restrained Specimen Test (TSRST), suggested by Monismith et al.(43) in 1965.

In this study, the IDT test is of interest, and therefore will be described in detail. The description will also include further modifications suggested by ASU.

2.1.c.9 IDT Test Methodology and Protocol

Tensile creep and tensile strength test data are major material inputs required for the MEPDG 2002 Design Guide (30), when a thermal fracture analysis is desired. The predictions in this design guide are based on a module called TCMODEL, developed during the SHRP research. The IDT is used to develop the tensile stresses along the

diametral axis of the test specimen. The test is conducted by applying a compressive load to a cylindrical specimen through two diametrically opposite arc shaped rigid platens. Based on the theory of elasticity, the strain can be expressed in three-dimensions, that can be ideally reduced to a two-dimensional analysis for special loading conditions. Concerning the circular disk, the 2-D analysis can be categorized as plane stress, according to Way et al. in 2006 (48).

The Figure 10 shows a schematic diagram of the IDT:

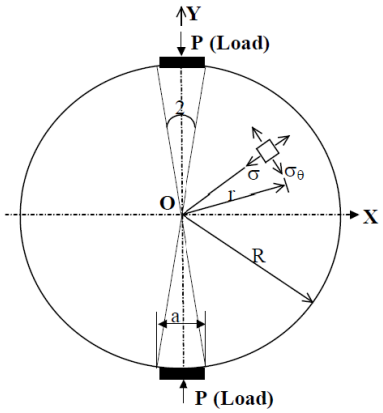


*Figure 10- Schematic Diagram of the IDT Test (31)*

Furthermore, a creep compliance data is needed to predict the tensile stress development in the asphalt concrete layers resulting from temperature cycling. The material inputs for the fracture model are the tensile strength at -10$^{o}$C and the m-value. The tensile strength can be obtained directly for the IDT test, whereas the m-value is the slope of the creep compliance master curve and is obtained using compliance data from the Indirect Tensile Creep Test. The creep compliance curve is obtained from the IDT creep testing. Both values of the tensile strength and creep compliance are used in a linear viscoelastic

analysis to calculate the low temperature and fatigue cracking potential of the asphalt concrete.

The IDT Tensile Test procedure was carried out and developed by Roque et al.(24) It was described in the AASHTO TP0-02. Two modifications were suggested to the original protocol. The first one includes the original LVDT's gage length of 1.5 inches to 3.0 inches, center to center. The second one suggests using a temperature of -15ºC instead of -20ºC.

Concerning the Indirect Creep Test, a constant static load is applied to the specimen for 100,000 seconds while recording the horizontal deformations. The horizontal deformations are recorded also for another 1,000 seconds after the load is removed to calculate the recovery of the specimen. Poisson's ratio is also calculated based on the vertical and horizontal deformations measured by the LVDT's. The Figure 11 shows the elastic and viscoelastic strain components that exist during both loading and unloading conditions. The plastic and visco-plastic components only exist during the loading portion:

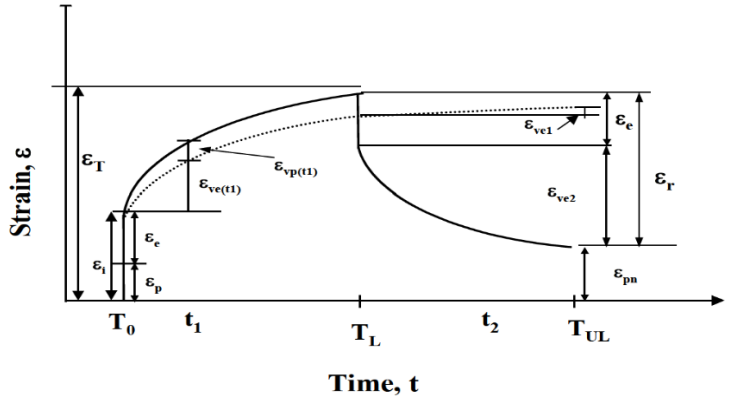


*Figure 11- Total Strain Response for Typical Indirect Creep Test (31)*

The Roque et al. (24) IDT protocol is now based on the use of a 100 second creep test. Enhanced data analysis techniques through the program MASTER as used to get accurate evaluations of the time-temperature shift factors ($a_T$) and the creep compliance mode fit and creep compliance master curve.

The phenomenon of static creep shown in the figure above illustrates the strain-time response of an asphalt mixture. It is divided into recoverable and non-recoverable components (time-dependent or time-independent):

Where the total strain $\varepsilon_T$ is found using this concept:

$$\varepsilon_T = \varepsilon_e + \varepsilon_p + \varepsilon_{ve} + \varepsilon_{vp}$$

Where

$\varepsilon_e$= the elastic strain, recoverable and time independent

$\varepsilon_p$= the plastic strain, irrecoverable and time independent

$\varepsilon_{ve}$= the viscoelastic strain, recoverable and time dependent

$\varepsilon_{vp}$= the visco-plastic strain, irrecoverable and time-dependent

As vertical and horizontal LVDT's are mounted on the specimen, the horizontal and vertical deformation during the IDT Creep test were measured. The test was conducted at three different temperatures: 0 $^oC$, -10 $^oC$ and -15 $^oC$. The obtained data was extrapolated to obtain the creep compliance parameters at -20 $^oC$. The tensile creep was determined by applying a static load of a fixed magnitude along the diametral axis of the specimen. As the vertical and horizontal deformations were measured near the center of the specimen, the tensile creep compliance could be calculated as a function of time. It is important to select the right loads to keep the horizontal strains in the linear viscoelastic range during the creep test.

The tensile strength is immediately determined after conducting the creep test, by applying a constant rate of vertical deformation to failure.

A modified method is suggested to measure the tensile strength allowing the determination of the energy until failure and total fracture energy that was applied. For this method, the vertical LVDT's were removed due to the possible damage in the post-failure phase of the test.

2.1.c.10 Calculation of the Creep Compliance Parameters

The creep compliance derived from the indirect tensile test is similar from the one determined from the Triaxial Compressive Creep Test. It is given by the following equation:

$$D(t) = D_1 * t^m$$

Where D(t) is the total compliance at any time

t is the loading time

$D_1$ and m are the material regression coefficients

The regression coefficients are referred to as the compliance parameters and they are general indicators of the creep behavior of the material: $D_1$ is the intercept of the log of the creep compliance curve and 1/m is the slope of this curve. It is plotted in terms of log of the time.

Creep compliance for the biaxial stress state exists and is obtained through Hooke's law by the following formula:

$$D(t) = \frac{\varepsilon_x}{\sigma_x - \upsilon * \sigma_y} \; when \; \sigma_z = 0$$

It has been corrected later by Roque et al (24) as per the following:

$$D(t) = \frac{\varepsilon(t)}{\sigma} = \frac{(H_m(t) * D * T)}{P * GL} * C_{cmpl}$$

Where as $C_{cmpl} = 0.6354 * \left(\frac{X}{Y}\right)^{-1} - 0.332$

$0.20 \leq \frac{t}{D} \leq 0.65$ and $\left[0.704 - 0.213 * \left(\frac{b_{avg}}{D_{avg}}\right)\right] \leq C_{cmpl} \leq \left[1.556 - 0.195 * \left(\frac{b_{avg}}{D_{avg}}\right)\right]$

D(t) is the creep compliance response at time t

$H_M(t)$ is the measured horizontal deflection at time t

GL is the gage length

P is the creep load

t is the specimen thickness

D is the specimen diameter

μ is the Poisson's Ratio

The value of $\frac{X}{Y}$ is also used to calculate the Poisson's ratio of the material during testing:

$v = -0.10 + 1.480 * \left(\frac{X}{Y}\right)^2 - 0.778 \left(\frac{t}{D}\right)^2 \left(\frac{X}{Y}\right)^2$ and $0.05 \leq v \leq 0.5$

The next step is to calculate the tensile stress corrected for the 3D effects. It has the following formula below:

$\sigma_x = \frac{2*P}{\pi*t*D} * C_{sx}$ and $C_{sx} = 0.,948 - 0.01114 * \left(\frac{t}{D}\right) - 0.2693 * (v) + 1.436 * \left(\frac{t}{D}\right) * (v)$

The maximum tensile strain corrected is found by the following equation:

$$\varepsilon_x = \frac{H_M}{GL_{1.072}} * C_{BX}$$

With $C_{BX} = 1.03 - 0.189 * \left(\frac{t}{D}\right) - 0.081 * (v) - 0.089 * \left(\frac{t}{D}\right)^2$.

The master creep compliance curve fit to a Power model is defined by the following equation. The results of the development of the master curve are needed to continue the calculations.

$$D(\xi) = D_0 + D_1 * \xi^m$$

Where ξ is the reduced time

D(ξ) is the creep compliance at reduced time ξ

$D_0$, $D_1$ and m are the power model parameters

2.1.c.11 Calculation of the Tensile Strength

The tensile strength is used to evaluate the effect of moisture within the pavement structure and determine its fracture resistance. It is accurately determined by conducting the IDT test. It is determined right after determining the tensile creep by applying a constant rate of 12.5 mm/min of vertical deformation to failure.

The model computes the failure strength of each test specimen, which is defined as the stress at which the first failure occurs. The tensile strength of the mixture, at the three temperatures noted are also required. The TCMODEL however only needs the value at -10°C.

In the IDT Protocol, a special procedure is utilized to determine the failure load achieved during the Indirect Tensile Test. Therefore, at the instant failure, the failure load can be defined and the tensile strength computed from:

$$S_t = \frac{2 * P_r * C_{sx}}{\pi * D * t} * C_{sx}$$

$P_f$= failure load, $C_{sx}$= correction factors (previously defined), t = specimen thickness and D = specimen diameter

The parameters from the Indirect Tensile Strength test that can be considered for the cracking performance of the mixture are the Indirect Tensile Strength ($S_t$), the Tensile Strain at Failure ($\varepsilon_{ff}$), the Fracture Energy to Failure ($\Gamma_{fa}$) and the Total Fracture Energy ($\Gamma_{fr}$). It is important to consider the energy approach to the thermal analysis of asphalt pavements since it doesn't only consider the maximum force the specimen is able to hold but also the amount of deformation that the mixture can experience without cracking.

The tensile strain at failure is the horizontal strain corresponding to the failure strength. The horizontal strain is calculated as an average deformation, measured by the horizontal LVDTs and divided by the gage length GL (typically 3 inches).

The energy until failure is simply the area under the load-vertical deformation curve, until the maximum load had occurred.

The total fracture energy is the entire area under the load-vertical deformation curve.

### 2.1.c.12 MEPDG Level 3 Thermal Cracking Prediction Equation

The ASU research team was responsible of developing the flexible pavement part for the MEPDG software. Therefore, the level 3 analysis had numerical optimization techniques developed related to the creep compliance and tensile strength of the pavement mixtures to be studied. As these predictions were developed, they were based on correlations of the creep compliance and tensile strength data with the volumetric properties of the mixtures. The creep compliance was still determined as the following response:

$$D(t) = D_1 * t^m$$

Where $D_1$ (1/psi) and m are the fracture coefficients obtained from the creep compliance of the mixture and t is the loading time in seconds.

The $D_1$ and m parameters were calculated for each temperature of -20, -10 and 0°C. Once they were selected for each mixture by nonlinear regression analysis, they were correlated to different volumetric properties (Air voids, VFA, Penetration, A and VTS). The following correlation was found by the research team:

$$\log(D_{1)} = -8.5241 + 0.01306T + 0.7957\log(V_a) + 2.0103\log(VFA) - 1.923\log(A_{RTFO})$$

Where:

T = Test temperature (°C) (i.e., 0, -10, and –20 °C)

$V_a$= Air voids (%)

VFA = Void filled with asphalt (%) = $\frac{V_{beff}}{V_{beff}+V_a} * 100$

$A_{RTFO}$ = Intercept of binder Viscosity-Temperature relationship for the RTFO condition

For the *m** parameter, the best relationship found was:

$$m = 1.1628 - 0.04596V_a - 0.01126VFA + 0.0024 * Pen_{77} + 0.001683 * Pen_{77}^{0.4605}T$$

Where

T= Test temperature (°C) (i.e., 0, -10, and –20 °C)

$V_a$= Air voids (%)

VFA = Void filled with asphalt (%)

$Pen_{77}$= Penetration at 77 °F = $10^{290.5013\sqrt{8.1177.288+257.0694*10^{A+2.72973*VTS}}}$

$A_{RTFO}$= Intercept of binder Viscosity-Temperature relationship for the RTFO condition

$VTS_{RTFO}$ = Slope of binder Viscosity-Temperature relationship for the RTFO condition

The tensile strength (in psi) at -10°C was also correlated with the volumetric properties as follows:

$$S_t = 7416.712 - 114.016 * V_a - 0.304 * V_a^2 - 122.592\, VFA + 0.704 VFA^2 + 405.71 \log(Pen_{77}) - 2039.296 * \log(A_{RTFO}).$$

# CHAPTER 3

# 3 THE PREDICTIVE MODELS

## 3.1 Effective Temperature Concept and Model

In this part of the study, the temperature at which distresses occur is of interest. For this reason, the effective temperature concept is applied. It is defined as the temperature at which the sample will accumulate the same amount of damage as if it was obtained for the cumulative load damage at a certain location for different climates.

### 3.1.a Effective Rutting Temperature

According to Witczak et al. (1992) (8), the temperatures considered in this study depend on the type of the distresses evaluated. First, the effective temperature will be assessed for the Rutting distress. For the predicted permanent deformation, it will be evaluated as a single temperature, at which rutting is to be expected due to the seasonal fluctuations under cumulative damage principles. In other words, the effective temperature is used in the predictive permanent deformation model to assess the rutting that would happen under temperature fluctuations throughout the annual environmental cycle and different traffic loadings.

In 2005, Sotil (45) improved the initial Effective temperature model developed by Witczak in 1992. It included the loading frequency, environmental factors such as the Mean Annual Average Temperature (MAAT), air temperature, wind speed, sunshine and rainfall.

In 2008, El-Basyouny and Jeong (47) improved the 2005 model, giving it a final form as follows:

$$T_{eff} = 41.534 - 3.261 \times \ln(Freq) - 9.021 \times z + 1.11 \times MAAT + 1.254 \times \sigma_{MMAT}$$
$$- 1.132 \times Wind + 0.337 \times Sunshine + 0.071 \times Rain$$

Where

Freq is the loading frequency (Hz)

Z is the depth in the asphalt layer at which the temperature is desired (in)

MAAT is the Mean Annual Average Temperature ($^{o}$F)

$\sigma_{MMAT}$ is the standard deviation of the mean annual air temperature of a period of years for a design site ($^{o}$F)

Wind is the mean annual speed (mph)

Sunshine is the mean annual sunshine percentage (%)

Rain is the cumulative annual rainfall depth (in).

In 2010, Rodezno (46) further modified this model based on a larger database, to tailor the changes in the environment selected. The finalized model, that is also going to be used in this study is the following:

$$T_{eff} = 14.62 - 3.361 \times \ln(Freq) - 10.94 \times z + 1.121 \times MAAT + 1.718 \times \sigma_{MMAT}$$
$$- 0.431 \times Wind + 0.333 \times Sunshine + 0.08 \times Rain$$

For the purpose of this study, the loading frequency is taken to be equivalent to 18 Hz. The loading frequency is relative to the functional specification of the road, and how often traffic loading is to be expected.

The MAAT is calculated based on the monthly recorded temperature for the location under study. It is obtained by the average of the high and low annual temperatures.

The standard deviation $\sigma_{MMAT}$ is calculated based on the measured monthly temperatures.

The depth of the asphalt z is considered to be equal to 2cm (or 0.78 in) from the surface. This is the average depth to where rutting normally happens.

The wind speed is the annual wind speed recorded for each city, along with the annual sunshine percentage and the cumulative rainfall for one year.

### 3.1.b Effective Fatigue Temperature

As it was previously stated, the effective temperature has to be associated with the distress under consideration. In terms of fatigue, according to AASHTO TP 107, the testing temperature is selected based on the 98% reliability of the PG (Performance Grade) on the climatic region. The testing temperature is determined as the average of the high and low temperature of the PG- temperature, minus 3ºC. (i.e., for a PG of $64^0$C, the effective fatigue temperature is calculated to be $\frac{64-22}{2} - 3 = 18^oC$)

## 3.2 The Flow Number Predictive Model

The knowledge of the flow number for a specific HMA mixture provides valuable information. Considering laboratory testing, it would give valuable information for selecting the appropriate stress and temperature conditions. By having the FN, a suitable deviator stress and temperature will allow the failure of the sample within a reasonable time period and ensure the occurrence of the three stages of the RLPD Test (Primary, Secondary and Tertiary).

Furthermore, it will be used as a tool to assess and rank the mix designs based on the predictions, knowing only the fundamental mix properties as described in the future chapters.

In 2010, Rodezno (46) developed a predictive Flow Number model. A large database was generated and put together in order to make the model as comprehensive as possible, under different stress levels, temperature combinations, gradations and binder types.

The variables selected for the development of this model are the following:

- Testing Temperature ($^oF$)
- Binder Viscosity at Testing Temperature, defined in terms of Ai and VTSi, $V_1$
- Aggregate Gradation, more specifically the percent of aggregates retained on sieves ¾'', No. 4, and the percent passing on sieve No. 200 ( $R_{34}$, $R_{04}$ and $P_{200}$)
- The Air Void content ($V_a$) in percent
- The Normal Stress p (psi)
- The Maximum Shear Stress q (psi)

As described in Section 2.1.a.1, p and q allow the evaluation of the state of stresses and are significant factors for the flow number predictions. These stresses are associated with the principal stresses developed during the triaxial testing and reflect the stresses that are applied by the traffic loading in the design site. The presence of these two parameters in the model shows the importance of the stress levels applied to the samples.

It was also decided that FN results are limited to 100,000 cycles. The FN results that lasted beyond this limit were found to not have reached the tertiary flow. In total, 1801 FN tests were part of the analysis.

The relationship between the standard deviation and mean flow number values was explored for both confined and unconfined testing. It was shown that at low flow number values, the dispersion for both confined and unconfined testing is higher than at high flow

number values. Also, the standard deviation increases with the increase in flow number values.

A stepwise regression analysis was involved to determine a more suitable model using arithmetic and logarithmic terms. The stepwise regression analysis was run for the entire database. Based on the results of the correlation matrix, the most significant variable was the log of the viscosity of the binder at testing temperature ($V_1$). The testing temperature is taken to be the effective pavement temperature in the future, to evaluate the predicted permanent deformation.

The model had a coefficient of determination $R^2$ of 0.64 and is considered to be reasonable. In Figure 12 below, the distribution of the measured vs predicted Flow Number values is shown.

The final model that is going to be used in this study has the following form:

$$\log FN = 0.485 + 0.644 \times \log(V_1) + 0.0874 \times P_{200} - 3.323 \times \log p + 0.0129 \times R_{04} - 0.0803 \times V_a + 2.593 \times \log q - 0.0142 \times R_{34}$$

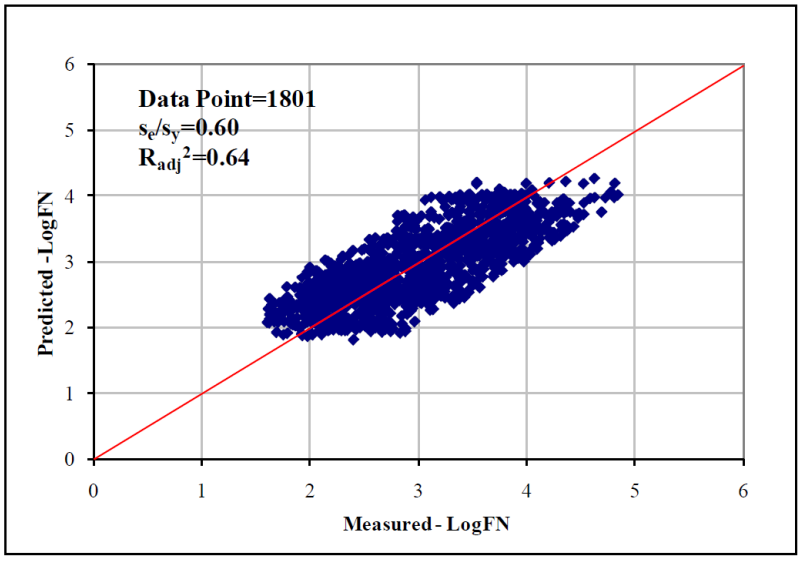


*Figure 12- Measured vs. Predicted Flow Number Values (46)*

### 3.2.a Sensitivity Analysis

In terms of sensitivity analysis, a summary table including the maximum, minimum and average values for each of the variables used in the model has been provided. (Table 1). Three variables were included in addition to the ones in the model since they contribute indirectly to it. These variables are the principal stresses $\sigma_1$ and $\sigma_3$ as well as the test temperature. The first two variables are needed to compute the normal and maximum shear stresses p and q, where as the temperature is needed to calculate the binder viscosity $V_1$ in terms of Ai and VTSi.

The findings of the sensitivity analysis are summarized as follows:

1. The Flow Number decreases with an increase in air voids. It is found to be approximately equal to 20% for every 1% increase in air voids.
2. The Flow Number increases with an decrease in Viscosity. Stiffer binder will have a higher Flow Number. In other terms, at higher temperatures, the binder will result in lower Flow Number values.
3. The Flow Number decreases with an increase in deviator stresses. Also, it will increase with an increase in confinement stress levels.
4. The Flow Number will decrease with higher percent passing the ¾'' sieve. As for the percentage retained on sieve No. 200 and passing No. 4, the Flow Number will increase with the increase of these percentages.

*Table 1- Summary of the Maximum and Minimum values used for the development of the FN Model*

| Parameters | Mean | Minimum | Maximum |
|---|---|---|---|
| **Va (%)** | 7 | 1 | 13 |
| **$R_{34}$ (%)** | 2 | 0 | 26 |
| **$R_{04}$ (%)** | 46 | 14 | 78 |
| **$P_{200}$ (%)** | 5 | 3 | 12 |
| **V1 (Poise)** | 2.49E+05 | 1.02E+03 | 4.56E+06 |
| **T (ºF)** | 117 | 85 | 150 |
| **P (psi)** | 55 | 2 | 235 |
| **Q (psi)** | 51 | 2 | 225 |
| **$\sigma_1$ (psi)** | 106 | 4 | 460 |
| **$\sigma_3$ (psi)** | 3 | 0 | 30 |

3.3 The Rutting/Permanent Deformation Predictive Model

As explained in the previous section, a predictive model for the flow number of pavement mixtures have been developed. Based on this prediction, a Permanent Deformation predictive model was also developed by Rodezno, 2010 (46). Kaloush (10) was the first to present this approach by relating the flow number obtained in the laboratory to the rut depth measured in the field. The new model by Rodezno covers a wider range for analysis, as well as higher levels of traffic for different asphalt layer thicknesses. It also covers different stress conditions (confined and unconfined) as they are replicated in the Flow Number predictive model established. Hypothetically, is it determined that the rutting depth increases with an increase of traffic loading but decreases with the increase in Flow Number and Asphalt layer thickness.

In her study, Rodezno used the MEPDG software to generate necessary data for the analysis. Also, the MEPDG was a necessary tool to generate the HMA rutting values

for a wide range of climatic locations and pavement structure. Having this output in hand, in addition to the prediction of the flow number using the same pavement mixtures and different traffic levels, the model was developed.

Concerning the generation of the flow number values, a typical stress of 120 psi for a standard tire pressure was taken into consideration, with a confinement level of 20 psi. This confinement level is the most commonly used in laboratory testing for the RLPD test. Even though permanent deformation occurs at different temperatures and different stress conditions, it was considered safe to assume these stress conditions for the analysis of the results. This stress condition represents a safe densification condition by still representing a good portion of the distress happening.

In order to develop the model, a wide range of asphalt mixtures was used. For each climatic region (20 regions in total), two binder types were selected, along with four different gradations, two air void contents. The following Table 2 summarizes the levels of the variables used in the flow number prediction for this analysis.

*Table 2- Variables used for the Flow Number Prediction*

| Variable | Levels | Description | | | |
|---|---|---|---|---|---|
| **Climatic Region** | 20 | Cold to Hot Climate | | | |
| **Air Voids** | 2 | 4 and 10% | | | |
| **Gradations** | 4 | R 3/4 | R 3/8 | R 4 | P 200 |
| | | 0.4 | 5.8 | 27 | 5.4 |
| | | 0 | 24.6 | 51.1 | 3.5 |
| | | 3 | 35.5 | 57.7 | 3.54.2 |
| | | 9.2 | 47.9 | 70 | 6 |

Using the Effective Rutting Temperature model (the Modified Witczak Effective Temperature for Rutting), the temperatures for each location has been assessed and the

Flow Number determined at the respective temperature. The values required for the Mean Annual Air Temperature, Mean Annual Average Wind Speed, Mean Annual Sunshine Percentage, Cumulative Annual Precipitation and Mean Monthly Air Temperature Standard Deviation were obtained from the MEPDG EICM Database (Enhanced Integrated Climatic Model).

The MEPDG rutting value generation was based on a basic pavement structure including a varying HMA layer in thickness, a 10-in base with a Modulus of Resilience of 40,000 psi and a subgrade with a Modulus of Resilience of 20,000 psi.
Three traffic levels were also considered among the different gradations and air void levels defined previously.

Concerning the type of binder used, it was generated from the LTPPBind 3.1 based on the locations chosen. As this software recommends modifying the binder based on traffic levels, two binder types were selected per location: one binder for each traffic level: 3 million ESAL and 10 to 30 million ESAL.

Finally, those combinations generated a total of 1,440 permanent deformation predictions.

An initial assessment was made in order to determine the relationship between the rutting values and the flow number predicted values. It was noticed that for a certain AC layer structure, 2 traffic levels at 20 different locations and for 4 different gradations, the predicted flow number was quite different. However, the rutting values were similar. For this reason, a power and non-linear relationship between the flow number, ESALs and asphalt layer thickness was established.

After performing a non-linear regression analysis on the 1,440 combinations, the final version of the model is presented below:

$$R = 0.00462 \times FN^{-0.242} \times ESALs^{0.483} \times h^{-1.021}$$

Where FN is the predicted flow number

ESALs is the traffic level chosen

And h is the thickness of the asphalt layer in inches.

The model has an adjusted $R^2$ of 0.86, with an Se/Sy ratio of 0.36. This shows that the model has a great accuracy. The AC rutting values from the MEPDG simulations are plotted with the rutting predictive values from the models generated in Figure 13:

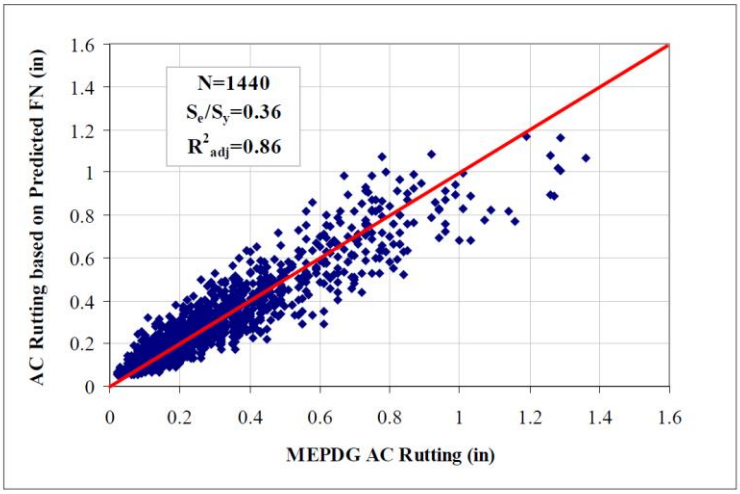


*Figure 13- Comparison of the MEPDG Rutting Values and the Rutting Values based on the Predicted FN (46)*

This model is a great tool that allows the prediction of the permanent deformation based on the traffic level and flow number prediction. The flow number predictive model itself is only based on the chosen stress levels and pavement mix designs. This tool allows to have an idea about the future behavior of the mix in terms of permanent deformation, while taking into consideration its proper characteristics. Having this tool beforehand will

allow further modification, as well as the classification of the mixture in terms of acceptable/unacceptable permanent deformation behavior.

## 3.4 Fatigue Predictive Model

In this section, a detailed explanation of the fatigue predictive model taken into consideration in this study is presented. In general, this model relates the fatigue life of binders to the fatigue life of pavement mixtures.

Initially, the binder fatigue parameter $|G^*|sin\delta$ is based on small strain rheology, and therefore does not consider damage resistance. For this reason, the Linear Amplitude Sweet Test (LAS) was proposed to further investigate the binder fatigue resistance. The LAS is a strain controlled cyclic torsion test, conducted on a Dynamic Shear Rheometer, at certain fixed frequency, loading cycles and increasing strain levels by increments. A total of 3,000 cycles are applied at a frequency of 10Hz for 1% strain increments from 0 to 30%. The total duration of the test is essentially less than 5 minutes. This test is considered instead of the Time Sweep Test due to its certainty concerning the test duration. The Time Sweep Test is a conventional fatigue test with repeated cyclic loading at constant strain amplitudes. It evaluates the ability of asphalt binder to resist fatigue damage. It consists of two major phases. The first one includes a frequency sweep to test the undamaged material properties and evaluate the rheological characteristics of the binder, whereas the second one includes the damage characteristics of the binder by employing a linear strain sweep test.

The damage characterization is also conducted in the LAS test according to AASHTO, by considering the Simplified Viscoelastic Continuum Damage (S-VECD) formulation.

The NCHRP 9-59 developed a new approach to assess asphalt binder fatigue analysis called GFTAB, standing for the General Failure Theory for Asphalt Binders. This is another way to analyze the LAS Test. It will be used to develop the new model, as it is more difficult to use the S-VECD method to correlate binder test data to fatigue performance of asphalt mixtures, since the test data has a wide range of stiffnesses and the samples are being tested at multiple strain levels, as well as having a different failure criteria for both binder and mixtures in terms of fatigue.

Developing the model has been carried on 3 distinguished phases. First, the binder fatigue performance has been investigated using the LAS along with the evaluation of the $|G^*|\sin\delta$ parameter. Then, the mixture fatigue performance has been studied using the Axial Fatigue Test and S-VECD. The third part was used to evaluate the relationship between binder and mixture fatigue performance.

The $|G^*|\sin\delta$ parameter is a simple indication obtained from the Dynamic Shear Rheometer at a frequency of 10 rad/sec, according to AASHTO T315. It should be less than 5000 kPa from RTFO and PAV aged binders to control fatigue.

Considering the GFTAB model, it relies on the failure of the material rather than its damage accumulation. Based on this concept, the FSC (Fatigue Strain Capacity) was defined. It refers to the fatigue life at the maximum strain level and was calculated by the ratio of the amount of binder strain to the effective binder content.

$$N_{failure} = \left( \frac{\left( (FSC) * \left( \frac{VBE}{100} \right) \right)}{\varepsilon_t} \right)^{k_1 * \frac{90}{\delta}}$$

Where FSC is the binder fatigue strain capacity, in %

VBE is the mixture effective binder content by volume, in %

$\varepsilon_t$ is the mixture's maximum tensile strain, in %

$K_1$ is the fatigue exponent coefficient

δ is the binder phase angle, in degrees

This equation was later reformulated in the following form:

$$FSC = N_f^{\frac{k1}{2*90}} * \left( \varepsilon_t * \frac{100}{VBE} \right)$$

These formulas refer that the material failure occurs when the binder strain is equal to the fatigue strain capacity. According the Christensen (27) (AAPT 2019), the FSC should be closely related to measures of binder failure strain. However, the binder inside the mixture is confined and has different stress concentrations. Therefore, it is possible that the FSC and failure strain may be highly correlated but different in magnitude.

In order to determine the value of FSC, a certain strain value must be kept constant. Also, at failure, the damage function should be equal to 1.

The damage function has the following form: $D = \sum_{i=1}^{n} N_i \left( \frac{(\varepsilon_t)_i}{FSC_i} * \left( \frac{VBE}{100} \right) \right)^{2\left(\frac{90}{\delta}\right)}$

Equating this to 1 at failure, the following formula for the FSC s determined:

$$FSC = \sum_{i=1}^{nf} [N_i \left[ \frac{(\varepsilon_t)_i}{\frac{VBE}{100}} \right]^{2\left(\frac{90}{\delta}\right)}]^{\left(\frac{\delta}{2(90)}\right)}$$

The values of FSC using the LAS are calculated by setting the term VBE/100 equal to 1. Under a range of temperatures and loading rates, the function of FSC in terms of binder modulus shows the failure envelope (Heulekom, 1996) (27).

A typical FSC value (FSC*) can be determined from direct tension data, defining the general failure envelope (Refer to Figure 14). This FSC* can be estimated as follows:

$$FSC * = \frac{1}{6.56 \times 10^{-3} \times S(T,t)^{0.0482} + 1.35 \times 10^{-9} \times S(T,t)^{1.10}}$$

Where S(T,t) is the initial stiffness of the material at a certain temperature

And FSC* is the typical failure envelope.

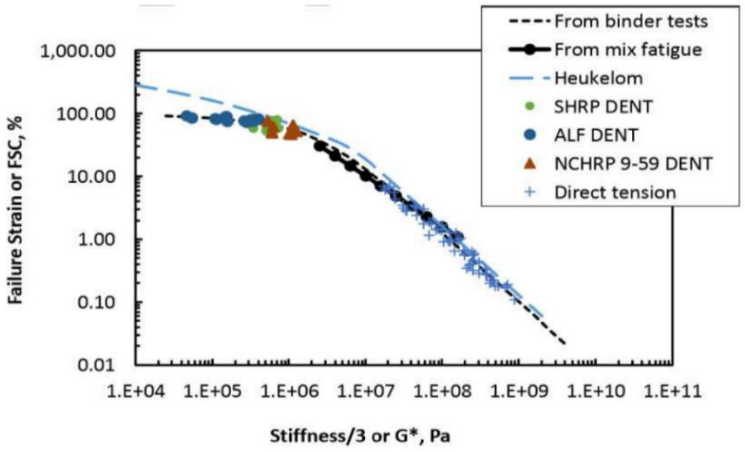


*Figure 14- Binder failure envelopes as defined in the NCHRP 9-59 (28)*

The binder is said to have good fatigue performance if the ratio of the strain capacity calculated for a specific binder with the typical binder fatigue strain capacity is greater

than one. This ratio is defined as the FFPR, the fracture/fatigue performance ratio (FFPR). It goes by the following formula:

$$FFPR = \frac{FSC_{binder}}{FSC^*}$$

The main advantage of the FFPR is to characterize the fatigue performance and eliminate the effect of modulus on fracture and fatigue properties. The strain capacity decreases substantially with increased modulus, which can also result in a decreased fatigue life at higher strain levels.

In order to study the correlation between binder and mixture fatigue, the data of FFPR, FCS* and initial complex shear modulus at 10 Hz and 18$^{o}$C will be taken into consideration.

Concerning the asphalt mixtures, the Axial Fatigue test was conducted at 18$^{o}$C at four different strain levels. The mixtures were expected to fail for less than 10,000 cycles, between 10,000 and 50,000 cycles, between 50,000 and 100,000 cycles and greater than 100,000 cycles. The test data was analyzed using the simplified viscoelastic continuum damage theory (S-VECD). The results are plotted in the form of Material Integrity "C" versus Damage "D". Having more accumulated damage and higher material integrity percentage show a good fatigue performance. And based on these criteria, the asphalt mixtures were ranked. However, this test is not enough to assess the fatigue performance. Therefore, a different strain level needs to be estimated for higher number of cycles (10,000, 100,000 and 1,000,000 cycles).

Having the viscoelastic fatigue parameter $|G^*|\sin\delta$, the nonlinear viscoelastic

binder fatigue parameter based on the LAS, and the axial fatigue test data for mixtures, the relationship between the binder and asphalt mixtures is studied.

The |G*|sinδ is reported to be a bad indicator of asphalt mixture's fatigue performance due to the poor correlation between |G*|sinδ and the axial fatigue test data.

Using Microsoft Excel Solver, the model was developed by testing the Number of Cycles to Failure at three different strain levels: 300, 350 and 400με. The ageing had a great effect on the model, as it introduced some variability into the model. The $R^2$ value changed from 80 to 96% when asphalt ageing (PAV and extracted STOA) were introduced.

Finally, the final model was presented as the following:

$$N_f = \left( \frac{\left( (FSC^*)(\frac{VBE}{100}) \right)}{\varepsilon_t} \right)^{(\frac{3.7}{\varepsilon_t})(\frac{90}{\delta})}$$

Where FSC* is defined as follows:

$$FSC^* = \frac{1}{6.56 \times 10^{-3} \times G_b(T,t)^{0.0482} + 1.35 \times 10^{-9} \times G_b(T,t)^{1.10}}$$

And $G^*_b$ is the dynamic shear modulus of the asphalt binder

VBE is the effective binder content by volume in percent

δ is the phase angle associated with the $|G^*_b|$ calculated by:

$$\delta_b = 90 + (-7.3146 - 2.6162 * VTS') * \log(f_s * \eta_{s,T}) + (0.1124 + 0.2029 * VTS') * \log(f_s * \eta_{s,T})^2$$

The Dynamic Shear Modulus of the Asphalt Binder is calculated as follows:

$$|G *_b| = 0.0051 f_s \eta_{s,T} (sin\delta)^{7.1542 - 0.4929 f_s + 0.0211 f_s^2}$$

Having $f_s$ as the dynamic shear frequency (10 Hz)

$\eta_{s,T}$ the viscosity of the asphalt binder at the frequency and temperature T in cP calculated by:

$$loglog\,\eta_{s,T} = 0.9699 f_s^{-0.0527} * A + 0.9668 f_s^{-0.0575} * VTS log T_R$$

With $T_R$ being the effective fatigue temperature in Rankine.

And $VTS' = 0.9668 f_s^{-0.0575} * VTS$

These formulas were developed by the Cox-Mertz rule using correction factors for the non-Newtonian behaviors.

The final model along with the final FSC* formula will be used in this study to develop the fatigue criterion for each mixture.

3.4.a Sensitivity Analysis

A sensitivity analysis has been carried in order to understand the behavior of this model by modifying each variable at a time.

- By increasing the VBE from 14 to 15%, the $N_f$ increased by 14.7%
- By increasing the strain applied on the structure from 0.035 to 0.036, the $N_f$ decreased by 29%
- By increasing the phase angle δ from 47.74 to 48, the $N_f$ decreased by 6%
- By increasing the FSC* from 48 to 52, the $N_f$ increased by 21%
- By changing the PG-Binder from 76-22 to 82-10, the $N_f$ decreased by 19%

It is important to note that the fatigue behavior of an HMA essentially happens in the lower lifts of the structure. The proposed model can be applied to any mix design throughout the structure to study the potential fatigue resistance. In this study, since the

majority of the mixes collected are surface mixtures, the models are used with the data provided.

## 3.5 Thermal Cracking Prediction Models

The thermal cracking prediction models used in this study are the calibrated versions of the original TCMODEL proposed by Roque and Buttlar (24). Part of the database gathered for the implementation of these new models served as a thermal fracture characterization for the mixtures. Mixtures from five different aggregate sources were used, with 5 different gradation types as well as four different binder types through Arizona (PG 58-28, PG 64-22, PG 70-10 and PG 76-16). A few steps were conducted before inputting the creep compliance data used for the TCMODEL.

The first step consisted of smoothing the creep compliance data. Test results were available for 1, 2, 5, 10, 20, 50, 100, 200, 500 and 1000 seconds. Some errors were associated with the data for 1 and 2 seconds as they did not conform with the resulted expected from the Roque-Buttlar (24) studies. A power function was utilized using the data points for every test temperature for 5, 10, 20, 50 and 100 seconds as previously defined in section 2.1.c.9:

$$D(t) = D_1 * t^m$$

The values at 1 and 2 seconds were back calculated once the regression parameters $D_1$ and m were found. There parameters were back calculated for each temperature.

Next, the creep compliance data was extrapolated from the temperature -15$^o$C to -20 $^o$C as the protocols requires. The following function was used to extrapolate the data from the previous temperatures of 0, -10 and -15 $^o$C.

$$D(t) = P * e^{Q(Temp)}$$

Where

D(t) is the creep compliance

Temp is the extrapolated temperature in $^{o}$C (-20 $^{o}$C)

P, Q are the regression coefficients dependent on the mixture

In all the cases above, the $R^2$ values were higher for higher loading times (50seconds+) with values higher than 0.95. For lower loading times (<20seconds), the correlation was still considered to be good with $R^2$ values ranging between 0.70 to 0.90. For the remaining loading times, the $R^2$ values were between 0.80 and 0.95.

Initially, the creep compliance data and master curve for the mixtures tested by the ASU-ADOT project (the 11 mixtures mentioned above) where compared to mixes from the Roque-Buttlar database. The results of the master curves were located within the Roque-Buttlar data Zone. Therefore, the results for the creep compliance data was considered to be comparable.

For the tensile strength data, the tensile strength values at 0 $^{o}$C and -10 $^{o}$C were taken for both the ASU-ADOT and Roque-Buttlar mixes. After conducting a statistical analysis, it was found that the difference in the tensile strength values was insignificant for 3 out of 4 cases, for 2 binders at 0 $^{o}$C and for PG58-28 at -10 $^{o}$C. However, for the samples at -10 $^{o}$C for the PG64-22, the difference was statistically different, whereas the ASU-ADOT mixtures had a higher average strength than the ones from the Roque-Buttlar. However, it was concluded that the results of the tensile strength were comparable between both the ASU-ADOT and Roque Buttlar (24) Databases.

As a next time, the creep compliance for the eleven ASU-ADOT mixtures was predicted using the MEPDG Level 3 prediction models for a loading duration of 1000 seconds. The thermal fracture parameter m and $D_1$ were found as well. The predicted creep compliance data was plotted against the measured ones reaching 330 data points. It was found that for the ASU-ADOT database, the results correlate poorly with the predicted values from the MEPDG (Figure 15).

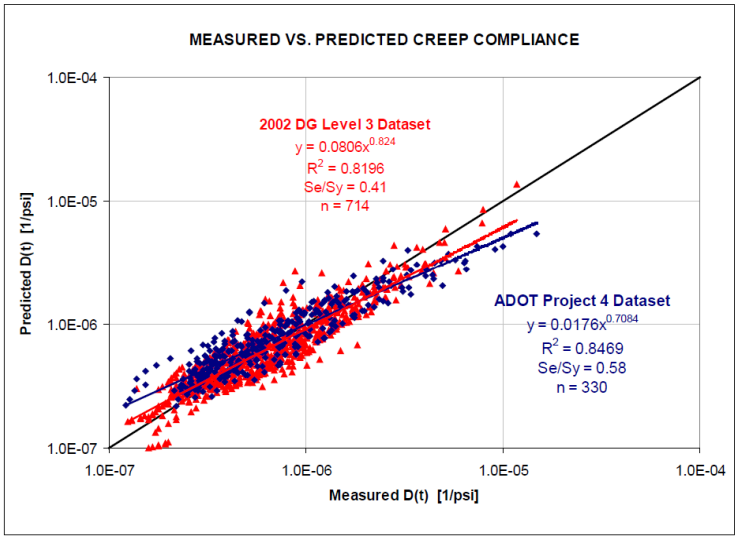


*Figure 15- Predicted vs Measured Creep Compliance for the ASU-ADOT database (31)*

Now considering the tensile strength data, it was measured at a temperature of -10°C and predicted using the Level 3 MEPDG. The following (Figure 16) curve shows the results plotted of measured vs predicted tensile strength for the ASU-ADOT database:

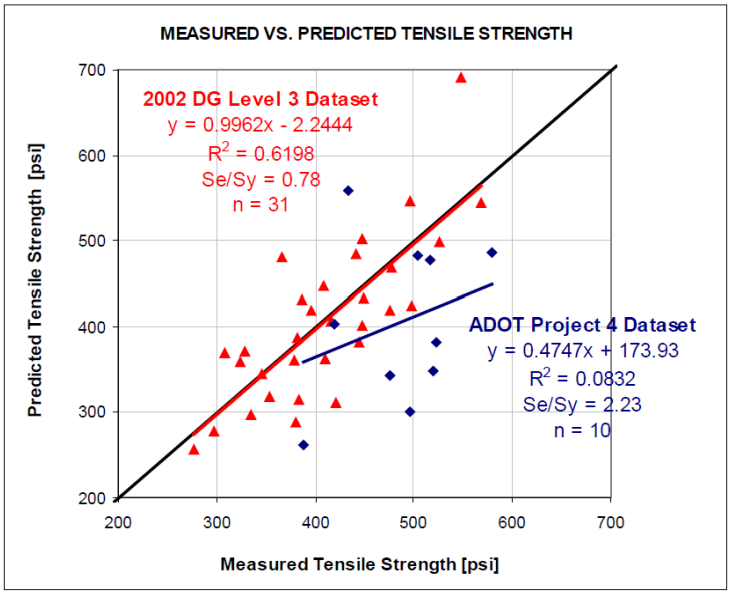


*Figure 16- Predicted vs. Measured Tensile Strength for the ASU-ADOT Database (31)*

It was concluded that the proposed tensile strength prediction models greatly underestimate the real tensile strength of the mixtures, and that a significant difference exists between the MEPDG predicted values and the measured values for the ASU-ADOT database.

In addition, the binder content variation had to be studied and corrected, as it has been shown that when the binder content increases, the number of thermal cracks increases. This is not rational, as the behavior of the mixture becomes softer with more binder added to it, and thermal cracking is increasing. Therefore, the modification of the thermal predictive model was needed for the level 3 analysis. A new set of predictive equations for $D_1$ and m was developed and validated, as well as for the tensile strength at -10$^{o}$C.

3.5.a Existing Set of Predictive Equations for Level 3 Thermal Fracture Analyses

An existing set of predictive equations was already developed for the thermal fracture parameters $D_1$ and m, correlating with the volumetric properties of the pavement

mixtures by the ASU Research team. They were found for each testing temperature of -20, -10 and 0°C. These equations were already explained in Section 2.1.c.12 and are inserted below for simplicity:

$$\log(D_1) = -8.5241 + 0.01306T + 0.7957\log(V_a) + 2.0103\log(VFA) - 1.923\log(A_{RTFO})$$

and

$$m = 1.1628 - 0.04596V_a - 0.01126VFA + 0.0024 * Pen_{77} + 0.001683 * Pen_{77}^{0.4605}T$$

These two values were calculated and plotted in the creep compliance equation, and a total of 714 datapoints were used to come up with these correlation by plotting the measured vs the predicted creep compliance data. These correlations have an $R^2$ of 0.8 and Se/Sy of 0.45. The regressions were considered to be acceptable.

In addition, the tensile strength was predicted at -10 °C as it was correlated with the volumetric properties of the mixture. A total of 31 data points was used to develop this correlation, obtaining a $R^2$ of 0.62 and Se/Sy of 0.68. The correlation was considered to be acceptable as well.

$$S_t = 7416.712 - 114.016 * V_a - 0.304 * V_a^2 - 122.592\,VFA + 0.704VFA^2 + 405.71\log(Pen_{77}) - 2039.296 * \log(A_{RTFO}).$$

Where St is in psi.

However, a problem was identified in the set of prediction models defined above, as a provisional sensitivity analysis of the variation of the binder content shed lights to an unrealistic result pattern. Also, an additional observation was made as the slope of the creep compliance decreased with an increase in the effective binder content. This was in

violation to the common understanding of the thermal fracture development and was identified as a source of the problem existing with the set of the predictive models suggested.

Another problem was discovered after comparing the measured and predicted creep compliance values. As the creep compliance was plotted separately for each temperature, the quality of the prediction was decreasing and was shown to be biased. The $R^2$ values were getting lower for lower temperatures. Therefore, a set of separate equations for each temperature was suggested and developed using an expanded database considering 10 new lab blended mixtures from the ASU-ADOT databases. Four different PG binder grades were considered, ranging from PG 58-28 to PG 76-16 with five different aggregate gradations.

3.5.b New Set of Predictive Equations for "m" and "$D_1$" of the Creep Compliance

As the existing form of the predictive equations for the creep compliance parameters was developed for all the test temperatures, the "T" term was removed from the equations. Separate models were optimized independently for each testing temperature as follows:

For the $D_1$ fracture parameter:

$$\log(D_1)_{-20^oC} = -11.92540 + 1.52206 * \log(V_a) + 4.49876 * \log(VFA) - 3.81320 * \log(A_{RTFO})$$

$$\log(D_1)_{-10^oC} = -10.76560 + 1.51960 * \log(V_a) + 3.49983 * \log(VFA) - 2.99870 * \log(A_{RTFO})$$

$$Log(D_1)_{0^oC} = -9.80626 + 1.50845 * \log(V_a) + 2.99000 * \log(VFA) - 2.90157 * \log(A_{RTFO})$$

Where $V_a$ is the air void content (%), VFA is the Void Filled with Asphalt (%) and $A_{RTFO}$ is the intercept of the binder Viscosity-Temperature relationship for the RTFO (Short-term ageing) condition.

For the "m" parameter, the equation was also split in terms of temperature. In addition, in order to address the binder content discussed previously, the VFA term which caused the value of the "m" parameter to decrease was removed from the equation. The best relationships found were the following:

$$m_{-20^oC} == 1.75987 + 1.78187 * V_a^{0.02030} + 0.00089 * Pen_{77}^{0.96870}$$

$$m_{-10^oC} = -1.8269 + 1.94218 * V_a^{0.01600} + 0.00098 * Pen_{77}^{0.96857}$$

$$m_{0^oC} = -2.41043 + 2.59093 * V_a^{0.01547} + 0.00199 * Pen_{77}^{0.97247}$$

Where $V_a$ is the air void content (%) and the $Pen_{77}$ is the Penetration of the binder at 77 °F given by the following formula:

$$Pen_{77} = 10^{290.5013\sqrt{8.1177.288+257.0694*10^{A+2.72973*VTS}}}$$

A total of 939 data points was used, where 313 point were accorded to each testing temperature. The final comparison between the measured and predicted values of the creep compliance is shown below, with a final $R^2$ of 0.80 and Se/Sy of 0.45 (Figure 17).

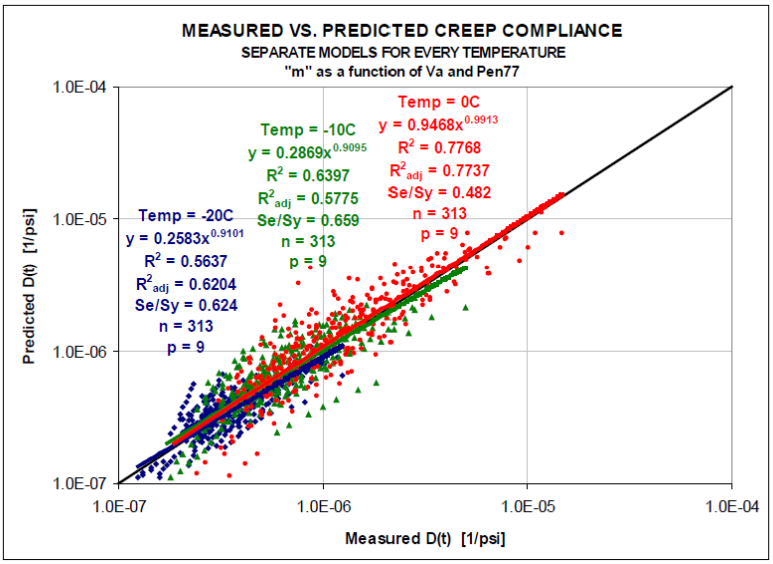


*Figure 17- New Comparison between the Measured & Predicted Creep Compliance for the ASU-ADOT Database (31)*

Lastly, a new form of the tensile strength predictive model was suggested having the same form of the previous model:

$$S_t = 4976.34 - 42.49 * V_a - 2.73 * V_a^2 - 80.61 * VFA + 0.465 * VFA^2 + 174.35 * \log(Pen_{77}) - 1{,}217.54 * \log(A_{RTFO})$$

A total of 42 data points was used, resulting in $R^2$ of 0.47 and Se/Sy of 0.73. The correlation was poor but accepted as the way the tensile strength affects the current TCMODEL is still questionable and should be modified in further versions of the TCMODEL. The result of this equation is supposed to be the undamaged strength, measured during the IDT Test. Also, it was supposed during the SHRP study that -10°C was considered the best temperature to measure the tensile strength. However, different mixtures having different binder grades would have their maximum tensile strength at different temperatures. For this reason, measuring the tensile strength at only one temperature is not significant and do not provide reliable information. This causes a great

difficulty in developing a prediction model based on the volumetric characteristics of the mixture, and thus lead to this poor correlation.

### 3.5.c Total Fracture Energy Prediction

It was determined and concluded that the total fracture energy is a better indicator of the thermal fracture resistance of pavement mixtures than the tensile strength. It can be divided into two terms: the post peak energy measured after the tensile strength was observed, and the energy until failure when the maximum tensile strength has occurred. It can also be associated with the first stage of the cracking process, whereas the post peak energy is associated with the propagation of the thermal cracking. Therefore, the higher the post peak energy, the longer the propagation of the thermal cracking leading a lower observed cracking mechanism.

The following relationship has been introduced, for the total fracture energy at -10°C using 16 conventional asphalt mixtures and rubber mixtures. It was correlated to the mixture's volumetrics as per the following:

$$\Gamma_{\text{tfr}} = 4497.832 - 439.057 * AC + 46.284 * AC^2 - 2057.821 * AV + 40.009 * AV^2 + 12612.114 * \log(V_{beff}) + 13.571.050 * \log(VMA) - 345.948 * VFA + 8.056 * Pen_{77} - 0.052 * Pen_{77}^2 + 1.044 * AC * Rubber\%$$

Where:

AC = Asphalt content (%)

AV = Air voids (%)

$V_{beff}$ = Effective Binder Content (%)

VMA = Voids in mineral aggregate (%) = Effective binder content (%)

VFA = Voids filled with asphalt (%)

Pen77 = Penetration of the binder at 77$^{o}$F

Rubber% = Percent of rubber in binder

This developed correlation had shown a high level of accuracy with $R^2$=0.99 and Se/Sy= 0.176 when the measured vs predicted total fracture energy was plotted.

### 3.5.d Sensitivity Analysis of the Creep Compliance Parameters $D_1$ and m

In this section, the sensitivity analysis of both the fracture parameters $D_1$ and m.

First, considering the sensitivity of $D_1$, it has been determined to increase when $V_b$ increases. Also, the air void content has an effect of $D_1$. As the Air void content $V_a$ increases, $D_1$ decreases.

In other words, when $D_1$ changes with respect to $V_b$ with increasing air void content, the following has been noticed: a pavement mixture with 4% air void content had the highest $D_1$ value compared to the other mixtures, at $V_b$=7%, but had the lowest $D_1$ value when $V_b$ was equal to 14%.

In addition, $D_1$ decreases and becomes less sensitive to the variation of $V_b$ when temperature decreases. Finally, $D_1$ is not considered to be highly sensitive to the change in binder gradation.

Second, concerning the slope of the creep compliance “m”, it is defined to decrease when $V_b$ decreases, and when $V_a$ increases. Also, “m” decreases with a decrease in temperature and increase in binder stiffness. This parameter has a significant importance, as a lower value of the slope of creep compliance will decrease it for the mixture and lead to a higher potential of thermal cracking. It is also to be noted that the

"m" fracture parameter influences the Crack Depth Model in a complex manner. By decreasing "m", it was noticed that the predicted thermal cracking increase and decreased in some way.

As previously mentioned, the Paris law fracture parameter "n" is equal to $0.8 * (1 + \frac{1}{m})$. And by decreasing the "m" value, the Paris law parameter will increase. Therefore, a higher "n" will decrease the fracture parameter "A" and result in a decrease in thermal cracking. However, it will increase the effect of the stress intensity factor ΔK and leading to an increase in thermal cracking. Finally, a lower m would increase the predicted number of thermal fractures in the mix.

### 3.5.e Sensitivity Analysis of Tensile Strength $S_t$ at -10°C

In this section, the sensitivity of the tensile strength will be studied. The tensile strength is noted to decrease with an increase of $V_b$. Also, $S_t$ is to be decreasing with increasing binder stiffness.

$S_t$ is also very sensitive to the air void content variation: the higher the air void content in the mixture, the more sensitive the tensile strength $S_t$ is to the changes in $V_b$. In the case of the study, at $V_b$=7%, with a higher value of $V_a$, $S_t$ is higher, and the difference is significant.

At $V_b$=10%, with a higher value of $V_a$, $S_t$ is higher but with a smaller difference.

At $V_b$=14%, the analysis is reversed, with a higher value of air void content, the tensile strength became lower.

In order to interpret the significance of the parameter $S_t$, the following has been concluded:

The lower the $S_t$ value due to the increase in binder content will cause the Paris law parameter A to increase, leading to a faster crack growth and a higher thermal cracking prediction.

# CHAPTER 4

# 4 CLIMATIC ZONES AND ANALYSIS OF PRE-EXISTING LTPP PAVEMENT SECTIONS

## 4.1 LTPP Climatic Zones and Regions in the United States

For this study, new and approved pavement mixtures have been collected among the United States. As the Long-Term Pavement Performance (LTPP) represents one of the biggest databases for pavements behavior and design throughout history, some of its data goes back far in time. Distresses are quantified according to their deterioration and implemented rehabilitation over the years. In order to create a new and up-to-date database, the collected data from all around the States has been studied according to the volumetric characteristics provided by the contacted State Engineers.

One of the objectives of this study is to compare the recently collected and previously dated designs, and asses the improvements in terms of volumetric characteristics made by the State Agencies. This comparison will allow to determine if the governing distresses in each state were addressed in terms of design.

The pavement mixtures collected are mostly dated within 5 years from today (2020), and will be implemented in future projects; mostly highways with high traffic volume.

It is known that several factors affect the pavement performance. Two of these factors are considered: traffic level and environmental conditions.

In the first case, highways with high traffic volumes are considered (10 million $\leq$ ESAL$\leq$ 30 million) for this study.

Concerning the environmental conditions, the pavement mixtures and volumetric characteristics collected belong to the different climate zones in each state.

According to the LTPP, North America is divided into 4 environmental conditions (Refer to Figure 18):

1. Wet and Freeze
2. Wet and Non-Freeze
3. Dry and Freeze
4. Dry and Non-Freeze


*Figure 18- LTPP Climatic Zones*

After selecting the states to be studied, sections having similar classification, traffic volume and location (as per the climatic regions of the state) have been identified from the LTPP Database. It is important to note that structural differences were not taken into consideration between the recent and previous pavement mixtures. However, the

corresponding locations, estimated traffic conditions as well as environmental conditions were chosen to be the same as much as possible in order to be able to assess the potential behaviors. As the foundation of each structure is affecting pavement performance, it is assumed that the mix designs are closely situated, and that the pavement structures should respectively be similar due to comparable effect of traffic.

As for the PG-binders for the surface layers used in these sections, they have been identified using LTPPBind V3.1 based on the location and weather station chosen for each state.

As the LTPP contains a great amount of pavement sections, only a few met the comparison criteria. In order to fit the comparison, the pavement section must belong to the same climatic region as the one provided by the state engineers, and also has to fit the functional classification defined. In addition, all the required distresses (rutting, fatigue and thermal cracks) will have to be measured and recorded throughout the pavement life of the pavement section. Also, the pavement mixture's volumetrics will have to be recorded in the datafile. If these values are not presented, the comparison and prediction of the distresses will not be possible.

Once the pavement section has been identified and met all the requirements, the pavement mixture's volumetrics for the surface course have been recorded. Since the predictive models implemented in this thesis are all based on the mixture's volumetrics, the rutting, number of cycles to fatigue as well as tensile strength and fracture energy will be predicted for all of the sections selected.

The required data for the models and predictions goes as far as the Aggregate Gradation ($\%R_{04}$, $\%R_{34}$, $\%R_{38}$ and $\%P_{200}$), Asphalt Content (%), Air Void Content ($V_a$, %), Voids

Filled by Minerals (VMA, %), and the PG-Binder. The viscosity of the binder is depending on the effective temperature in Rankine, as well as the two parameters "$A_i$" and "$VTS_i$".

4.2. Description of the Data Collected from the LTPP

Only a few states have been selected from the four main LTPP climatic regions. These states were selected in accordance to the new mix designs gathered from the state engineers in order to carry a good comparison in terms of mix, climate, volumetrics and expected performance over an average pavement life of 20 years. The following Figure 19 shows the states chosen from the LTPP for further analysis:

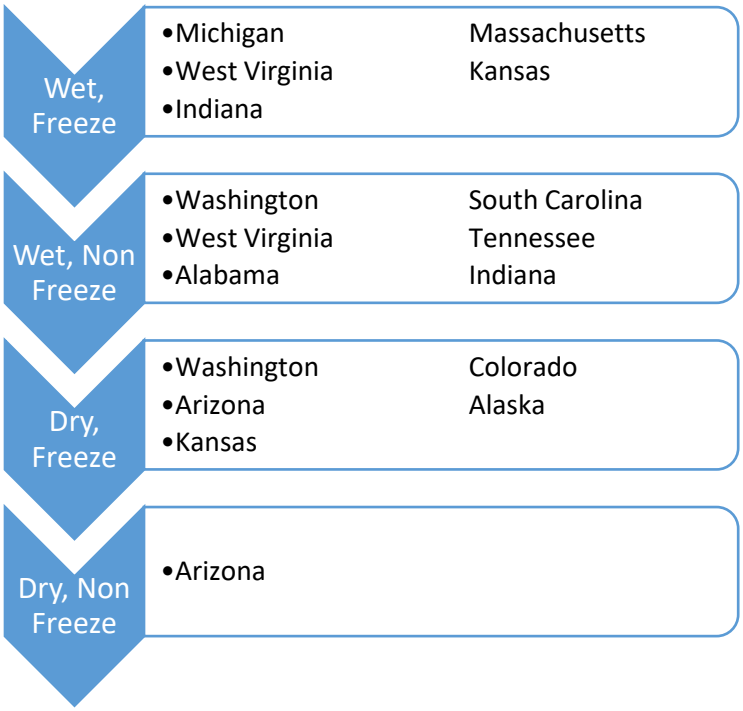


*Figure 19- States chosen to be studied from the LTPP*

The regions stated above all do have the measured data required for our analysis, as well as the mixture's volumetrics required.

In : below are the data gathered summarized per State, Region, Climatic Regions and finally the section number taken into consideration:

*Table 3- States, Cities, Climate Regions Section Number*

| State | City | Climate Zone | Section Number |
|---|---|---|---|
| **Washington** | *Spokane* | *Dry, Freeze* | A320 |
| **Colorado** | *Yuma* | *Dry, Freeze* | 502 |
| **Colorado** | *El Paso* | *Dry, Freeze* | 7783 |
| **Colorado** | *Rio Blanco* | *Dry, Freeze* | 1053 |
| **Arizona** | *Flagstaff* | *Dry, Freeze* | 669 |
| **Alaska** | *Anchorage* | *Dry, Freeze* | 1004 |
| **Arizona** | *Tucson* | *Dry, No Freeze* | 6054 |
| **Arizona** | *Kingman* | *Dry, No Freeze* | 1022 |
| **Arizona** | *Phoenix* | *Dry, No Freeze* | B961 |
| **Massachusetts** | *Boston* | *Wet, Freeze* | 1003 |
| **Michigan** | *Marquette* | *Wet, Freeze* | 1004 |
| **West Virginia** | *Kanawha* | *Wet, Freeze* | 1640 |
| **Kansas** | *Cherokee* | *Wet, Freeze* | 1005 |
| **Michigan** | *Alpena* | *Wet, Freeze* | 6016 |
| **Michigan** | *Port Huron* | *Wet, Freeze* | D330 |
| **Indiana** | *La Porte* | *Wet, Freeze* | 5528 |
| **Michigan** | *Grand Rapids* | *Wet, Freeze* | 901 |
| **Indiana** | *Jackson* | *Wet, Freeze* | A902 |
| **Massachusetts** | *Springfield* | *Wet, Freeze* | 1002 |
| **Washington** | *Seattle* | *Wet, No Freeze* | 6049 |
| **South Carolina** | *Columbia/Lexington* | *Wet, No Freeze* | 1024 |
| **West Virginia** | *Charleston* | *Wet, No Freeze* | 7008 |
| **Tennessee** | *Memphis* | *Wet, No Freeze* | 3109 |
| **Alabama** | *Montgomery* | *Wet, No Freeze* | 4125 |
| **Alabama** | *Tuscaloosa* | *Wet, No Freeze* | 6012 |
| **Indiana** | *Jefferson* | *Wet, No Freeze* | 18-1028 |
| **Arkansas** | *Little Rock* | *Wet, No Freeze* | A606 |
| **Kansas** | *Scott* | *Wet, No Freeze* | 1006 |

The following Figure 20 shows the variation of the data gathered as per the climatic region:

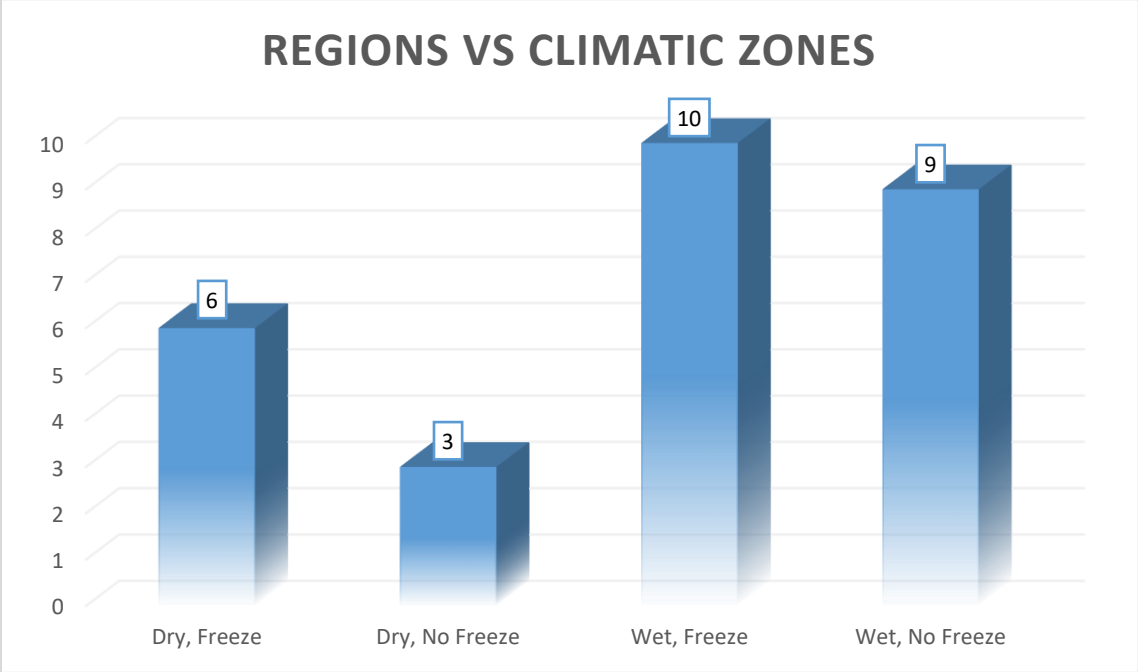


*Figure 20- Regions vs Climatic Regions*

Limited data was gathered from the Dry, No Freeze zone as very few sections fit into the comparison criteria.

Next, the PG-Binders of these sections were found for the surface course using the LTPPBind (v.3) for 98% reliability according to the nearest weather station found next to the section under study. The PG-binders are found in the following Figure 21.

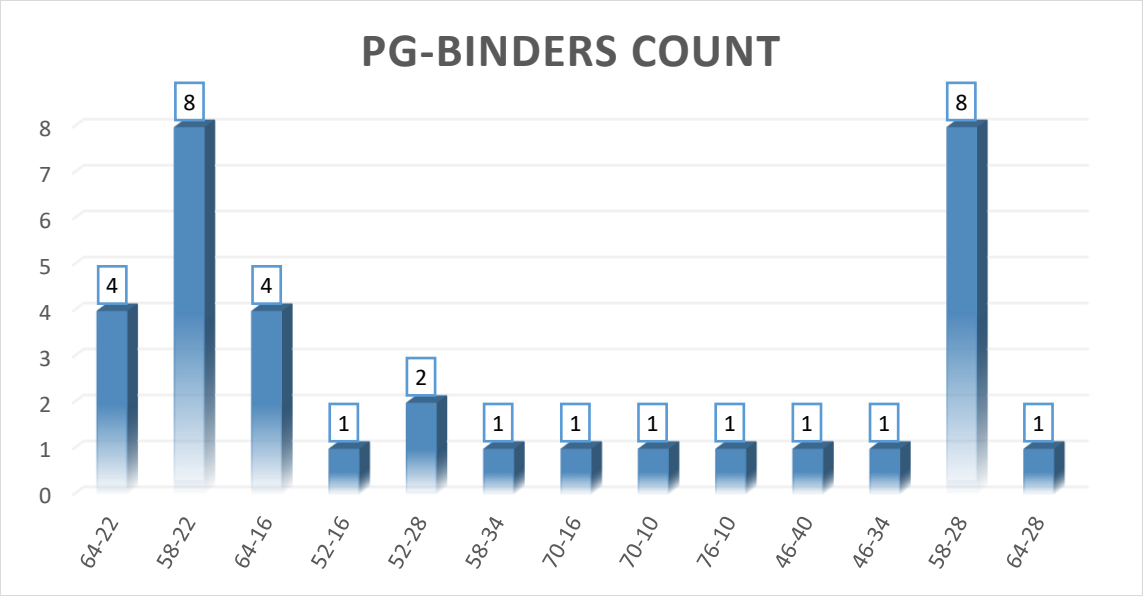


*Figure 21- PG-Binders Count*

This concludes a total number of sections under consideration of **28**.

Now separating these 28 mixes into their respective states, the following results are obtained (Figure 22):

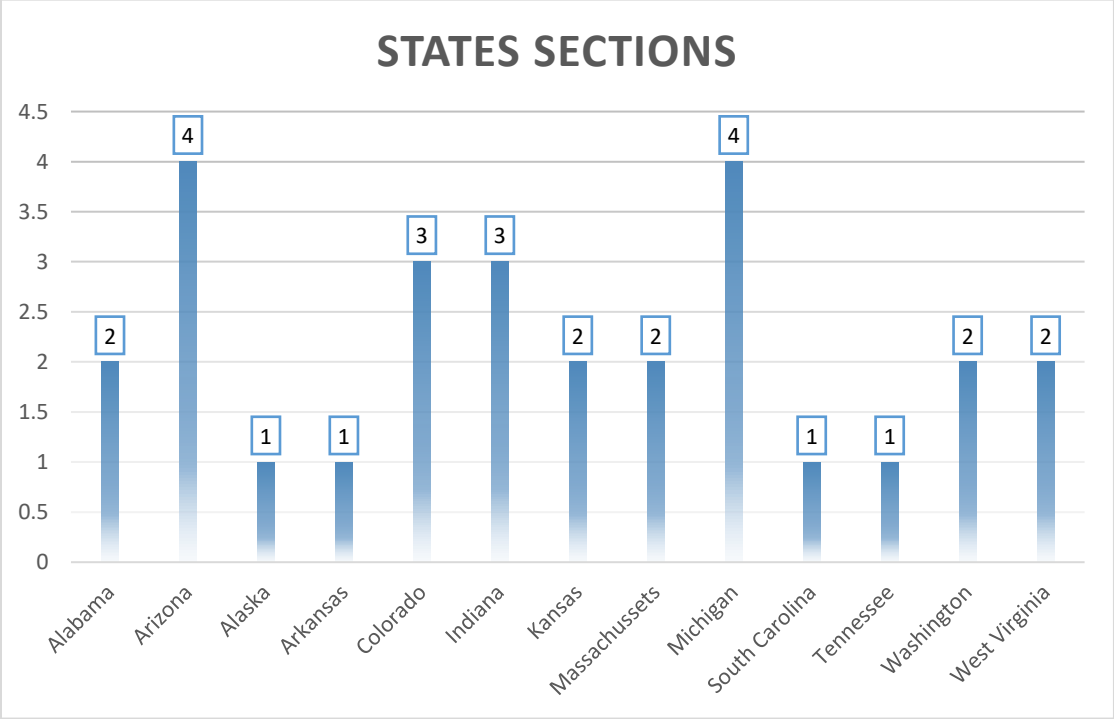


*Figure 22- State Sections Count*

Once these sections were finalized, their volumetrics and measured distresses were gathered. The following Figures Figure 23 to Figure 31 show the descriptive statistics about the data gathered. The first Table 4 shows the maximum, minimum and mean average of all the variables collected from the LTPP and needed for the development of the models within this study. The second Table 5 shows the variation of the distresses measured in terms of the three main distresses considered. The distresses measured and taken into consideration are: Rutting, Alligator cracking, Longitudinal cracking and Transverse cracking. In terms of fatigue, both longitudinal and alligator cracking are taken into consideration. As for the longitudinal cracking, two types of cracking were measured and recorded in the LTPP Database: Wheel Path (WP) and Non-Wheel Path (NWP) cracking.

*Table 4- LTPP Data Collected Minimum, Mean and Maximum Values*

| | LTTP Database | | |
|---|---|---|---|
| Number of Sections: 28 | Min | Mean | Max |
| $V_a$ (%) | 2.30 | 4.92 | 8.90 |
| Ac (%) | 3.70 | 5.26 | 6.50 |
| $V_{be}$ (%) | 5.10 | 9.44 | 12.30 |
| VMA (%) | 13.50 | 14.36 | 16.60 |
| VFA (%) | 36.43 | 65.74 | 83.57 |
| $R_{34}$ (%) | 0.00 | 3.27 | 17.00 |
| $R_{38}$ (%) | 2.00 | 21.11 | 42.00 |
| $R_{04}$ (%) | 14.00 | 43.36 | 63.00 |
| $P_{200}$ (%) | 2.00 | 5.80 | 9.60 |
| $H_{HMA}$ (in) | 1.60 | 7.90 | 21.90 |

Now for the distresses measured:

*Table 5- LTPP Database Distresses Measured Ranges*

| | LTPP Database | | |
|---|---|---|---|
| **Number of Sections: 28** | Min | Mean | Max |
| **Rut Depth (in)** | 0.00 | 0.31 | 0.98 |
| **Longitudinal Cracks (NWP) (length, m)** | 0.00 | 181.88 | 609.80 |
| **Longitudinal Cracks (WP) (length, m)** | 0.00 | 3.85 | 39.80 |
| **Alligator Cracks ($m^2$)** | 0.00 | 65.58 | 274.50 |
| **Thermal Cracks (count)** | 0.00 | 61.68 | 256.00 |

Concerning the frequency distribution of the variables, the graphs are shown below (Figure 23 to Figure 31):

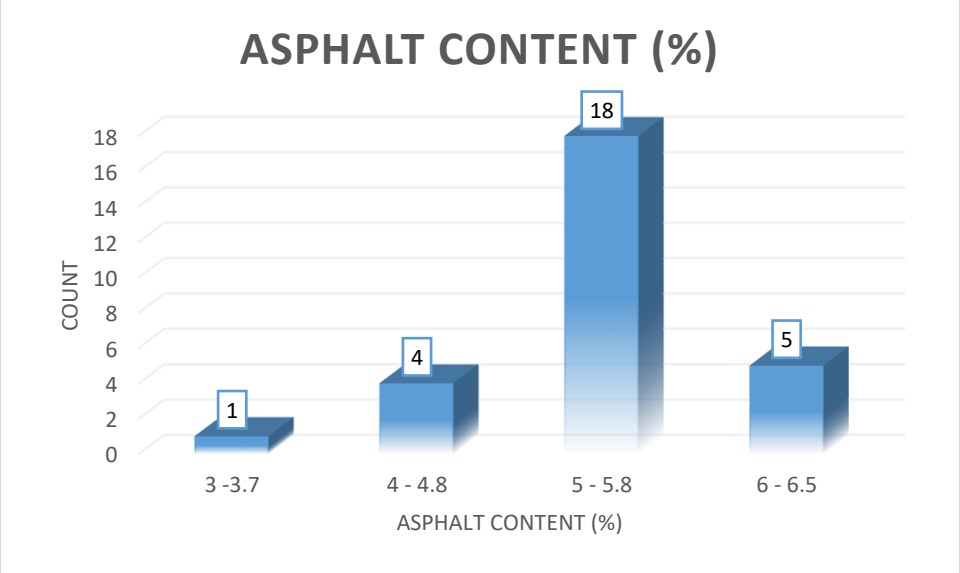


*Figure 23- LTPP Database Asphalt Content (%) Observations*

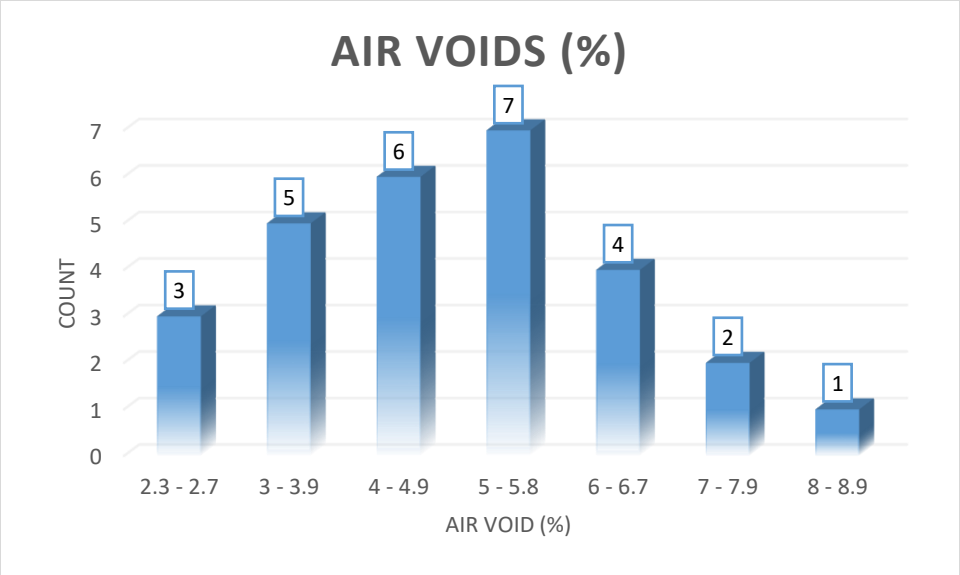


*Figure 24- LTPP Database Air Void Content (%) Observations*

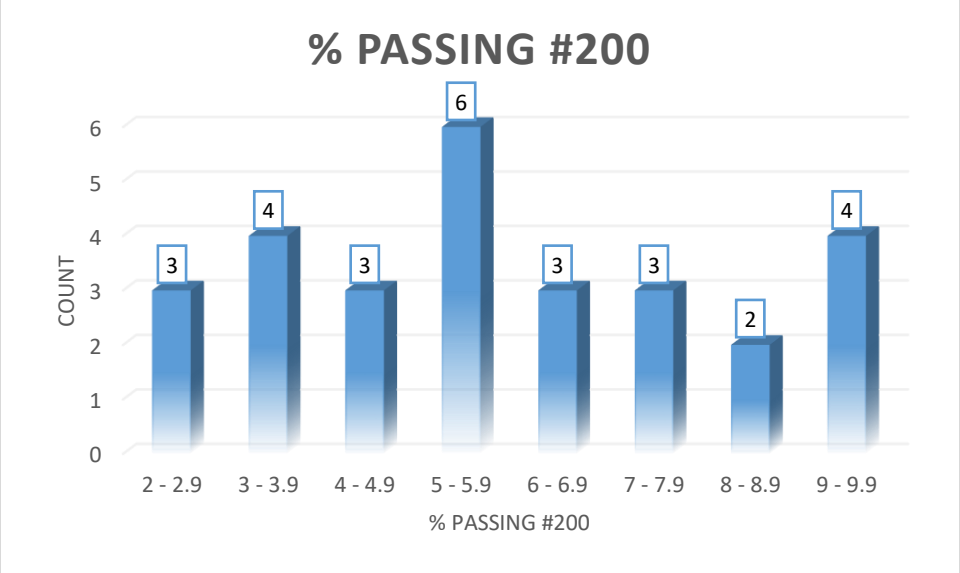


*Figure 25- LTPP Database %P200 Observations*

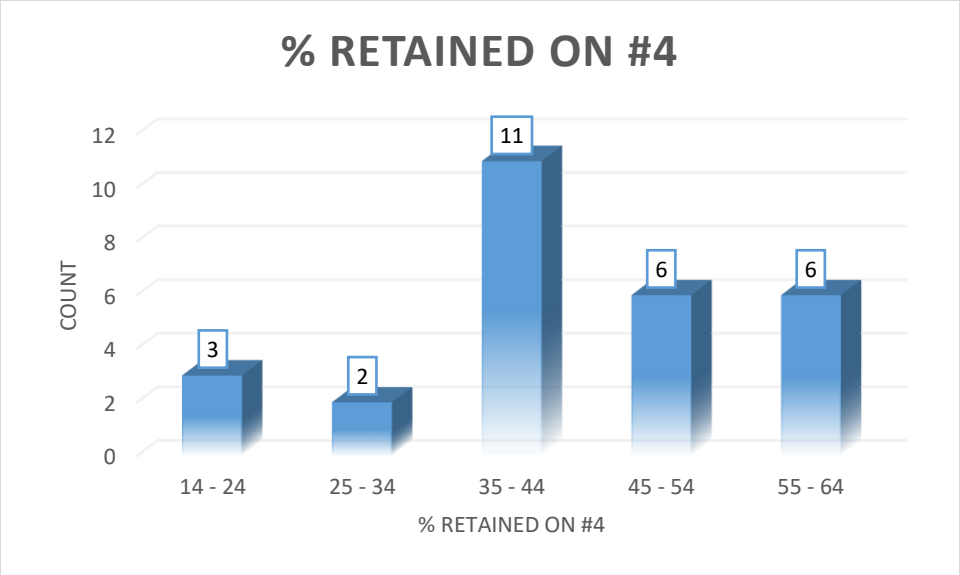


*Figure 26- LTPP Database %R04 Observations*

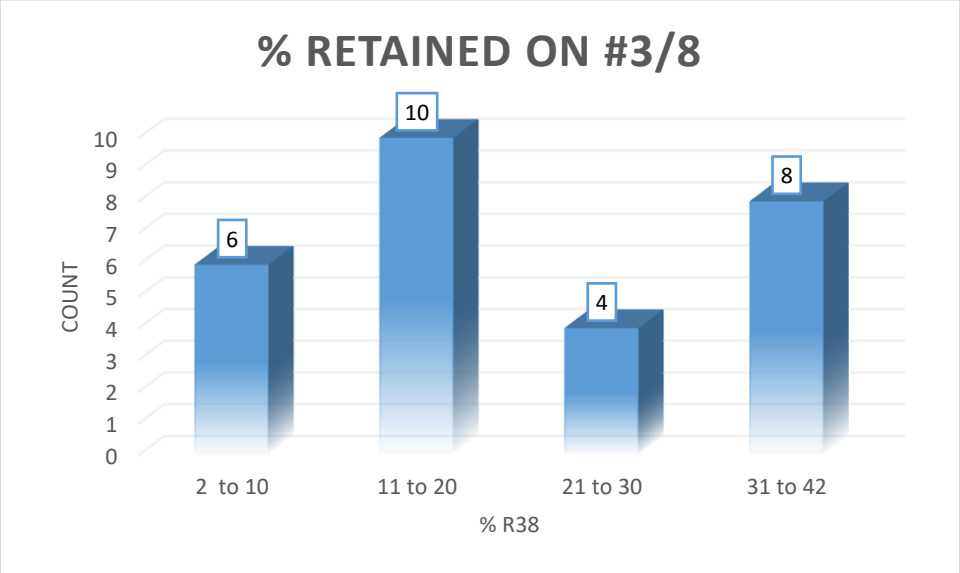


*Figure 27- LTPP Database % Retained on #3/8 Observations*

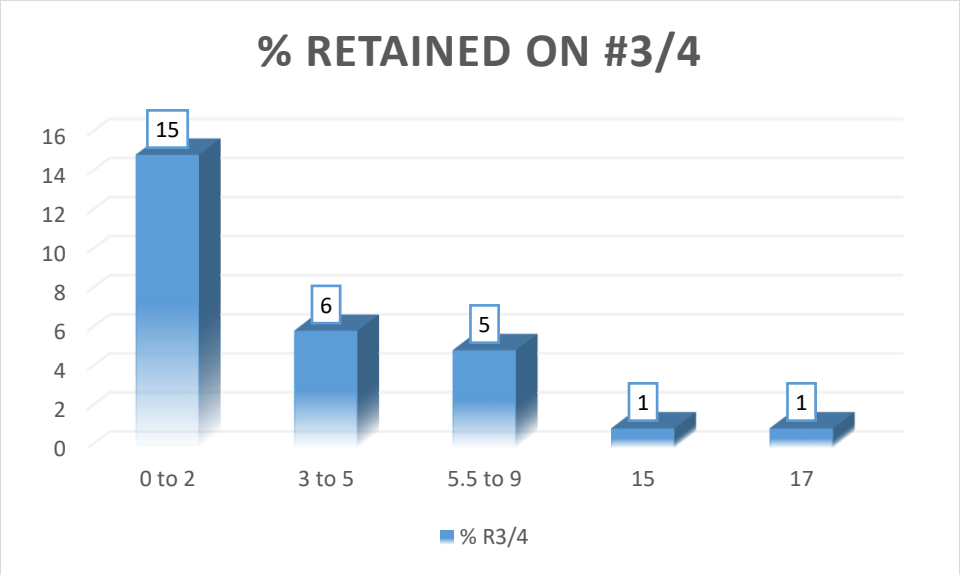


*Figure 28- LTPP Database % Retained on #3/4 Observations*

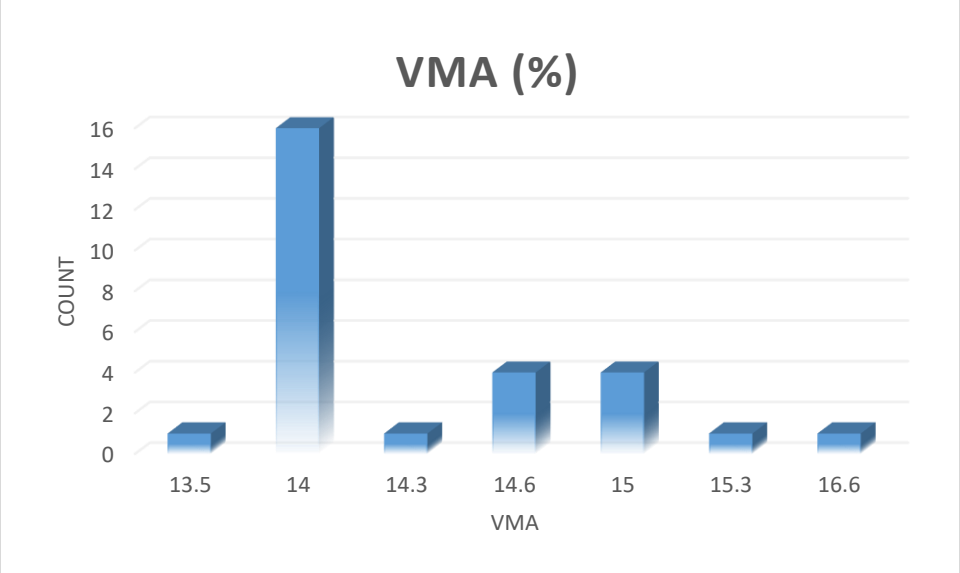


*Figure 29- LTPP Database of VMA (%) Ranges*

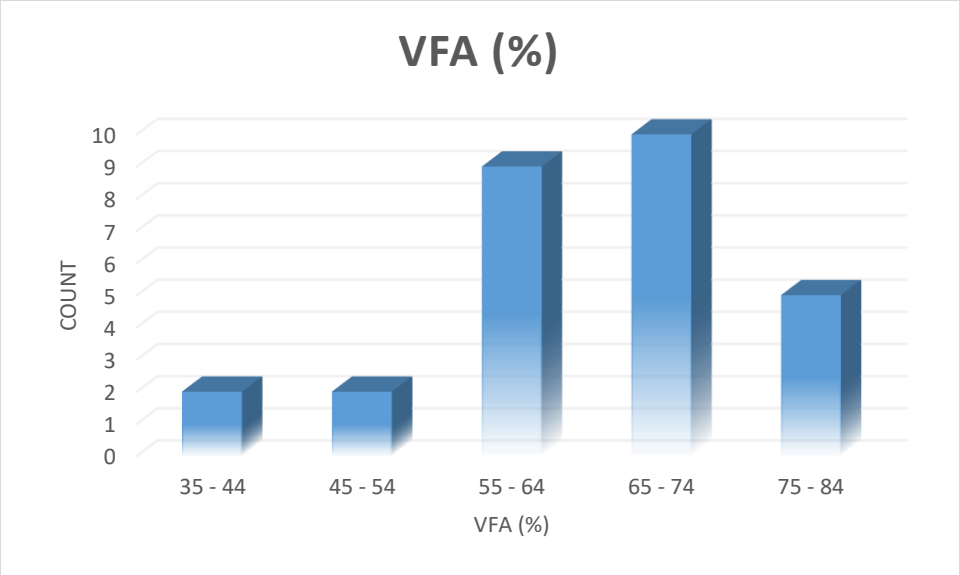


*Figure 30- LTPP Database of VFA (%) Ranges*

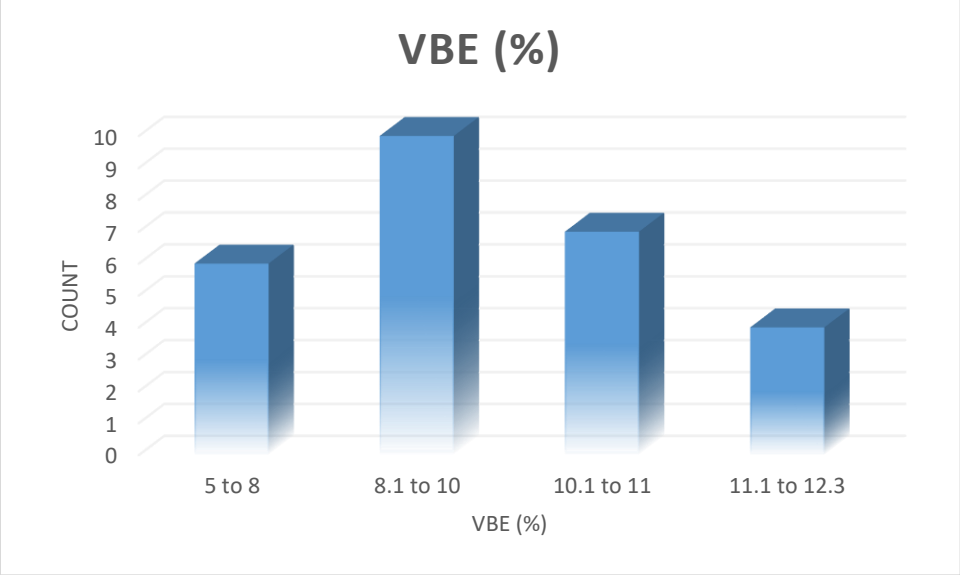


*Figure 31- LTPP Database VBE (%) Ranges*

Having this gathered database on hand, the development of the needed variables for the models is found in detail in the following sections of the chapter. The first step was to develop the Rutting Depth based on the Flow Number Predictive Model (Refer to 3.2 and 0).

4.3.Generation of the Rutting Depth

4.3.a. Calculation of the Effective Rutting Temperature

The Effective Temperature is the temperature at which the specimen is going to accumulate the same amount of damage in the laboratory testing as if it is located according to the different climate changes in the field (as defined in section 0)

In this project, it is also the temperature at which the predicted rutting (or permanent pavement deformation) will occur according to the different climate conditions. The formula is inserted below for ease.

El Basyouny and Jeong (2008) (47) developed the following formula, depending on the climatic conditions of each section chosen:

- $T_{eff} = 14.62 - 3.36 \times \ln(Freq) - 10.94 \times z + 1.121 \times MAAT + 1.718 \times (\sigma_{MMAT}) - 0.431 \times Wind + 0.333 \times Sunshine + 0.08 \times Rain$

Where:

Freq is the Driving Frequency, taken to be 18 Hz in case of Highways

z is the depth at which $T_{eff}$ is measured to be critical, which is 2 in from the surface in this study

MAAT is the Mean Annual Temperature, calculated based on the location

$\sigma_{MMAT}$ is the standard deviation for the Monthly Average Temperature based on the location

Wind is the mean annual wind speed in mph

Sunshine is the mean annual sunshine in percentage

Rain is the cumulative annual rainfall depth, in inches

This temperature is the Effective Rutting Temperature, at which the pavement will accumulate permanent deformation at a critical depth. The first step is to calculate the MAAT for the different regions under study. For this reason, the monthly highest and lowest temperatures were gathered from online sources such as “U.S. Climate Data”. Once the monthly data is gathered, the average of the high temperature and the average of low temperature is found. Then, the average of both values is found, which is the MAAT needed.

The standard deviation of the monthly average temperature is also found using the gathered data. In addition, the mean annual wind speed, sunshine percentage and the cumulative rainfall depth were recorded. A sample of the data gathered is found below in Table 6:

*Table 6- Data Collected for the Calculation of Effective Temperature in Phoenix, Arizona*

| **Phoenix/ Months** | **1** | **2** | **3** | **4** | **5** | **6** | **7** | **8** | **9** | **10** | **11** | **12** |
|---|---|---|---|---|---|---|---|---|---|---|---|---|
| **Average high in °F:** | 67 | 71 | 77 | 85 | 95 | 104 | 106 | 104 | 100 | 89 | 76 | 66 |
| **Average low in °F:** | 46 | 49 | 53 | 60 | 69 | 78 | 83 | 83 | 77 | 65 | 53 | 45 |
| **Avg T /month** | 56.5 | 60 | 65 | 72.5 | 82 | 91 | 94.5 | 93.5 | 88.5 | 77 | 64.5 | 55.5 |
| **Avg. Precipitation (in)** | 0.91 | 0.91 | 0.98 | 0.28 | 0.12 | 0.04 | 1.06 | 0.98 | 0.63 | 0.59 | 0.67 | 0.87 |
| **Cum. Precipitation (in)** | 0.91 | 1.82 | 2.8 | 3.08 | 3.2 | 3.24 | 4.3 | 5.28 | 5.91 | 6.5 | 7.17 | 8.04 |
| **Wind speed (mph)** | 7 | 6.8 | 6.9 | 7.5 | 7.3 | 7.2 | 6.4 | 5.7 | 6.3 | 6.6 | 6.8 | 7 |
| **Sunshine % per year** | 57.8 | | | | | | | | | | | |

The MAAT is found to be equal to 75$^{o}$F, the standard deviation of the mean monthly average temperature is 14.7 and the sunshine percentage per year is the number of sunny days divided by 365. Finally, the Effective Rutting Temperature is found to be equal to 129$^{o}$F.

The same analysis is done for all the states under study and different cities within each state. Since different climate is expected in the cities chosen, the MAAT and Effective Rutting Temperatures are summarized in the Table 7:

*Table 7- Effective Rutting Temperature for States under Study*

| State | City | Section Number | MAAT (°F) | Effective Rutting T (°F) |
|---|---|---|---|---|
| **Alabama** | *Montgomery* | 4125 | 65 | 120 |
| | *Tuscaloosa* | 6012 | 65 | 104 |
| **Arizona** | *Tucson* | 6054 | 72 | 123 |
| | *Phoenix* | B961 | 75 | 130 |
| | *Flagstaff* | 669 | 46 | 92 |
| | *Kingman* | 1022 | 61 | 121 |
| **Alaska** | *Anchorage* | 1004 | 36 | 84 |
| **Arkansas** | *Little Rock* | A606 | 63 | 121 |
| **Colorado** | *Rio Blanco* | 1053 | 47 | 97 |
| | *El Paso* | 7783 | 76 | 113 |
| | *Yuma* | 502 | 51 | 105 |
| **Indiana** | *La Porte* | 5528 | 50 | 104 |
| | *Jackson* | A902 | 53 | 110 |
| | *Jefferson* | 18-1028 | 56 | 112 |
| **Kansas** | *Cherokee* | 1005 | 57 | 116 |
| | *Scott* | 1006 | 52 | 113 |
| **Massachusetts** | *Boston* | 1003 | 51 | 105 |
| | *Springfield* | 1002 | 51 | 108 |
| **Michigan** | *Port Huron* | D330 | 65 | 103 |
| | *Alpena* | 6016 | 44 | 97 |
| | *Marquette* | 1004 | 44 | 96 |
| | *Grand Rapids* | 901 | 49 | 102 |
| **South Carolina** | *Columbia/Lexington* | 1024 | 64 | 121 |
| **Tennessee** | *Memphis* | 3109 | 63 | 121 |
| **Washington** | *Seattle* | 6049 | 53 | 95 |
| | *Spokane* | A320 | 48 | 98 |
| **West Virginia** | *Kanawha* | 1640 | 53 | 109 |
| | *Charleston* | 7008 | 56 | 110 |

The following graph shows the values obtained for the effective rutting temperatures for the different states considered:

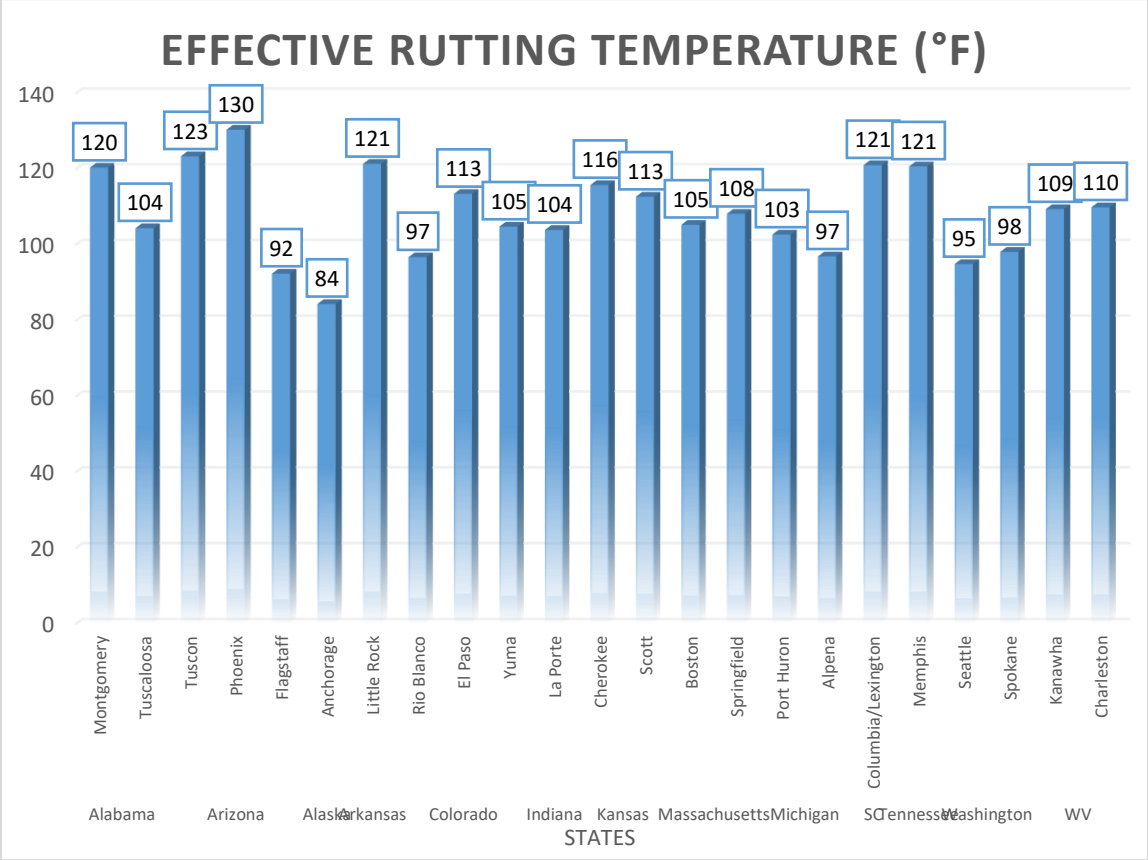


*Figure 32- Effective Rutting Temperature (F) Calculations*

4.3.b. Calculation of the Viscosity at Effective Rutting Temperature

The viscosity (V1 in Poise) is the second needed input in order to find the Flow Number values based on the flow number predictive model (Refer to Chapter 3 Section b).

The viscosity is calculated based on the "$A_i$" and "$VTS_i$" values respective to each PG-Binder of the mix designs. The "Ai" and "VTSi" values are obtained from the LTPP website and are regression coefficients or the intercept and the slope of the viscosity-temperature relationship. Also, the same values are inputted into the MEPDG Software to

compute the viscosity of the binder. The Table 8 below shows the typical “Ai” and “VTSi” values for each binder:

*Table 8- Typical "Ai" and "VTSi" values*

| Asphalt Binder Grade | A | VTS | Asphalt Binder Grade | A | VTS |
|---|---|---|---|---|---|
| **PG 46-34** | 11.504 | -3.901 | **PG 70-28** | 9.715 | -3.217 |
| **PG 46-40** | 10.101 | -3.393 | **PG 70-34** | 8.965 | -2.948 |
| **PG 46-46** | 8.755 | -2.905 | **PG 70-40** | 8.129 | -2.648 |
| **PG 52-10** | 13.386 | -4.57 | **PG 76-10** | 10.059 | -3.331 |
| **PG 52-16** | 13.305 | -4.541 | **PG 76-16** | 10.015 | -3.315 |
| **PG 52-22** | 12.755 | -4.342 | **PG 76-22** | 9.715 | -3.208 |
| **PG 52-28** | 11.84 | -4.012 | **PG 76-28** | 9.2 | -3.024 |
| **PG 52-34** | 10.707 | -3.602 | **PG 76-34** | 8.532 | -2.785 |
| **PG 52-40** | 9.496 | -3.164 | **PG 82-10** | 9.514 | -3.128 |
| **PG 52-46** | 8.31 | -2.736 | **PG 82-16** | 9.475 | -3.114 |
| **PG 58-10** | 12.316 | -4.172 | **PG 82-22** | 9.209 | -3.019 |
| **PG 58-16** | 12.248 | -4.147 | **PG 82-28** | 8.75 | -2.856 |
| **PG 58-22** | 11.787 | -3.981 | **PG 82-34** | 8.151 | -2.642 |
| **PG 58-28** | 11.01 | -3.701 | **AC-2,5** | 11.5167 | -3.89 |
| **PG 58-34** | 10.035 | -3.35 | **AC-5** | 11.2614 | -3.7914 |
| **PG 58-40** | 8.976 | -2.968 | **AC-10** | 11.0134 | -3.6454 |
| **PG 64-10** | 11.432 | -3.842 | **AC-20** | 10.7709 | -3.6017 |
| **PG 64-16** | 11.375 | -3.822 | **AC-3** | 10.6316 | -3.548 |
| **PG 64-22** | 10.98 | -3.68 | **AC-40** | 10.5338 | -3.5104 |
| **PG 64-28** | 10.312 | -3.44 | **PEN 40-50** | 10.5254 | -3.5047 |
| **PG 64-34** | 9.461 | -3.134 | **PEN 60-70** | 10.6508 | -3.5537 |
| **PG 64-40** | 8.524 | -2.798 | **PEN 85-100** | 11.8232 | -3.621 |
| **PG 70-10** | 10.69 | -3.566 | **PEN 120-150** | 11.0897 | -3.7252 |
| **PG 70-16** | 10.641 | -3.548 | **PEN 200-300** | 11.8107 | -4.0068 |
| **PG 70-22** | 10.299 | -3.426 | **-** | - | - |

Once the “$A_i$” and “$VTS_i$” values are gathered with respect to the PG-Binder needed, the viscosity of the binder at the effective rutting temperature following the equation below:

$$loglog(\eta) = A_i + VTS_i \log(T_R)$$

Where η is the viscosity in Centipoise (cP) and $T_R$ is the effective rutting temperature in Rankine.

A summary of the data needed for this formula is included below in Table 9:

*Table 9- Calculation of V1 in Poise*

| State | City | Section | PG | A | VTS | V1 (P) |
|---|---|---|---|---|---|---|
| **Alabama** | *Montgomery* | 4125 | 64-16 | 11.38 | -3.82 | 3.52E+04 |
| | *Tuscaloosa* | 6012 | 64-16 | 11.38 | -3.82 | 1.94E+05 |
| **Arizona** | *Tucson* | 6054 | 70-10 | 10.69 | -3.57 | 5.82E+04 |
| | *Phoenix* | B961 | 76-10 | 10.06 | -3.33 | 6.14E+04 |
| | *Flagstaff* | 669 | 58-28 | 11.01 | -3.70 | 2.13E+05 |
| | *Kingman* | 1022 | 70-16 | 10.64 | -3.55 | 7.25E+04 |
| **Alaska** | *Anchorage* | 1004 | 46-40 | 10.10 | -3.39 | 4.31E+04 |
| **Arkansas** | *Little Rock* | A606 | 64-16 | 11.38 | -3.82 | 3.19E+04 |
| **Colorado** | *Rio Blanco* | 1053 | 46-34 | 11.50 | -3.90 | 1.88E+04 |
| | *El Paso* | 7783 | 58-28 | 11.01 | -3.70 | 2.39E+04 |
| | *Yuma* | 502 | 64-28 | 10.31 | -3.44 | 1.16E+05 |
| **Indiana** | *La Porte* | 5528 | 58-28 | 11.01 | -3.70 | 6.11E+04 |
| | *Jackson* | A902 | 58-28 | 11.01 | -3.70 | 3.35E+04 |
| | *Jefferson* | 18-1028 | 58-28 | 11.01 | -3.70 | 2.79E+04 |
| **Kansas** | *Cherokee* | 1005 | 64-22 | 10.98 | -3.68 | 5.01E+04 |
| | *Scott* | 1006 | 64-28 | 10.31 | -3.44 | 5.42E+04 |
| **Massachusetts** | *Boston* | 1003 | 58-22 | 11.79 | -3.98 | 6.77E+04 |
| | *Springfield* | 1002 | 58-28 | 11.01 | -3.70 | 3.98E+04 |
| **Michigan** | *Port Huron* | D330 | 58-28 | 11.01 | -3.70 | 6.94E+04 |
| | *Alpena* | 6016 | 52-28 | 11.84 | -4.01 | 5.39E+04 |
| | *Marquette* | 1004 | 52-28 | 11.84 | -4.01 | 5.70E+04 |
| | *Grand Rapids* | 901 | 58-34 | 10.04 | -3.35 | 5.14E+04 |
| **South Carolina** | *Columbia/Lexington* | 1024 | 64-16 | 11.38 | -3.82 | 3.30E+04 |
| **Tennessee** | *Memphis* | 3109 | 64-22 | 10.98 | -3.68 | 3.11E+04 |
| **Washington** | *Seattle* | 6049 | 52-16 | 13.31 | -4.54 | 1.13E+05 |
| | *Spokane* | A320 | 58-28 | 11.01 | -3.70 | 1.13E+05 |
| **West Virginia** | *Kanawha* | 1640 | 64-22 | 10.98 | -3.68 | 9.56E+04 |
| | *Charleston* | 7008 | 64-22 | 10.98 | -3.68 | 9.09E+04 |

4.3.c. Calculation of the Predicted Flow Number

Having these values at hand, the flow number of each region was predicted, followed by the estimate (predicted) rutting depth. A summary of all the data gathered is found in Appendix A, Table 54 .

As mentioned in Chapter 3 (Section b), the flow number is calculated for a fixed value of the deviator stress of 100 psi and 20 psi confinement. This will represent the typical tire load of 120 psi on the pavement structure.

The following flow number values were generated for each city based on the following model (Table 10):

$$\log FN = 0.485 + 0.644 \times \log(V_1) + 0.0874 \times P_{200} - 3.323 \times \log p + 0.0129 \times R_{04} - 0.0803 \times V_a + 2.593 \times \log q - 0.0142 \times R_{34}$$

*Table 10- LTPP Database Predicted Flow Number*

| State | City | Section Number | Flow Number |
|---|---|---|---|
| **Alabama** | *Montgomery* | 4125 | 124 |
| | *Tuscaloosa* | 6012 | 711 |
| **Arizona** | *Tucson* | 6054 | 424 |
| | *Phoenix* | B961 | 214 |
| | *Flagstaff* | 669 | 642 |
| | *Kingman* | 1022 | 424 |
| **Alaska** | *Anchorage* | 1004 | 332 |
| **Arkansas** | *Little Rock* | A606 | 633 |
| **Colorado** | *Rio Blanco* | 1053 | 402 |
| | *El Paso* | 7783 | 353 |
| | *Yuma* | 502 | 463 |
| **Indiana** | *La Porte* | 5528 | 238 |
| | *Jackson* | A902 | 360 |
| | *Jefferson* | 18-1028 | 203 |
| **Kansas** | *Cherokee* | 1005 | 306 |
| | *Scott* | 1006 | 590 |
| **Massachusetts** | *Boston* | 1003 | 306 |
| | *Springfield* | 1002 | 139 |
| **Michigan** | *Port Huron* | D330 | 190 |
| | *Alpena* | 6016 | 309 |
| | *Marquette* | 1004 | 167 |
| | *Grand Rapids* | 901 | 649 |
| **South Carolina** | *Columbia/Lexington* | 1024 | 56 |
| **Tennessee** | *Memphis* | 3109 | 159 |
| **Washington** | *Seattle* | 6049 | 185 |
| | *Spokane* | A320 | 295 |
| **West Virginia** | *Kanawha* | 1640 | 151 |
| | *Charleston* | 7008 | 165 |

### 4.3.d. Calculation of the Traffic Level

The next step involves calculating the traffic level applied on each pavement structure. The LTPP Database has recorded the traffic level according to the functional classification of the road segment, truck factor, truck percentage, and growth factor. The recorded data has been carried on an annual basis. For this reason, considering 20 years of approximate pavement life, the number of ESALs (Equivalent Single Axle Load) applied on the road section was simply taken to be the summation of the yearly measurements over the last 20 years. In order to have accurate results, the ESALs were counted up to 20 years before the last rutting measurement was made. This means that the number of axles recorded 20 years prior to the rutting reading, were the actual traffic impacting the road segment in terms of permanent deformation. The following Table 11 summarizes the number of ESALs measured for the period of 20 years as per the LTPP traffic count and measurements:

*Table 11- LTPP Database Measured ESALs*

| State | City | Section Number | Measured ESALs |
|---|---|---|---|
| Alabama | *Montgomery* | 4125 | 6,125,491 |
| | *Tuscaloosa* | 6012 | 28,635,775 |
| Arizona | *Tucson* | 6054 | 6,790,044 |
| | *Phoenix* | B961 | 54,626,332 |
| | *Flagstaff* | 669 | 54,832,475 |
| | *Kingman* | 1022 | 30,809,129 |
| Alaska | *Anchorage* | 1004 | 2,839,318 |
| Arkansas | *Little Rock* | A606 | 20,420,809 |
| Colorado | *Rio Blanco* | 1053 | 2,143,699 |
| | *El Paso* | 7783 | 11,327,852 |
| | *Yuma* | 502 | 10,759,236 |
| Indiana | *La Porte* | 5528 | 5,967,296 |
| | *Jackson* | A902 | 82,299,713 |
| | *Jefferson* | 18-1028 | 18,354,638 |
| Kansas | *Cherokee* | 1005 | 1,065,225 |
| | *Scott* | 1006 | 1,174,183 |
| Massachusetts | *Boston* | 1003 | 654,719 |
| | *Springfield* | 1002 | 5,276,055 |
| Michigan | *Port Huron* | D330 | 1,669,321 |
| | *Alpena* | 6016 | 3,090,930 |
| | *Marquette* | 1004 | 1,330,708 |
| | *Grand Rapids* | 901 | 35,264,543 |
| South Carolina | *Columbia/Lexington* | 1024 | 26,048 |
| Tennessee | *Memphis* | 3109 | 2,376,525 |
| Washington | *Seattle* | 6049 | 6,541,155 |
| | *Spokane* | A320 | 957,197 |
| West Virginia | *Kanawha* | 1640 | 15,242,141 |
| | *Charleston* | 7008 | 40,565,999 |

4.3.e. Estimation of the Rutting Depth

All the required input has been set into an Excel file, where only the pavement mixture's volumetrics are required, as well as the estimated traffic and the asphalt layer's thickness. The rutting depth has been predicted based on the following equation, as mentioned in Section 0:

$$R = 0.00462 \times FN^{-0.242} \times ESALs^{0.483} \times h^{-1.021}$$

Where FN is the predicted Flow Number

ESALs is the number of single axle load repetitions

h is the asphalt layer thickness (in)

Since the asphalt layer thickness is also recorded for each section, the rutting depth was predicted, and the following results were obtained in Table 12:

*Table 12- Predicted Rutting*

| State | City | Section | Climate Zone | Flow Number | Measured ESAL | Asphalt Thickness (in) | Predicted Rutting (in) |
|---|---|---|---|---|---|---|---|
| **AL** | Montgomery | 4125 | W, NF | 124 | 6.13E+06 | 6 | 0.458 |
| | Tuscaloosa | 6012 | W, NF | 711 | 2.86E+07 | 5 | 0.760 |
| **AZ** | Tucson | 6054 | D, NF | 424 | 6.79E+06 | 9 | 0.236 |
| | Phoenix | B961 | D, NF | 214 | 5.46E+07 | 10 | 0.684 |
| | Flagstaff | 669 | D, F | 642 | 5.48E+07 | 6 | 0.885 |
| | Kingman | 1022 | D, NF | 424 | 3.08E+07 | 8.5 | 0.519 |
| **AK** | Anchorage | 1004 | D, F | 332 | 2.84E+06 | 5.4 | 0.277 |
| **AR** | Little Rock | A606 | W, NF | 633 | 2.04E+07 | 5 | 0.664 |
| **CO** | Rio Blanco | 1053 | D, F | 402 | 2.14E+06 | 6.8 | 0.182 |
| | El Paso | 7783 | D, F | 353 | 1.13E+07 | 9.7 | 0.293 |
| | Yuma | 502 | D, F | 463 | 1.08E+07 | 9.3 | 0.279 |
| **IN** | La Porte | 5528 | W, F | 238 | 5.97E+06 | 7.2 | 0.320 |
| | Jackson | A902 | W, F | 360 | 8.23E+07 | 6.8 | 1.090 |
| | Jefferson | 18-1028 | W, NF | 203 | 1.84E+07 | 18 | 0.224 |
| **KS** | Cherokee | 1005 | W, F | 306 | 1.07E+06 | 12.7 | 0.073 |
| | Scott | 1006 | W, NF | 590 | 1.17E+06 | 14 | 0.059 |
| **MS** | Boston | 1003 | W, F | 306 | 6.55E+05 | 6.6 | 0.113 |
| | Springfield | 1002 | W, F | 139 | 5.28E+06 | 7.8 | 0.316 |
| **MI** | Port Huron | D330 | W, F | 190 | 1.67E+06 | 2.2 | 0.613 |
| | Alpena | 6016 | W, F | 309 | 3.09E+06 | 4.6 | 0.346 |
| | Marquette | 1004 | W, F | 167 | 1.33E+06 | 4.2 | 0.293 |
| | Grand Rapids | 901 | W, F | 649 | 3.53E+07 | 8.6 | 0.494 |
| **SC** | Columbia | 1024 | W, NF | 56 | 2.60E+04 | 1.6 | 0.153 |
| **TN** | Memphis | 3109 | W, NF | 159 | 2.38E+06 | 7 | 0.233 |
| **WA** | Seattle | 6049 | W, NF | 185 | 6.54E+06 | 10.6 | 0.240 |
| | Spokane | A320 | D, F | 295 | 9.57E+05 | 2.7 | 0.342 |
| **WV** | Kanawha | 1640 | W, F | 151 | 1.52E+07 | 2.5 | 1.654 |
| | Charleston | 7008 | W, NF | 165 | 4.06E+07 | 3.9 | 1.650 |

4.3.f. Comparing the Predicted vs Measured Rutting Values

As mentioned previously in the Background Section, there are many performance indicators on how well the pavement is performing. These indicators include the visible distresses, the structural response, surface friction and roughness/serviceability of the

pavement. These indicators are classified either as Functional of Structural. The following Table 13 shows the difference in these indicators (FHWA Reference Manual, 2001):

*Table 13- Asphalt Pavement Performance Indicators*

| Performance Indicators | Functional | Structural |
|---|---|---|
| **Distress** | ✓ | ✓ |
| **Structural Response** | | ✓ |
| **Surface Friction** | ✓ | |
| **Roughness/Serviceability** | ✓ | |

Concerning Rutting, it is referred to as the permanent deformation due to the accumulation of small amounts of wheel loads leading to a significant depression of the pavement surface. It happens in the wheel paths, and the main problem associated to it happens during wet seasons. It increases the likelihood of vehicle accidents associated with hydroplaning.

Several factors affect the presence of permanent deformation and its location:

If it is only present in the surface, one or a combination of the following could be the reason:

- The HMA surface layer was overloaded
- The HMA layer was soft during a hot climate period and is affected by traffic loading

- The mix is unstable
- The asphalt is very temperature susceptible

If the rutting exists only in the base/subbase, different explanations exist:

- The surface layer is too thin
- The aggregates in the base/subbase were inadequately designed
- The layers were exposed to long periods of moisture

If the permanent deformation reached the subgrade, it means that the whole pavement structure is too thin to handle the applied loads or that the natural soil underneath is weak. The soil may have high moisture content generally.

In the case of the LTPP Database, the rutting has been measured only for the surface layer of the HMA pavement structure. Permanent Deformation may have happened in the layers underneath, however such information is not provided. In addition, the predictive models implemented in this study only cover the permanent deformation accumulated in the surface layer over the expected traffic and pavement life of the structure.

After having the results shown in the previous section 4.3.e, the predicted vs measured rutting values are plotted in Figure 33:

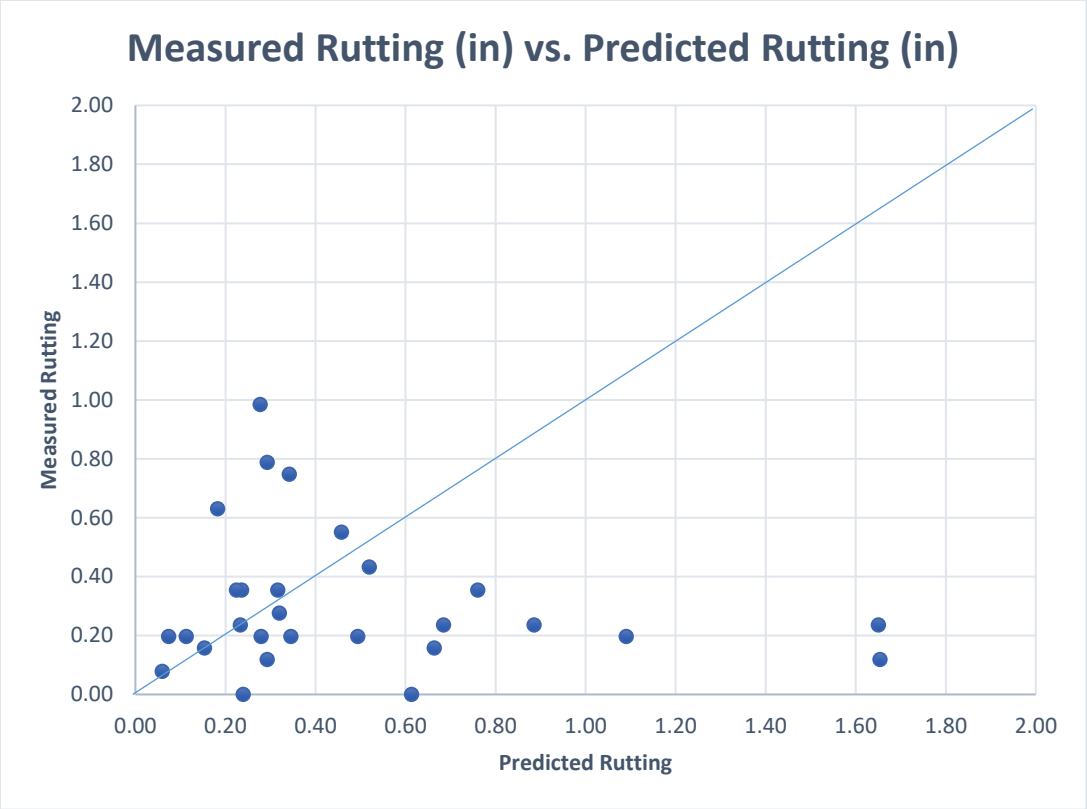


*Figure 33- Predicted vs Measured Rutting Values (in)*

The rutting values were predicted based on the measured ESAL values as well as the recorded Asphalt Thickness of the surface layer. It can be seen from the graph above that the values are widespread. However, for low values of rutting, the prediction seems to be more accurate than for highest values. In other words, for Flow number values less than 5,000 cycles, the predicted rutting values seem to be closer than the measured ones.

It is also to be considered that the model had an initial $R^2$ of 0.84 and a ratio Se/Sy of 0.36. This shows that the model is good and should be accurate. However, uncertainty also lays in the measured values provided by the LTPP. This uncertainty depends on the quality of the aggregates, how the pavement was constr, as well as the

quality control of the construction and mix. In addition, the weather modifications exhibited also affects the performance of the pavement structure in terms of rutting.
All in all, the coefficients of variation of the measured and predicted rutting values were calculated. The coefficient of variation for the measured rutting values was found to be 77%, whereas the coefficient of variation of the predicted values was found to be equal to 80%. This shows a rather high variability in the data to start with.

It is to be also noted that this model was originally developed with a different set of data. Also, it is highly depending on another predictive model, which is the Flow Number Predictive Model discussed previously. Therefore, the results obtained in the graph above are reflective the high variability of the results.

The model was developed using certain samples back in 2010 by Rodezno (46). Now, the model is being tested out of time and out of sample. Overfitting the sample may have happened. The model may accommodate the data gathered upon the development of the model, and therefore may not fit the current data.
The data gathered may be different than the one used in 2010, and therefore may not be adequate to the model. This explains the high variance and the high dispersion in the graph. All in all, the following **Error! Reference source not found.** shows the behavior o f rutting with the Flow Number, measured ESALs and Asphalt Thickness:


*Figure 34- Rutting Comparison*

In general, rutting is bound to happen more frequently in Wet Areas, as well as with Freeze climate.

This behavior is reflected in the prediction of rutting, whereas it is more frequent and in higher number for the Dry Freeze, Wet Freeze and Wet Non-Freeze. The Figure 35 summarizes the results obtained per climatic regions having the predicted rutting according to the model used:

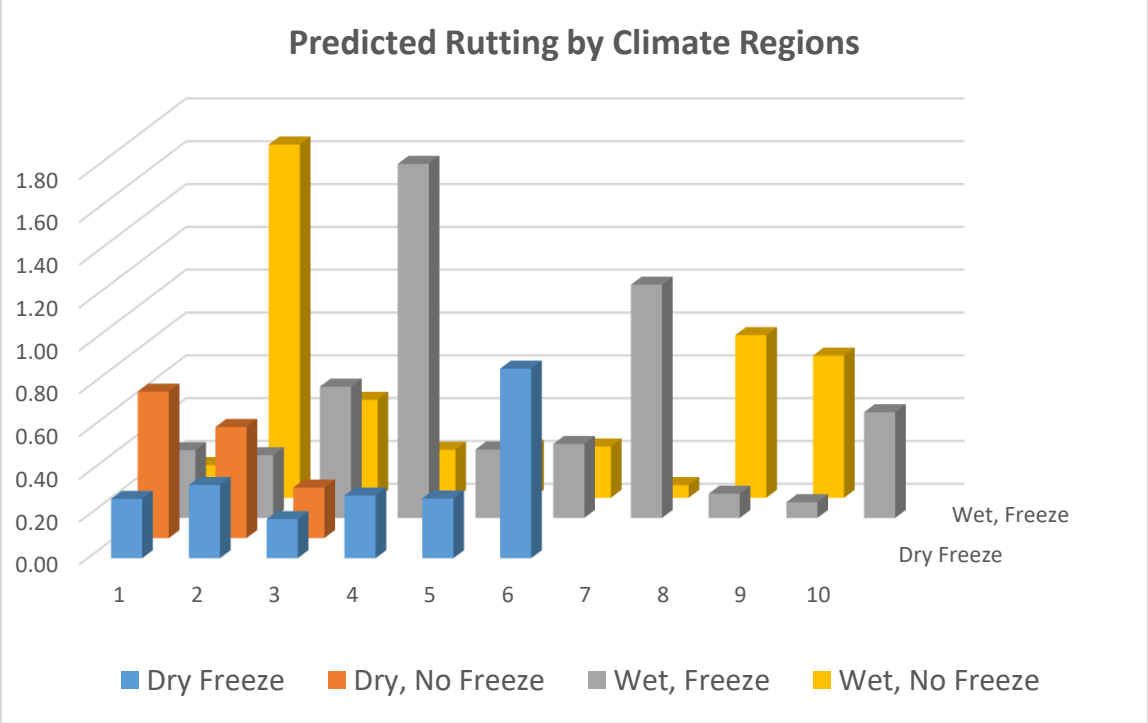


*Figure 35-Predicted Rutting per Climate Regions*

On average, the Dry, No Freeze region does expect some rutting, but in lower values than the other regions. The results coincide with the hypothesis. In addition, Rutting happen in bigger amount during freeze and thaw, where deformation is increasing.

All in all, the maximum rutting value predicted in the Dry Freeze is 0.52 inches, in the Dry Non-Freeze 0.34, in the Wet Non-Freeze, 0.60 inches and finally in the Wet Freeze 0.87 inches. The average rutting values per climatic region are found in Figure 36:

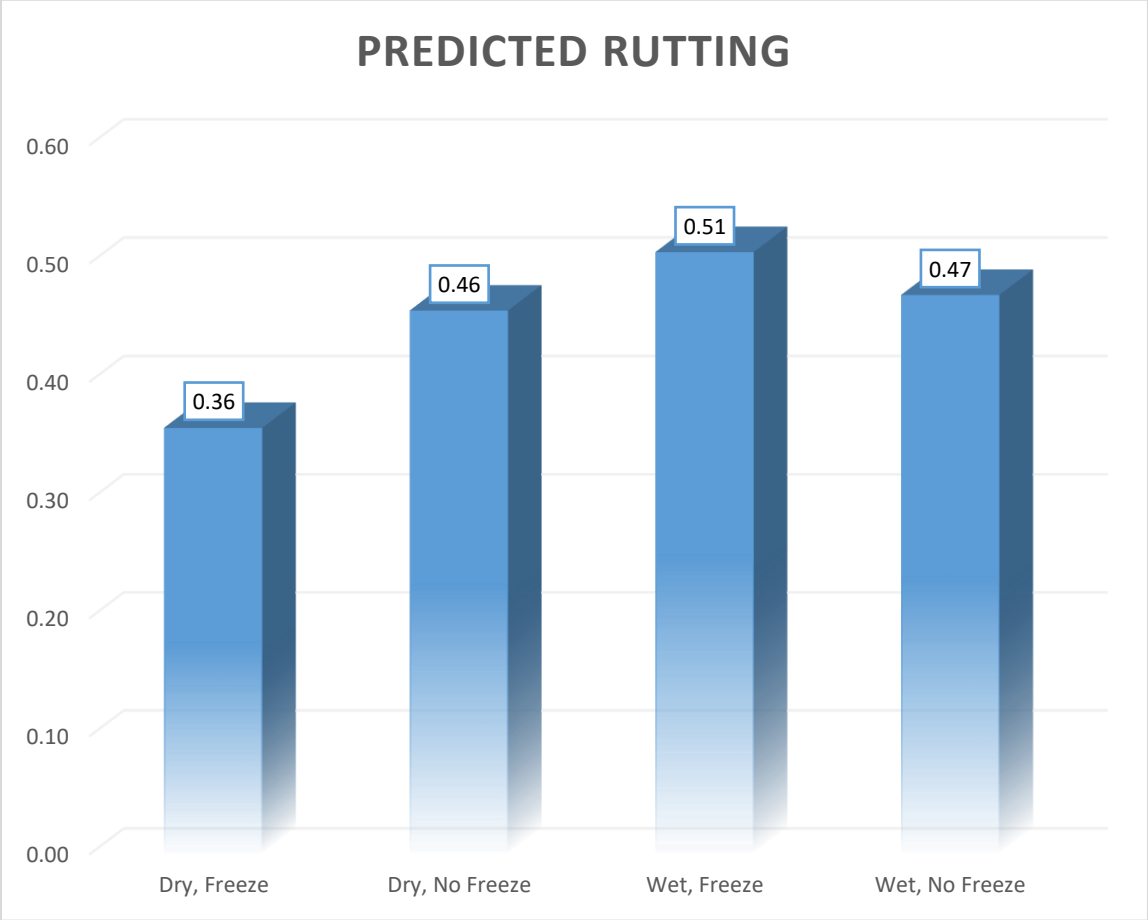


*Figure 36- Predicted Rutting per Climate Regions for the LTPP Database*

This graph shows that the predicted rutting for the sections is relatively the same for all the climatic regions, therefore no results can be concluded from this graph.

4.4.Generation of the Fatigue Behavior

In this section, the fatigue prediction is carried on based on the predictive model described in 3.4. This model specifically derives the number of cycles needed until failure, in other words, till the pavement structure reaches fatigue failure and a crack is

initiated. It is also referred to as the fatigue life at the maximum strain level. It has been derived by relating the fatigue life of the asphalt mixtures to the fatigue life of the asphalt binders. In order to proceed and generate the results needed, the following steps have been implemented.

4.4.a. Calculation of the Effective Fatigue Temperature

The first step is associated with developing the testing temperature at which fatigue is most likely to happen. According to AASHTO TP 107, the testing temperature is based on the PG of the binder as per the climatic region. The “Fatigue Temperature” is found by the averaging the high and low temperatures of the PG and deducting 3$^{o}$C from the total. The temperatures were found for the states into consideration and are listed below Table 14:

*Table 14- LTPP Database Effective Fatigue Temperature*

| State | City | Section Number | PG (LTTP Bind) | Effective Fatigue Temperature (°F) |
|---|---|---|---|---|
| **Alabama** | *Montgomery* | 4125 | 64-16 | 69.8 |
| | *Tuscaloosa* | 6012 | 64-16 | 69.8 |
| **Arizona** | *Tucson* | 6054 | 70-10 | 80.6 |
| | *Phoenix* | B961 | 76-10 | 86 |
| | *Flagstaff* | 669 | 58-28 | 53.6 |
| | *Kingman* | 1022 | 70-16 | 75.2 |
| **Alaska** | *Anchorage* | 1004 | 46-40 | 32 |
| **Arkansas** | *Little Rock* | A606 | 64-16 | 69.8 |
| **Colorado** | *Rio Blanco* | 1053 | 46-34 | 37.4 |
| | *El Paso* | 7783 | 58-28 | 53.6 |
| | *Yuma* | 502 | 64-28 | 59 |
| **Indiana** | *La Porte* | 5528 | 58-28 | 53.6 |
| | *Jackson* | A902 | 58-28 | 53.6 |
| | *Jefferson* | 18-1028 | 58-28 | 53.6 |
| **Kansas** | *Cherokee* | 1005 | 64-22 | 64.4 |
| | *Scott* | 1006 | 64-28 | 59 |
| **Massachusetts** | *Boston* | 1003 | 58-22 | 64.4 |
| | *Springfield* | 1002 | 58-28 | 53.6 |
| **Michigan** | *Port Huron* | D330 | 58-28 | 53.6 |
| | *Alpena* | 6016 | 52-28 | 48.2 |
| | *Marquette* | 1004 | 52-28 | 48.2 |
| | *Grand Rapids* | 901 | 58-34 | 48.2 |
| **South Carolina** | *Columbia* | 1024 | 64-16 | 69.8 |
| **Tennessee** | *Memphis* | 3109 | 64-22 | 64.4 |
| **Washington** | *Seattle* | 6049 | 52-16 | 59 |
| | *Spokane* | A320 | 58-28 | 53.6 |
| **West Virginia** | *Kanawha* | 1640 | 64-22 | 64.4 |
| | *Charleston* | 7008 | 64-22 | 64.4 |

The effective temperatures found are plotted on the Figure 37 below, to show the variation of the obtained values:

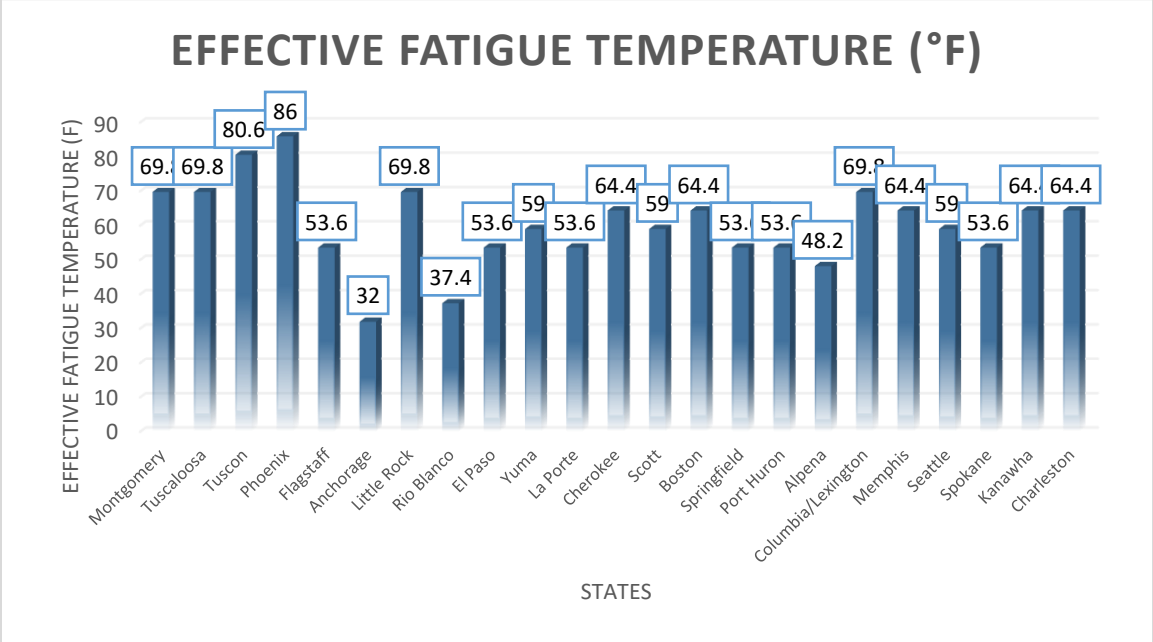


*Figure 37- Effective Fatigue Temperature (°F) Calculation*

Once the Effective Temperature at which fatigue is happening, i.e., testing temperature, the next step involves calculating the viscosity at the specific temperatures for each PG-binder.

4.4.b. Calculation of the Asphalt Binder Viscosity at Specific Temperature and Frequency

According to the equation below, the viscosity is calculated based on the "Ai" and "VTSi", as well as the Effective Temperature in Rankine, and the loading frequency. In this case, the frequency "f" is equal to 10 Hz for all cases:

$$loglog\ \eta_{s,T} = 0.9699 f_s^{-0.0527} * A + 0.9668 f_s^{-0.0575} * VTSlogT_R$$

This formula allows to find the viscosity at test temperature (°F) and frequency (Hz) in centipoise (cP) in Table 15.

*Table 15- LTPP Database Viscosity Calculation of the LTPP Database*

| State | City | Section | PG (LTTP Bind) | A | VTS | Effective Fatigue T. (°R) | η (cP) |
|---|---|---|---|---|---|---|---|
| **Alabama** | *Montgomery* | 4125 | 64-16 | 11.38 | -3.82 | 529.47 | 1.04E+09 |
| | *Tuscaloosa* | 6012 | 64-16 | 11.38 | -3.82 | 529.47 | 1.04E+09 |
| **Arizona** | *Tucson* | 6054 | 70-10 | 10.69 | -3.57 | 540.27 | 3.36E+08 |
| | *Phoenix* | B961 | 76-10 | 10.06 | -3.33 | 545.67 | 2.11E+08 |
| | *Flagstaff* | 669 | 58-28 | 11.01 | -3.70 | 513.27 | 1.52E+09 |
| | *Kingman* | 1022 | 70-16 | 10.64 | -3.55 | 534.87 | 3.47E+08 |
| **Alaska** | *Anchorage* | 1004 | 46-40 | 10.10 | -3.39 | 491.67 | 5.82E+08 |
| **Arkansas** | *Little Rock* | A606 | 64-16 | 11.38 | -3.82 | 529.47 | 1.04E+09 |
| **Colorado** | *Rio Blanco* | 1053 | 46-34 | 11.50 | -3.90 | 497.07 | 2.66E+09 |
| | *El Paso* | 7783 | 58-28 | 11.01 | -3.70 | 513.27 | 1.52E+09 |
| | *Yuma* | 502 | 64-28 | 10.31 | -3.44 | 518.67 | 7.88E+08 |
| **Indiana** | *La Porte* | 5528 | 58-28 | 11.01 | -3.70 | 513.27 | 1.52E+09 |
| | *Jackson* | A902 | 58-28 | 11.01 | -3.70 | 513.27 | 1.52E+09 |
| | *Jefferson* | 18-1028 | 58-28 | 11.01 | -3.70 | 513.27 | 1.52E+09 |
| **Kansas** | *Cherokee* | 1005 | 64-22 | 10.98 | -3.68 | 524.07 | 1.15E+09 |
| | *Scott* | 1006 | 64-28 | 10.31 | -3.44 | 518.67 | 7.88E+08 |
| **Massachusetts** | *Boston* | 1003 | 58-22 | 11.79 | -3.98 | 524.07 | 1.16E+09 |
| | *Springfield* | 1002 | 58-28 | 11.01 | -3.70 | 513.27 | 1.52E+09 |
| **Michigan** | *Port Huron* | D330 | 58-28 | 11.01 | -3.70 | 513.27 | 1.52E+09 |
| | *Alpena* | 6016 | 52-28 | 11.84 | -4.01 | 507.87 | 3.17E+09 |
| | *Marquette* | 1004 | 52-28 | 11.84 | -4.01 | 507.87 | 3.17E+09 |
| | *Grand Rapids* | 901 | 58-34 | 10.04 | -3.35 | 507.87 | 6.21E+08 |
| **South Carolina** | *Columbia* | 1024 | 64-16 | 11.38 | -3.82 | 529.47 | 1.04E+09 |
| **Tennessee** | *Memphis* | 3109 | 64-22 | 10.98 | -3.68 | 524.07 | 1.15E+09 |
| **Washington** | *Seattle* | 6049 | 52-16 | 13.31 | -4.54 | 518.67 | 5.60E+09 |
| | *Spokane* | A320 | 58-28 | 11.01 | -3.70 | 513.27 | 1.52E+09 |
| | *Kanawha* | 1640 | 64-22 | 10.98 | -3.68 | 524.07 | 1.15E+09 |

| | | | | | | | |
|---|---|---|---|---|---|---|---|
| **West Virginia** | *Charleston* | 7008 | 64-22 | 10.98 | -3.68 | 524.07 | 1.15E+09 |

4.4.c. Calculation of the Phase Angle δ based on Temperature and Frequency

By definition, the phase angle is the lag between the applied stresses and strains on a viscoelastic material. For the purpose of the analysis, it has been calculated using the following equation:

$$\delta_b = 90 + (-7.3146 - 2.6162 * VTS') * \log(f_s * \eta_{s,T}) + (0.1124 + 0.2029 * VTS') * \log(f_s * \eta_{s,T})^2$$

Having the frequency equal to 10 Hz, and the viscosity (in cP) calculated at the testing temperature and frequency in the previous step, the phase angle of the asphalt binder was estimated in Table 16:

*Table 16- Calculation of Phase Angle δ for the LTPP Database*

| State | City | Section Number | η (cP) | δ |
|---|---|---|---|---|
| **Alabama** | *Montgomery* | 4125 | 1.04E+09 | 46.92 |
| | *Tuscaloosa* | 6012 | 1.04E+09 | 46.92 |
| **Arizona** | *Tucson* | 6054 | 3.36E+08 | 50.18 |
| | *Phoenix* | B961 | 2.11E+08 | 50.62 |
| | *Flagstaff* | 669 | 1.52E+09 | 44.73 |
| | *Kingman* | 1022 | 3.47E+08 | 49.95 |
| **Alaska** | *Anchorage* | 1004 | 5.82E+08 | 47.11 |
| **Arkansas** | *Little Rock* | A606 | 1.04E+09 | 46.92 |
| **Colorado** | *Rio Blanco* | 1053 | 2.66E+09 | 43.21 |
| | *El Paso* | 7783 | 1.52E+09 | 44.73 |
| | *Yuma* | 502 | 7.88E+08 | 46.15 |
| **Indiana** | *La Porte* | 5528 | 1.52E+09 | 44.73 |
| | *Jackson* | A902 | 1.52E+09 | 44.73 |
| | *Jefferson* | 18-1028 | 1.52E+09 | 44.73 |
| **Kansas** | *Cherokee* | 1005 | 1.15E+09 | 45.80 |
| | *Scott* | 1006 | 7.88E+08 | 46.15 |
| **Massachusetts** | *Boston* | 1003 | 1.16E+09 | 47.26 |
| | *Springfield* | 1002 | 1.52E+09 | 44.73 |
| **Michigan** | *Port Huron* | D330 | 1.52E+09 | 44.73 |
| | *Alpena* | 6016 | 3.17E+09 | 42.91 |
| | *Marquette* | 1004 | 3.17E+09 | 42.91 |
| | *Grand Rapids* | 901 | 6.21E+08 | 46.63 |
| **South Carolina** | *Columbia/Lexington* | 1024 | 1.04E+09 | 46.92 |
| **Tennessee** | *Memphis* | 3109 | 1.15E+09 | 45.80 |
| **Washington** | *Seattle* | 6049 | 5.60E+09 | 42.36 |
| | *Spokane* | A320 | 1.52E+09 | 44.73 |
| **West Virginia** | *Kanawha* | 1640 | 1.15E+09 | 45.80 |
| | *Charleston* | 7008 | 1.15E+09 | 45.80 |

4.4.d. Calculation of the Complex Modulus of the Asphalt Binder

The Complex Shear Modulus of the asphalt binder $|G_b^*|$ is estimated based on the phase angle calculated in the step above and the viscosity (in cP) at testing temperature and frequency (Hz).

The following formula has been used to predict the dynamic shear modulus (Pa) needed for the analysis:

$$|G_b^*| = 0.0051 f_s \eta_{s,T} (sin\delta)^{7.1542 - 0.4929 f_s + 0.0211 f_s^2}$$

Calculating it for the different states and cities, the following Table 17 has been generated in Pascals:

*Table 17- Calculation of the Complex Modulus of the Asphalt Binder |G*b| for the LTPP Database*

| State | City | Section Number | η (cP) | δ | $\|G^*_b\|$ (Pa) |
|---|---|---|---|---|---|
| **Alabama** | *Montgomery* | 4125 | 1.04E+09 | 46.92 | 1.36E+07 |
| | *Tuscaloosa* | 6012 | 1.04E+09 | 46.92 | 1.36E+07 |
| **Arizona** | *Tucson* | 6054 | 3.36E+08 | 50.18 | 5.45E+06 |
| | *Phoenix* | B961 | 2.11E+08 | 50.62 | 3.52E+06 |
| | *Flagstaff* | 669 | 1.52E+09 | 44.73 | 1.70E+07 |
| | *Kingman* | 1022 | 3.47E+08 | 49.95 | 5.56E+06 |
| **Alaska** | *Anchorage* | 1004 | 5.82E+08 | 47.11 | 7.70E+06 |
| **Arkansas** | *Little Rock* | A606 | 1.04E+09 | 46.92 | 1.36E+07 |
| **Colorado** | *Rio Blanco* | 1053 | 2.66E+09 | 43.21 | 2.63E+07 |
| | *El Paso* | 7783 | 1.52E+09 | 44.73 | 1.70E+07 |
| | *Yuma* | 502 | 7.88E+08 | 46.15 | 9.75E+06 |
| **Indiana** | *La Porte* | 5528 | 1.52E+09 | 44.73 | 1.70E+07 |
| | *Jackson* | A902 | 1.52E+09 | 44.73 | 1.70E+07 |
| | *Jefferson* | 18-1028 | 1.52E+09 | 44.73 | 1.70E+07 |
| **Kansas** | *Cherokee* | 1005 | 1.15E+09 | 45.80 | 1.39E+07 |
| | *Scott* | 1006 | 7.88E+08 | 46.15 | 9.75E+06 |
| **Massachusetts** | *Boston* | 1003 | 1.16E+09 | 47.26 | 1.55E+07 |
| | *Springfield* | 1002 | 1.52E+09 | 44.73 | 1.70E+07 |
| **Michigan** | *Port Huron* | D330 | 1.52E+09 | 44.73 | 1.70E+07 |
| | *Alpena* | 6016 | 3.17E+09 | 42.91 | 3.05E+07 |
| | *Marquette* | 1004 | 3.17E+09 | 42.91 | 3.05E+07 |
| | *Grand Rapids* | 901 | 6.21E+08 | 46.63 | 7.94E+06 |
| **South Carolina** | *Columbia/Lexington* | 1024 | 1.04E+09 | 46.92 | 1.36E+07 |
| **Tennessee** | *Memphis* | 3109 | 1.15E+09 | 45.80 | 1.39E+07 |
| **Washington** | *Seattle* | 6049 | 5.60E+09 | 42.36 | 5.16E+07 |
| | *Spokane* | A320 | 1.52E+09 | 44.73 | 1.70E+07 |
| **West Virginia** | *Kanawha* | 1640 | 1.15E+09 | 45.80 | 1.39E+07 |
| | *Charleston* | 7008 | 1.15E+09 | 45.80 | 1.39E+07 |

The Figure 38 has been plotted for the different states to have a clearer idea about the variability of the results:

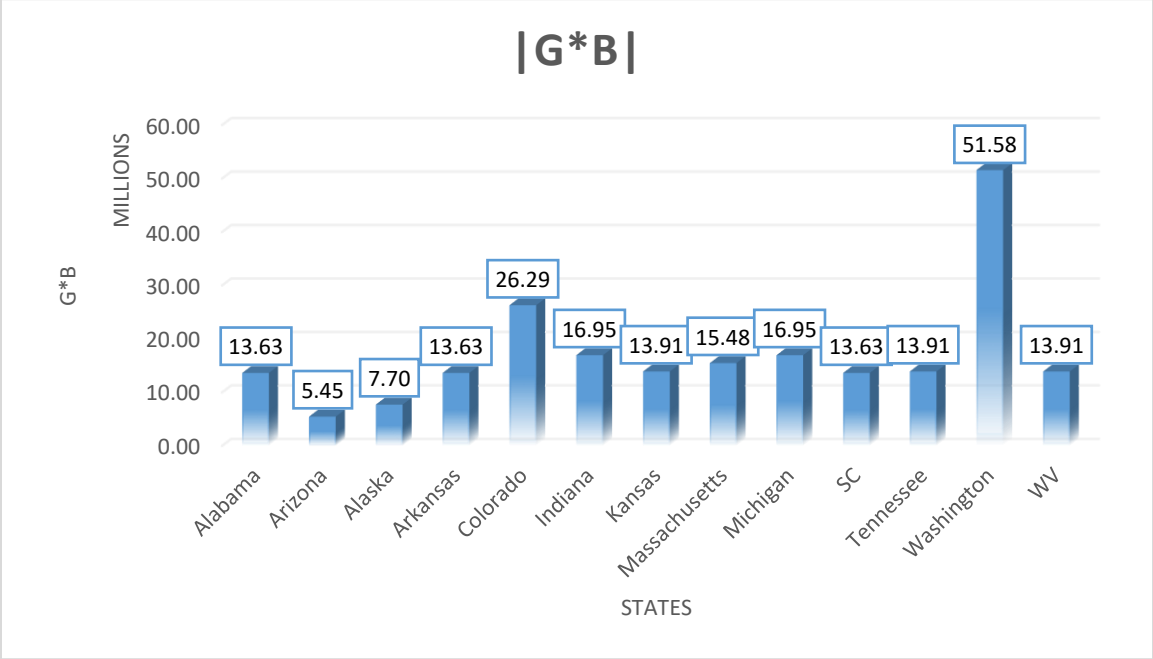


*Figure 38- Calculation of the Complex Shear Modulus of the Asphalt Binder for the LTPP Database*

4.4.e. Calculation of the FSC*, the Fatigue Strain Capacity or General Shear Envelope

The Fatigue Strain Capacity or FSC* is characterized as the maximum strain capacity for a specific asphalt binder. It is obtained as explained in Section 3.4. It is estimated as follows:

$$FSC^* = \frac{1}{6.56 \times 10^{-3} \times G_b(T,t)^{0.0482} + 1.35 \times 10^{-9} \times G_b(T,t)^{1.10}}$$

Where $G_b$ is the complex shear modulus of the asphalt binder for a specific testing temperature and frequency.

The results of the FSC* calculation is shown below in Table 18:

*Table 18- FSC* Calculation for the LTPP Database*

| State | City | Section Number | \|G*b\| Pa | FSC* |
|---|---|---|---|---|
| **Alabama** | *Montgomery* | 4125 | 1.36E+07 | 30 |
| | *Tuscaloosa* | 6012 | 1.36E+07 | 30 |
| **Arizona** | *Tucson* | 6054 | 5.45E+06 | 47 |
| | *Phoenix* | B961 | 3.52E+06 | 55 |
| | *Flagstaff* | 669 | 1.70E+07 | 27 |
| | *Kingman* | 1022 | 5.56E+06 | 47 |
| **Alaska** | *Anchorage* | 1004 | 7.70E+06 | 41 |
| **Arkansas** | *Little Rock* | A606 | 1.36E+07 | 30 |
| **Colorado** | *Rio Blanco* | 1053 | 2.63E+07 | 20 |
| | *El Paso* | 7783 | 1.70E+07 | 27 |
| | *Yuma* | 502 | 9.75E+06 | 36 |
| **Indiana** | *La Porte* | 5528 | 1.70E+07 | 27 |
| | *Jackson* | A902 | 1.70E+07 | 27 |
| | *Jefferson* | 18-1028 | 1.70E+07 | 27 |
| **Kansas** | *Cherokee* | 1005 | 1.39E+07 | 30 |
| | *Scott* | 1006 | 9.75E+06 | 36 |
| **Massachusetts** | *Boston* | 1003 | 1.55E+07 | 28 |
| | *Springfield* | 1002 | 1.70E+07 | 27 |
| **Michigan** | *Port Huron* | D330 | 1.70E+07 | 27 |
| | *Alpena* | 6016 | 3.05E+07 | 18 |
| | *Marquette* | 1004 | 3.05E+07 | 18 |
| | *Grand Rapids* | 901 | 7.94E+06 | 40 |
| **South Carolina** | *Columbia/Lexington* | 1024 | 1.36E+07 | 30 |
| **Tennessee** | *Memphis* | 3109 | 1.39E+07 | 30 |
| **Washington** | *Seattle* | 6049 | 5.16E+07 | 12 |
| | *Spokane* | A320 | 1.70E+07 | 27 |
| **West Virginia** | *Kanawha* | 1640 | 1.39E+07 | 30 |
| | *Charleston* | 7008 | 1.39E+07 | 30 |

It is to be mentioned that the FSC* and the Number of Cycles to Failure are directly proportional. This means that the higher the value of FSC*, the better the fatigue life of the asphalt mixture.

4.4.f. Calculation of the Number of Cycles to Fatigue Failure

The final model developed to predict the fatigue life of an asphalt mixture was developed based on the GFTAB analysis of asphalt binder based on the LAS test, and the axial fatigue testing on asphalt mixtures. The model has the following form:

$$N_f = \left( \frac{\left( (FSC^*)(\frac{VBE}{100}) \right)}{\varepsilon_t} \right)^{(\frac{3.7}{\varepsilon_t})(\frac{90}{\delta})}$$

For a constant strain level taken to be equal to 350 με in Table 19:

*Table 19- Number of Cycles to failure for the LTPP Database*

| State | City | Section | μ (cp) | δ | G*b Pa | FS C* | Nf |
|---|---|---|---|---|---|---|---|
| **Alabama** | *Montgomery* | 4125 | 1.04E+09 | 47 | 1.36E+07 | 55 | 7214 |
| | *Tuscaloosa* | 6012 | 1.04E+09 | 47 | 1.36E+07 | 55 | 8200 |
| **Arizona** | *Tucson* | 6054 | 3.36E+08 | 50 | 5.45E+06 | 64 | 10887 |
| | *Phoenix* | B961 | 2.11E+08 | 51 | 3.52E+06 | 69 | 13478 |
| | *Flagstaff* | 669 | 1.52E+09 | 45 | 1.70E+07 | 57 | 9435 |
| | *Kingman* | 1022 | 3.47E+08 | 50 | 5.56E+06 | 66 | 12750 |
| **Alaska** | *Anchorage* | 1004 | 5.82E+08 | 47 | 7.70E+06 | 70 | 15257 |
| **Arkansas** | *Little Rock* | A606 | 1.04E+09 | 47 | 1.36E+07 | 55 | 12999 |
| **Colorado** | *Rio Blanco* | 1053 | 2.66E+09 | 43 | 2.63E+07 | 54 | 7734 |
| | *El Paso* | 7783 | 1.52E+09 | 45 | 1.70E+07 | 57 | 7500 |
| | *Yuma* | 502 | 7.88E+08 | 46 | 9.75E+06 | 63 | 8234 |
| **Indiana** | *La Porte* | 5528 | 1.52E+09 | 45 | 1.70E+07 | 57 | 10987 |
| | *Jackson* | A902 | 1.52E+09 | 45 | 1.70E+07 | 57 | 13055 |
| | *Jefferson* | 18-1028 | 1.52E+09 | 45 | 1.70E+07 | 57 | 11617 |
| **Kansas** | *Cherokee* | 1005 | 1.15E+09 | 46 | 1.39E+07 | 57 | 8368 |
| | *Scott* | 1006 | 7.88E+08 | 46 | 9.75E+06 | 63 | 16943 |
| **Massachusetts** | *Boston* | 1003 | 1.16E+09 | 47 | 1.55E+07 | 57 | 4839 |
| | *Springfield* | 1002 | 1.52E+09 | 45 | 1.70E+07 | 57 | 14058 |
| **Michigan** | *Port Huron* | D330 | 1.52E+09 | 45 | 1.70E+07 | 57 | 10066 |
| | *Alpena* | 6016 | 3.17E+09 | 43 | 3.05E+07 | 49 | 7938 |
| | *Marquette* | 1004 | 3.17E+09 | 43 | 3.05E+07 | 49 | 4646 |
| | *Grand Rapids* | 901 | 6.21E+08 | 47 | 7.94E+06 | 67 | 16032 |
| **South Carolina** | *Columbia* | 1024 | 1.04E+09 | 47 | 1.36E+07 | 55 | 3136 |
| **Tennessee** | *Memphis* | 3109 | 1.15E+09 | 46 | 1.39E+07 | 57 | 6552 |
| **Washington** | *Seattle* | 6049 | 5.60E+09 | 42 | 5.16E+07 | 33 | 590 |
| | *Spokane* | A320 | 1.52E+09 | 45 | 1.70E+07 | 57 | 6262 |
| **West Virginia** | *Kanawha* | 1640 | 1.15E+09 | 46 | 1.39E+07 | 57 | 8100 |
| | *Charleston* | 7008 | 1.15E+09 | 46 | 1.39E+07 | 57 | 5417 |

It is to be noted that the higher the number of cycles to failure, the better the fatigue life of the mixture.

If multiple strains are to be considered, the accumulated Damage formula mentioned in Section 3.4 must be generated for multiple strain levels.

4.4.g. Comparing the Predicted vs. Measured Fatigue Values

In this section, the predicted and the measured fatigue indicators are compared. The LTPP provides measured fatigue areas (Alligator Cracking) in $m^2$. The measured distresses are found in Appendix A, Table 54. The mechanism of fatigue refers to the progressive process whereby a bound layer in the HMA pavement structure undergoes a certain number of repeated applications of stress/strain leading to its crack. The asphalt mixtures are recognized as having a viscoelastic behavior. In other terms, the elastic portion of the specimen concerns the energy stored when loaded, whereas the viscous portion represents the energy dissipated within the specimen. The lower the energy dissipated/higher the energy stored, the lower is the crack propagation. When too much stress/strain is accumulated within the sample, a crack forms to release them. The accumulation over time is the main cause of fatigue of the material.

In this study, the Number of Repetition to Failure $N_f$ was predicted and related to the estimated fatigue life of a mixture. The LTPP Database provides measurements of the area having forms of fatigue under the shape of Alligator Cracking. It refers to a surface damaged with a pattern looking like scales from the back of an alligator. It begins usually with longitudinal cracks, connected by transverse cracks. It is the most serious issue that can affect the asphalt surface and is almost always the result of neglecting the need to make repairs and protect the surface.

Longitudinal cracking appears as the onset of fatigue cracking. It allows moisture infiltration, roughness and onset of alligator cracking followed by structural failure. They are mostly caused by improper paving operations, bottom-up reflected cracks, shrinkage of the asphalt layer or poorly constructed joints. They are widely linked to fatigue behavior.

For this reason, in this section, the fatigue behavior collected from the LTPP Database is retrieved from data recorded in terms of Alligator Cracking (Fatigue) and Longitudinal Cracks. The longitudinal cracks are measured within the wheel path, and non-wheel path (WP, NWP) in meters. Normally, the transvers cracks could also be correlated with fatigue. However, as no background have been provided on the possible nature of the distresses recorded, only longitudinal and alligator cracks are taken into consideration in the analysis.

The following Table 20 has been generated:

*Table 20- LTPP Database Fatigue Comparison*

| State | City | Section Number | Long Cracking (Length, m) WP and NWP | | Fatigue ($m^2$) | $N_f$ |
|---|---|---|---|---|---|---|
| **Alabama** | *Montgomery* | 4125 | 0 | 0 | 76.6 | 7214 |
| | *Tuscaloosa* | 6012 | 4.3 | 95.9 | 125.6 | 8200 |
| **Arizona** | *Tucson* | 6054 | 0 | 0 | 1.2 | 10887 |
| | *Phoenix* | B961 | 0 | 29.7 | 46.3 | 13478 |
| | *Flagstaff* | 669 | 0 | 201.8 | 0 | 9435 |
| | *Kingman* | 1022 | 0 | 359.5 | 120.2 | 12750 |
| **Alaska** | *Anchorage* | 1004 | 0 | 84.8 | 2 | 15257 |
| **Arkansas** | *Little Rock* | A606 | 0 | 272.9 | 60.9 | 12999 |
| **Colorado** | *Rio Blanco* | 1053 | 0 | 609.8 | 8 | 7734 |
| | *El Paso* | 7783 | 0 | 414.8 | 111.4 | 7500 |
| | *Yuma* | 502 | 33 | 161.2 | 75.4 | 8234 |
| **Indiana** | *La Porte* | 5528 | 0 | 322 | 132.3 | 10987 |
| | *Jackson* | A902 | 0 | 305.1 | 0 | 13055 |
| | *Jefferson* | 18-1028 | 0 | 172.7 | 0 | 11617 |
| **Kansas** | *Cherokee* | 1005 | 1.4 | 188.9 | 154.5 | 8368 |
| | *Scott* | 1006 | 0 | 36.5 | 33.3 | 16943 |
| **Massachusetts** | *Boston* | 1003 | 12.5 | 30.6 | 104.5 | 4839 |
| | *Springfield* | 1002 | 0 | 99.8 | 203.4 | 14058 |
| **Michigan** | *Port Huron* | D330 | 2.5 | 235.5 | 0 | 10066 |
| | *Alpena* | 6016 | 13.3 | 160 | 0 | 7938 |
| | *Marquette* | 1004 | 0 | 207.5 | 2.2 | 4646 |
| | *Grand Rapids* | 901 | 0 | 287.5 | 274.5 | 16032 |
| **South Carolina** | *Columbia/Lexington* | 1024 | 0 | 53.3 | 22.6 | 3136 |
| **Tennessee** | *Memphis* | 3109 | 0 | 88 | 22 | 6552 |
| **Washington** | *Seattle* | 6049 | 39.8 | 0 | 0 | 590 |
| | *Spokane* | A320 | 0.9 | 198.3 | 1.3 | 6262 |
| **West Virginia** | *Kanawha* | 1640 | 0 | 171.3 | 258.1 | 8100 |
| | *Charleston* | 7008 | 0 | 305.1 | 0 | 5417 |

It is to be noted that the LTPP Database does not always provide Fatigue measurements. In the case where no values have been provided, a value of 0 was assigned in the respective column (Fatigue $m^2$) in Table 20. In addition, as we are considering fatigue behavior, the longitudinal cracks on the wheel-path were considered in the analysis.

Based on the analysis, it is safe to assume that the number of cycles to failure $N_f$ is said to be greater when a pavement structure is not expected to experience a lot of fatigue distresses. In other terms, the higher the number of cycles to failure $N_f$, the lower the fatigue behavior during the pavement life.

As the data presented in the LTPP is not in terms of $N_f$, the comparison the predicted vs measured data is different than the one presented for rutting. The results are presented in **Error! Reference source not found.** showing the number of cycles to f ailure in 1000, the length of longitudinal cracks on the wheel path, and the amount of alligator cracking in terms of area in $m^2$.

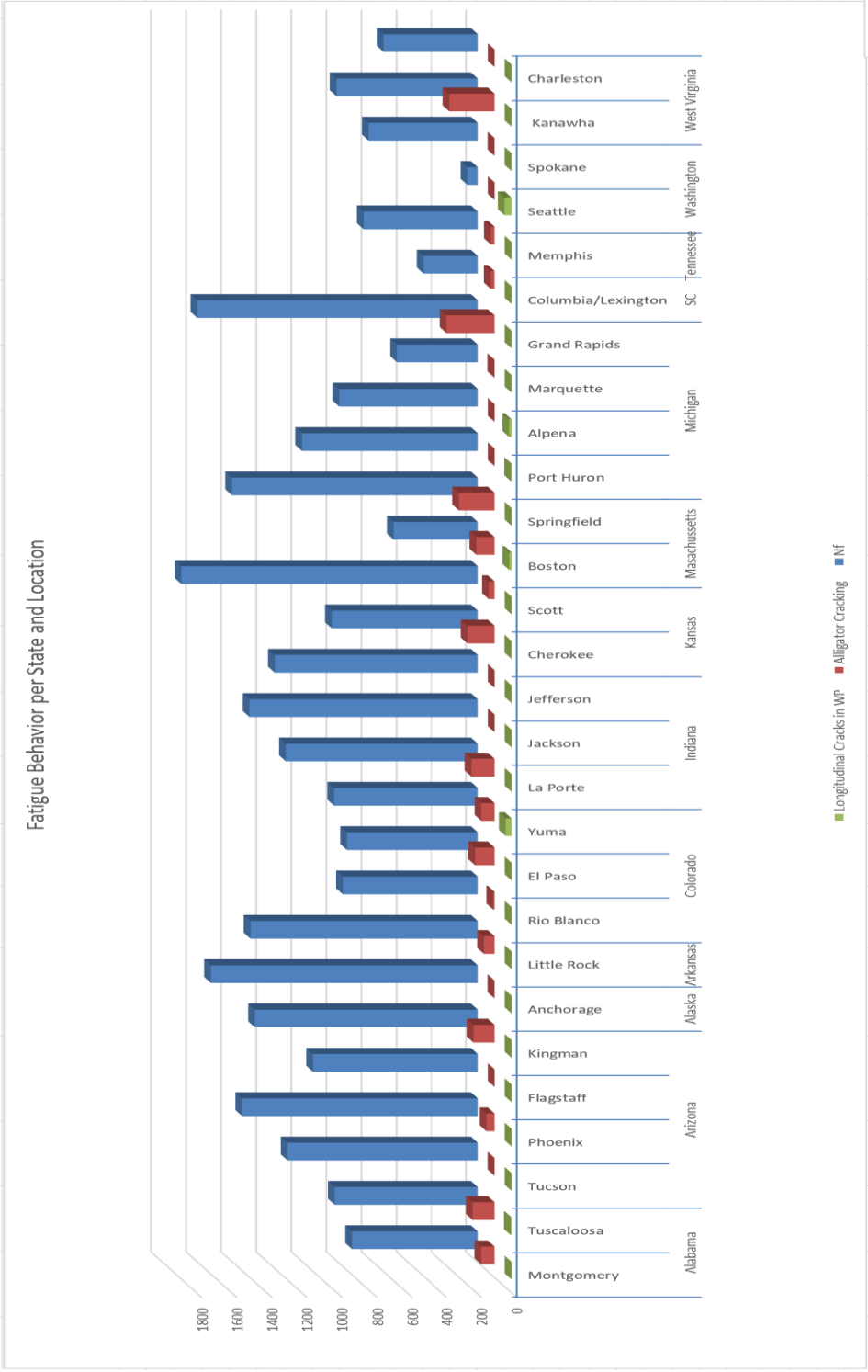


*Figure 39- Fatigue Comparison per State and Region for LTPP Database*

The preceding bar chart shows the fatigue behavior of each state. In order to give a better analysis of that has been obtained, a different chart has been plotted in terms of climatic regions. For most of the cases, it can be seen from the chart above that the initial proposed theory is somehow satisfied, as the number of cycles to failure increases, the fatigue behavior is better. However, some exceptions did occur. Based on the data collected, the following limitations have been concluded: For a maximum strain level of 350 με, the $N_f$ ranges have the following trend in Table 21:

*Table 21- Nf Behavior Ranges*

| | | |
|---|---|---|
| **$N_f$ Ranges** | **Low** | <6,000 |
| | **Satisfactory** | 6,000-10,000 |
| | **Good** | 10,000-15,000 |
| | **Excellent** | >15,000 |

The following ranges are observed from the bar chart above. However, it is to be noticed that even though these ranges are generalized, the fatigue behavior of each climatic region is differing. The Figure 40 showing the fatigue per climatic region is shown below.

From the climatic regions' graph, the following behaviors were recorded:

The highest fatigue areas were recorded in the Wet (Freeze and Non-Freeze) regions. The highest area recorded by the LTPP is of 274.5 $m^2$, happening in the Wet, Freeze Region.

Similarly, the highest length of longitudinal cracks has been recorded in the Wet, Freeze region with a length of 39.8 m. The different PG-Binder used in this analysis also

have a big effect on the number of cycles to failure, as $G^*_b$ and $\delta$ are dependent on the type of binder used. Also, the fatigue temperature developed is based on the PG of the binder. Therefore, the choice of the PG-binder plays a big role in this prediction. Choosing the right PG of the binder plays an important part in general within all of the predictions. It is important to choose the right binder for the right temperature set. At high temperatures, a stiffer binder is required to resist rutting and avoid the softening of the binder whereas at low temperatures, softer binders are required to avoid the stiffening of the binder at lower temperatures. In terms of fatigue, an elastic behavior is required, which means that more energy needs to be stored and released then dissipated. This is reflected by the $G^*\sin\delta$ factor < 5000 kPa. The list of the performance grades per climatic region is shown in Table 22:

*Table 22- PG-Binder per Climatic Regions*

| State | City | Section Number | PG (LTTP Bind) | MAAT (ºF) | Climate Zone |
|---|---|---|---|---|---|
| **Colorado** | *Yuma* | 502 | 64-28 | 46 | *Dry, Freeze* |
| **Washington** | *Spokane* | A320 | 58-28 | 61 | |
| **Alaska** | *Anchorage* | 1004 | 46-40 | 65 | |
| **Arizona** | *Flagstaff* | 669 | 58-28 | 65 | |
| **Colorado** | *Rio Blanco* | 1053 | 46-34 | 72 | |
| **Colorado** | *El Paso* | 7783 | 58-28 | 75 | |
| **Arizona** | *Tucson* | 6054 | 70-10 | 36 | *Dry, No Freeze* |
| **Arizona** | *Kingman* | 1022 | 70-16 | 47 | |
| **Arizona** | *Phoenix* | B961 | 76-10 | 63 | |
| **Kansas** | *Cherokee* | 1005 | 64-22 | 50 | *Wet, Freeze* |
| **Michigan** | *Marquette* | 1004 | 52-28 | 51 | |
| **Indiana** | *Jackson* | A902 | 58-28 | 51 | |
| **Michigan** | *Grand Rapids* | 901 | 58-34 | 51 | |
| **Michigan** | *Alpena* | 6016 | 52-28 | 52 | |
| **Massachusetts** | *Boston* | 1003 | 58-22 | 53 | |
| **Massachusetts** | *Springfield* | 1002 | 58-28 | 56 | |
| **Michigan** | *Port Huron* | D330 | 58-28 | 57 | |
| **West Virginia** | *Kanawha* | 1640 | 64-22 | 65 | |
| **Indiana** | *La Porte* | 5528 | 58-28 | 76 | |
| **Alabama** | *Montgomery* | 4125 | 64-16 | 44 | *Wet, No Freeze* |
| **Alabama** | *Tuscaloosa* | 6012 | 64-16 | 44 | |
| **Tennessee** | *Memphis* | 3109 | 64-22 | 48 | |
| **Arkansas** | *Little Rock* | A606 | 64-16 | 49 | |
| **Washington** | *Seattle* | 6049 | 52-16 | 53 | |
| **South Carolina** | *Columbia* | 1024 | 64-16 | 53 | |
| **West Virginia** | *Charleston* | 7008 | 64-22 | 56 | |
| **Kansas** | *Scott* | 1006 | 64-28 | 63 | |
| **Indiana** | *Jefferson* | 18-1028 | 58-28 | 64 | |

The highest temperatures are experienced in the Dry, Freeze and Dry, No-Freeze regions. In the dry-freeze region, the PG Binders are stiff at high temperatures and soft at low temperatures. However, all the performance grades vary from 46 to 76 in terms of high temperatures, and from 10 to 34 in terms of low temperatures.

In the following section, each climatic region is divided as per the 4 regions discussed earlier in Section 4.1. In addition, the cumulative graph of all the sections is shown below in Figure 40.

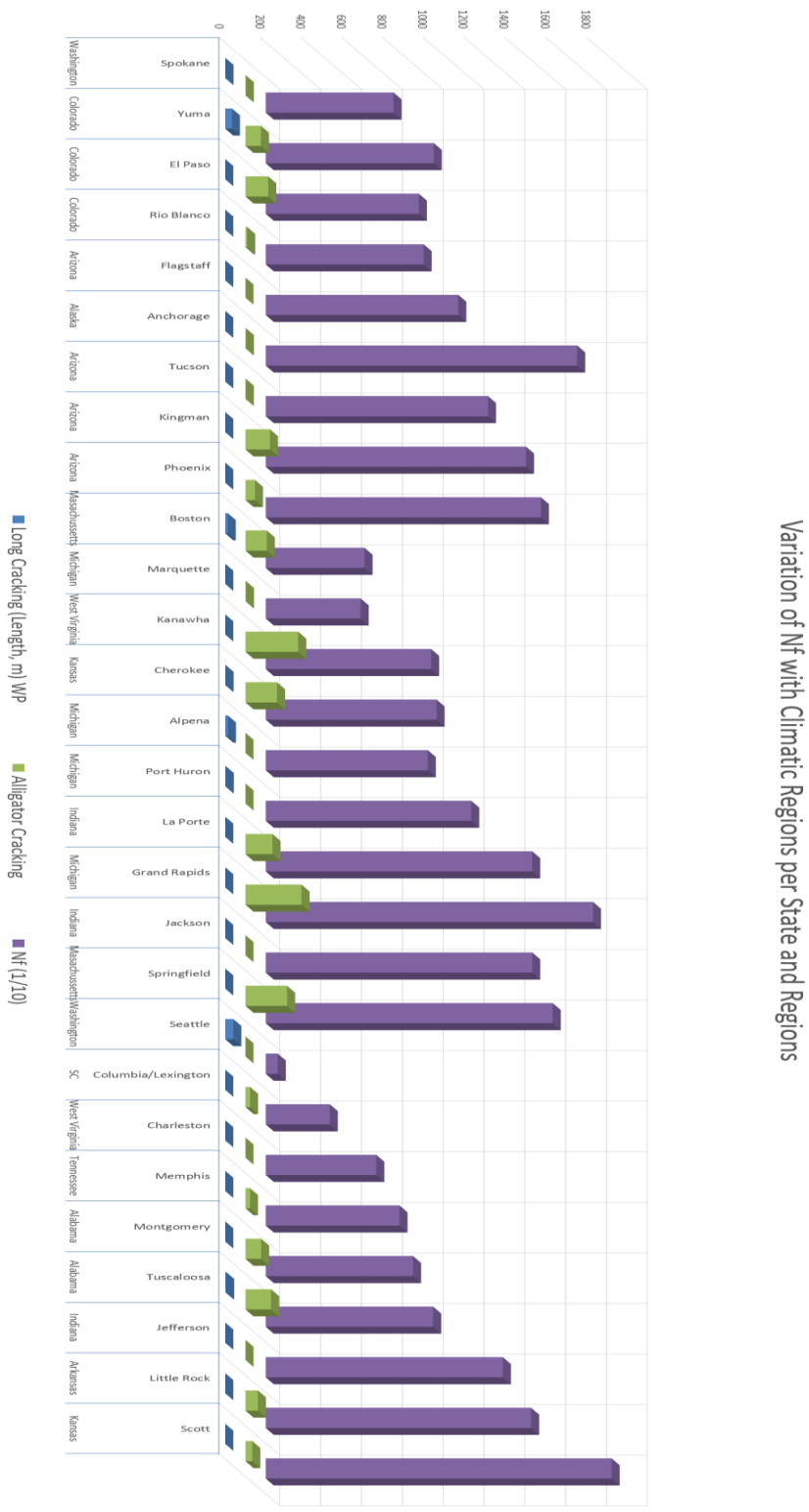


*Figure 40- Nf Variation with Climatic Regions per State and Regions*

4.4.g.1.Fatigue Analysis: Dry-Freeze Region

For the Dry Freeze Region, the highest number of cycles to failure is of 15260, with only 2 $m^2$ of alligator cracking. This number of cycles to failure according to the general criteria falls within the Satisfactory range. As the $N_f$ goes lower, more fatigue areas are recorded. The Figure 41 below must be taken into consideration:

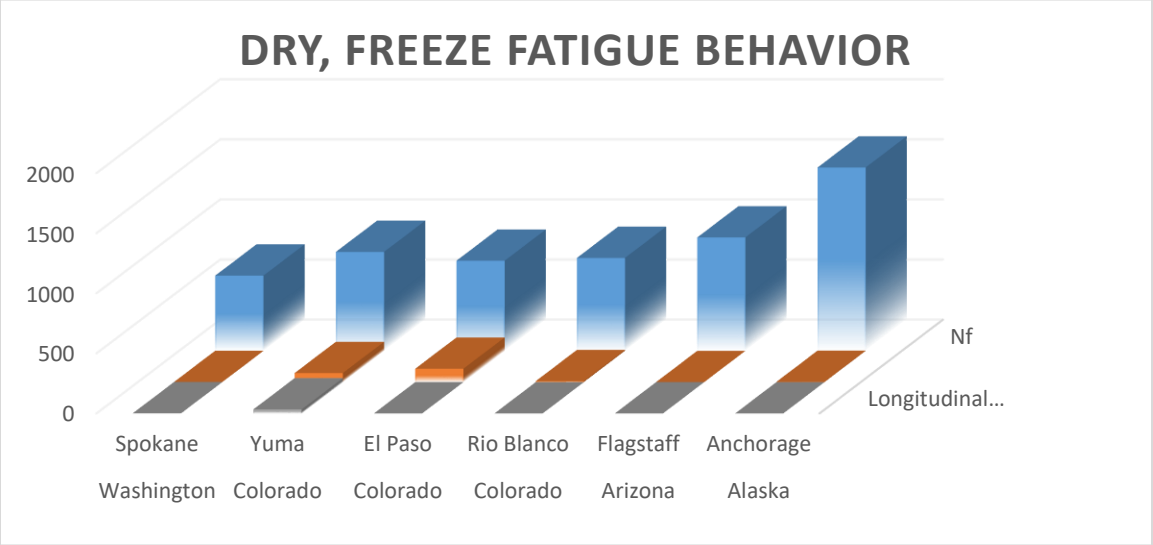


*Figure 41- Dry- Freeze Fatigue Behavior Data*

The fatigue behavior in Spokane, Arizona do not stick with the trend suggested above. As for the other section, the behavior fit the trend proposed above. Even though the number of cycles to failure falls within the Satisfactory Range, the fatigue behavior seems to be looking good. This could be justified by the number and date of data collection included in the LTPP, as the results are not the most recent compared to the other sections. For this reason, this section could be removed from the analysis.

4.4.g.2.Fatigue Analysis: Dry, Non-Freeze Region

For the Dry, Non-Freeze region, the highest number of cycles to failure is recorded to be 10890, with 1.2 $m^2$ of alligator cracking. In this climatic zone, the number of cycles to failure for all of the sections fall within the Good range. The trend is followed except for the section located in Tucson (Figure 42). This can also be verified as the inputted data is not the most recent one, and that newer measurements should be conducted.

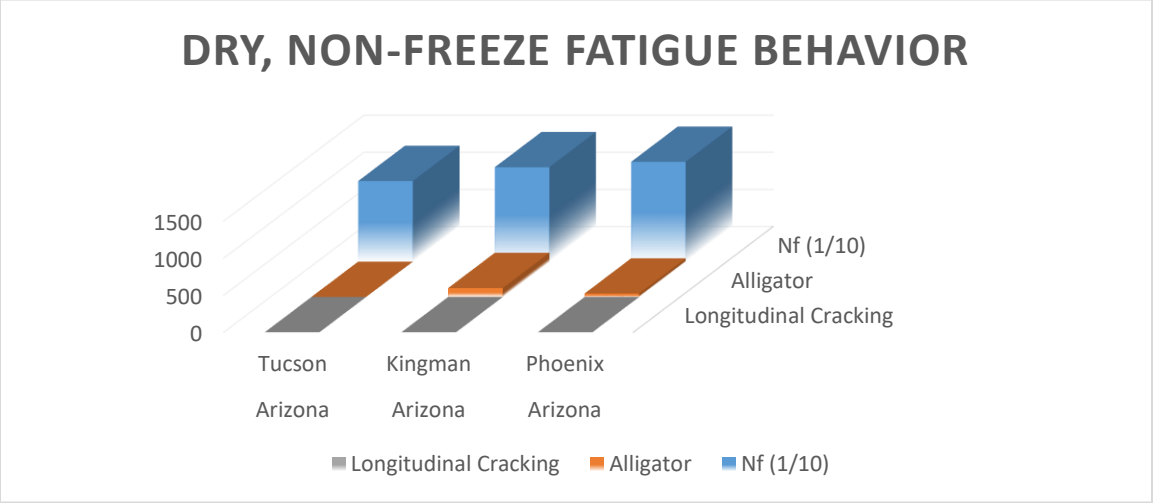


*Figure 42- Dry, Non-Freeze Fatigue Behavior*

4.4.g.3.Fatigue Analysis: Wet, Freeze Region

For the Wet, Freeze Region, the worst fatigue behavior is experience in both terms of alligator cracking. The highest alligator cracking area that has been recorded is 258.1 $m^2$.

The number of cycles to failure within this region ranges from 4840 till 16030. However, some inconsistencies are presented in this case, as high fatigue is expected in this type of climate. Moisture by itself is considered to have a negative effect of asphalt. In the freeze part of this climatic region, freeze and thaw phenomena affects the performance of the asphalt pavement structure drastically.

The following Figure 43 shows the fatigue behavior of the Wet, Freeze region:

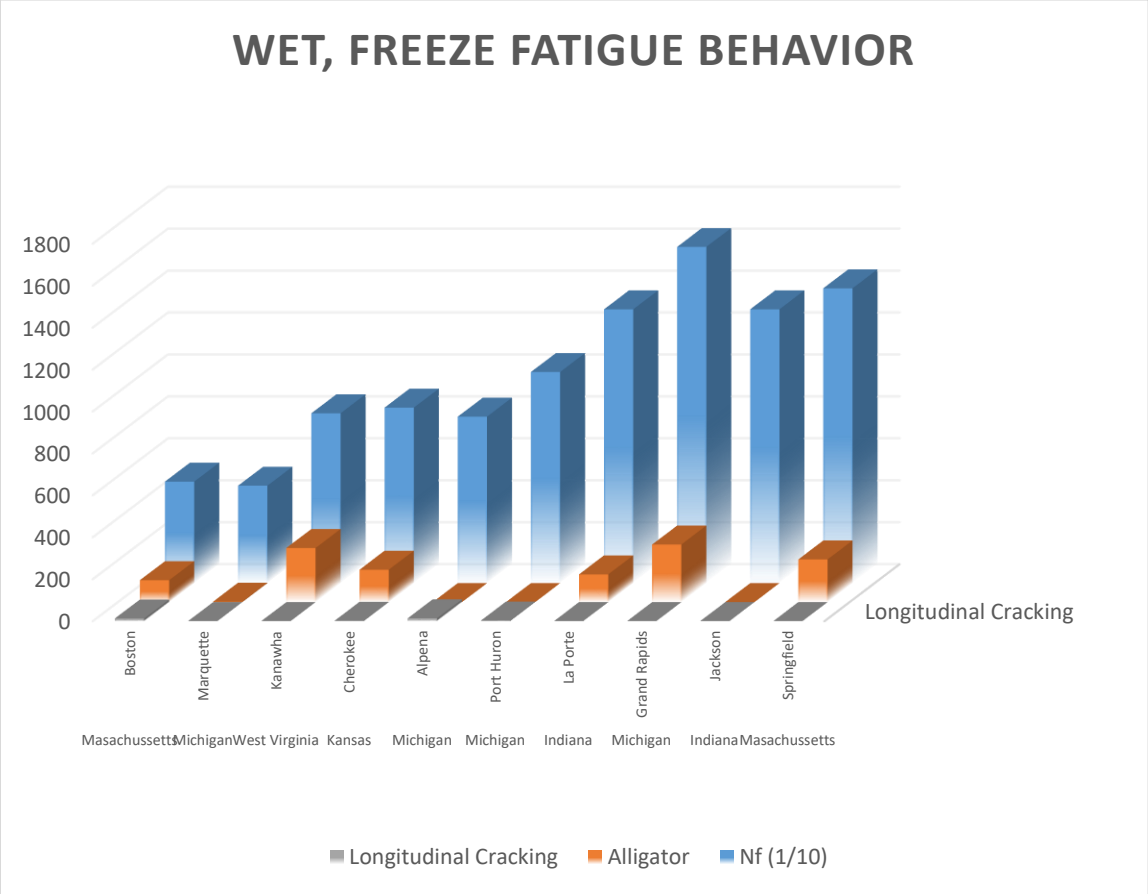


*Figure 43- Wet, Freeze Fatigue Behavior*

4.4.g.4.Fatigue Analysis: Wet, Non-Freeze Region

In this region the highest number of cycles to failure is found to be 10440. In terms of measured rutting, the trend is approximately followed. The amount of alligator cracking recorded is logical in terms of $N_f$. However, the increase/decrease with respect to the number of cycles to failure is somehow consistent. As the number $N_f$ increases, the alligator cracking area should decrease. The trend is observed in certain cases except for Seattle-Washington and Charleston-Virginia. This is explained in the case where the data is not the most recent (Figure 44).

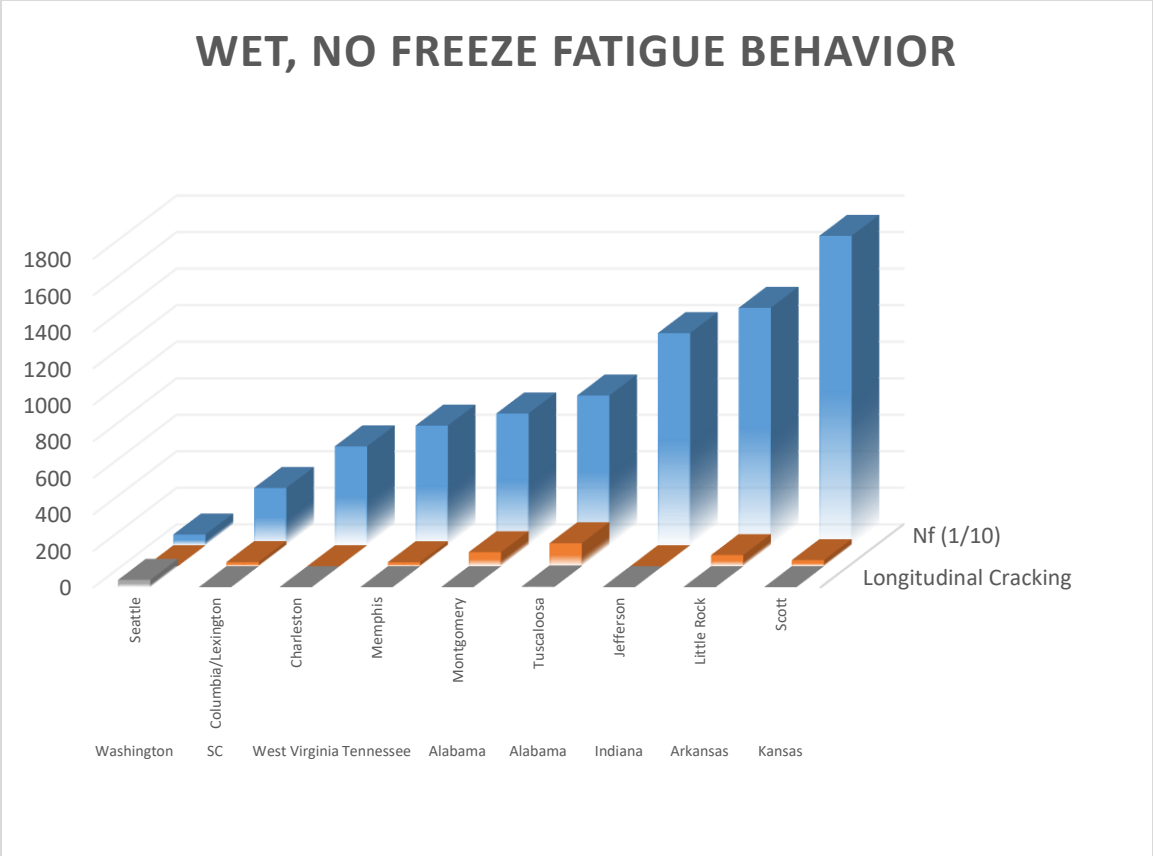


*Figure 44- Wet, Non-Freeze Fatigue Behavior*

## 4.5. Generation of the Total Effective Fracture Energy and Tensile Strength

In this section, an estimation of the thermal cracking behavior is observed. The predictive models were described and defined in the previous chapter, Section 3.5. However, not enough data was available in order to run the new TCMODEL suggested by Zborowski in 2007(31). For this reason, all the parameter that could be developed with the available data are listed in this section. The outcome of this analysis is to relate all the parameters found, with the trends that are expected for the thermal cracking mechanism behavior. The creep compliance at 1000 seconds, the $D_1$ and m parameters, as well as the tensile strength and total effective fracture energy were found for all the available mixtures from the LTPP Database.

4.5.a. Calculation of the $D_1$ fracture parameter for the Creep Compliance

First, the calculation of the $D_1$ parameter was calculated for each testing temperature of -20°C, -10 °C and 0 °C. The formulas used are inserted below for simplicity in 1/psi:

- ➔ $\log(D_1)_{-20^oC} = -11.92540 + 1.52206 * \log(V_a) + 4.49876 * \log(VFA) - 3.81320 * \log(A_{RTFO})$
- ➔ $\log(D_1)_{-10^oC} = -10.76560 + 1.51960 * \log(V_a) + 3{,}49983 * \log(VFA) - 2.99870 * \log(A_{RTFO})$
- ➔ $\log(D_1)_{0^oC} = -9.80626 + 1.50845 * \log(V_a) + 2.99000 * \log(VFA) - 2.90157 * \log(A_{RTFO})$

The results are summarized in the Table 23:

*Table 23- D1 calculation for the LTPP Database*

| State | City | Climate Zone | Section | Va | Vbe | D1 -20°C | D1 -10°C | D1 0°C |
|---|---|---|---|---|---|---|---|---|
| **AZ** | Flagstaff | Dry, F | 669 | 4.9 | 9.7 | 2.4E-07 | 3.7E-07 | 4.9E-07 |
| **AK** | Anchorage | Dry, F | 1004 | 3.9 | 10.1 | 2.5E-07 | 3.5E-07 | 4. 4E-07 |
| **CO** | Rio Blanco | Dry, F | 1053 | 4 | 10.3 | 2.6E-07 | 3.6E-07 | 4.6E-07 |
| **CO** | El Paso | Dry, F | 7783 | 5.3 | 8.7 | 2.0E-07 | 3.3E-07 | 4.5E-07 |
| **CO** | Yuma | Dry, F | 502 | 7.4 | 7.6 | 1.6E-07 | 3.0E-07 | 4.6E-07 |
| **WA** | Spokane | Dry, F | A320 | 6 | 8 | 1.7E-07 | 3.0E-07 | 4.2E-07 |
| **AZ** | Tucson | Dry, NF | 6054 | 4.6 | 10 | 2.6E-07 | 3.8E-07 | 5.0E-07 |
| **AZ** | Phoenix | Dry, NF | B961 | 4.5 | 10.1 | 2.6E-07 | 3.8E-07 | 4.9E-07 |
| **AZ** | Kingman | Dry, NF | 1022 | 3.9 | 10.7 | 2.7E-07 | 3.8E-07 | 4.7E-07 |
| **IN** | La Porte | Wet, F | 5528 | 6.2 | 10.4 | 2.7E-07 | 4.3E-07 | 5.9E-07 |
| **IN** | Jackson | Wet, F | A902 | 2.7 | 11.3 | 2.4E-07 | 3.0E-07 | 3.6E-07 |
| **KS** | Cherokee | Wet, F | 1005 | 5 | 9 | 2.3E-07 | 3.5E-07 | 4.7E-07 |
| **MS** | Boston | Wet, F | 1003 | 5.6 | 8.4 | 1.9E-07 | 3.2E-07 | 4.4E-07 |
| **MS** | Springfield | Wet, F | 1002 | 2.3 | 11.7 | 2.2E-07 | 2.6E-07 | 3.1E-07 |
| **MI** | Port Huron | Wet, F | D330 | 4 | 10 | 2.5E-07 | 3.5E-07 | 4.5E-07 |
| **MI** | Alpena | Wet, F | 6016 | 2.7 | 11.3 | 2.4E-07 | 3.0E-07 | 3.6E-07 |
| **MI** | Marquette | Wet, F | 1004 | 5.1 | 8.9 | 2.1E-07 | 3.5E-07 | 4.5E-07 |
| **MI** | Grand Rapids | Wet, F | 901 | 3.5 | 10 | 3.7E-07 | 4.6E-07 | 5.77E-07 |
| **WV** | Kanawha | Wet, F | 1640 | 5.1 | 8.86 | 2.2E-07 | 3.4E-07 | 4.71E-07 |
| **AL** | Montgomery | Wet, NF | 4125 | 5.8 | 9.2 | 1.8E-07 | 3.0E-07 | 4.2E-07 |
| **AL** | Tuscaloosa | Wet, NF | 6012 | 5.2 | 9.8 | 2.0E-07 | 3.2E-07 | 4.34E-07 |
| **AR** | Little Rock | Wet, NF | A606 | 3 | 12.3 | 2.1E-07 | 2.8E-07 | 3.52E-07 |
| **IN** | Jefferson | Wet, NF | 1028 | 4.3 | 10.69 | 2.7E-07 | 3.8E-07 | 4.97E-07 |
| **KS** | Scott | Wet, NF | 1006 | 3.2 | 10.8 | 2.9E-07 | 3.7E-07 | 4.55E-07 |
| **SC** | Columbia | Wet, NF | 1024 | 7.9 | 6.1 | 6.1E-08 | 1.5E-07 | 2.43E-07 |
| **TV** | Memphis | Wet, NF | 3109 | 6 | 8 | 1.77E-07 | 3.07E-07 | 4.39E-07 |
| **WA** | Seattle | Wet, NF | 6049 | 8.9 | 5.1 | 4.07E-08 | 1.12E-07 | 2E-07 |
| **WV** | Charleston | Wet, NF | 7008 | 6.7 | 7.3 | 1.39E-07 | 2.64E-07 | 3.94E-07 |

The behavior of this parameter reflects the trend that is expected: for the same level of air void content, $D_1$ decreases with the increase of $V_b$ and vice versa. Also, the values are within an acceptable range of the model.

It is also noticed that $D_1$ increases with the increase in temperature. This reflects the trend stating that with higher temperature, and higher creep compliance, the resistance to thermal cracking is increasing. This is also reflected by the fact that, at higher temperatures, the asphalt binder is softer. The Figure 45 shows the variation of $D_1$ with respect to the temperatures -20°C, -10°C and 0°C.

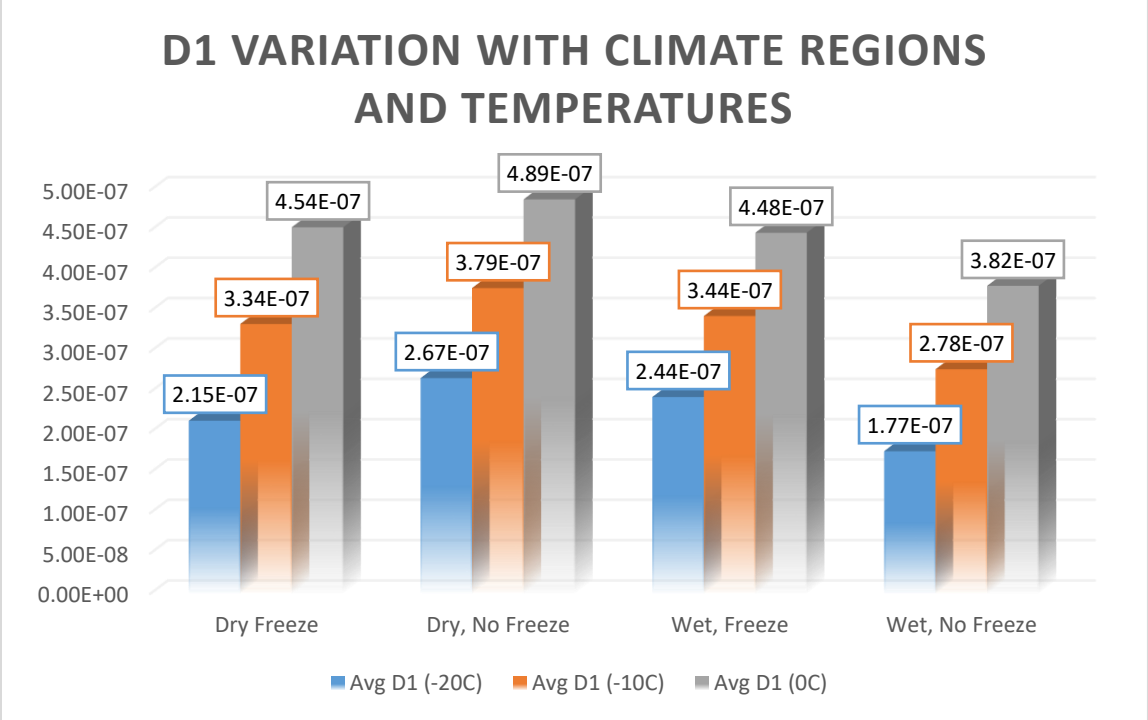


*Figure 45-D1 Variation with Temperature per Climate Region*

4.5.b. Calculation of the Penetration Parameter at 77°F

In order to calculate the slope of the creep compliance curve "m", the penetration of the asphalt binders at 77°F is needed as one input parameter in the suggested relationships.

As no data was gathered for the asphalt binders at this specific temperature, it was estimated using the following equation in 1/10 mm, and is depending on “Ai” and “VTSi” of the binder:

$$Pen_{77} = 10^{290.5013\sqrt{8.1177.288+257.0694*10^{A+2.72973*VTS}}}$$

The results are summarized in the Table 24:

*Table 24- Binder Penetration per Climatic Region*

| State | City | Climate Zone | PG | Pen 77 |
|---|---|---|---|---|
| **Colorado** | Rio Blanco | Dry, Freeze | 46-34 | 234 |
| **Alaska** | Anchorage | Dry, Freeze | 46-40 | 307 |
| **Arizona** | Flagstaff | Dry, Freeze | 58-28 | 92 |
| **Colorado** | El Paso | Dry, Freeze | 58-28 | 92 |
| **Washington** | Spokane | Dry, Freeze | 58-28 | 92 |
| **Colorado** | Yuma | Dry, Freeze | 64-28 | 70 |
| **Arizona** | Tucson | Dry, No Freeze | 70-10 | 35 |
| **Arizona** | Kingman | Dry, No Freeze | 70-16 | 42 |
| **Arizona** | Phoenix | Dry, No Freeze | 76-10 | 28 |
| **Michigan** | Alpena | Wet, Freeze | 52-28 | 131 |
| **Michigan** | Marquette | Wet, Freeze | 52-28 | 131 |
| **Massachusetts** | Boston | Wet, Freeze | 58-22 | 72 |
| **Indiana** | La Porte | Wet, Freeze | 58-28 | 92 |
| **Indiana** | Jackson | Wet, Freeze | 58-28 | 92 |
| **Massachusetts** | Springfield | Wet, Freeze | 58-28 | 92 |
| **Michigan** | Port Huron | Wet, Freeze | 58-28 | 92 |
| **Michigan** | Grand Rapids | Wet, Freeze | 58-34 | 126 |
| **Kansas** | Cherokee | Wet, Freeze | 64-22 | 54 |
| **West Virginia** | Kanawha | Wet, Freeze | 64-22 | 54 |
| **Washington** | Seattle | Wet, No Freeze | 52-16 | 89 |
| **Indiana** | Jefferson | Wet, No Freeze | 58-28 | 92 |
| **Alabama** | Montgomery | Wet, No Freeze | 64-16 | 46 |
| **Alabama** | Tuscaloosa | Wet, No Freeze | 64-16 | 46 |
| **Arkansas** | Little Rock | Wet, No Freeze | 64-16 | 46 |
| **South Carolina** | Columbia/Lexington | Wet, No Freeze | 64-16 | 46 |
| **Tennessee** | Memphis | Wet, No Freeze | 64-22 | 54 |
| **West Virginia** | Charleston | Wet, No Freeze | 64-22 | 54 |

| | | | | |
|---|---|---|---|---|
| **Kansas** | Scott | Wet, No Freeze | 64-28 | 70 |

It is noticed that in the Freeze Regions, the Asphalt binders do get softer in terms of consistency, as the higher the value of $Pen_{77}$, the softer it is. The results agree with the expected trend as well, as the PG-Binders' type also correspond to the values obtained. A stiffer binder has a higher upper bound temperature. This is observed as well within the results in the Table 24.

Softer binders are also used in freeze and wet regions. However, in the Dry and Non-Freeze region, the binders are way stiffer than the other regions, which is in accordance with the expectation.

4.5.c. Calculation of the m parameter, slope of the Creep Compliance curve

In this section, the slope of the creep compliance curve is calculated according to the three formulas suggested in Section 3.5. The formulas are inserted below:

$$m_{-20^oC} == 1.75987 + 1.78187 * V_a^{0.02030} + 0.00089 * Pen_{77}^{0.96870}$$

$$m_{-10^oC} = -1.8269 + 1.94218 * V_a^{0.01600} + 0.00098 * Pen_{77}^{0.96857}$$

$$m_{0^oC} = -2.41043 + 2.59093 * V_a^{0.01547} + 0.00199 * Pen_{77}^{0.97247}$$

After the calculation of the Penetration value at 77°F in the previous section, the m values obtained are summarized below in Table 25:

*Table 25- Variation of the m parameters in terms of Va and Vb at Different Temperatures*

| State | City | Climate Zone | Va | Vbe | m -20°C | m -10°C | m 0°C |
|---|---|---|---|---|---|---|---|
| **Arizona** | Flagstaff | Dry, Freeze | 4.9 | 9.7 | 0.152 | 0.243 | 0.407 |
| **Alaska** | Anchorage | | 3.9 | 10.1 | 0.301 | 0.406 | 0.758 |
| **Colorado** | Rio Blanco | | 4 | 10.3 | 0.249 | 0.349 | 0.638 |
| **Colorado** | El Paso | | 5.3 | 8.71 | 0.154 | 0.245 | 0.410 |
| **Colorado** | Yuma | | 7.4 | 7.61 | 0.150 | 0.237 | 0.385 |
| **Washington** | Spokane | | 6 | 8 | 0.159 | 0.249 | 0.415 |
| **Arizona** | Tucson | Dry, No Freeze | 4.6 | 10 | 0.106 | 0.193 | 0.305 |
| **Arizona** | Phoenix | | 4.5 | 10.1 | 0.099 | 0.187 | 0.292 |
| **Arizona** | Kingman | | 3.9 | 10.7 | 0.105 | 0.194 | 0.311 |
| **Indiana** | La Porte | Wet, Freeze | 6.18 | 10.4 | 0.160 | 0.250 | 0.416 |
| **Indiana** | Jackson | | 2.7 | 11.3 | 0.129 | 0.224 | 0.382 |
| **Kansas** | Cherokee | | 5 | 9 | 0.123 | 0.212 | 0.342 |
| **Massachusetts** | Boston | | 5.6 | 8.4 | 0.141 | 0.231 | 0.378 |
| **Massachusetts** | Springfield | | 2.3 | 11.7 | 0.124 | 0.219 | 0.376 |
| **Michigan** | Port Huron | | 4 | 10 | 0.144 | 0.236 | 0.398 |
| **Michigan** | Alpena | | 2.7 | 11.3 | 0.158 | 0.255 | 0.449 |
| **Michigan** | Marquette | | 5.1 | 8.87 | 0.182 | 0.275 | 0.475 |
| **Michigan** | Grand Rapids | | 3.5 | 10 | 0.164 | 0.259 | 0.451 |
| **West Virginia** | Kanawha | | 5.1 | 8.86 | 0.124 | 0.213 | 0.343 |
| **Alabama** | Montgomery | Wet, No Freeze | 5.8 | 9.2 | 0.123 | 0.210 | 0.335 |
| **Alabama** | Tuscaloosa | | 5.2 | 9.8 | 0.119 | 0.207 | 0.330 |
| **Arkansas** | Little Rock | | 3 | 12.3 | 0.099 | 0.189 | 0.308 |
| **Indiana** | Jefferson | | 4.3 | 10.7 | 0.147 | 0.238 | 0.401 |
| **Kansas** | Scott | | 3.2 | 10.8 | 0.119 | 0.211 | 0.351 |
| **South Carolina** | Columbia | | 7.9 | 6.1 | 0.135 | 0.220 | 0.347 |
| **Tennessee** | Memphis | | 6 | 8 | 0.130 | 0.218 | 0.349 |
| **Washington** | Seattle | | 8.9 | 5.1 | 0.171 | 0.259 | 0.425 |
| **West Virginia** | Charleston | | 6.7 | 7.3 | 0.134 | 0.221 | 0.354 |

The trend of the m parameter also coincides with the concepts discussed. With increase of temperature, the m-parameter is increasing, leading to a higher value of the creep compliance.

In terms of climatic regions, the higher values of the m parameter are relatively observed in the freeze regions. The Figure 46 below shows this behavior for each climate region:

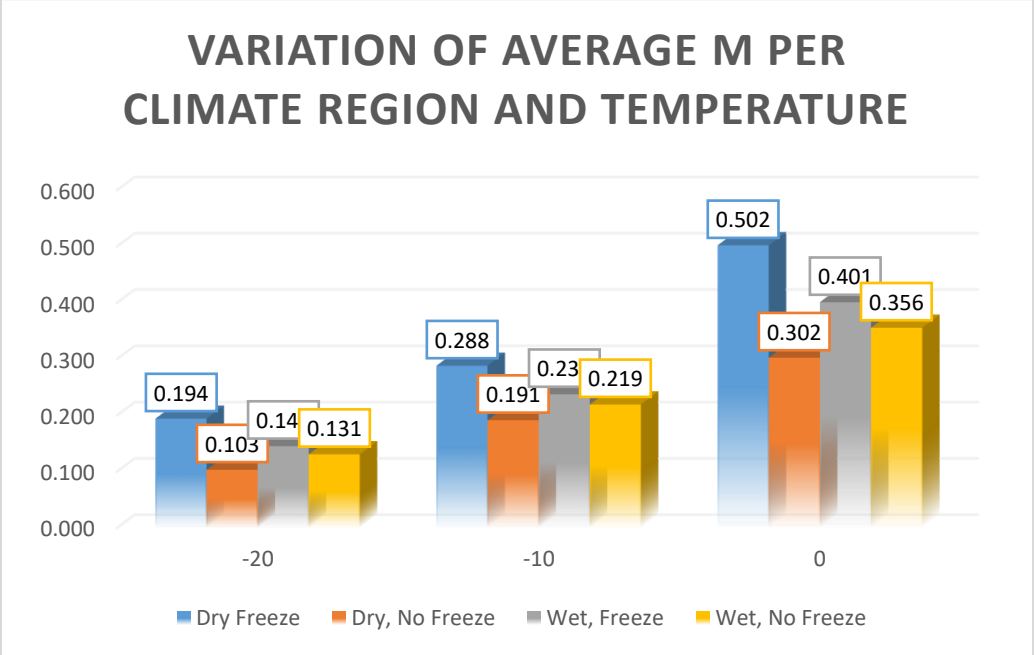


*Figure 46- Variation of the m parameter with temperature and climate regions*

The average values of the m-parameter are shown in the graph above. The variation observed per temperature follows the expected trend, as the creep compliance increase with increasing temperatures, the "m" fracture parameter increases too. Also, it can be noticed that the values of this parameter are different within the different climate zones. It is noticeable that some of the highest values happen at the wet regions.

4.5.d. Calculation of the Creep Compliance values at 100 seconds

Typical creep compliance values were calculated for a loading time of 100 seconds using the previous parameters. A typical response was used in the following form:

$$D(t) = D_1 * t^m$$

The creep compliance was found respectively for the three testing temperatures. The results are summarized below in Table 26:

*Table 26- Creep Compliance Variation with respect to Temperature and Climate Region*

| State | City | Climate Zone | D (100) -20°C | D (100) -10°C | D (100) 0°C |
|---|---|---|---|---|---|
| **Arizona** | Flagstaff | Dry, Freeze | 4.92E-07 | 1.13E-06 | 3.19E-06 |
| **Alaska** | Anchorage | Dry, Freeze | 1.00E-06 | 2.25E-06 | 1.46E-05 |
| **Colorado** | Rio Blanco | Dry, Freeze | 8.13E-07 | 1.80E-06 | 8.67E-06 |
| **Colorado** | El Paso | Dry, Freeze | 4.17E-07 | 1.02E-06 | 2.98E-06 |
| **Colorado** | Yuma | Dry, Freeze | 3.19E-07 | 9.09E-07 | 2.71E-06 |
| **Washington** | Spokane | Dry, Freeze | 3.52E-07 | 9.32E-07 | 2.86E-06 |
| **Arizona** | Tucson | Dry, No Freeze | 4.26E-07 | 9.27E-07 | 2.02E-06 |
| **Arizona** | Phoenix | Dry, No Freeze | 4.18E-07 | 9.00E-07 | 1.90E-06 |
| **Arizona** | Kingman | Dry, No Freeze | 4.47E-07 | 9.17E-07 | 1.98E-06 |
| **Indiana** | La Porte | Wet, Freeze | 5.65E-07 | 1.36E-06 | 3.99E-06 |
| **Indiana** | Jackson | Wet, Freeze | 4.30E-07 | 8.26E-07 | 2.07E-06 |
| **Kansas** | Cherokee | Wet, Freeze | 4.03E-07 | 9.33E-07 | 2.29E-06 |
| **Massachusetts** | Boston | Wet, Freeze | 3.64E-07 | 9.14E-07 | 2.52E-06 |
| **Massachusetts** | Springfield | Wet, Freeze | 3.84E-07 | 7.14E-07 | 1.75E-06 |
| **Michigan** | Port Huron | Wet, Freeze | 4.83E-07 | 1.04E-06 | 2.80E-06 |
| **Michigan** | Alpena | Wet, Freeze | 4.92E-07 | 9.54E-07 | 2.82E-06 |
| **Michigan** | Marquette | Wet, Freeze | 4.91E-07 | 1.19E-06 | 4.06E-06 |
| **Michigan** | Grand Rapids | Wet, Freeze | 8.05E-07 | 1.53E-06 | 4.60E-06 |
| **West Virginia** | Kanawha | Wet, Freeze | 3.93E-07 | 9.25E-07 | 2.29E-06 |
| **Alabama** | Montgomery | Wet, No Freeze | 3.15E-07 | 8.04E-07 | 1.98E-06 |
| **Alabama** | Tuscaloosa | Wet, No Freeze | 3.48E-07 | 8.36E-07 | 1.98E-06 |
| **Arkansas** | Little Rock | Wet, No Freeze | 3.49E-07 | 6.91E-07 | 1.45E-06 |
| **Indiana** | Jefferson | Wet, No Freeze | 5.43E-07 | 1.16E-06 | 3.16E-06 |
| **Kansas** | Scott | Wet, No Freeze | 5.10E-07 | 9.77E-07 | 2.29E-06 |
| **South Carolina** | Columbia | Wet, No Freeze | 1.14E-07 | 4.07E-07 | 1.20E-06 |
| **Tennessee** | Memphis | Wet, No Freeze | 3.23E-07 | 8.38E-07 | 2.19E-06 |
| **Washington** | Seattle | Wet, No Freeze | 8.95E-08 | 3.67E-07 | 1.42E-06 |
| **West Virginia** | Charleston | Wet, No Freeze | 2.58E-07 | 7.31E-07 | 2.01E-06 |

The creep compliance values are observed to increase with increasing temperature. Also, the regions with freeze are noted to have a higher compliance. As the binder gets stiffer, the

pavement structure will behave in a brittle manner leading to more thermal cracking (lower compliance)/

The following Figure 47 shows the described trend by the average creep compliance values with respect to the climate regions:

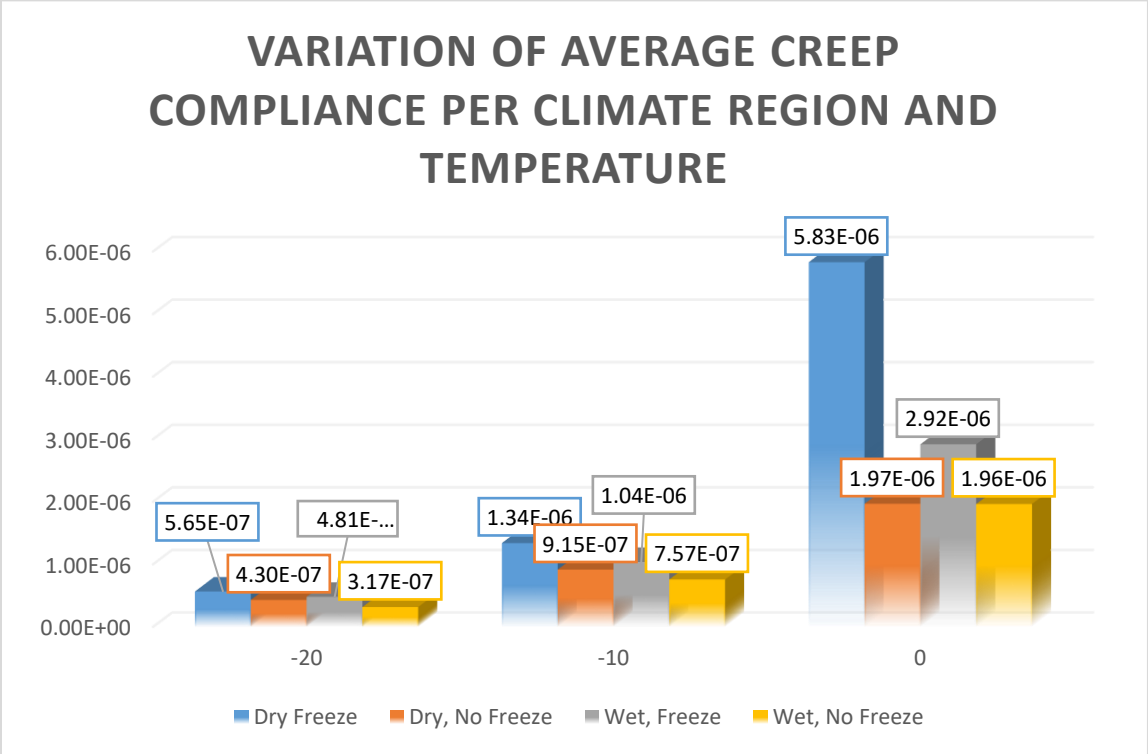


*Figure 47- Average Creep Compliance Variation with Temperature and Climate Region at 100 seconds*

The following observations can be concluded:

a. When the temperature increases, the creep compliance increases. The asphalt binder gets softer, and is more prone to resist thermal cracking

b. The highest creep compliance values are exhibited in the Dry Freeze and Wet Freeze regions, due to the soft choice of the PG-Binder. Because softer binders are chosen for the Freezing regions, the compliance is higher.

c. Since the values of the creep compliance are higher in the freeze regions, they are more prone to resist thermal cracking.

4.5.e. Calculation of the Total Effective Energy

The total effective energy is the energy needed to fracture the sample. In other words, the energy needed to initiate and crack, and propagate it. The total effective energy is the total of the effective energy to failure, and the post-peak energy as described in Section 3.5.

The following relationship has been introduced at a specific temperature of -10°C.

$$\Gamma_{tfr} = 4497.832 - 439.057 * AC + 46.284 * AC^2 - 2057.821 * AV + 40.009 * AV^2 + 12612.114 * \log(V_{beff}) + 13.571.050 * \log(VMA) - 345.948 * VFA + 8.056 * Pen_{77} - 0.052 * Pen_{77}^2 + 1.044 * AC * Rubber\%$$

The results are summarized in the Table 27 below:

*Table 27- Effective Fracture Energy*

| State | City | Climate Zone | Fracture Energy |
|---|---|---|---|
| **Arizona** | Flagstaff | Dry, Freeze | -101.68 |
| **Alaska** | Anchorage | Dry, Freeze | -3109.29 |
| **Colorado** | Rio Blanco | Dry, Freeze | -1568.32 |
| **Colorado** | El Paso | Dry, Freeze | -118.39 |
| **Colorado** | Yuma | Dry, Freeze | 271.91 |
| **Washington** | Spokane | Dry, Freeze | 60.49 |
| **Arizona** | Tucson | Dry, No Freeze | -224.70 |
| **Arizona** | Phoenix | Dry, No Freeze | -260.23 |
| **Arizona** | Kingman | Dry, No Freeze | -281.67 |
| **Indiana** | La Porte | Wet, Freeze | 248.46 |
| **Indiana** | Jackson | Wet, Freeze | -574.19 |
| **Kansas** | Cherokee | Wet, Freeze | -56.94 |
| **Massachusetts** | Boston | Wet, Freeze | -13.66 |
| **Massachusetts** | Springfield | Wet, Freeze | -645.89 |
| **Michigan** | Port Huron | Wet, Freeze | -374.86 |
| **Michigan** | Alpena | Wet, Freeze | -729.83 |
| **Michigan** | Marquette | Wet, Freeze | -291.67 |
| **Michigan** | Grand Rapids | Wet, Freeze | -738.12 |
| **West Virginia** | Kanawha | Wet, Freeze | -97.91 |
| **Alabama** | Montgomery | Wet, No Freeze | 99.60 |
| **Alabama** | Tuscaloosa | Wet, No Freeze | 32.49 |
| **Arkansas** | Little Rock | Wet, No Freeze | -80.44 |
| **Indiana** | Jefferson | Wet, No Freeze | -34.87 |
| **Kansas** | Scott | Wet, No Freeze | -457.88 |
| **South Carolina** | Columbia/Lexington | Wet, No Freeze | 353.10 |
| **Tennessee** | Memphis | Wet, No Freeze | 42.37 |
| **Washington** | Seattle | Wet, No Freeze | 518.95 |
| **West Virginia** | Charleston | Wet, No Freeze | 224.91 |

It is widely noticed that some values of this effective energy are negative. The concept behind this equation is that the higher the effective energy, the more resistant the mixture is to thermal

cracking. Once developed, this model had shown an extremely high level of accuracy ($R^2$=0.99) and Se/Sy =0.176, which means that this correlation is extremely reliable.

Therefore, it was determined that the range of this model are rather limited, and not all the inputted volumetrics will generate a reliable output. Based on observation, the following limiting criteria was developed for this relationship in Table 28:

*Table 28- Limitation Criteria for the Effective Thermal Cracking Predictive Model*

| **Limitation Criteria** | |
|---|---|
| **4< AC <6** | |
| **3.5 <Va< 7.5** | |
| **VMA** | >14 |
| **56 < VFA < 74** | |
| **VBE** | >8 |
| **24< PEN 77 <130** | |

These limitation criteria are however approximate, as the data by itself doesn't have a linear relationship in between the input data. However, the following trends have been recorded, by changing one input variable at a time:

- Concerning the asphalt content values (AC), the total effective energy decreases for values of AC less than 5 and increases for values greater than 5%.
- For the air void content $V_a$, it decreases with an increase of air void content
- For the VMA, it increases with an increase in VMA and is sensitive to it
- For $V_{beff}$, it increases with an increase in $V_{beff}$ and is highly sensitive to it
- With increasing $Pen_{77}$, the effective energy increases.

4.5.f. Calculation of Tensile strength $S_t$

Next, the tensile strength $S_t$ is generated for the available data based on the previously described model:

$$S_t = 4976.34 - 42.49 * V_a - 2.73 * V_a^2 - 80.61 * VFA + 0.465 * VFA^2 + 174.35$$

$$* \log(Pen_{77}) - 1{,}217.54 * \log(A_{RTFO})$$

The results are summarized in Table 29 below:

*Table 29- Tensile Strength at -10C in psi*

| State | City | Climate Zone | Tensile Strength |
|---|---|---|---|
| **Arizona** | *Flagstaff* | *Dry, Freeze* | 486 |
| **Alaska** | *Anchorage* | *Dry, Freeze* | 551 |
| **Colorado** | *Rio Blanco* | *Dry, Freeze* | 526 |
| **Colorado** | *El Paso* | *Dry, Freeze* | 546 |
| **Colorado** | *Yuma* | *Dry, Freeze* | 708 |
| **Washington** | *Spokane* | *Dry, Freeze* | 621 |
| **Arizona** | *Tucson* | *Dry, No Freeze* | 399 |
| **Arizona** | *Phoenix* | *Dry, No Freeze* | 377 |
| **Arizona** | *Kingman* | *Dry, No Freeze* | 389 |
| **Indiana** | *La Porte* | *Wet, Freeze* | 468 |
| **Indiana** | *Jackson* | *Wet, Freeze* | 451 |
| **Kansas** | *Cherokee* | *Wet, Freeze* | 487 |
| **Massachusetts** | *Boston* | *Wet, Freeze* | 558 |
| **Massachusetts** | *Springfield* | *Wet, Freeze* | 461 |
| **Michigan** | *Port Huron* | *Wet, Freeze* | 463 |
| **Michigan** | *Alpena* | *Wet, Freeze* | 478 |
| **Michigan** | *Marquette* | *Wet, Freeze* | 558 |
| **Michigan** | *Grand Rapids* | *Wet, Freeze* | 548 |
| **West Virginia** | *Kanawha* | *Wet, Freeze* | 499 |
| **Alabama** | *Montgomery* | *Wet, No Freeze* | 448 |
| **Alabama** | *Tuscaloosa* | *Wet, No Freeze* | 405 |
| **Arkansas** | *Little Rock* | *Wet, No Freeze* | 354 |
| **Indiana** | *Jefferson* | *Wet, No Freeze* | 445 |
| **Kansas** | *Scott* | *Wet, No Freeze* | 449 |
| **South Carolina** | *Columbia/Lexington* | *Wet, No Freeze* | 845 |
| **Tennessee** | *Memphis* | *Wet, No Freeze* | 587 |
| **Washington** | *Seattle* | *Wet, No Freeze* | 1146 |
| **West Virginia** | *Charleston* | *Wet, No Freeze* | 682 |

The trend of the results of the tensile strength values do follow the analysis in the previous chapter Section 3.5.e. As the binder is stiffer, the tensile strength decreases. The results are also more sensitive to the change in the effective binder content with a higher air void content. However, in terms of climate regions, the average results are shown below in Figure 48:

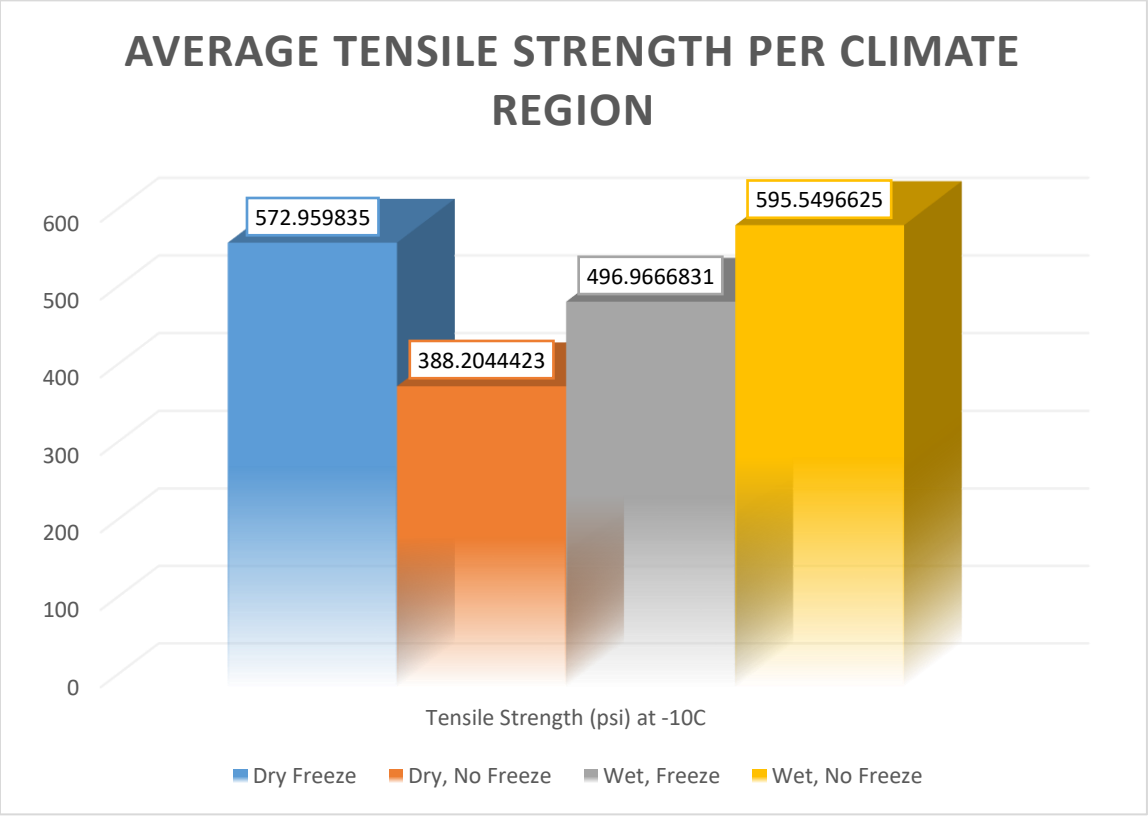


*Figure 48- Average Tensile Strength Values for Different Climatic Regions*

As mentioned previously, the softer the binder, the higher the values of the tensile strength. As mentioned previously, very soft binders are used in the Freeze Regions, which explains the high values of the tensile strength, whereas very stiff binders are used in the Dry, No Freeze region.

However, the amount of thermal cracks do not solely depend on the values of the tensile strength, but on all the variables generated within this section together. For this reason, the

TCMODEL generates the amount of cracking based on these variables and give an estimate of the expected thermal cracking that would happen during the pavement life.

As the TCMODEL was not run for this study due to some input data missing, an observation was made by comparing all of the obtained results in order to estimate the amount of thermal cracking that could be expected, with respect to the amount of transverse cracks measured by the LTPP Database.

4.5.g. Estimation of the Amount of Thermal Cracking

As mentioned in the previous section, the amount of transverse cracking was recorded by the LTPP for each section. This gathered data will be used to compare all the input variables generated for the TCMODEL and give an estimate of the thermal cracking that would happen.

Zborowski (2007) (31) have run the thermal cracking model (TCMODEL) and have generated the amount of thermal cracks to be expected along a certain number of years. Only the results obtained after the first year were considered for the comparison, as the generation of the first crack will mean that the tensile strength has been reached.

In addition to the transverse cracks, the longitudinal cracks in the Non-Wheel path have been added to the analysis, as they are part of the thermal cracking happening on the asphalt pavement structure. This data has been gathered from the first few years after the construction of the pavement section, as thermal cracking is assumed to happen in the early years of the pavement life.

The APPENDIX A

DATA AND RESULTS FOR THE LTPP DATABASE

*Table 54-Collected LTPP Database*

| LOCATIONS | | | MEASURED DISTRESSES | | | | |
|---|---|---|---|---|---|---|---|
| **State** | **City** | **Section** | **Fatigue (ft2)** | **Transverse Cracks (count)** | **Long. NWP (ft)** | **Long. In the WP (ft)** | **Rutting (in)** |
| **Alabama** | *Montgomery* | 4125 | 825 | 80 | 0 | 0 | 0.55 |
| | *Tuscaloosa* | 6012 | 1352 | 57 | 314.63 | 14.11 | 0.35 |
| **Arizona** | *Tucson* | 6054 | 13 | 87 | 731.63 | 0.00 | 0.35 |
| | *Phoenix* | B961 | 498 | 4 | 0.00 | 0.00 | 0.24 |
| | *Flagstaff* | 669 | 0 | 97 | 239.50 | 0.00 | 0.24 |
| | *Kingman* | 1022 | 1294 | 0 | 32.81 | 0.00 | 0.43 |
| **Alaska** | *Anchorage* | 1004 | 22 | 0 | 141.08 | 0.00 | 0.98 |
| **Arkansas** | *Little Rock* | A606 | 656 | 0 | 16.40 | 0.00 | 0.16 |
| **Colorado** | *Rio Blanco* | 1053 | 926 | 14 | 61.68 | 0.00 | 0.63 |
| | *El Paso* | 7783 | 1199 | 12 | 75.46 | 0.00 | 0.79 |
| | *Yuma* | 502 | 812 | 5 | 397.64 | 108.3 | 0.20 |
| **Indiana** | *La Porte* | 5528 | 1424 | 75 | 1000.6 | 0.00 | 0.28 |
| | *Jackson* | A902 | 0 | 4 | 291.99 | 0.00 | 0.20 |
| | *Jefferson* | 18-1028 | 0 | 24 | 524.93 | 0.00 | 0.35 |
| **Kansas** | *Cherokee* | 1005 | 1663 | 58 | 619.75 | 4.59 | 0.20 |
| | *Scott* | 1006 | 358 | 37 | 119.75 | 0.00 | 0.08 |
| **Massachusetts** | *Boston* | 1003 | 1125 | 75 | 100.39 | 41.01 | 0.20 |
| | *Springfield* | 1002 | 2189 | 96 | 246.06 | 0.00 | 0.35 |
| **Michigan** | *Port Huron* | D330 | 0 | 56 | 772.64 | 8.20 | 0.00 |
| | *Alpena* | 6016 | 0 | 53 | 121.39 | 43.64 | 0.20 |
| | *Marquette* | 1004 | 24 | 40 | 505.25 | 0.00 | 0.12 |
| | *Grand Rapids* | 901 | 2955 | 7.4 | 941.60 | 0.00 | 0.20 |
| **South Carolina** | *Columbia* | 1024 | 243 | 0 | 9.84 | 0.00 | 0.16 |
| **Tennessee** | *Memphis* | 3109 | 237 | 0 | 0.00 | 0.00 | 0.24 |
| **Washington** | *Seattle* | 6049 | 0 | 2 | 130.58 | 130.58 | 0.00 |
| | *Spokane* | A320 | 14 | 29 | 649.61 | 2.95 | 0.75 |
| **West Virginia** | *Kanawha* | 1640 | 2778 | 0 | 374.02 | 0.00 | 0.12 |
| | *Charleston* | 7008 | 0 | 12 | 1000.9 | 0.00 | 0.24 |

| LOCATIONS | | DATA COLLECTED | | | | | | | | | | | |
|---|---|---|---|---|---|---|---|---|---|---|---|---|---|
| City | Section | $H_{HMA}$ (in) | PG | AC | $V_a$ | $P_{200}$ | $R_{04}$ | $R_{38}$ | $R_{34}$ | VMA | VFA | $V_{BE}$ | Meas ESAL |
| *Montgomery* | 4125 | 6 | 64-16 | 6 | 5.8 | 4.7 | 40 | 42 | 4 | 15 | 61 | 9 | 6.13E+06 |
| *Tuscaloosa* | 6012 | 5 | 64-16 | 6 | 5.2 | 4 | 63 | 12 | 4 | 15 | 65 | 10 | 2.86E+07 |
| *Tucson* | 6054 | 9 | 70-10 | 5 | 4.6 | 7.5 | 42 | 25 | 2 | 14.6 | 68 | 10 | 6.79E+06 |
| *Phoenix* | B961 | 10 | 76-10 | 5.3 | 4.5 | 3.8 | 50 | 35 | 9 | 14.6 | 69 | 10 | 5.46E+07 |
| *Flagstaff* | 669 | 6 | 58-28 | 4.6 | 4.9 | 4.7 | 52 | 39 | 5 | 14.6 | 66 | 10 | 5.48E+07 |
| *Kingman* | 1022 | 8.5 | 70-16 | 4.5 | 3.9 | 5.3 | 50 | 28 | 4 | 14.6 | 73 | 11 | 3.08E+07 |
| *Anchorage* | 1004 | 5.4 | 46-40 | 5.5 | 3.9 | 7.2 | 39 | 20 | 3 | 14 | 72 | 10 | 2.84E+06 |
| *Little Rock* | A606 | 5 | 64-16 | 5 | 3 | 9.4 | 60 | 39 | 15 | 15.3 | 80 | 12 | 2.04E+07 |
| *Rio Blanco* | 1053 | 6.8 | 46-34 | 4.8 | 4 | 9.1 | 48 | 19 | 0 | 14.3 | 72 | 10 | 2.14E+06 |
| *El Paso* | 7783 | 9.7 | 58-28 | 5 | 5.29 | 9.6 | 43 | 15 | 0 | 14 | 62 | 9 | 1.13E+07 |
| *Yuma* | 502 | 9.3 | 64-28 | 5 | 7.39 | 8.7 | 37 | 22 | 0 | 15 | 51 | 8 | 1.08E+07 |
| *La Porte* | 5528 | 7.2 | 58-28 | 4.8 | 6.18 | 5.9 | 40 | 33 | 0 | 16.6 | 63 | 10 | 5.97E+06 |
| *Jackson* | A902 | 6.8 | 58-28 | 5.4 | 2.7 | 5.8 | 46 | 35 | 0 | 14 | 81 | 11 | 8.23E+07 |
| *Jefferson* | 18-1028 | 18 | 58-28 | 3.7 | 4.303 | 3.1 | 59 | 35 | 0 | 15 | 71 | 11 | 1.84E+07 |
| *Cherokee* | 1005 | 12.7 | 64-22 | 6.5 | 5 | 9.5 | 21 | 14 | 0 | 14 | 64 | 9 | 1.07E+06 |
| *Scott* | 1006 | 14 | 64-28 | 5.8 | 3.2 | 8.2 | 39 | 19 | 0 | 14 | 77 | 11 | 1.17E+06 |
| *Boston* | 1003 | 6.6 | 58-22 | 5.6 | 5.6 | 5.4 | 46 | 18 | 0 | 14 | 60 | 8 | 6.55E+05 |
| *Springfield* | 1002 | 7.8 | 58-28 | 5 | 2.3 | 3.7 | 22 | 4 | 0 | 14 | 84 | 12 | 5.28E+06 |
| *Port Huron* | D330 | 2.2 | 58-28 | 5 | 4 | 6.2 | 14 | 9 | 0 | 14 | 71 | 10 | 1.67E+06 |
| *Alpena* | 6016 | 4.6 | 52-28 | 5 | 2.7 | 2.3 | 63 | 12 | 8 | 14 | 81 | 11 | 3.09E+06 |
| *Marquette* | 1004 | 4.2 | 52-28 | 5 | 5.12 | 6 | 30 | 13 | 7 | 14 | 63 | 9 | 1.33E+06 |
| *Grand Rapids* | 901 | 8.6 | 58-34 | 5 | 3.5 | 7 | 60 | 38 | 6 | 13.5 | 74 | 10 | 3.53E+07 |
| *Columbia* | 1024 | 1.6 | 64-16 | 5.2 | 7.9 | 3.7 | 30 | 8 | 0 | 14 | 44 | 6 | 2.60E+04 |
| *Memphis* | 3109 | 7 | 64-22 | 5.6 | 6 | 6 | 58 | 10 | 17 | 14 | 57 | 8 | 2.38E+06 |
| *Seattle* | 6049 | 10.6 | 52-16 | 5.5 | 8.9 | 5.2 | 42 | 23 | 2 | 14 | 36 | 5 | 6.54E+06 |

| | | | | | | | | | | | | | |
|---|---|---|---|---|---|---|---|---|---|---|---|---|---|
| ***Spokane*** | A320 | 2.7 | 58-28 | 5.6 | 6 | 5.6 | 41 | 16 | 5.6 | 14 | 57 | 8 | 9.57E +05 |
| ***Kanawha*** | 1640 | 2.5 | 64-22 | 6 | 5.14 | 2 | 35 | 6 | 0 | 14 | 63 | 9 | 1.52E +07 |
| ***Charleston*** | 7008 | 3.9 | 64-22 | 6 | 6.7 | 2.7 | 44 | 2 | 0 | 14 | 52 | 7 | 4.06E +07 |

*Table 55- Summary of the LTTP Database Thermal Input*

| State | City | Section | Climate Zone | D(100) @ -20°C | D(100) @ -10°C | D(100) @ 0°C | St (psi) | FE | Meas Transverse | Meas. Long. In the NWP |
|---|---|---|---|---|---|---|---|---|---|---|
| **Arizona** | *Flagstaff* | 669 | *DF* | 1.00E-06 | 2.25E-06 | 1.46E-05 | 551 | -3109.29 | 0 | 43 |
| **Alaska** | *Anchorage* | 1004 | | 4.92E-07 | 1.13E-06 | 3.19E-06 | 486 | -101.68 | 97 | 73 |
| **Colorado** | *Rio Blanco* | 1053 | | 8.13E-07 | 1.80E-06 | 8.67E-06 | 526 | -1568.32 | 14 | 18.8 |
| **Colorado** | *El Paso* | 7783 | | 4.17E-07 | 1.02E-06 | 2.98E-06 | 546 | -118.39 | 12 | 23 |
| **Colorado** | *Yuma* | 502 | | 3.19E-07 | 9.09E-07 | 2.71E-06 | 708 | 271.91 | 5 | 121.2 |
| **Washington** | *Spokane* | A320 | | 3.52E-07 | 9.32E-07 | 2.86E-06 | 621 | 60.49 | 29 | 198 |
| **Arizona** | *Tucson* | 6054 | *D, NF* | 4.26E-07 | 9.27E-07 | 2.02E-06 | 399 | -224.70 | 87 | 223 |
| **Arizona** | *Phoenix* | B961 | | 4.18E-07 | 9.00E-07 | 1.90E-06 | 377 | -260.23 | 4 | 0 |
| **Arizona** | *Kingman* | 1022 | | 4.47E-07 | 9.17E-07 | 1.98E-06 | 389 | -281.67 | 0 | 10 |
| **Indiana** | *La Porte* | 5528 | *W, F* | 5.65E-07 | 1.36E-06 | 3.99E-06 | 468 | 248.46 | 75 | 305 |
| **Indiana** | *Jackson* | A902 | | 4.30E-07 | 8.26E-07 | 2.07E-06 | 451 | -574.19 | 4 | 89 |
| **Kansas** | *Cherokee* | 1005 | | 4.03E-07 | 9.33E-07 | 2.29E-06 | 487 | -56.94 | 58 | 188.9 |
| **Massachusetts** | *Boston* | 1003 | | 3.64E-07 | 9.14E-07 | 2.52E-06 | 558 | -13.66 | 75 | 30.6 |
| **Massachusetts** | *Springfield* | 1002 | | 3.84E-07 | 7.14E-07 | 1.75E-06 | 461 | -645.89 | 96 | 75 |
| **Michigan** | *Port Huron* | D330 | | 4.83E-07 | 1.04E-06 | 2.80E-06 | 463 | -374.86 | 56 | 235.5 |
| **Michigan** | *Alpena* | 6016 | | 4.92E-07 | 9.54E-07 | 2.82E-06 | 478 | -729.83 | 53 | 37 |
| **Michigan** | *Marquette* | 1004 | | 4.91E-07 | 1.19E-06 | 4.06E-06 | 558 | -291.67 | 40 | 154 |
| **Michigan** | *Grand Rapids* | 901 | | 8.05E-07 | 1.53E-06 | 4.60E-06 | 548 | -738.12 | 7.4 | 287 |
| **West Virginia** | *Kanawha* | 1640 | | 3.93E-07 | 9.25E-07 | 2.29E-06 | 499 | -97.91 | 0 | 114 |
| **Alabama** | *Montgomery* | 4125 | *W, NF* | 3.15E-07 | 8.04E-07 | 1.98E-06 | 448 | 99.60 | 80 | 0 |
| **Alabama** | *Tuscaloosa* | 6012 | | 3.48E-07 | 8.36E-07 | 1.98E-06 | 405 | 32.49 | 57 | 95.9 |

| | | | | | | | | | | |
|---|---|---|---|---|---|---|---|---|---|---|
| **Arkansas** | *Little Rock* | A606 | | 3.49E-07 | 6.91E-07 | 1.45E-06 | 354 | -80.44 | 0 | 5 |
| **Indiana** | *Jefferson* | 18-1028 | | 5.43E-07 | 1.16E-06 | 3.16E-06 | 445 | -34.87 | 24 | 160 |
| **Kansas** | *Scott* | 1006 | | 5.10E-07 | 9.77E-07 | 2.29E-06 | 449 | -457.88 | 37 | 36.5 |
| **South Carolina** | *Columbia* | 1024 | | 1.14E-07 | 4.07E-07 | 1.20E-06 | 845 | 353.10 | 0 | 3 |
| **Tennessee** | *Memphis* | 3109 | | 3.23E-07 | 8.38E-07 | 2.19E-06 | 587 | 42.37 | 0 | 0 |
| **Washington** | *Seattle* | 6049 | | 8.95E-08 | 3.67E-07 | 1.42E-06 | 1146 | 518.95 | 2 | 39.8 |
| **West Virginia** | *Charleston* | 7008 | | 2.58E-07 | 7.31E-07 | 2.01E-06 | 682 | 224.91 | 12 | 305.1 |

that has all of the computed variables joined for the comparison is found in Appendix A

Table 55.

The observed trend for the results can be explained in the following method:

- The higher the tensile strength, the less is the measured number of cracks (approximately in all the cases stated)
- The higher the creep compliance, the lower the number of measured thermal cracking.

  However, the trend in the chart below is only verified for the Dry, Freeze Region as the measured thermal cracking outcomes are low compared to a high tensile strength and creep compliance value. For the Wet, No Freeze Region, the number of cracks observed is within the good range of thermal behavior, with a moderate value of creep compliance.

  For the other regions, (Dry No Freeze and Wet Freeze) the behaviors are very similar, whereas the measured and predicted values are very close to each other. The potential for thermal cracking for these 2 regions is the highest among the four different climates.
- The Figure 49 below indicates that tensile strength and creep compliance for only one temperature (-10$^{o}$C) at one loading rate (100 seconds) is not representative of the thermal cracking behavior that may happen in the field, and the values of tensile strength are not significantly related to the thermal behavior of the pavement.
- Generally, thermal cracking would occur at lower temperatures and colder climates, due to the stiffening of the binder. Potentially, the Freeze regions are

more susceptible to this kind of behavior. However, it all depends on the kind of mixtures implemented by the agencies in the field and what type of improvements they implement to help against the formation of distresses.

- It is also noticed from the graph below that the Wet, Freeze Regions, which are the most susceptible to Low Temperature Cracking, that despite having high tensile strength and creep compliance, the measured distresses are still high. This means that there is room for improving their mix designs, even though they are supposed to perform better than expected.

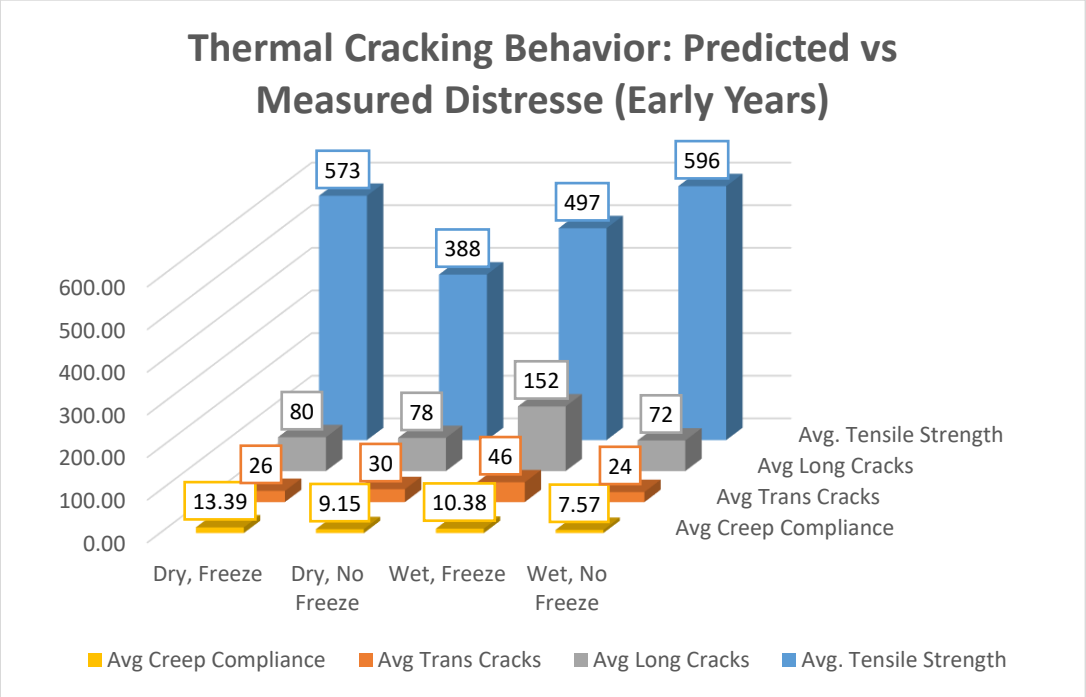


*Figure 49- Thermal Cracking Behavior: Predicted Variables vs Measured Distresses for the LTPP Database*

- The transverse cracks were not separated from reflective cracks. As the data has been gathered by the LTPP, it was not possible to conduct such distinction. Therefore, the transverse cracks all in all were considered as thermal cracks. This could possibly alter the results, but the overall analysis is not affected.

In the following scatterplot Figure 50, the predicted variables are plotted against the measured distresses. The plot does not have consistent units, but basically show a potential increase in tensile strength when the measured distresses (i.e. thermal and transverse cracking) are still low. This could lead to a possible relationship between the two. However, this theory still needs to be further detailed and proven by extensive field testing.

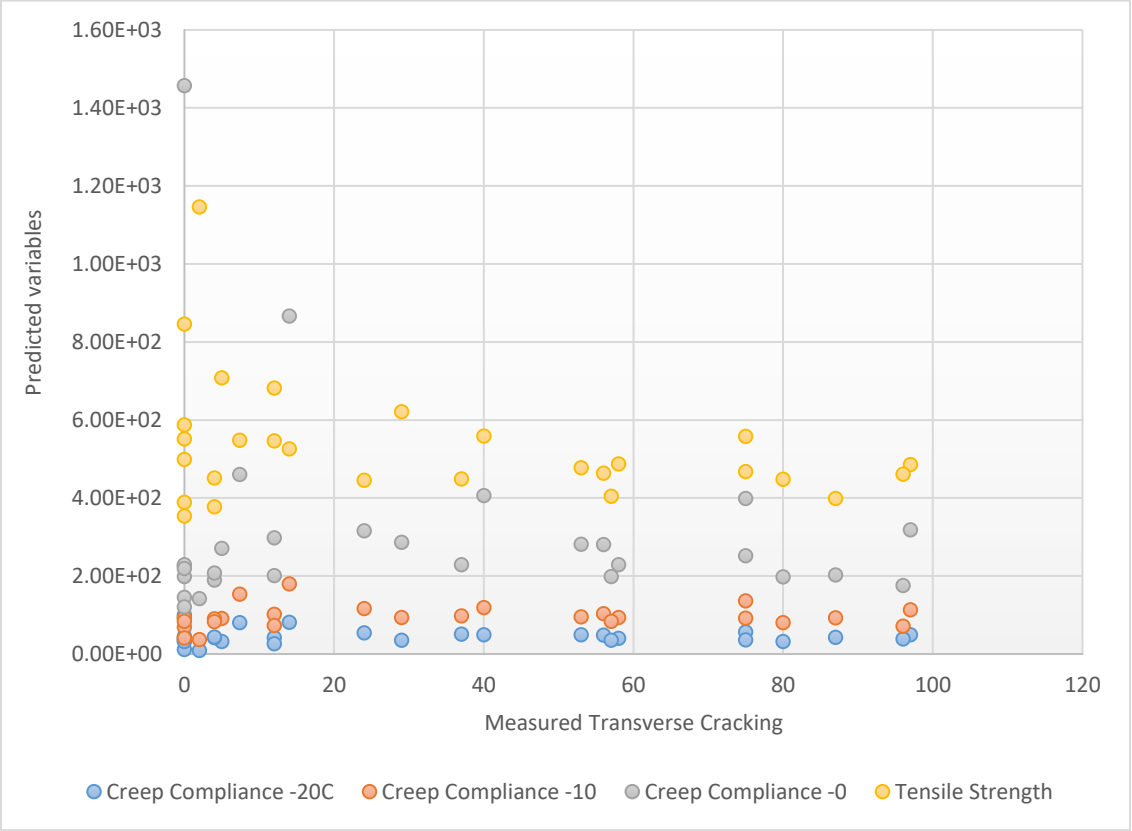


*Figure 50- Average Values Visualization*

# CHAPTER 5

# 5 DESCRIPTION AND ANALYSIS OF THE NEW U.S. PAVEMENT MIXTURES

## 5.1 Data Gathering and Description of the Data Collected from the USA

The Long-Term Pavement Performance, also known as the LTPP, is one of the greatest pavement databases known in North America. As most of the data collected in this database goes far in time, one of the objectives tackled for this study was to gather brand new pavement mixtures. The purpose of this new data collection is to study the advancement of the designs implemented and see how agencies are addressing the distresses arising along the pavement life of the structures.

The first step in this data collection required the gathering of the contact information of the current State Engineers all over the United States. A formal e-mail was put together and sent out for the unique purpose of graduate research at ASU. Only 50% of the state engineers ccontacted were responsive to the research call and provided with the data requested.

The requested data had to include the pavement volumetrics used for HMA pavements (Hot Mix Asphalt). This was the main target, as other types of pavements would be collected further in the future. In addition, these pavement mixtures had to be dated recently, and applied on Highways (i.e.: Heavy Traffic) as Surface Mixtures. One of the most important requests was the gathering of multiple HMA pavement mixtures belonging to several climate zones within the same state. This highlights the difference between the data collected per climatic regions and per state location.

Another objective of this study is to study the difference between the old and new pavement mixtures, belonging to the same climatic regions as well as traffic volumes within the same state. For this reason, the LTPP sections gathered previously falls within the same regions, serves the same purpose and have approximately the same climatic conditions with the new pavement mixtures gathered.

Having 25 responses from 25 states, the data was gathered and summarized in the Table 57 in Appendix C per state and per location.

The following Figure 51 shows how many sections belong to each climate zone:

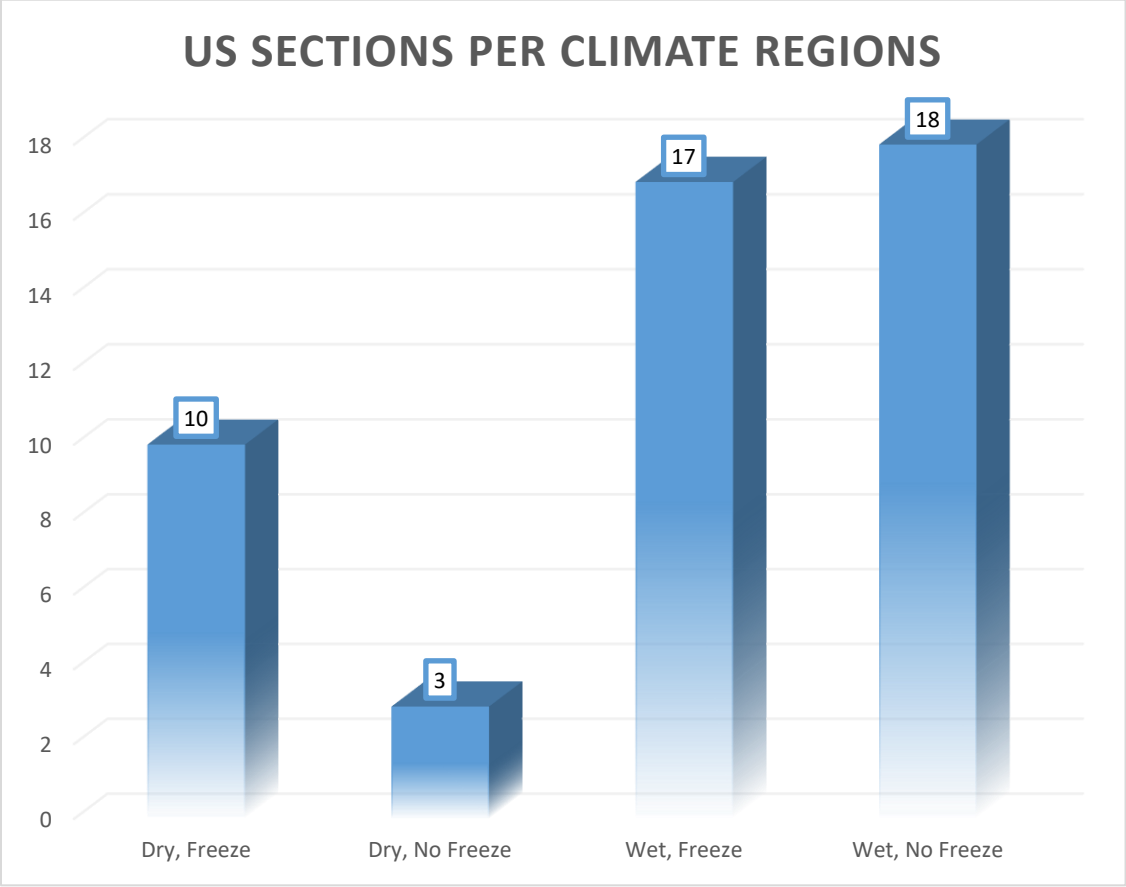


*Figure 51- Number of new US Sections per Climatic Regions*

Then, the distribution of the asphalt binders was observed and summarized in the following Figure 52:

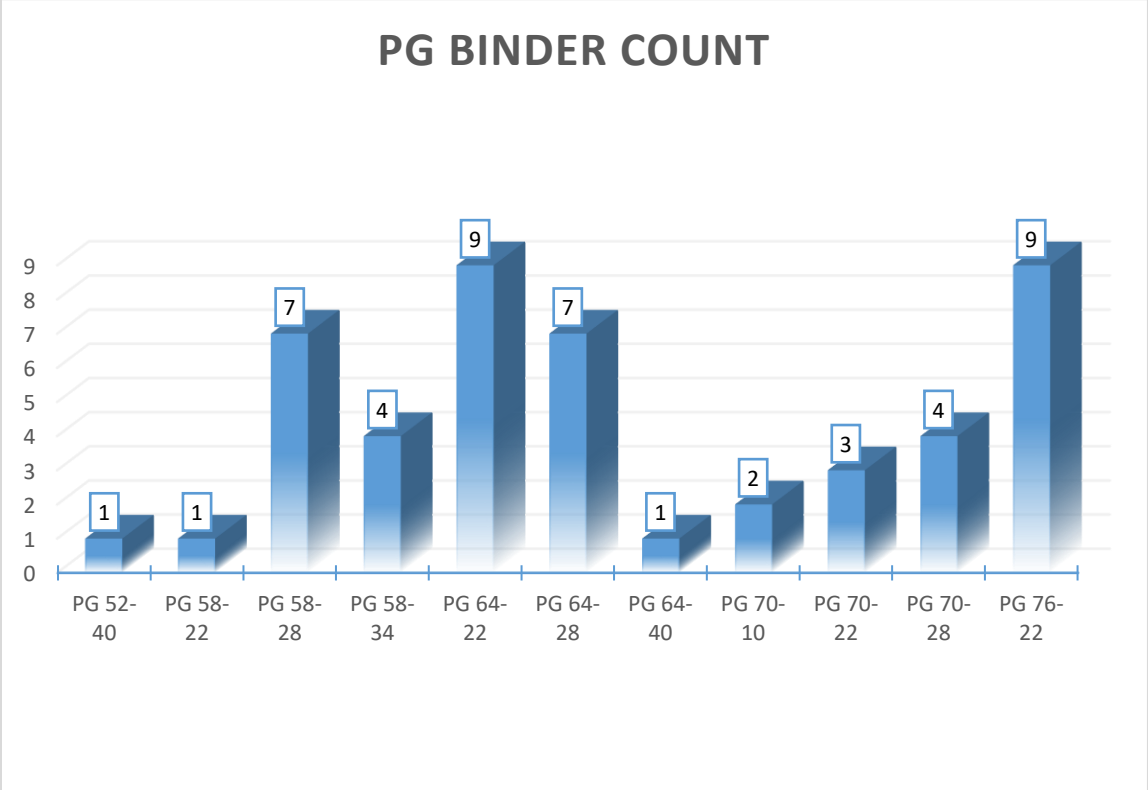


*Figure 52- PG-Binder Distribution for the new US pavement mixtures*

Referring to the table above, the Freeze zones (Dry, Freeze and Wet, Freeze) have on average stiffer binders than the regions with No Freeze. However, the binder chosen all over the regions have closer ranges than the ones found in the LTPP Database.

A total of 48 sections have been gathered and included in this study. The following Figure 53 shows how many sections belong to the specific states:

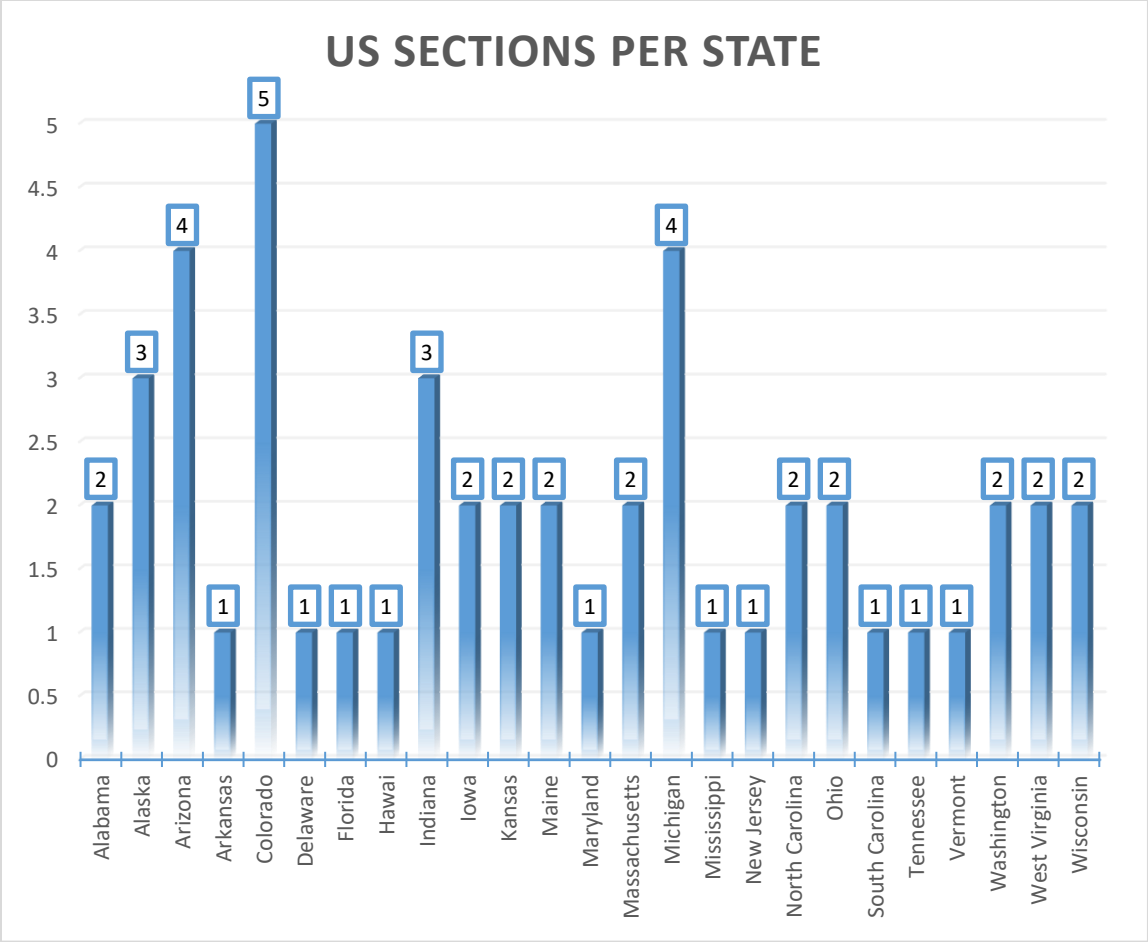


*Figure 53- US Sections per State*

The following table shows the minimum, maximum and average values for the volumetrics gathered from the mix designs collected. It also includes variables needed to develop the predictive models describe in Chapter 3. All the data gathered will then be compared in Chapter 6 to see the evolution of the designs and if the agencies are modifying their designs as per the expected pavement performance. The distresses were not measured for these pavement mixtures, as few of them have not been yet implemented in the field. The performance of these mixtures will be assessed based on the predictive models implemented in the previous chapter.

The following Table 30 summarizes the mean, maximum and minimum values for the volumetrics. The remaining of the data for this database is found in Appendix C, Table 57.

*Table 30-Volumetric Values for US Database*

| | US Database | | |
|---|---|---|---|
| **Number of Sections: 48** | **Min** | **Mean** | **Max** |
| **$V_a$ (%)** | 3.3 | 4.05333 | 5.8 |
| **Ac (%)** | 3.9 | 5.59833 | 6.7 |
| **$V_{be}$ (%)** | 8 | 11.591 | 14.5 |
| **VMA (%)** | 12 | 15.6444 | 18.3 |
| **VFA (%)** | 64.8 | 73.9 | 80.6 |
| **$R_{34}$ (%)** | 0 | 2.19583 | 35 |
| **$R_{38}$ (%)** | 0 | 14.8854 | 55 |
| **$R_{04}$ (%)** | 3.0 | 40.7229 | 67 |
| **$P_{200}$ (%)** | 3.33 | 5.40104 | 10 |

Concerning the frequency distribution of the variables, the following graphs have been generated to describe the data collected from Figure 54 to Figure 62:

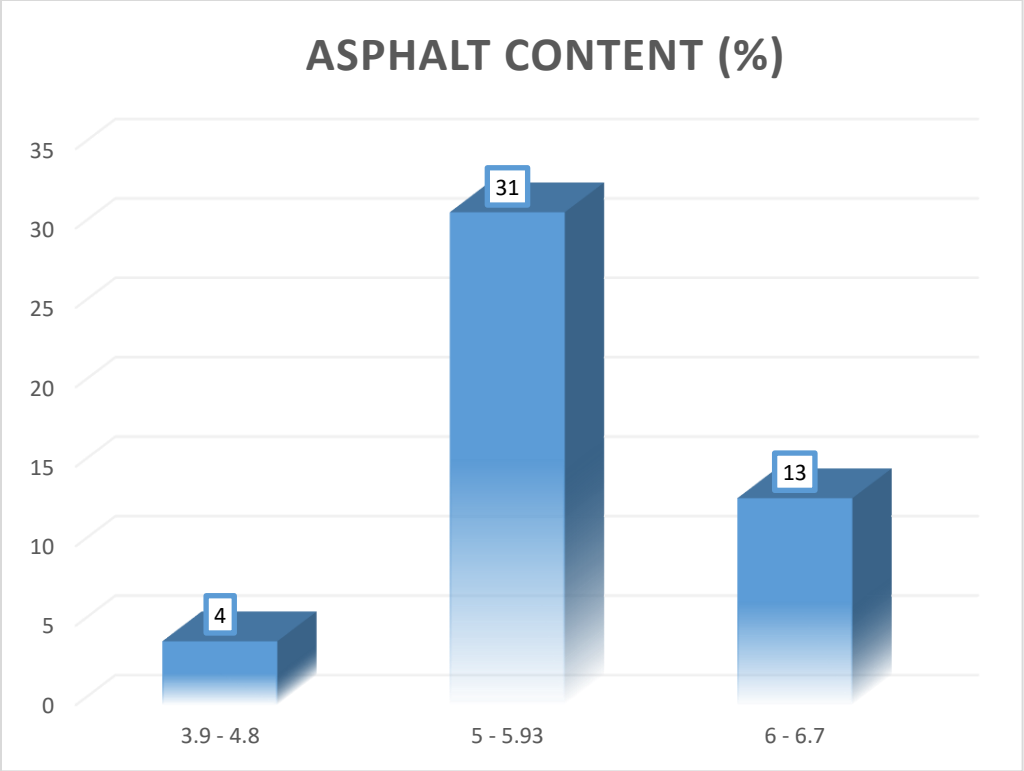


*Figure 54- US Database Asphalt Content (%) Observation*

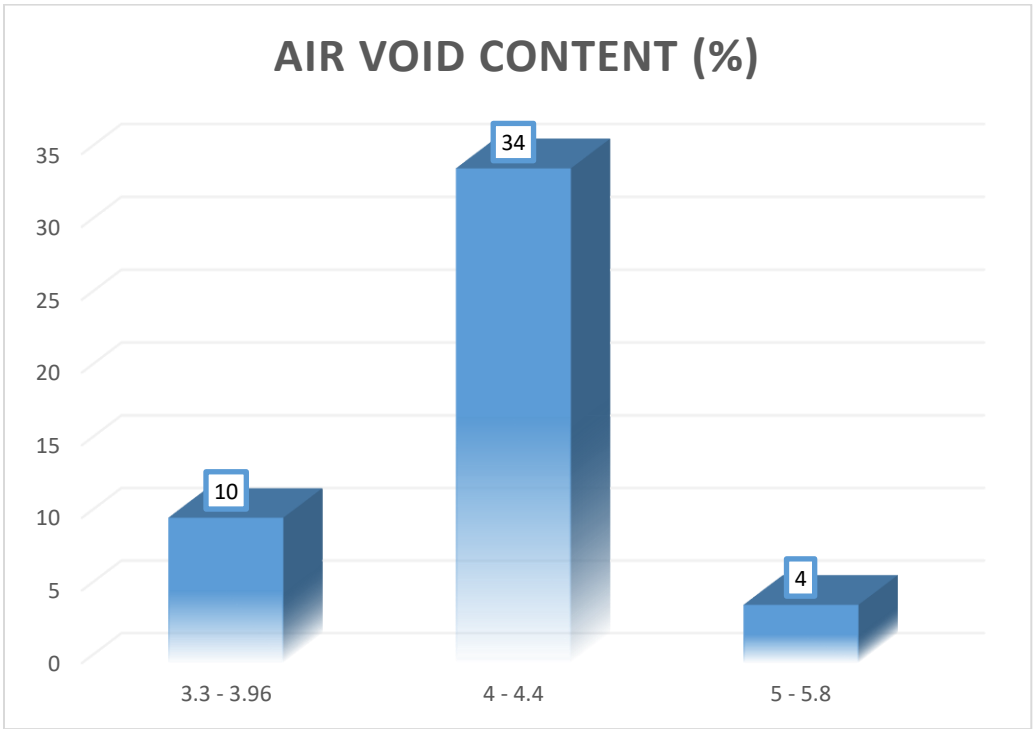


*Figure 55- US Database Air Void Content (%)*

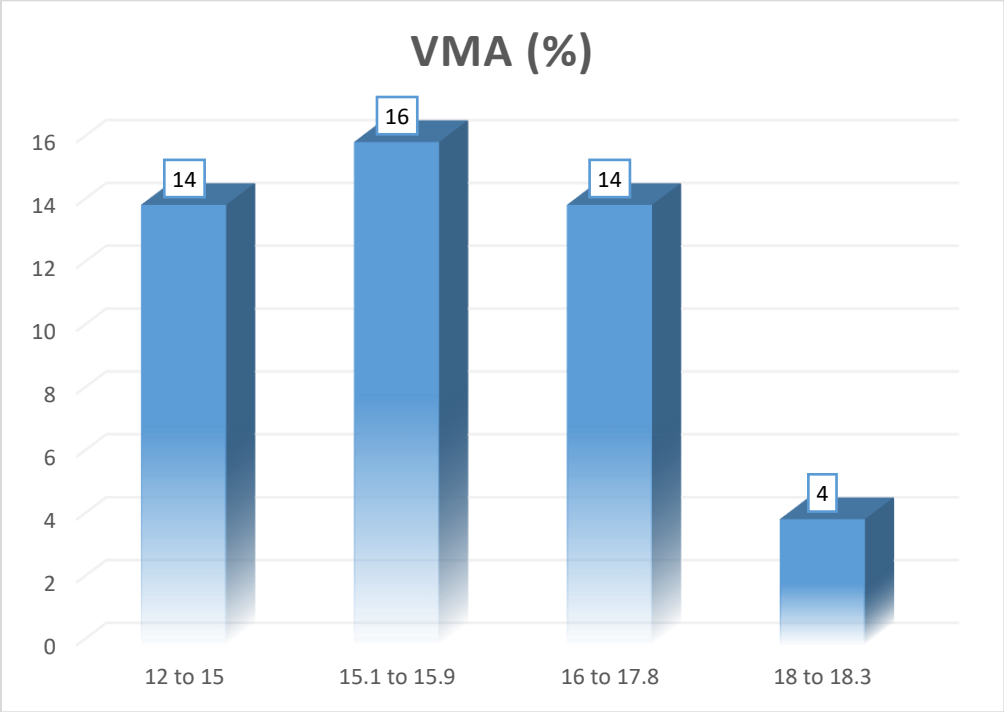


*Figure 56- US Database VMA Ranges (%)*

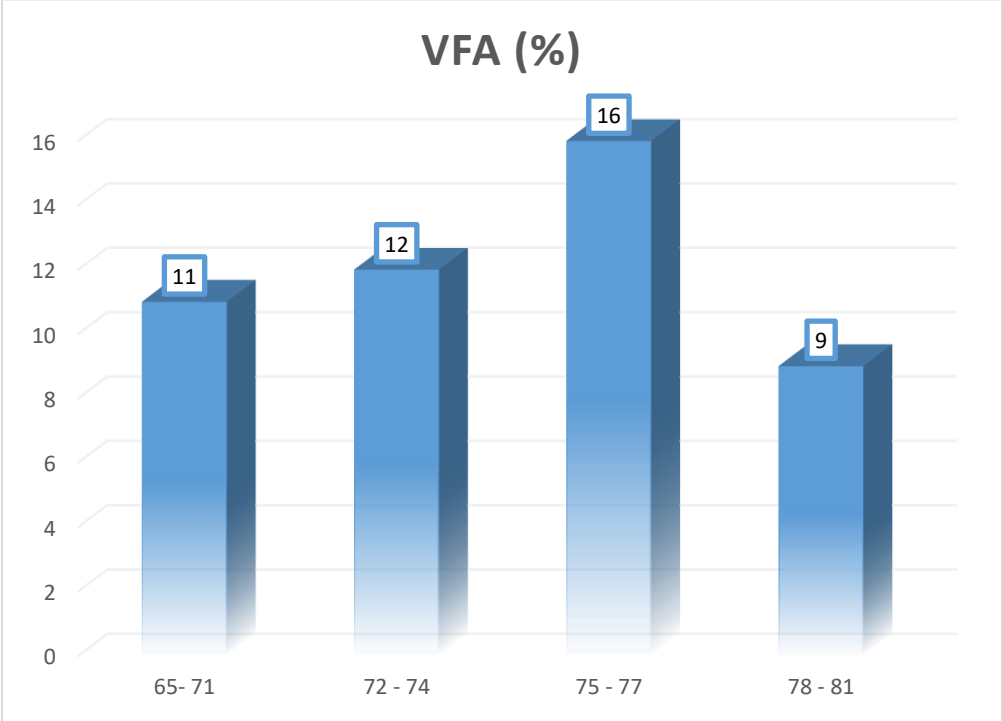


*Figure 57- US Database VFA Ranges in (%)*

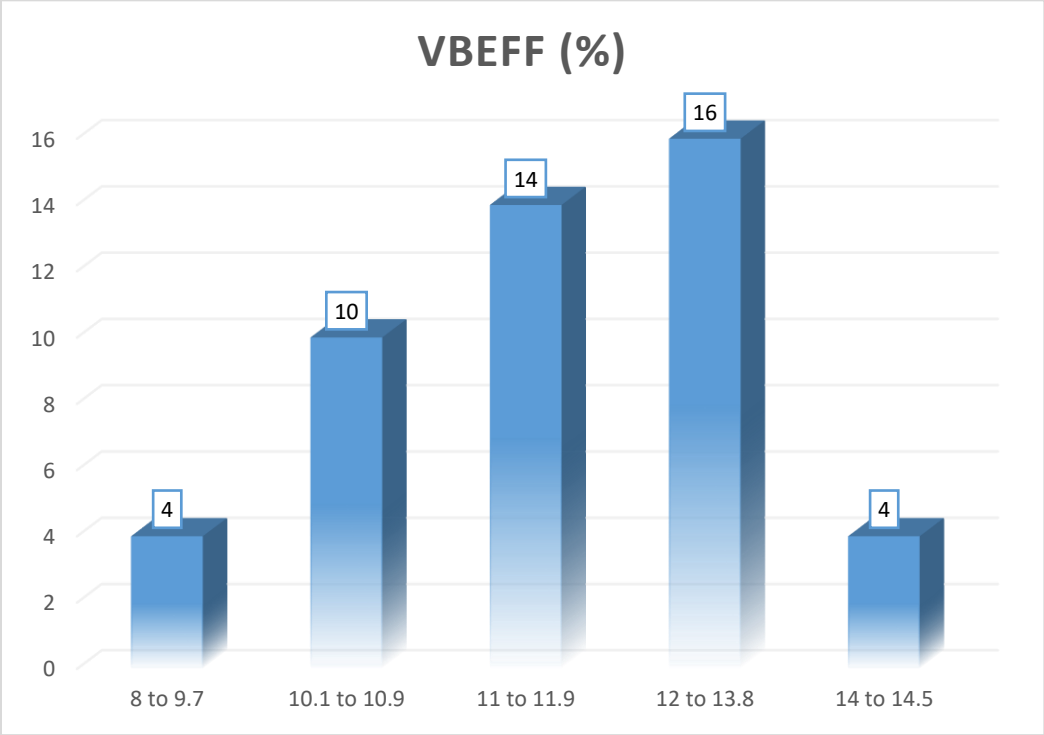


*Figure 58- US Database Vbeff Ranges in (%)*

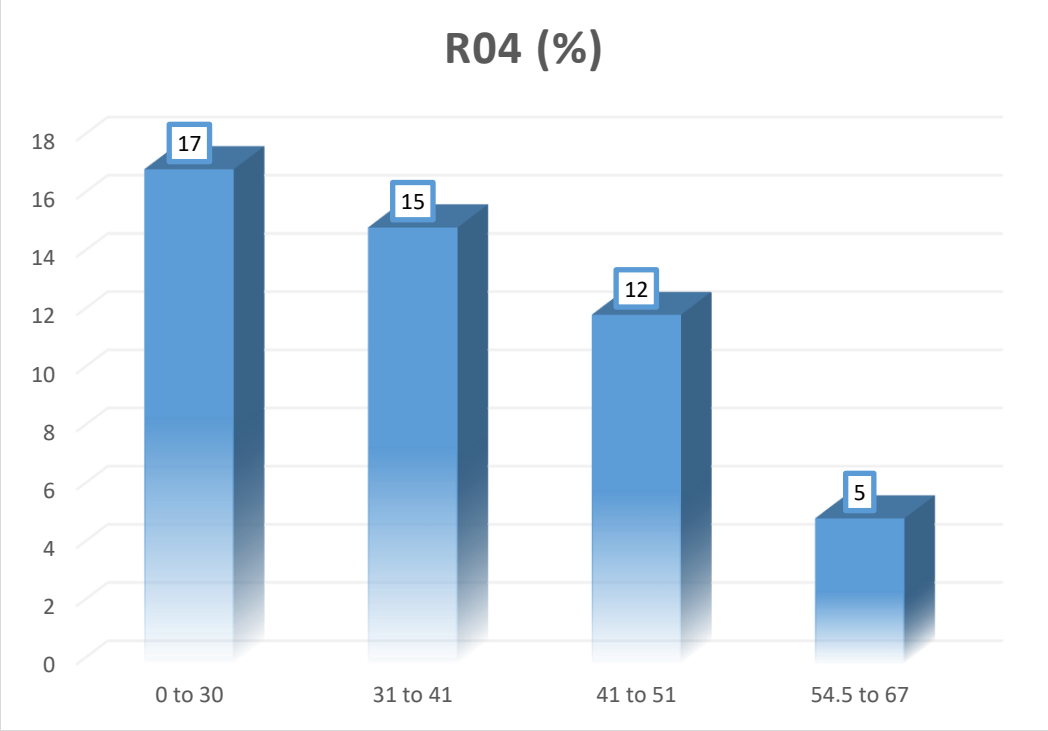


*Figure 59- US Database R04 Ranges in (%)*

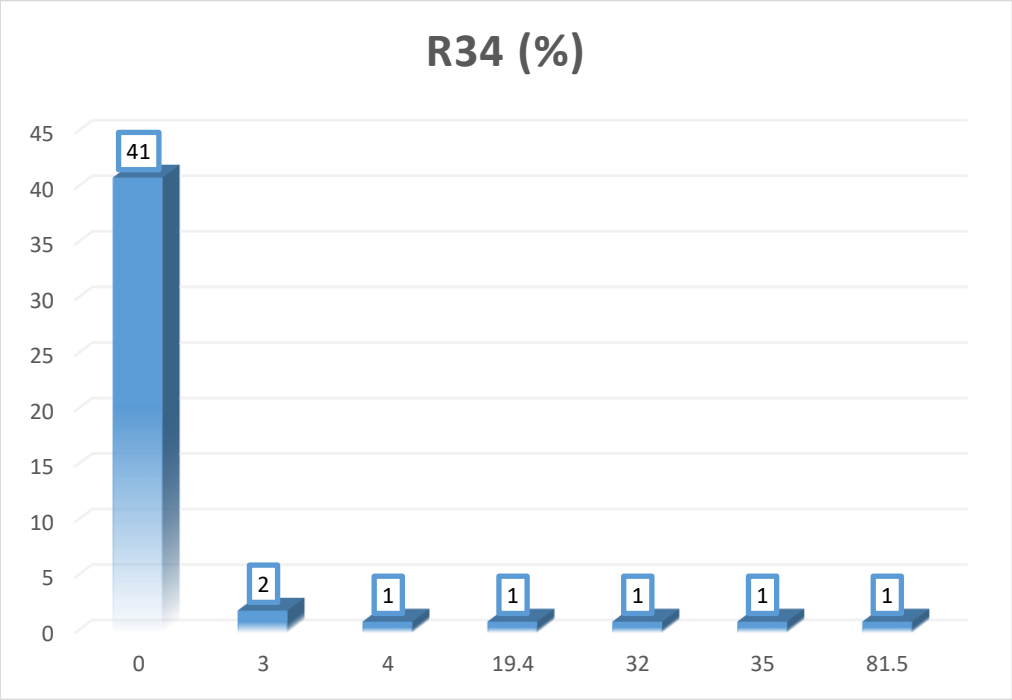


*Figure 60- US Database R34 Ranges in (%)*

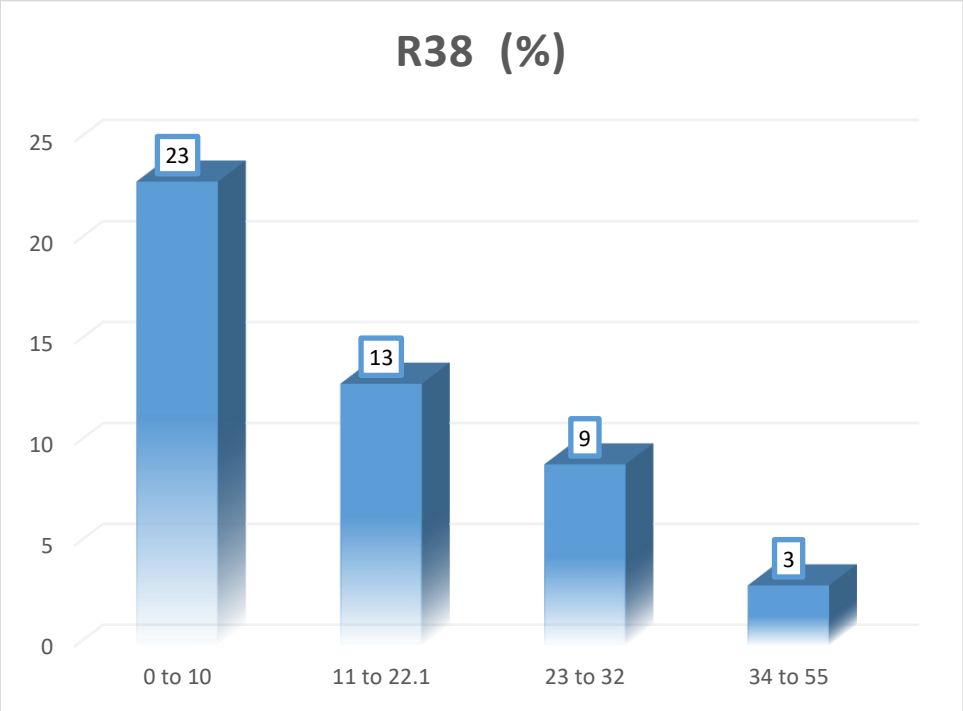


*Figure 61- US Database R38 Ranges in (%)*

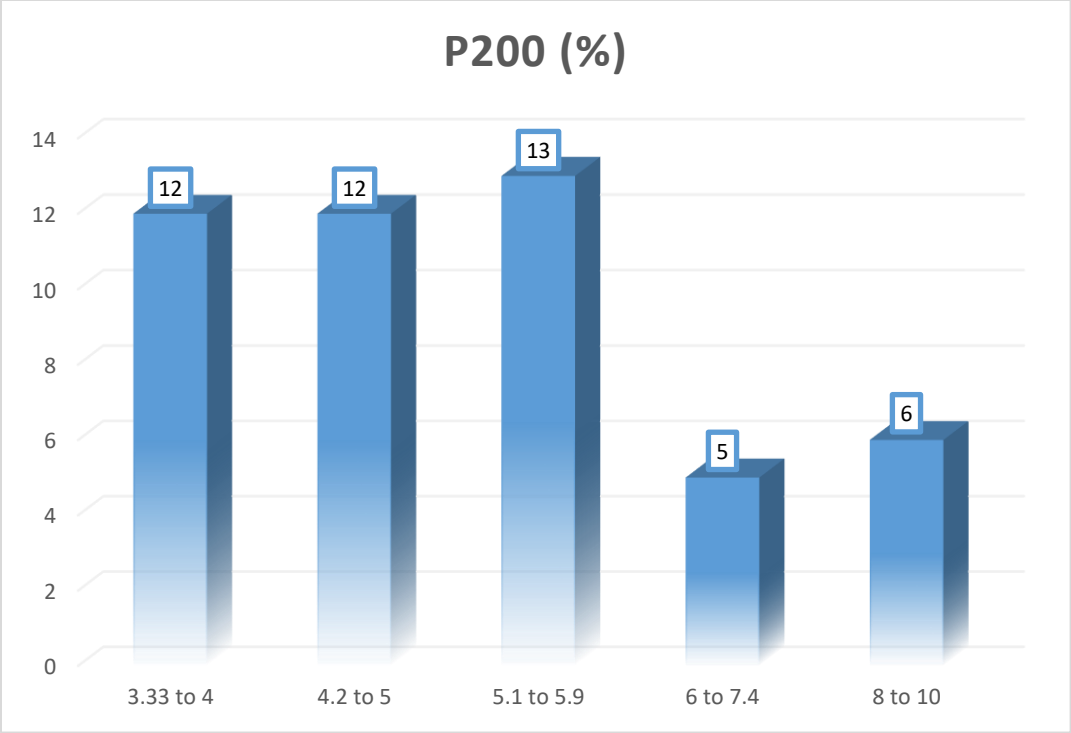


*Figure 62- US Database P200 Ranges in (%)*

In the following section, the development of the predicted models discussed in the previous chapter (Chapter 0). The same procedure has been developed for the new set of data. The first step was to develop the rutting predictive model, similar to the LTPP database collected. The purpose of developing these values is to be able to determine the quality of the pavement mixtures and whether modifications are needed to address the pavement performance of the mixture to be built.

## 5.2 Generation of the Rutting Depth

In order to develop the rutting predictive model, the effective rutting temperature had to be generated in order to evaluate to binder's viscosity at the rutting temperature. The same model has been used for the effective rutting temperature (as defined in 0).

### 5.2.a Calculation of the Effective Rutting Temperature

The effective rutting temperature has been generated for the same conditions considered earlier which includes a frequency of 18 Hz, and 2-inches from the surface.

The MAAT for each location has been calculated from data collected online, as well as the standard deviation for the Monthly Average Temperature based on the location, mean annual wind speed, mean annual sunshine in percentage and the cumulative rainfall depth. The results were included in the previous section and are repeated for the remaining U.S. locations in Appendix C, Table 58.

The Figure 63 below shows the variation of the effective rutting temperature along all the United States locations considered in this study:

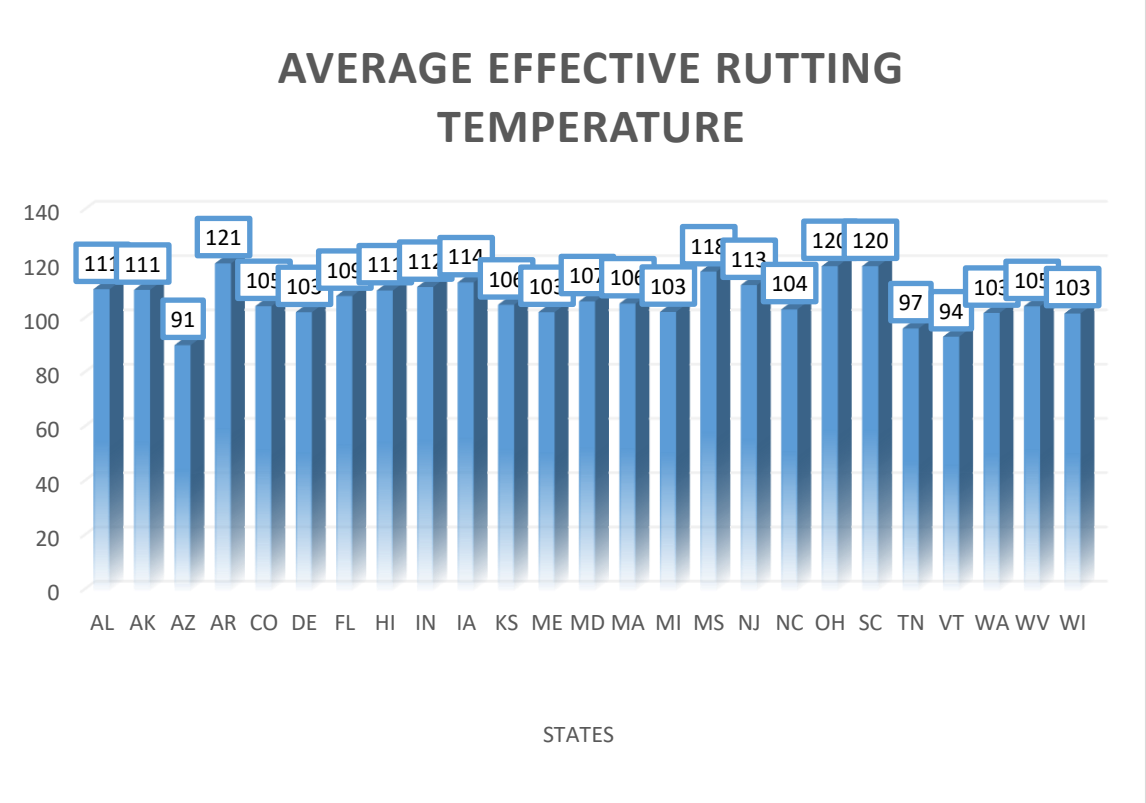


*Figure 63- Average Rutting Temperature in ºF per State*

### 5.2.b Calculation of the Viscosity at Effective Rutting Temperature

The viscosity (V1 in Poise) is another needed input to find the flow number prediction. Based on the binder type collected from the mix design collected. In addition, the "$A_i$" and "$VTS_i$". The same formulas have been used to generate the viscosities. The results are presented in Appendix C Table 59

### 5.2.c Calculation of the Predicted Flow Number

In this section, the flow number (FN) will be generated using the model assigned in the previous chapter. As all the needed variables have been developed in the previous sections for the United States taken into consideration, the same conditions have been assumed as the LTPP sections for the flow number analysis. A standard tire pressure has been assumed as principal stress ($\sigma_1$) of 120 psi. Therefore, a deviator stress of 100 psi and a confinement level of 20 psi are assumed for the flow number analysis.

The results are summarized in the Table 60 in Appendix C.

The results obtained have been displayed on Figure 64, in order to further visualize the variation of the estimated from number across the United States:

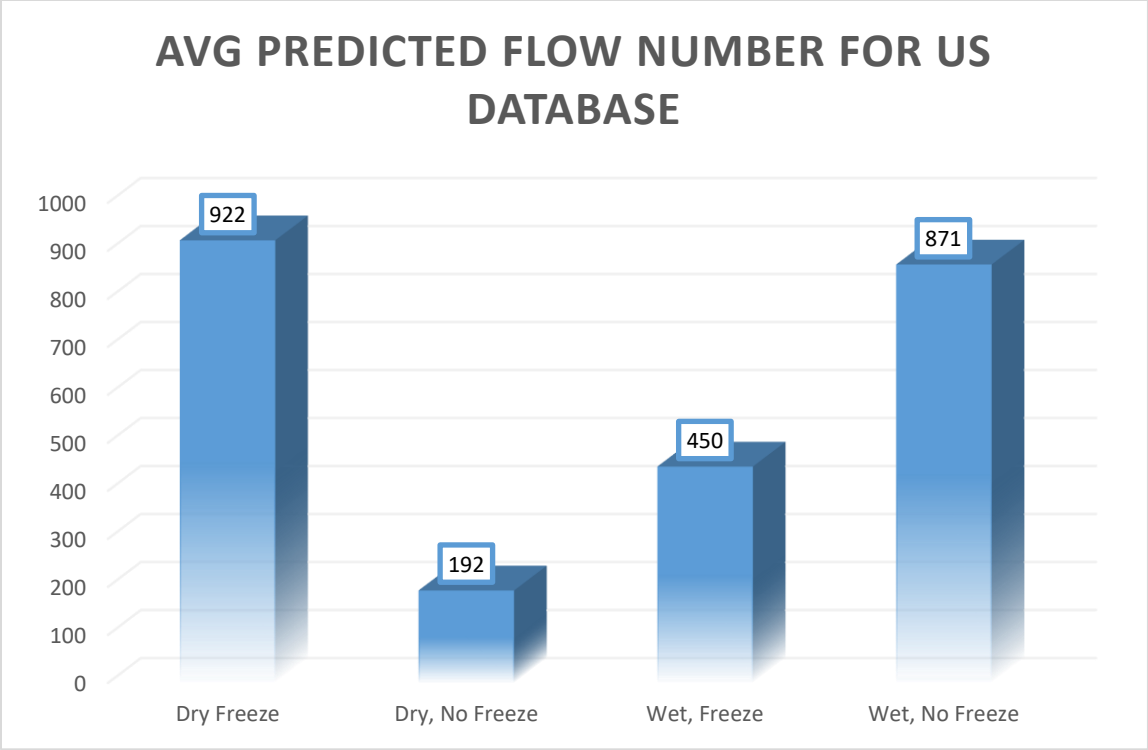


*Figure 64- Flow Number Distribution for the US Database*

A comparison between the obtained flow numbers for the two databases will be included in the next chapters for all of the developed results. It can be seen that the Flow number is rather low for the majority of the states, and therefore will mean a higher potential for rutting over the life of the pavement.

### 5.2.d Estimation of the Rutting Depth

In order to generate the rutting depth all over the United States sections acquired, the following conditions have been assumed in order to homogenize the results and ease the comparison between the values:

Two ESAL levels were assumed to simulate the possible effect of traffic that these pavement sections: 2 million and 30 million ESALs.

Concerning the thickness of the asphalt pavement, as no information was gathered on the thickness of the structures and their design as well as the type of bases and subbases underneath, a typical 4'' thickness was assumed for all the states.

The Rutting Depth have been generated for the sections taken into consideration. A comparison of the results as well as the meaning of them will be provided in the following chapter, as well as the comparison with the other generated results.

The Table 61 in Appendix C includes the generation of the rutting depth for the 2 ESAL levels assigned above.

On a first glance, it is noticed that the rutting depth increases with the increase in ESALs. The next step involving the results of this prediction is to compare it with the results obtained from the other database and compare the mix design information gathered to the final assessed criteria and identify the quality of the mix provided.

In the following Figure 65, the average rutting by climatic region is shown:

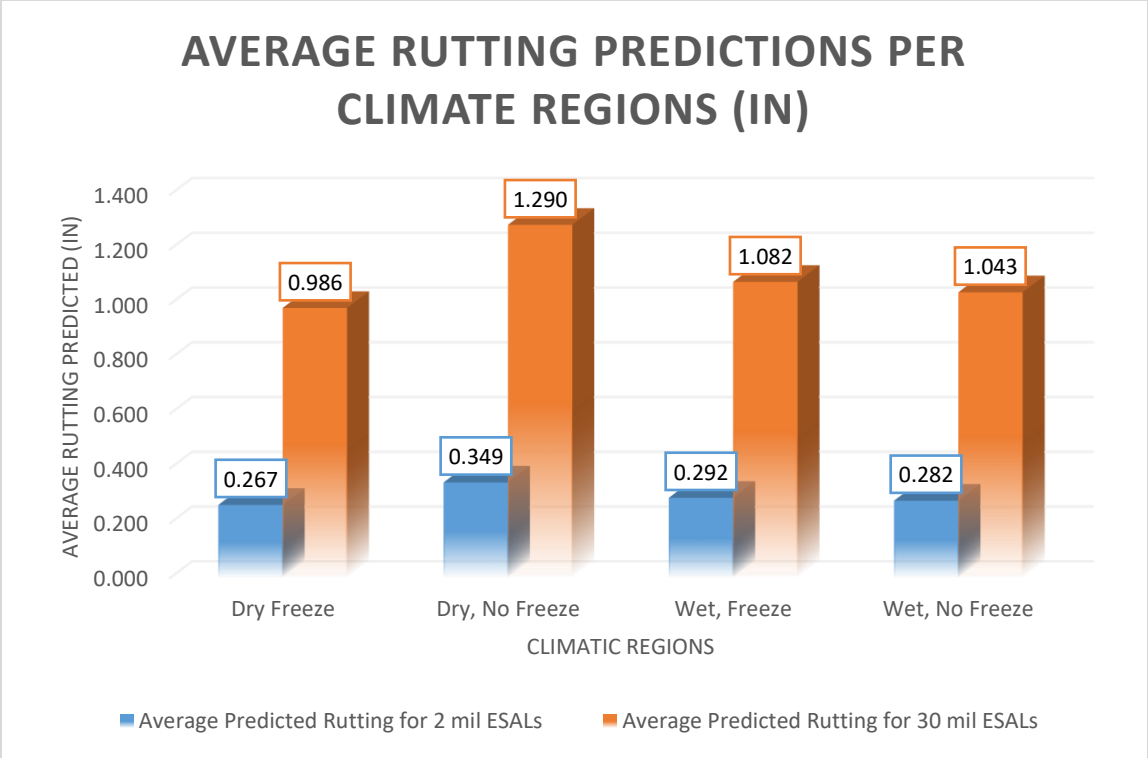


*Figure 65- Average Rutting Predictions Per Climate Regions*

In comparison with the other graph generated for the LTPP sections per climatic regions. Also, the highest rutting has been recorded in the Freeze Regions, where the change of seasons affects the deformation of the pavement structure during freeze and thaw events.

## 5.3 Generation of the Fatigue Behavior

The number of cycles to fatigue failure has also been developed for this dataset by assuming the same strain level of 350 με. The process includes the same steps and variable generation in order. And finally, the number of cycles to failure is generated.

### 5.3.a Calculation of the Effective Fatigue Temperature

The effective fatigue temperature has been generated according to the AASHTO TP-107 which is based on the type of the PG-Binders for each pavement mixtures acquired. The results are summarized in the

Table 62 in Appendix C

The table's results are summarized in the Figure 66 below to show the variation of the effective fatigue temperatures throughout the United States:

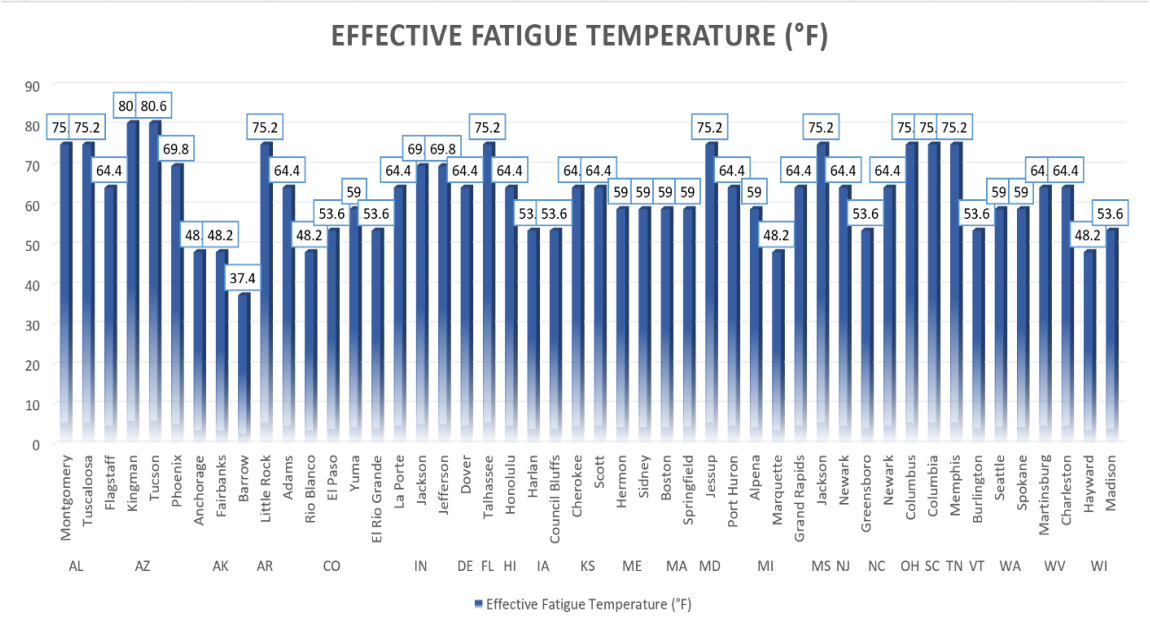


*Figure 66- Effective Fatigue Temperature for the US Database*

## 5.3.b Calculation of the Asphalt Binder Viscosity at Specific Temperature and Frequency

The next step involves in calculating the viscosity in (cP) for the asphalt binders at the effective fatigue temperatures. The calculations are included in

Table 63 in appendix C.

### 5.3.c Calculation of the Phase Angle δ based on Temperature and Frequency

The next step involves calculating the phase angle at the testing temperature, which is the effective fatigue temperature and frequency, which is taken to be equal to 10 Hz.

The results are found in

Table 64 in appendix C for the US Database.

### 5.3.d Calculation of the Complex Modulus of the Asphalt Binder

The next step involves in calculating the complex modulus of the binder, based on the phase angle previously calculated and the assumed frequency of 10 Hz.

The results are summarized in the

Table 65 in Appendix C

The Figure 67 has been plotted for the different states to have a clearer idea about the variability of the results:

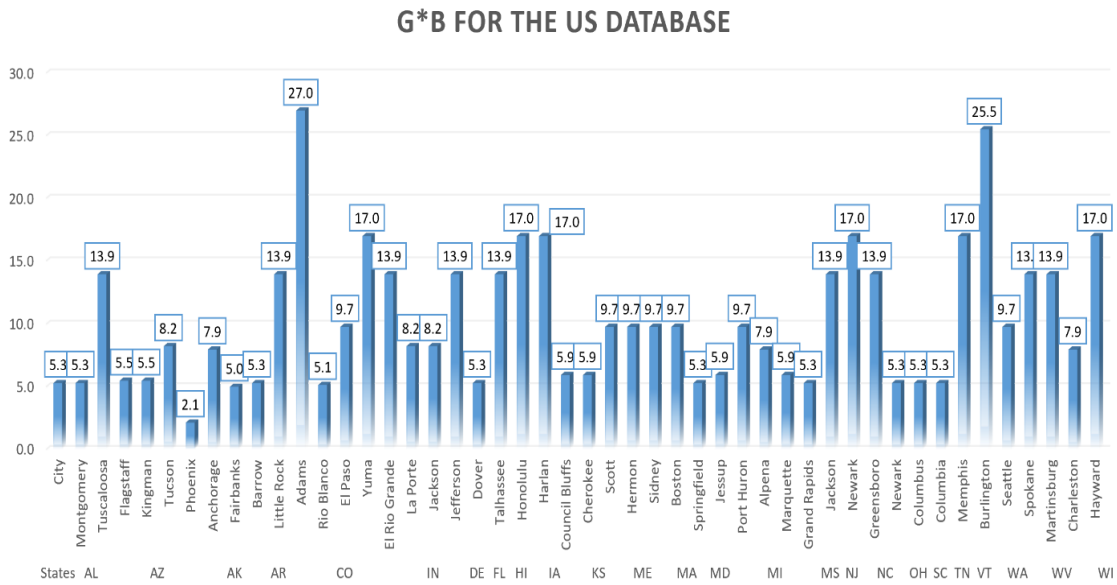


*Figure 67- G*b for the US Database*

Concerning the variation per climatic region, the average values of the Complex Shear Modulus for the asphalt binder has been calculated and plotted as follows in Figure 68:

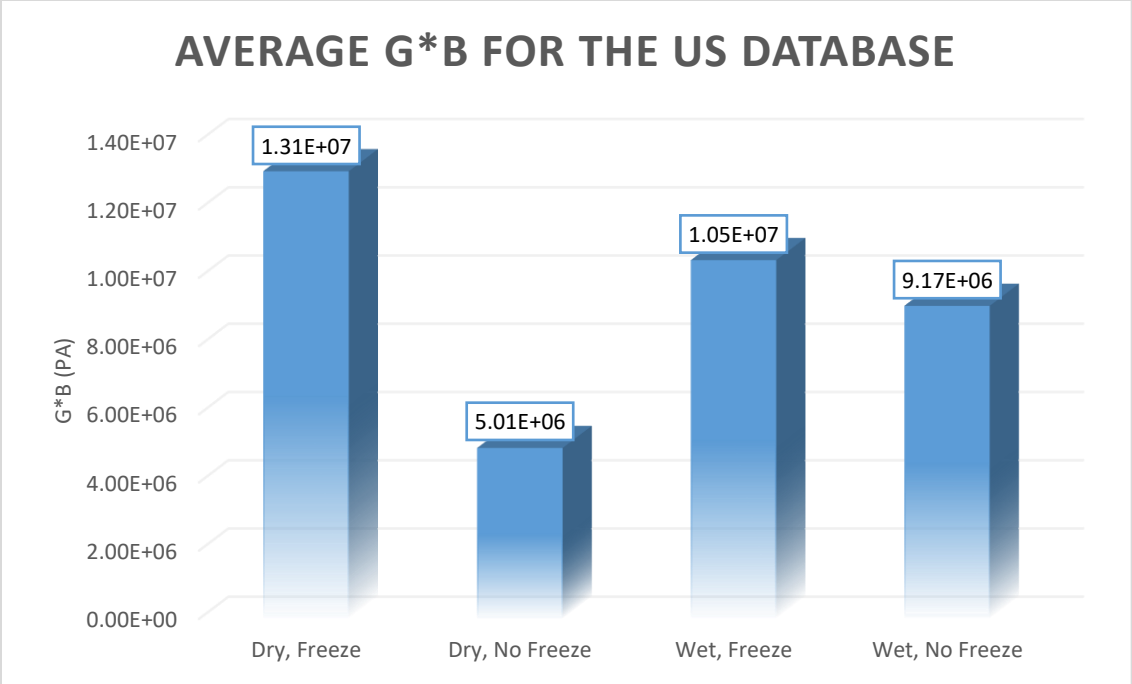


*Figure 68- G*b variation for the US Database*

Concerning this graph, it can be clearly seen that the binder is stiffer in the Freeze Regions, despite choosing softer binder types.

### 5.3.e Calculation of the FSC*, the Fatigue Strain Capacity or General Shear Envelope

The Fatigue Strain Capacity (FSC*) is the maximum strain capacity for a specific asphalt binder. It is found according to the FSC* equation included previously in Chapter 3, Section 4. The results are summarized in the

Table 66 in Appendix C.

### 5.3.f Calculation of the Number of Cycles to Fatigue Failure

For a strain level of 350 με, the number of cycles to failure are generated in order to estimate the number of cycles to failure in Table 67 in Appendix C.

To summarize this table, the following Figure 69 has been generated per climate region, with the average number of cycles to failure in order to assess the average fatigue life of asphalt pavements with respect to the climate in general.

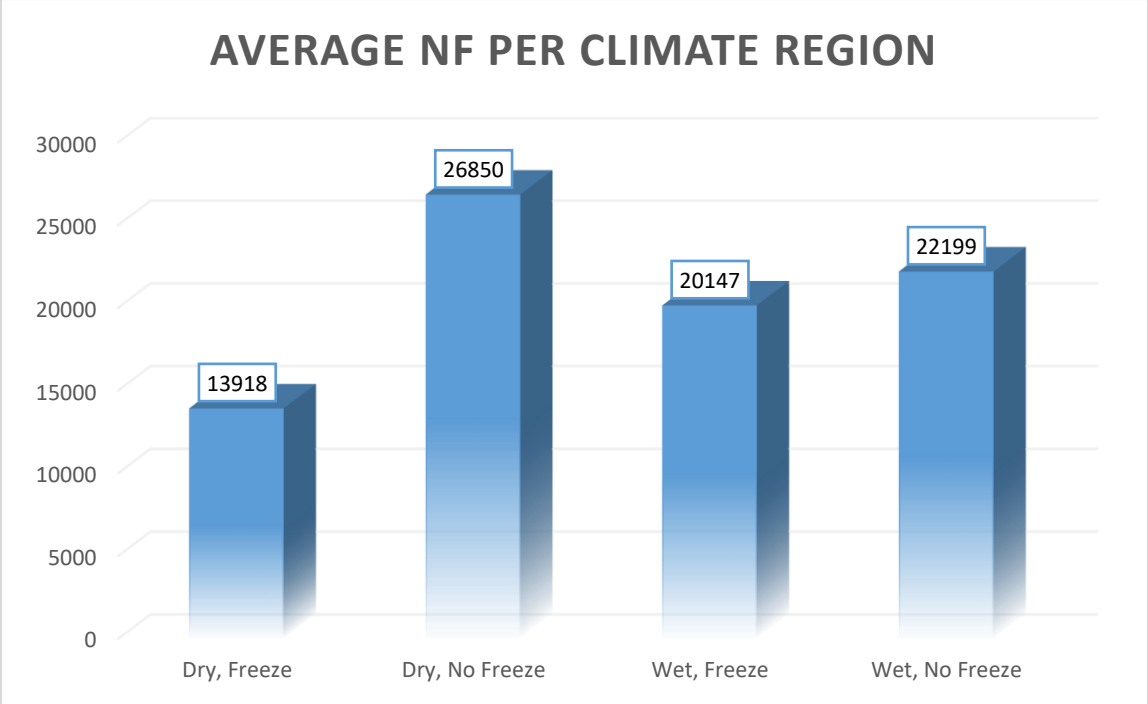


*Figure 69- Nf Variation with different climate zones for the US Database*

The Number of cycles to failure or the fatigue behavior of asphalt mixtures greatly depend on how elastic the mixture is. In other words, the stiffer the binder, the more fatigue is to be expected from the mixture. This chart shows that the freezing regions have lower fatigue lives, or lower number of cycles to failure. It is in accordance with the

previous chart, showing the stiffness of the binders at the effective fatigue temperature and phase angle.

## 5.4 Calculation of the Total Effective Fracture Energy and Tensile Strength

In order to predict the potential thermal cracking of the new pavement mixtures, the same variables have been found as the LTPP Database. Since no measured distresses were provided for the new mixtures, comparing the variables with the previously obtained results is crucial to understand the trend that the new mixtures will follow in the future. In the following chapters, a comparison of the new and old mix designs will be assessed, and a ranking criterion will be developed in order to assess the quality of the new mixtures in terms of all the defined distresses.

### 5.4.a Calculation of the $D_1$ fracture parameter for the Creep Compliance

The first step defines the calculation of $D_1$, the fracture parameter at three different temperatures: -20$^o$C, -10$^o$C and 0$^o$C. The equation used have been defined previously in details in Section 3.5.b

The values in 1/psi are summarized in Table 68 in Appendix C.

The model has shown a similar trend to the expected behavior, as the fracture parameter $D_1$ increases with the increase in temperature. This leads to an increase in creep compliance and therefore an increase in the potential resistance to thermal cracking.

The average values of $D_1$ are shown in Figure 70:

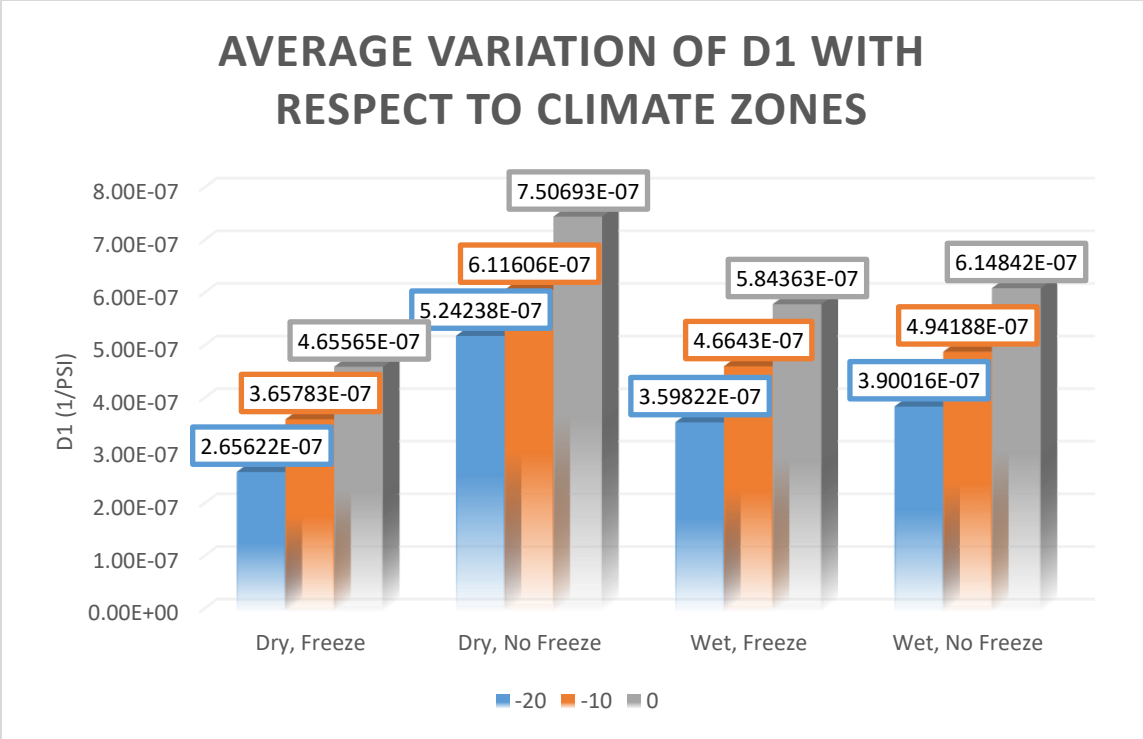


*Figure 70- Average Variation of D1 with the Different Climate Zones for the US Database*

The variation of $D_1$ is widely shown in this Figure 70. As the binder gets softer, the potential for thermal cracking is lower. It has been previously shown that the PG-binders have a stiffer behavior in the freezing zones, which is also reflected here by having a lower fracture parameter $D_1$.

### 5.4.b Calculation of the Penetration Parameter at 77°F

The next step involves calculating the penetration values at 77°F, which are a valuable input for the calculation of the slope of the creep compliance curve, "m".

Similarly, the penetration was calculated for the different binders using the formula previously defined along with the respective "Ai" and "VTSi" for each binder. The results are found in Table 69 in Appendix C.

In the following Figure 71, the average penetration for each climatic region is shown. However, the average values of penetration are not conclusive for each climate zone, as the PG-binder's type is widely spread within each region. As the creep compliance parameter $D_1$ depends on the volumetric properties of the mix as well, it explains the different trends observed.

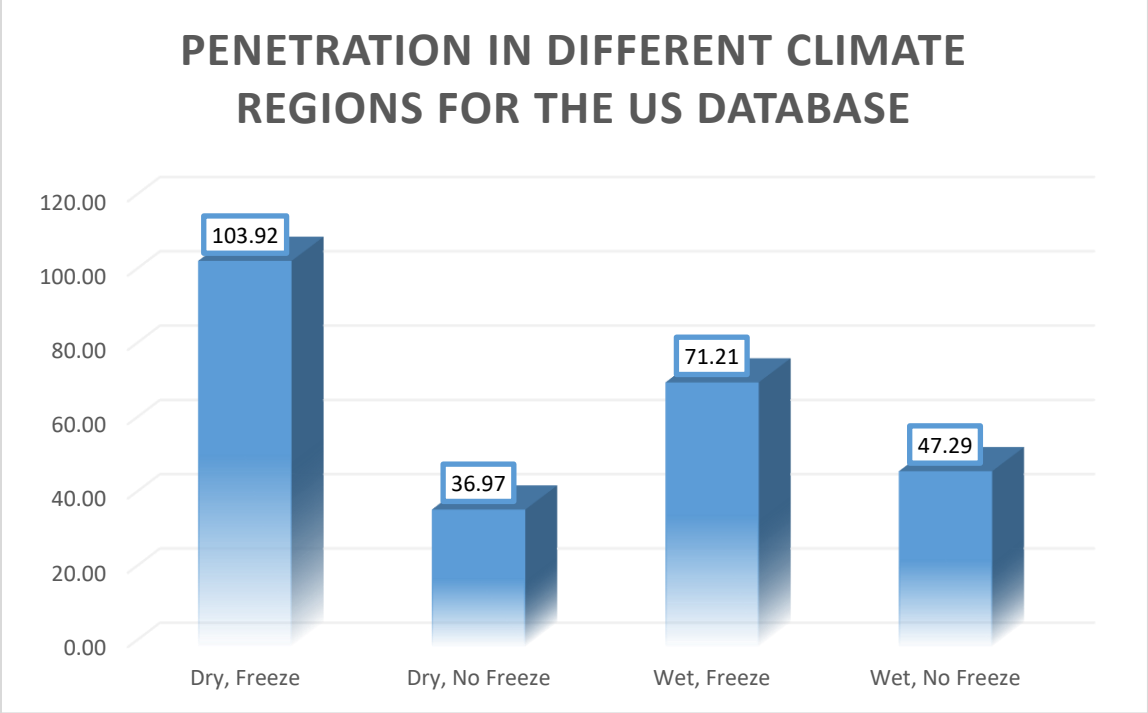


*Figure 71- Penetration in Difference Climates Regions for the US Database*

5.4.c Calculation of the m parameter, slope of the Creep Compliance curve

The slope of the creep compliance according to the three different formulas respective to the three testing temperatures are calculated in this section for all the U.S. sections under study. The results are found in Table 70 in Appendix B.

The average values of the m parameter are shown in the following Figure 72:

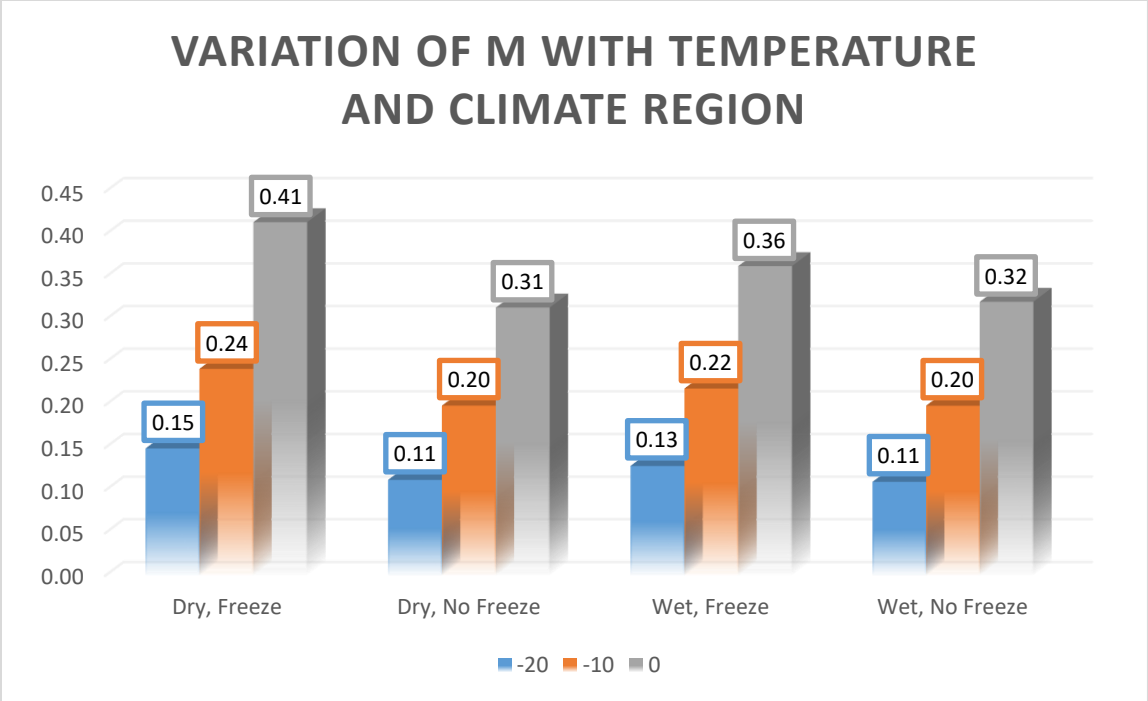


*Figure 72- Variation of the average m-parameter for the US Database*

The variation of the m fracture parameter reflects the slope of the creep compliance curve. The m fracture parameter depends on the values of the penetration of each binder, calculated in the previous step. The m parameter is known to increase with an increase in temperature. Also, when the temperature increases, the penetration increases, leading to a higher creep compliance and greater potential to thermal cracking resistance. A higher potential m parameter value is experienced for the Dry, freeze region, as the binder used in these cities is shown to be the softest according to the new mix designs.

5.4.d Calculation of the Creep Compliance values at 100 seconds

Similar to the complementing section for the LTPP Database, the creep compliance has been generated at 100 seconds for the three considered temperatures. The creep compliance should have an increasing trend with increasing temperature and softer binders, as reflected by the binders' types for each region.

The results found are summarized in Table 71 in Appendix C.

The average creep compliance values have been developed and shown in the following Figure 73:

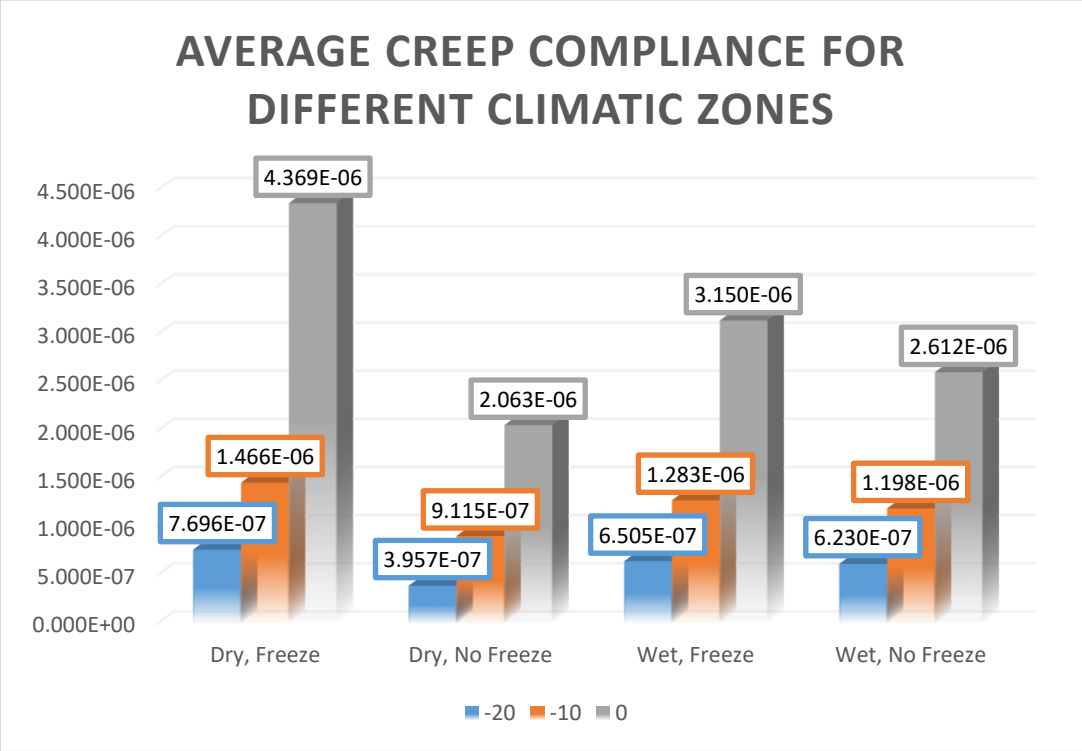


*Figure 73- Average Creep Compliance Values for Different Climatic Regions for the US Database*

The observed results show that the highest creep compliance is recorded in the Dry, Freeze Region. It is to be noted that the values depend on the new volumetric properties of each pavement mixture. As the binder type does not follow a specific choice pattern, the creep compliance does not specifically reflect the results obtained for the LTPP database sections. However, the trend following the temperatures is still applied, and therefore the model is still valid and verified.

The following observations were made based on the results obtained for the new database:

- With the increase in temperature, the creep compliance still increases. In addition, softer binders lead to higher creep compliance values and therefore more resistance to thermal cracking
- The new binder type is chosen within a certain range, from mildly stiff to stiffer. Very few soft binders. For this reason, the highest creep compliance happened in the Dry, No Freeze region followed by the Dry Freeze region. The results are based on the new volumetric properties introduced, and therefore do not refer to the same trends observed for the LTPP Database

### 5.4.e Calculation of the Total Effective Energy

In this section, the total effective energy needed to fracture is developed for the new database. It reflects the energy needed to initiate, crack and propagate the crack on the asphalt surface.

As explained in the previous Chapter, Chapter 4, Section 3, part e, the model doesn't cover all the possible ranges of the mixtures' volumetrics. For this reason, some negative values are generated for the new U.S. database, as the volumetrics do not fit into the developed limiting criteria in Table 31:

*Table 31- Limitation Criteria for the Effective Thermal Cracking Predictive Model*

| **Limitation Criteria** | |
|---|---|
| **4< AC <6** | |
| **3.5 <Va< 7.5** | |
| **VMA** | >14 |
| **56 < VFA < 74** | |
| **VBE** | >8 |
| **24< PEN 77 <130** | |

The generated values for the effective fracture energy are in the table in Table 72 in Appendix C.

The fracture energy for the Wet, No Freeze Region is rather high. Referring to the creep compliance values for this zone, it is referred to have a good value compared to the other regions. Similarly, the creep compliance is referred to be the lowest for the Dry No Freeze Region, reflecting low values for effective fracture energy. Due to the presence of negative values, a proper assessment cannot be concluded concerning this parameter. In the future analysis, the average of the effective fracture energy will be used to represent the behavior of it.

### 5.4.f Calculation of Tensile Strength $S_t$

The last input parameter required for the thermal cracking assessment is the calculation of the tensile strength at -10°C. The results are found below in Figure 74:

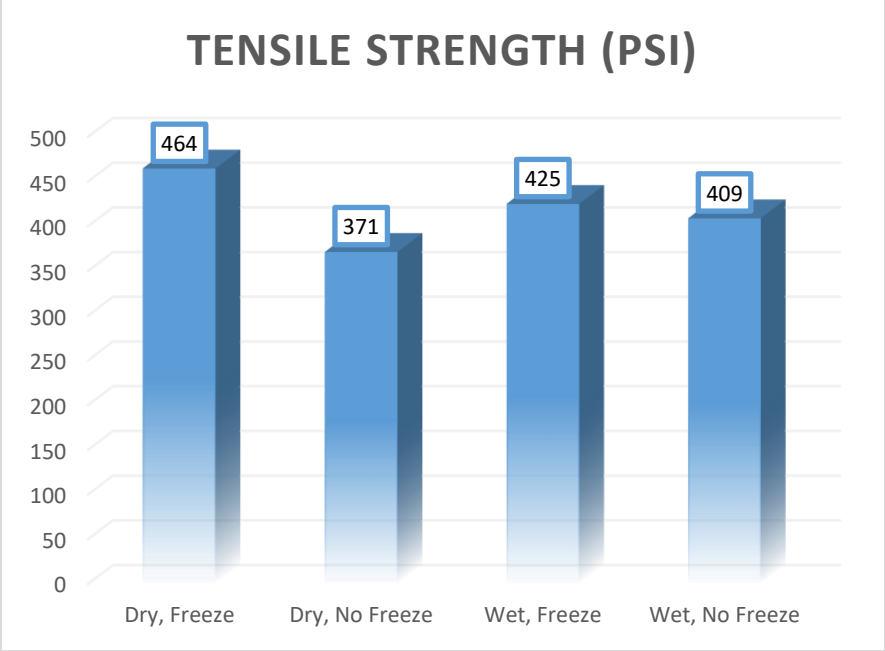


*Figure 74- Tensile Strength Calculation at -10C for the US Database*

The tensile strength value for the Dry Freeze region is reported to be the highest among the four average values. The tensile strength values are rather close to each other for the remaining of the climatic regions, and therefore do not provide additional information regarding the thermal cracking behavior explicitly.

However, the same trend is observed in terms of creep compliance as well. Further analysis is to be conducted in the section below.

### 5.4.g Estimation of the Amount of Thermal Cracking

The reported input variables are all set next to each other in one table in order to be able to generate a certain judgement concerning the potential and expected thermal cracking behavior of the new pavement mixtures gathered. The Variables generated are also the required input values to run the TCMODEL and found in Table 73 in Appendix C.
In the following graphs, the average of the input variables has been plotted to show the potential thermal cracking resistance within the different climate region:

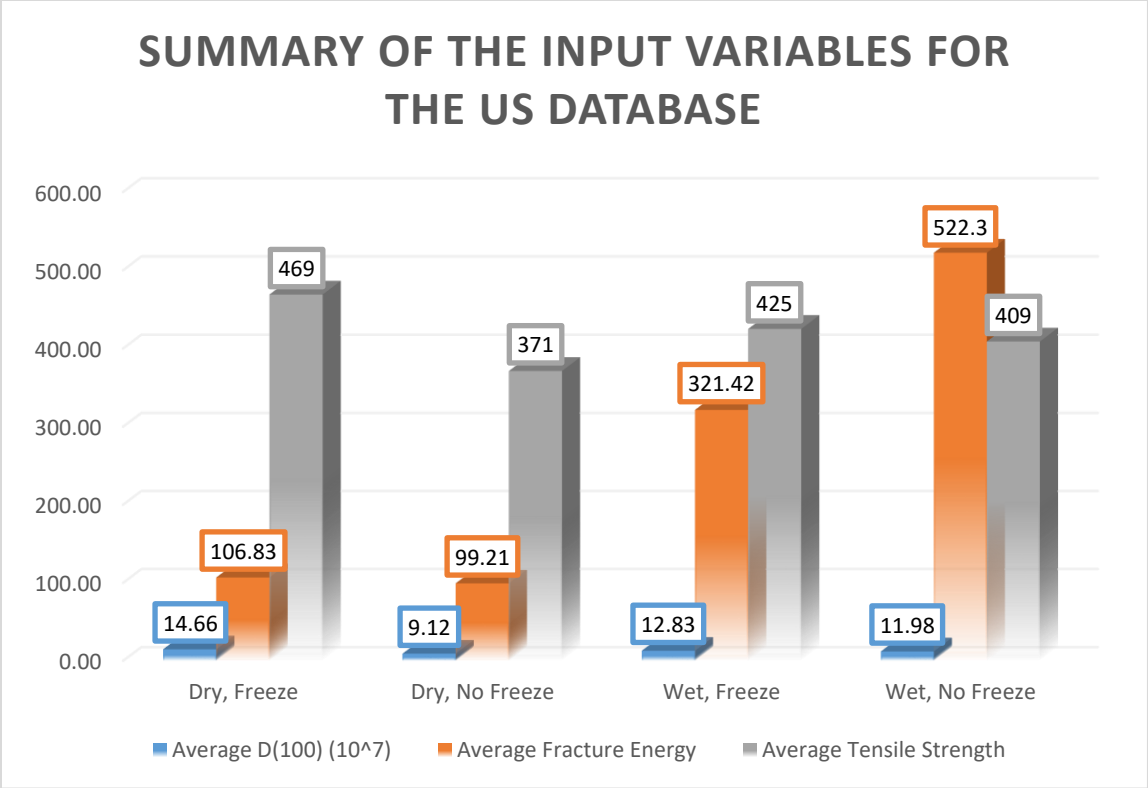


*Figure 75- Summary of the input variables for thermal cracking resistance for the US Database*

The following has been observed:

- The creep compliance has been found to be the highest in the Dry Freeze region and the lowest at the No Dry Freeze one.
- The Dry No Freeze region, having the lowest values of tensile strength and effective fracture energy as well as creep compliance is the more susceptible to thermal cracking behavior.
- The Wet, Freeze region has high effective fracture energy, good creep compliance and relatively good tensile strength values. It can be safe to say that this region will have a good potential with regards to thermal cracking resistance.
- As for the Wet No Freeze Region, the obtained values fall within the moderate range, which leads to a potential good thermal cracking resistance as well.

- The creep compliance value plays a big role in determining the expected thermal behavior. The tensile strength is not directly related to thermal cracking behavior, but may give some indication about the expectations. However, based on the observed trends between creep compliance and tensile strength, the creep compliance is increasing with higher tensile strength and vice versa.
- The choice of the pavement mixture highly affects the values obtained in terms of resistance to cracking, as the binder choice, air void content and gradation greatly affect the performance of the mix.
- Concerning the Wet Freeze Region, it has the lowest potential to resist thermal cracking. However, based on the graph above, having a high effective fracture energy shows that these regions are modifying their pavement mixtures in order to accommodate the thermal cracking problem.
- Finally, having most of the effective fracture energy values outside the model's range, very few values were left to compute the average. Therefore, the values obtained are not considered to be a 100% reliable.

In the next chapter, the decisive criterion will determine how these mixtures behave in terms of all the distresses presented and will quantify the quality of the mixtures.

# CHAPTER 6

# 6 FINAL ASSESSEMENT: COMPARISON AND ANALYSIS

In this chapter, a comparison of the old and new mix designs will be developed in order to see what are the potential changes that happened over the course of the years. The comparison is followed by an analysis of the results obtained from the LTPP database and the US Database to show how they relate to each other. Finally, the mix designs will be ranked according to a developed criterion to assess the quality of the mix. By finding the quality of the mixture, it can be determined if the mixture needs to be modified or needs some modifiers for it to perform better. For each distress discussed in this study, a criterion will be presented, ranking the mix designs as Poor, Good or Excellent in terms of Permanent Deformation, Fatigue and Thermal Cracking behaviors.

## 6.1 Comparison of the New and Old Pavement Mixtures

In the previous chapters, the LTPP Sections chosen were described in terms of pavement volumetrics, followed by the description of the pavement mixtures gathered from all over the United States. The descriptions were individually presented in Sections 4.2 and 5.1 respectively.

First, for the sake of comparison, only the sections having the same locations and regions are considered from both databases. Therefore, a total of 28 sections are considered for this purpose.

### 6.1.a Comparison of the PG-Binders Types

The first thing to consider is the choice of the PG-Binder as per the location of each region with respect to the climatic zone.

The Table 32 summarizes the sections considered, as well as the location and the PG-binder:

*Table 32- PG-Binder Comparison for both databases*

| State | City | Climatic Zone | PG (LTTP Database) | PG (US Database) |
|---|---|---|---|---|
| **Arizona** | *Flagstaff* | *Dry, Freeze* | PG 58-28 | PG 58-34 |
| **Alaska** | *Anchorage* | *Dry, Freeze* | PG 46-40 | PG 58-34 |
| **Colorado** | *Rio Blanco* | *Dry, Freeze* | PG 46-34 | PG 70-10 |
| **Colorado** | *El Paso* | *Dry, Freeze* | PG 58-28 | PG 70-22 |
| **Colorado** | *Yuma* | *Dry, Freeze* | PG 64-28 | PG 64-22 |
| **Washington** | *Spokane* | *Dry, Freeze* | PG 58-28 | PG 58-28 |
| **Arizona** | *Tucson* | *Dry, No Freeze* | PG 70-10 | PG 64-28 |
| **Arizona** | *Phoenix* | *Dry, No Freeze* | PG 76-10 | PG 58-28 |
| **Arizona** | *Kingman* | *Dry, No Freeze* | PG 70-16 | PG 58-28 |
| **Indiana** | *La Porte* | *Wet, Freeze* | PG 58-28 | PG 64-28 |
| **Indiana** | *Jackson* | *Wet, Freeze* | PG 58-28 | PG 64-28 |
| **Kansas** | *Cherokee* | *Wet, Freeze* | PG64-22 | PG 58-34 |
| **Massachusetts** | *Boston* | *Wet, Freeze* | PG 58-22 | PG 58-34 |
| **Massachusetts** | *Springfield* | *Wet, Freeze* | PG 58-28 | PG 58-28 |
| **Michigan** | *Port Huron* | *Wet, Freeze* | PG 58-28 | PG 76-22 |
| **Michigan** | *Alpena* | *Wet, Freeze* | PG 52-28 | PG 76-22 |
| **Michigan** | *Marquette* | *Wet, Freeze* | PG 52-28 | PG 76-22 |
| **Michigan** | *Grand Rapids* | *Wet, Freeze* | PG 58-34 | PG 70-22 |
| **WV** | *Kanawha* | *Wet, Freeze* | PG64-22 | PG 76-22 |
| **Alabama** | *Montgomery* | *Wet, No Freeze* | PG 64-16 | PG 64-22 |
| **Alabama** | *Tuscaloosa* | *Wet, No Freeze* | PG 64-16 | PG 64-40 |
| **Arkansas** | *Little Rock* | *Wet, No Freeze* | PG 64-16 | PG 64-28 |
| **Indiana** | *Jefferson* | *Wet, No Freeze* | PG 58-28 | PG 64-28 |
| **Kansas** | *Scott* | *Wet, No Freeze* | PG 64-28 | PG 70-28 |
| **SC** | *Columbia/Lexington* | *Wet, No Freeze* | PG 64-16 | PG 76-22 |
| **Tennessee** | *Memphis* | *Wet, No Freeze* | PG 64-22 | PG 76-22 |
| **Washington** | *Seattle* | *Wet, No Freeze* | PG 52-16 | PG 64-22 |
| **WV** | *Charleston* | *Wet, No Freeze* | PG 64-22 | PG 76-22 |

For the first climatic region, the Dry Freeze region, it is observed that stiffer binders are being used newly in the year 2018 compared to the older designs. The origin date of the LTPP Database's mix design is not known. However, the roads have been mostly constructed in the 1980's.

For the second climatic region, the Dry No Freeze region, softer binders are being used recently.

The third climatic region, the Wet Freeze, stiffer binders are being implemented in the recent dates.

Fourth, the Wet No Freeze region, stiffer binders are being used as well.

All in all, stiffer binders are being used in 3 out of the 4 regions in the recent years. The Dry, No Freeze region has been employing softer binders. The choice of binders may be linked to the potential behaviors in terms of pavement performance, which is to be assessed further on in this chapter. Employing stiffer binders may be done to address the problem of permanent deformation.

### 6.1.b Comparison of the Air Void Content

In this section, the change in Air Void Content in percent will be evaluated for the old and new pavement mixtures. The Air Void Content is an important parameter that directly affects the pavement performance of the mixture when subjected to traffic loads. Having a higher air void content will affect the durability of the pavement, as well as make it more permeable to water penetration. Being susceptible to water penetration affects the structure negatively in terms of distresses and will cause them to happen in a higher frequency and amount.

The Table 33below shows the air void content in percent for the old and new pavement mixtures:

*Table 33- Va (%) Comparison*

| State | City | Climatic Zone | *Va (%) (LTPP Database)* | Va (%) (US Database) |
|---|---|---|---|---|
| **Arizona** | *Flagstaff* | *Dry, Freeze* | 4.9 | 3.96 |
| **Alaska** | *Anchorage* | *Dry, Freeze* | 3.9 | 4 |
| **Colorado** | *Rio Blanco* | *Dry, Freeze* | 4 | 3.5 |
| **Colorado** | *El Paso* | *Dry, Freeze* | 5.292 | 3.5 |
| **Colorado** | *Yuma* | *Dry, Freeze* | 7.39 | 3.5 |
| **Washington** | *Spokane* | *Dry, Freeze* | 6 | 4.4 |
| **Arizona** | *Tucson* | *Dry, No Freeze* | 4.6 | 5.6 |
| **Arizona** | *Phoenix* | *Dry, No Freeze* | 4.5 | 5 |
| **Arizona** | *Kingman* | *Dry, No Freeze* | 3.9 | 5.2 |
| **Indiana** | *La Porte* | *Wet, Freeze* | 6.18 | 3.4 |
| **Indiana** | *Jackson* | *Wet, Freeze* | 2.7 | 4 |
| **Kansas** | *Cherokee* | *Wet, Freeze* | 5 | 4 |
| **Massachusetts** | *Boston* | *Wet, Freeze* | 5.6 | 4 |
| **Massachusetts** | *Springfield* | *Wet, Freeze* | 2.3 | 4 |
| **Michigan** | *Port Huron* | *Wet, Freeze* | 4 | 4 |
| **Michigan** | *Alpena* | *Wet, Freeze* | 2.7 | 4 |
| **Michigan** | *Marquette* | *Wet, Freeze* | 5.125 | 4 |
| **Michigan** | *Grand Rapids* | *Wet, Freeze* | 3.5 | 4 |
| **WV** | *Kanawha* | *Wet, Freeze* | 5.14 | 4.4 |
| **Alabama** | *Montgomery* | *Wet, No Freeze* | 5.8 | 3.5 |
| **Alabama** | *Tuscaloosa* | *Wet, No Freeze* | 5.2 | 3.5 |
| **Arkansas** | *Little Rock* | *Wet, No Freeze* | 3 | 4 |
| **Indiana** | *Jefferson* | *Wet, No Freeze* | 4.303 | 4 |
| **Kansas** | *Scott* | *Wet, No Freeze* | 3.2 | 4 |
| **SC** | *Columbia/Lexington* | *Wet, No Freeze* | 7.9 | 5.8 |
| **Tennessee** | *Memphis* | *Wet, No Freeze* | 6 | 4 |
| **Washington** | *Seattle* | *Wet, No Freeze* | 8.9 | 4.4 |
| **WV** | *Charleston* | *Wet, No Freeze* | 6.7 | 4 |

For the Dry Freeze region, it can be seen that the Air Void content has been decreased, and thus the permeability of the asphalt structure has been decreased. This

tackles the problem of freeze and thaw, leading to permanent deformation and higher deflections, since water cannot penetrate as easily as before.

For the Dry No Freeze region, the air void content has been increased in the new mixtures.

For the Wet Freeze region, the air void contents have been changed to have an average of 4% air void content. Some states had a $V_a$ of 2.3%, 2.7% and 3.4,% which have been increased to 4%. Also, higher air void contents have been lowered to the value of 4%.

For the last region, the Wet No Freeze, the air void content has been decreased conveniently to a lower range of 4% to 5%, making the structure less permeable in this wet climate zone. (Figure 76)

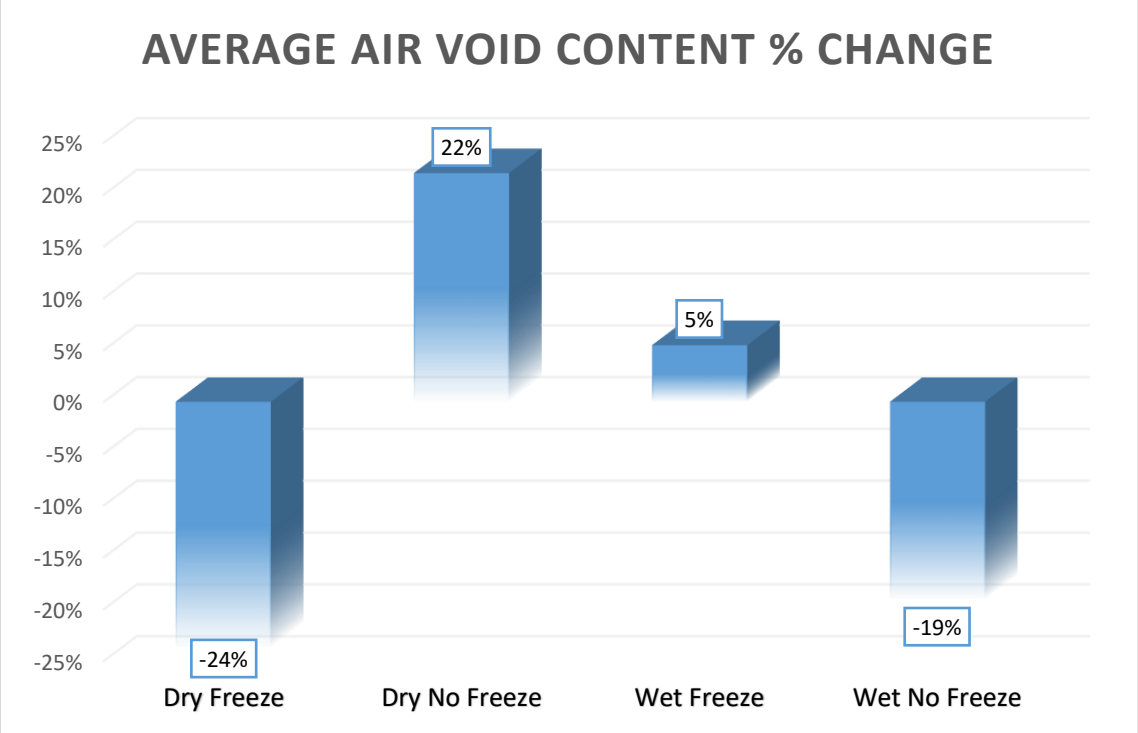


*Figure 76- Average Change in Air Void Content (%)*

### 6.1.c Comparison of the Asphalt Content

In terms of asphalt content, the changes made between the old and new mix designs are shown in the Table 34 below:

*Table 34- Asphalt Content % Comparison*

| State | City | Climatic Zone | AC (%) (LTPP Database) | AC (%) (US Database) |
|---|---|---|---|---|
| **Arizona** | *Flagstaff* | *Dry, Freeze* | 4.6 | 5.3 |
| **Alaska** | *Anchorage* | *Dry, Freeze* | 5.5 | 5.2 |
| **Colorado** | *Rio Blanco* | *Dry, Freeze* | 4.8 | 5.7 |
| **Colorado** | *El Paso* | *Dry, Freeze* | 5 | 5.7 |
| **Colorado** | *Yuma* | *Dry, Freeze* | 5 | 5.7 |
| **Washington** | *Spokane* | *Dry, Freeze* | 5.6 | 6.1 |
| **Arizona** | *Tucson* | *Dry, No Freeze* | 5 | 6.3 |
| **Arizona** | *Phoenix* | *Dry, No Freeze* | 5.3 | 5 |
| **Arizona** | *Kingman* | *Dry, No Freeze* | 4.5 | 5 |
| **Indiana** | *La Porte* | *Wet, Freeze* | 4.8 | 6.6 |
| **Indiana** | *Jackson* | *Wet, Freeze* | 5.4 | 6.2 |
| **Kansas** | *Cherokee* | *Wet, Freeze* | 6.5 | 6.2 |
| **Massachusetts** | *Boston* | *Wet, Freeze* | 5.6 | 5.4 |
| **Massachusetts** | *Springfield* | *Wet, Freeze* | 5 | 5.8 |
| **Michigan** | *Port Huron* | *Wet, Freeze* | 5 | 5.93 |
| **Michigan** | *Alpena* | *Wet, Freeze* | 5 | 5.81 |
| **Michigan** | *Marquette* | *Wet, Freeze* | 5 | 5.62 |
| **Michigan** | *Grand Rapids* | *Wet, Freeze* | 5 | 5.86 |
| **WV** | *Kanawha* | *Wet, Freeze* | 6 | 6 |
| **Alabama** | *Montgomery* | *Wet, No Freeze* | 6 | 5.9 |
| **Alabama** | *Tuscaloosa* | *Wet, No Freeze* | 6 | 6.1 |
| **Arkansas** | *Little Rock* | *Wet, No Freeze* | 5 | 5 |
| **Indiana** | *Jefferson* | *Wet, No Freeze* | 3.7 | 6.2 |
| **Kansas** | *Scott* | *Wet, No Freeze* | 5.8 | 5.6 |
| **SC** | *Columbia/Lexington* | *Wet, No Freeze* | 5.2 | 5.8 |
| **Tennessee** | *Memphis* | *Wet, No Freeze* | 5.6 | 5.7 |
| **Washington** | *Seattle* | *Wet, No Freeze* | 5.5 | 5.6 |
| **WV** | *Charleston* | *Wet, No Freeze* | 6 | 3.9 |

It can be seen that the asphalt content for all the regions has been increasing to reach values in between 5 and 6%. Having a higher percent of asphalt content will make the asphalt pavement structure behave in a softer way. Depending on the type of asphalt binder used, a higher asphalt content helps in fatigue resistance, as softer and more flexible behavior is to be expected. Also, with regards to thermal cracking, having a softer behavior promotes the resistance of the mix to crack. However, too much asphalt is not relatively good in terms of permanent deformation. Therefore, the optimum asphalt content, which is also depending on the aggregates' gradation, should be determined to answer all the distresses that may be encountered. Some states are more susceptible to distresses than others and suffer from a certain type of distresses more than others. These will be defined later on in the chapter.

The following Figure 77 shows the average percent increase of the asphalt binder content from the old to the new pavement mixtures:

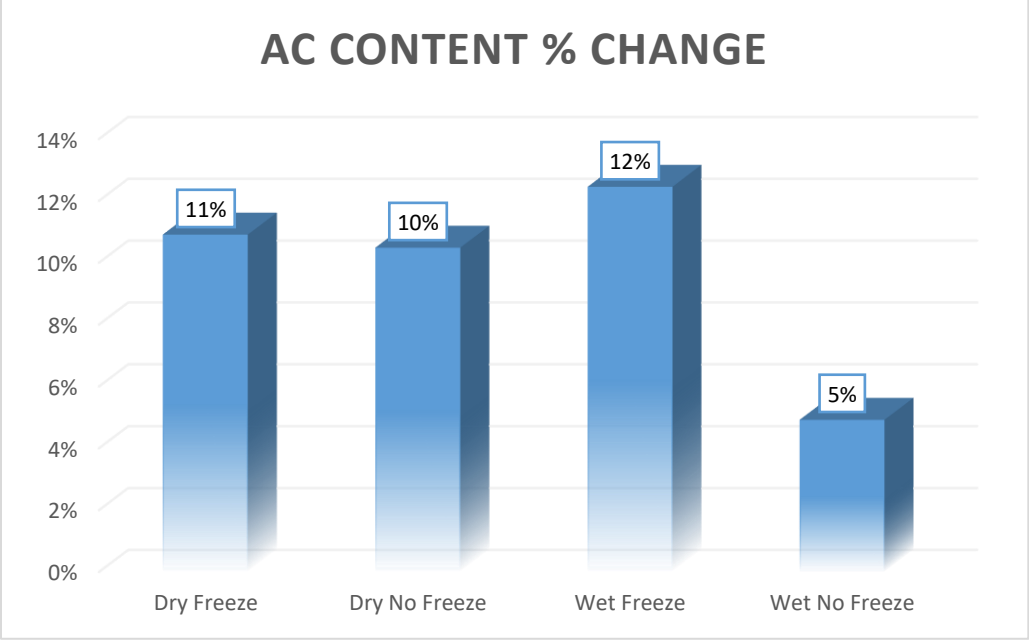


*Figure 77- Average Asphalt Content Change %*

### 6.1.d Comparison of the Effective Binder Content by Volume ($V_{beff}$)

The effective binder content by volume is compared for both databases. It is observed that the $V_{beff}$ is being increased in the recent years, which is reflected also by the increase in asphalt binder content. The Table 35 shows the previous and recent values, followed by a chart showing the percent change from the LTPP Sections and the US Sections.

*Table 35- Vbeff (%) Comparison*

| State | City | Climatic Zone | Vbe (LTPP) | Vbe (US) |
|---|---|---|---|---|
| **Arizona** | *Flagstaff* | *Dry, Freeze* | 9.7 | 11.6 |
| **Alaska** | *Anchorage* | *Dry, Freeze* | 10.1 | 11.4 |
| **Colorado** | *Rio Blanco* | *Dry, Freeze* | 10.3 | 11.9 |
| **Colorado** | *El Paso* | *Dry, Freeze* | 8.708 | 12.2 |
| **Colorado** | *Yuma* | *Dry, Freeze* | 7.61 | 11.3 |
| **Washington** | *Spokane* | *Dry, Freeze* | 8 | 10.8 |
| **Arizona** | *Tucson* | *Dry, No Freeze* | 10 | 10.3 |
| **Arizona** | *Phoenix* | *Dry, No Freeze* | 10.1 | 10.5 |
| **Arizona** | *Kingman* | *Dry, No Freeze* | 10.7 | 10.2 |
| **Indiana** | *La Porte* | *Wet, Freeze* | 10.42 | 12.1 |
| **Indiana** | *Jackson* | *Wet, Freeze* | 11.3 | 11.9 |
| **Kansas** | *Cherokee* | *Wet, Freeze* | 9 | 12.4 |
| **Massachusetts** | *Boston* | *Wet, Freeze* | 8.4 | 13.3 |
| **Massachusetts** | *Springfield* | *Wet, Freeze* | 11.7 | 12.1 |
| **Michigan** | *Port Huron* | *Wet, Freeze* | 10 | 12.3 |
| **Michigan** | *Alpena* | *Wet, Freeze* | 11.3 | 11.4 |
| **Michigan** | *Marquette* | *Wet, Freeze* | 8.875 | 11.37 |
| **Michigan** | *Grand Rapids* | *Wet, Freeze* | 10 | 11 |
| **WV** | *Kanawha* | *Wet, Freeze* | 8.86 | 11.3 |
| **Alabama** | *Montgomery* | *Wet, No Freeze* | 9.2 | 14 |
| **Alabama** | *Tuscaloosa* | *Wet, No Freeze* | 9.8 | 13.8 |
| **Arkansas** | *Little Rock* | *Wet, No Freeze* | 12.3 | 11.5 |
| **Indiana** | *Jefferson* | *Wet, No Freeze* | 10.697 | 11.2 |
| **Kansas** | *Scott* | *Wet, No Freeze* | 10.8 | 11.1 |
| **SC** | *Columbia/Lexington* | *Wet, No Freeze* | 6.1 | 12.4 |
| **Tennessee** | *Memphis* | *Wet, No Freeze* | 8 | 10.7 |
| **Washington** | *Seattle* | *Wet, No Freeze* | 5.1 | 9.3 |
| **WV** | *Charleston* | *Wet, No Freeze* | 7.3 | 8.4 |

It is noticed that the new values of the $V_{beff}$ range between 10 and 12 approximately. It is also noticeable that the $V_{beff}$ values are higher in the freeze regions, as more asphalt binder is added to soften the behavior of the structure at lower weather temperatures. (Figure 78)

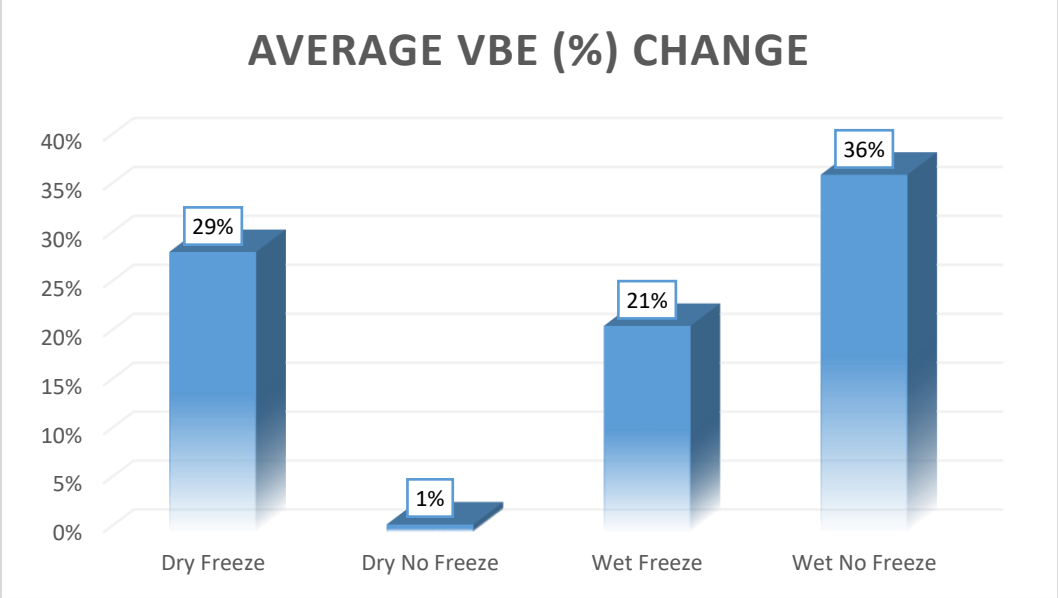


*Figure 78- Average VBE (%) Change*

### 6.1.e Comparison of the Voids in Mineral Aggregates (VMA)

In this section, the changes in Voids in Mineral Aggregates are being evaluated for the old and new pavement mixtures. Basically, the VMA represents the space between the rocks that can be filled with asphalt. When VMA is too low, there is not enough room in the mixture to add enough asphalt binder to adequately coat the individual aggregate particles. VMA is critical to a mixture's durability and crack resistance. When VMA is lowered, the asphalt binder content for a given air void level is lowered. For this reason, the SuperPave has set minimum values for VMA based on the NMAS of the mix:

A 9.5 mm mix has a minimum VMA of 15.0 percent, a 12.5 mm mix is 14.0 percent, and a 19 mm mix is 13.0 percent. Smaller stone mixes have more aggregate surface area to coat, thus requiring more VMA and more asphalt.

The following Table 36 summarizes the values of the VMAs for the old and new pavement mixtures:

*Table 36- VMA (%) Comparison*

| State | City | Climatic Zone | VMA (LTPP Database) | VMA (US Database) |
|---|---|---|---|---|
| **Arizona** | *Flagstaff* | *Dry, Freeze* | 14.6 | 15.56 |
| **Alaska** | *Anchorage* | *Dry, Freeze* | 14 | 15.4 |
| **Colorado** | *Rio Blanco* | *Dry, Freeze* | 14.3 | 15.4 |
| **Colorado** | *El Paso* | *Dry, Freeze* | 14 | 15.7 |
| **Colorado** | *Yuma* | *Dry, Freeze* | 15 | 14.8 |
| **Washington** | *Spokane* | *Dry, Freeze* | 14 | 13.7 |
| **Arizona** | *Tuscon* | *Dry, No Freeze* | 14.6 | 15.9 |
| **Arizona** | *Phoenix* | *Dry, No Freeze* | 14.6 | 15.5 |
| **Arizona** | *Kingman* | *Dry, No Freeze* | 14.6 | 15.4 |
| **Indiana** | *La Porte* | *Wet, Freeze* | 16.6 | 16.1 |
| **Indiana** | *Jackson* | *Wet, Freeze* | 14 | 15.9 |
| **Kansas** | *Cherokee* | *Wet, Freeze* | 14 | 16.4 |
| **Massachusetts** | *Boston* | *Wet, Freeze* | 14 | 17.3 |
| **Massachusetts** | *Springfield* | *Wet, Freeze* | 14 | 16.1 |
| **Michigan** | *Port Huron* | *Wet, Freeze* | 14 | 16.3 |
| **Michigan** | *Alpena* | *Wet, Freeze* | 14 | 15.4 |
| **Michigan** | *Marquette* | *Wet, Freeze* | 14 | 15.37 |
| **Michigan** | *Grand Rapids* | *Wet, Freeze* | 13.5 | 15 |
| **WV** | *Kanawha* | *Wet, Freeze* | 14 | 15.7 |
| **Alabama** | *Montgomery* | *Wet, No Freeze* | 15 | 17.5 |
| **Alabama** | *Tuscaloosa* | *Wet, No Freeze* | 15 | 17.3 |
| **Arkansas** | *Little Rock* | *Wet, No Freeze* | 15.3 | 15.5 |
| **Indiana** | *Jefferson* | *Wet, No Freeze* | 15 | 15.2 |
| **Kansas** | *Scott* | *Wet, No Freeze* | 14 | 15.1 |
| **SC** | *Columbia/Lexington* | *Wet, No Freeze* | 14 | 18.2 |
| **Tennessee** | *Memphis* | *Wet, No Freeze* | 14 | 14.7 |
| **Washington** | *Seattle* | *Wet, No Freeze* | 14 | 15.2 |
| **WV** | *Charleston* | *Wet, No Freeze* | 14 | 12.4 |

It can be seen that the VMAs all answer to the minimum values required by the SuperPave for surface mixtures. However, over the years, as the asphalt binder content has been increased, the VMAs also will increase. This replies to the needs of thermal cracking and fatigue behaviors.

The following Figure 79 shows the average change in VMAs for the old and new pavement mixtures:

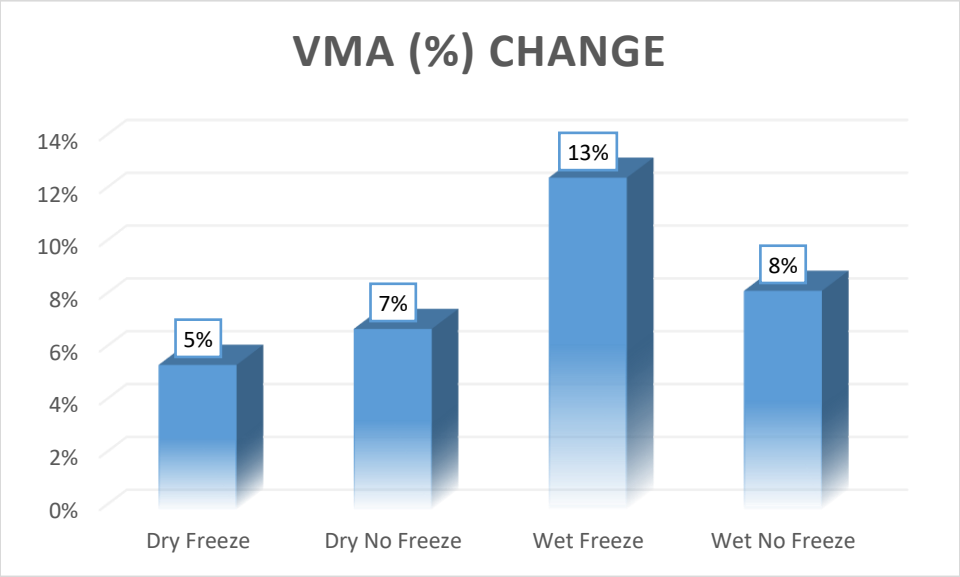


*Figure 79- Average VMA (%) Change*

### 6.1.f Comparison of the Volume Filled with Asphalt (VFA)

The volume Filled with Asphalt (VFA) represents the portion of the voids in the mineral aggregate that contain asphalt binder. It can also be described as the percent of the volume of the VMA that is filled with binder. VFA is inversely related to air voids: as air voids decrease, the VFA increases.

In the case of the pavement mixtures' change considered in this study, increase and decreases of air voids are observed over the climate regions. The changes in VFA are examined and reported in the Table 37 below:

*Table 37- VFA (%) Comparison*

| State | City | Climatic Zone | VFA (LTPP Database) | VFA (US Database) |
|---|---|---|---|---|
| **Arizona** | *Flagstaff* | *Dry, Freeze* | 66 | 74.6 |
| **Alaska** | *Anchorage* | *Dry, Freeze* | 72 | 74.0 |
| **Colorado** | *Rio Blanco* | *Dry, Freeze* | 72 | 77.3 |
| **Colorado** | *El Paso* | *Dry, Freeze* | 62 | 77.7 |
| **Colorado** | *Yuma* | *Dry, Freeze* | 51 | 76.4 |
| **Washington** | *Spokane* | *Dry, Freeze* | 57 | 67.9 |
| **Arizona** | *Tucson* | *Dry, No Freeze* | 68 | 64.8 |
| **Arizona** | *Phoenix* | *Dry, No Freeze* | 69 | 67.7 |
| **Arizona** | *Kingman* | *Dry, No Freeze* | 73 | 66.2 |
| **Indiana** | *La Porte* | *Wet, Freeze* | 63 | 75.2 |
| **Indiana** | *Jackson* | *Wet, Freeze* | 81 | 74.8 |
| **Kansas** | *Cherokee* | *Wet, Freeze* | 64 | 75.6 |
| **Massachusetts** | *Boston* | *Wet, Freeze* | 60 | 76.9 |
| **Massachusetts** | *Springfield* | *Wet, Freeze* | 84 | 75.2 |
| **Michigan** | *Port Huron* | *Wet, Freeze* | 71 | 75.5 |
| **Michigan** | *Alpena* | *Wet, Freeze* | 81 | 74.0 |
| **Michigan** | *Marquette* | *Wet, Freeze* | 63 | 74.0 |
| **Michigan** | *Grand Rapids* | *Wet, Freeze* | 74 | 73.3 |
| **WV** | *Kanawha* | *Wet, Freeze* | 63 | 72.0 |
| **Alabama** | *Montgomery* | *Wet, No Freeze* | 61 | 80.0 |
| **Alabama** | *Tuscaloosa* | *Wet, No Freeze* | 65 | 79.8 |
| **Arkansas** | *Little Rock* | *Wet, No Freeze* | 80 | 74.2 |
| **Indiana** | *Jefferson* | *Wet, No Freeze* | 71 | 73.7 |
| **Kansas** | *Scott* | *Wet, No Freeze* | 77 | 73.5 |
| **SC** | *Columbia/Lexington* | *Wet, No Freeze* | 44 | 68.1 |
| **Tennessee** | *Memphis* | *Wet, No Freeze* | 57 | 72.8 |
| **Washington** | *Seattle* | *Wet, No Freeze* | 36 | 71.1 |
| **WV** | *Charleston* | *Wet, No Freeze* | 52 | 67.7 |

It is expected for the VFA to decrease with increase Air Void Content and vice versa. Taking the average values, the following trends have been observed (Figure 80):

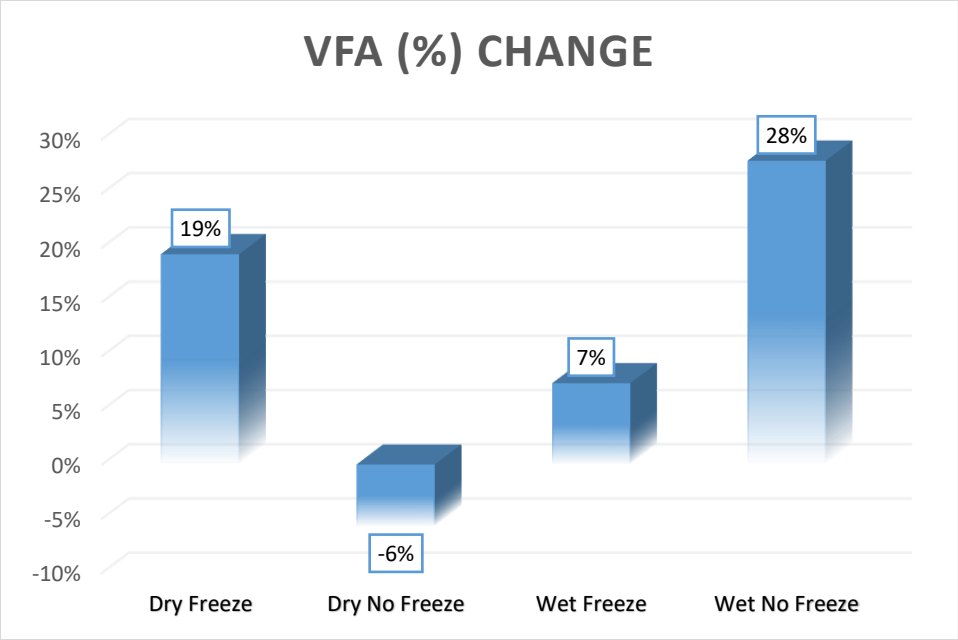


*Figure 80- VFA (%) Change*

The changes in VFA do reflect the ones for Air Void Content except for the Wet Freeze region, where the air void content increased and the VFA still increased. The change in VFA is only about 6% on average. As the VFA is the portion containing asphalt binder in the VMA, if VMA and Va increases, the change may cause the VFA to increase, as VFA is calculated by:

$$VFA = \frac{V_{beff}}{VMA} * 100 \text{ and } V_{beff} = VMA - V_a$$

The change in gradation will have to be studied in this case.

6.1.g Comparison of the Change in Gradation

In this section, the gradation changes will be compared in terms of the percent retained on Sieves #4. ¾'', 3/8'', and percent passing Sieve #200.

The following Table 38 summarizes the gradation results for both the old and new mix designs:

*Table 38- Gradation Comparison for %R04, %R34, %R38, %P200*

| | | | LTPP Database | | | | US Database | | | |
|---|---|---|---|---|---|---|---|---|---|---|
| **State** | **City** | **Climate Zone** | **$R_{04}$** | **$R_{38}$** | **$R_{34}$** | **$P_{200}$** | **$R_{04}$** | **$R_{38}$** | **$R_{34}$** | **$P_{200}$** |
| **AZ** | *Flagstaff* | *DF* | 52 | 39 | 5 | 4.7 | 50 | 29 | 3 | 3.33 |
| **AK** | *Anchorage* | | 39 | 20 | 3 | 7.2 | 52 | 24 | 0 | 5.2 |
| **CO** | *Rio Blanco* | | 48 | 19 | 0 | 9.1 | 36 | 22 | 0 | 4.3 |
| **CO** | *El Paso* | | 43 | 15 | 0 | 9.6 | 45 | 10 | 0 | 4.8 |
| **CO** | *Yuma* | | 37 | 22 | 0 | 8.7 | 42 | 23 | 0 | 4.8 |
| **WA** | *Spokane* | | 41 | 16 | 5.6 | 5.6 | 45 | 18 | 0 | 6.3 |
| **AZ** | *Tucson* | *D, NF* | 42 | 25 | 2 | 7.5 | 40 | 26 | 3 | 3.7 |
| **AZ** | *Phoenix* | | 50 | 35 | 9 | 3.8 | 57 | 37.9 | 3 | 4.2 |
| **AZ** | *Kingman* | | 50 | 28 | 4 | 5.3 | 45 | 24 | 0 | 3.8 |
| **IN** | *La Porte* | *W, F* | 40 | 33 | 0 | 5.9 | 43 | 8.2 | 0 | 5.4 |
| **IN** | *Jackson* | | 46 | 35 | 0 | 5.8 | 37.7 | 5.7 | 0 | 5.2 |
| **KS** | *Cherokee* | | 21 | 14 | 0 | 9.5 | 33 | 13 | 0 | 7.4 |
| **MS** | *Boston* | | 46 | 18 | 0 | 5.4 | 45 | 2 | 0 | 4.2 |
| **MS** | *Springfield* | | 22 | 4 | 0 | 3.7 | 39 | 12 | 0 | 4 |
| **MI** | *Port Huron* | | 14 | 9 | 0 | 6.2 | 18.8 | 4.3 | 0 | 5.6 |
| **MI** | *Alpena* | | 63 | 12 | 8 | 2.3 | 24.3 | 2.2 | 0 | 5.2 |
| **MI** | *Marquette* | | 30 | 13 | 7 | 6 | 29.8 | 6.5 | 0 | 5.6 |
| **MI** | *Grand Rapids* | | 60 | 38 | 6 | 7 | 19.3 | 0.5 | 0 | 5.3 |
| **WV** | *Kanawha* | | 35 | 6 | 0 | 2 | 48 | 34 | 4 | 5 |
| **AL** | *Montgomery* | *W, NF* | 40 | 42 | 4 | 4.7 | 44 | 4 | 0 | 8 |
| **AL** | *Tuscaloosa* | | 63 | 12 | 4 | 4 | 51 | 5 | 0 | 8.4 |
| **AR** | *Little Rock* | | 60 | 39 | 15 | 9.4 | 41 | 14 | 0 | 5.9 |
| **IN** | *Jefferson* | | 59 | 35 | 0 | 3.1 | 33.6 | 3 | 0 | 5 |
| **KS** | *Scott* | | 39 | 19 | 0 | 8.2 | 31 | 13 | 0 | 3.8 |
| **SC** | *Columbia* | | 30 | 8 | 0 | 3.7 | 30 | 9.1 | 0 | 5.32 |
| **TV** | *Memphis* | | 58 | 10 | 17 | 6 | 39 | 13 | 0 | 5.6 |
| **WA** | *Seattle* | | 42 | 23 | 2 | 5.2 | 41 | 6 | 0 | 5.5 |
| **WV** | *Charleston* | | 44 | 20 | 0 | 2.7 | 67 | 55 | 35 | 3.9 |

The average values for each climate region were found and the Figure 81 below has been generated:

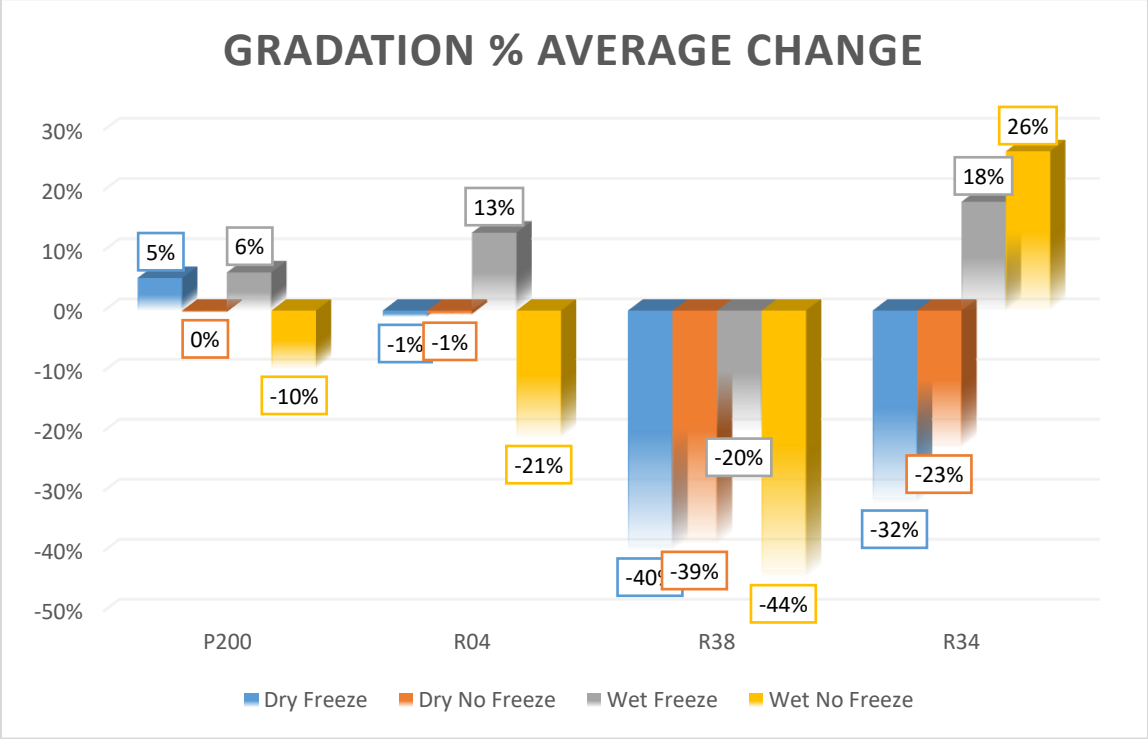


*Figure 81- Average Gradation % Change*

For the Dry Freeze Region, an increase in fine aggregate by only 5% was observed, facing a decrease in the coarse aggregates retained. Having coarse aggregates in the mixture has been proven to reduce the permanent deformation of the pavement structure, by increasing its overall strength.

For the Dry No Freeze region, a decrease in the retained coarse aggregates is noted only, making the pavement structure more flexible.

As for the Wet Freeze region, there is an increase in the amount of ¾'' sized aggregates present in them mix. This leads to believe that the problem in the wet and freeze regions, the agencies are trying to modify their pavement structures according to types of distresses such as permanent deformation.

Concerning the Wet No Freeze region, there is decrease in the aggregate sizes of 3/8'' and 0.187 inches considered, except for the fines passing #200 and ¾''. In this region, the gradation is getting more uniform for all the sizes. The considered improvement in terms of distresses is yet to be determined in the following sections.

The following Table 39 shows in summary what are the changes exhibited by the pavement mixtures over the course of the years:

*Table 39- Summary of the Changes in Pavement Mix Designs*

| Input Parameters | Variation | | | |
|---|---|---|---|---|
| | **Dry, Freeze** | **Dry, No Freeze** | **Wet, Freeze** | **Wet, No Freeze** |
| **PG-Binder type** | Stiffer | Softer | Stiffer | Stiffer |
| **Va (%)** | Decrease (-24%) | Increase (22%) | Increase (5%) | Decrease (-19%) |
| **Ac (%)** | Increase (11%) | Increase (10%) | Increase (12%) | Increase (5%) |
| **Vbeff (%)** | Increase (29%) | Increase (1%) | Increase (21%) | Increase (36%) |
| **VMA (%)** | Increase (5%) | Increase (7%) | Increase (13%) | Increase (8%) |
| **VFA (%)** | Increase (19%) | Decrease (-6%) | Increase (7%) | Increase (28%) |
| **Aggregate Gradation** | Decrease in Coarse Decrease in Fines | Decrease in Coarse | Increase in all Aggregate Types Except for 3/8" | Increase in Aggregates 3/4" Decrease in all other types |

Overall, all the climate regions are decreasing their 3/8'' aggregates. However, The Dry Regions are also decreasing the ¾'' aggregates. This indicates that more binder is needed, and a more flexible behavior is intended. Whereas for the Freeze Regions, an increase of the ¾'' aggregates is observed, trying to make the mixture stronger.

## 6.2 Comparison of the Flow Number and Rutting Behaviors

### 6.2.a Comparison of the Flow Number Values

In the previous chapters (4 and 5), the Flow Number of each section from the LTPP Database as well as from the U.S. database has been predicted based on the provided volumetrics for each climate zone. As the flow number defines the number of repetitions to reach tertiary flow, or permanent deformation, it is a great indicator of the potential of each section to resist rutting. As the "FN" increases, the pavement structure is most likely set to resist rutting longer. Before discussing the rutting parameters, it is important to define the quality of the mix and decide if this mixture will have a good behavior in terms of permanent deformation once the traffic level is forecasted.

The FN values have been predicted for both databases assuming a standard tire pressure of 120 psi, and a confinement level of 20 psi. In the Table 40 below are the predicted FN:

*Table 40- Comparison of FN for Both Databases*

| State | City | Climatic Zone | FN (LTPP) | FN (U.S.) |
|---|---|---|---|---|
| **Arizona** | *Flagstaff* | *Dry, Freeze* | 642 | 1206 |
| **Alaska** | *Anchorage* | *Dry, Freeze* | 332 | 1198 |
| **Colorado** | *Rio Blanco* | *Dry, Freeze* | 402 | 412 |
| **Colorado** | *El Paso* | *Dry, Freeze* | 353 | 170 |
| **Colorado** | *Yuma* | *Dry, Freeze* | 463 | 503 |
| **Washington** | *Spokane* | *Dry, Freeze* | 295 | 866 |
| **Arizona** | *Tucson* | *Dry, No Freeze* | 424 | 154 |
| **Arizona** | *Phoenix* | *Dry, No Freeze* | 214 | 190 |
| **Arizona** | *Kingman* | *Dry, No Freeze* | 424 | 232 |
| **Indiana** | *La Porte* | *Wet, Freeze* | 238 | 685 |
| **Indiana** | *Jackson* | *Wet, Freeze* | 360 | 587 |
| **Kansas** | *Cherokee* | *Wet, Freeze* | 306 | 460 |
| **Massachusetts** | *Boston* | *Wet, Freeze* | 306 | 431 |
| **Massachusetts** | *Springfield* | *Wet, Freeze* | 139 | 288 |
| **Michigan** | *Port Huron* | *Wet, Freeze* | 190 | 462 |
| **Michigan** | *Alpena* | *Wet, Freeze* | 309 | 493 |
| **Michigan** | *Marquette* | *Wet, Freeze* | 167 | 312 |
| **Michigan** | *Grand Rapids* | *Wet, Freeze* | 649 | 459 |
| **WV** | *Kanawha* | *Wet, Freeze* | 151 | 410 |
| **Alabama** | *Montgomery* | *Wet, No Freeze* | 124 | 1086 |
| **Alabama** | *Tuscaloosa* | *Wet, No Freeze* | 711 | 3916 |
| **Arkansas** | *Little Rock* | *Wet, No Freeze* | 633 | 551 |
| **Indiana** | *Jefferson* | *Wet, No Freeze* | 203 | 442 |
| **Kansas** | *Scott* | *Wet, No Freeze* | 590 | 251 |
| **SC** | *Columbia/Lexington* | *Wet, No Freeze* | 56 | 266 |
| **Tennessee** | *Memphis* | *Wet, No Freeze* | 159 | 523 |
| **Washington** | *Seattle* | *Wet, No Freeze* | 185 | 822 |
| **WV** | *Charleston* | *Wet, No Freeze* | 165 | 218 |

It can be clearly seen that most of the Flow Number values have increased over time, which certainly means an increase in rutting resistance. This also means that the rutting problem has been considered by the agencies. However, the extent of this enhancement can only be shown with the effects of the asphalt layer thickness and the expected traffic over the pavement life of the structure. (Figure 82)

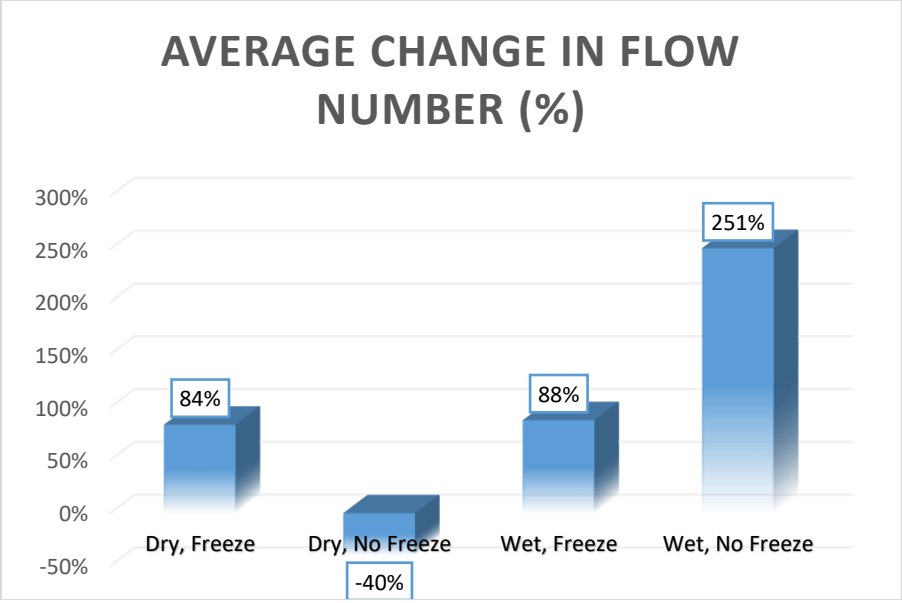


*Figure 82- Average Change in Flow Number (%)*

It can be observed that the changes implemented by the agencies to the asphalt volumetrics did quite affect the flow number values. Three of the four climatic regions have exhibited great increases in the flow number values, leading to a potential improvement on rutting.

However, for the Dry No Freeze, the Flow Number values seem to be decreasing. By considering the changes to the pavement mix designs (Table 39, it can be seen that for the Dry, No Freeze region, a choice of a softer binder has been recorded, as well as an increase in the asphalt content and air voids. All these modifications are pointing towards a softer behavior of the mix. In order to have a high Flow Number value and thus less expected Rutting, a stiffer behavior is recommended to resist permanent deformation. A slight decrease in the coarse aggregates has been done to the mixture.

### 6.2.b Comparison of the Rutting Values

In this section, the predicted rutting values as per the Flow Number values, measured ESALs and asphalt thickness are generated for both the old and new pavement mixtures. As the flow number values have been compared in the previous section, the rutting values in here will be compared for each location as per the climatic regions. In order to be able to compare the two predicted rutting values, the rutting has been predicted using the Asphalt Thicknesses provided by the LTPP for all the databases, for a constant traffic level of 30 million ESALs.

The summarized values are found below in Table 41.

*Table 41- Predicted Rutting Depth Comparison*

| *State* | *Climate Zone* | *Rutting of LTPP Database for 30 mil* | *Rutting Using LTPP Thickness and 30 mil* |
|---|---|---|---|
| **Flagstaff** | *Dry, Freeze* | 0.63 | 0.57 |
| **Anchorage** | *Dry, Freeze* | 0.83 | 0.64 |
| **Rio Blanco** | *Dry, Freeze* | 0.62 | 0.65 |
| **El Paso** | *Dry, Freeze* | 0.45 | 0.56 |
| **Yuma** | *Dry, Freeze* | 0.44 | 0.45 |
| **Spokane** | *Dry, Freeze* | 1.73 | 1.40 |
| **Tucson** | *Dry, No Freeze* | 0.46 | 0.62 |
| **Phoenix** | *Dry, No Freeze* | 0.49 | 0.53 |
| **Kingman** | *Dry, No Freeze* | 0.49 | 0.60 |
| **La Porte** | *Wet, Freeze* | 0.67 | 0.62 |
| **Jackson** | *Wet, Freeze* | 0.64 | 0.60 |
| **Cherokee** | *Wet, Freeze* | 0.35 | 0.34 |
| **Boston** | *Wet, Freeze* | 0.69 | 0.67 |
| **Springfield** | *Wet, Freeze* | 0.70 | 0.62 |
| **Port Huron** | *Wet, Freeze* | 2.37 | 2.01 |
| **Alpena** | *Wet, Freeze* | 0.99 | 1.06 |
| **Marquette** | *Wet, Freeze* | 1.26 | 1.02 |
| **Grand Rapids** | *Wet, Freeze* | 0.44 | 0.55 |
| **Wet Freeze Region/ Kanawha** | *Wet, Freeze* | 2.20 | 1.82 |
| **Montgomery** | *Wet, No Freeze* | 0.94 | 0.59 |
| **Tuscaloosa** | *Wet, No Freeze* | 0.75 | 0.52 |
| **Little Rock** | *Wet, No Freeze* | 0.77 | 0.83 |
| **Jefferson** | *Wet, No Freeze* | 0.27 | 0.23 |
| **Scott** | *Wet, No Freeze* | 0.27 | 0.35 |
| **Columbia/Lexington** | *Wet, No Freeze* | 4.42 | 3.18 |
| **Memphis** | *Wet, No Freeze* | 0.76 | 0.53 |
| **Seattle** | *Wet, No Freeze* | 0.48 | 0.35 |
| **Charleston** | *Wet, No Freeze* | 1.37 | 1.34 |

The average change in the expected rutting has been calculated, and the following results have been obtained Figure 83:

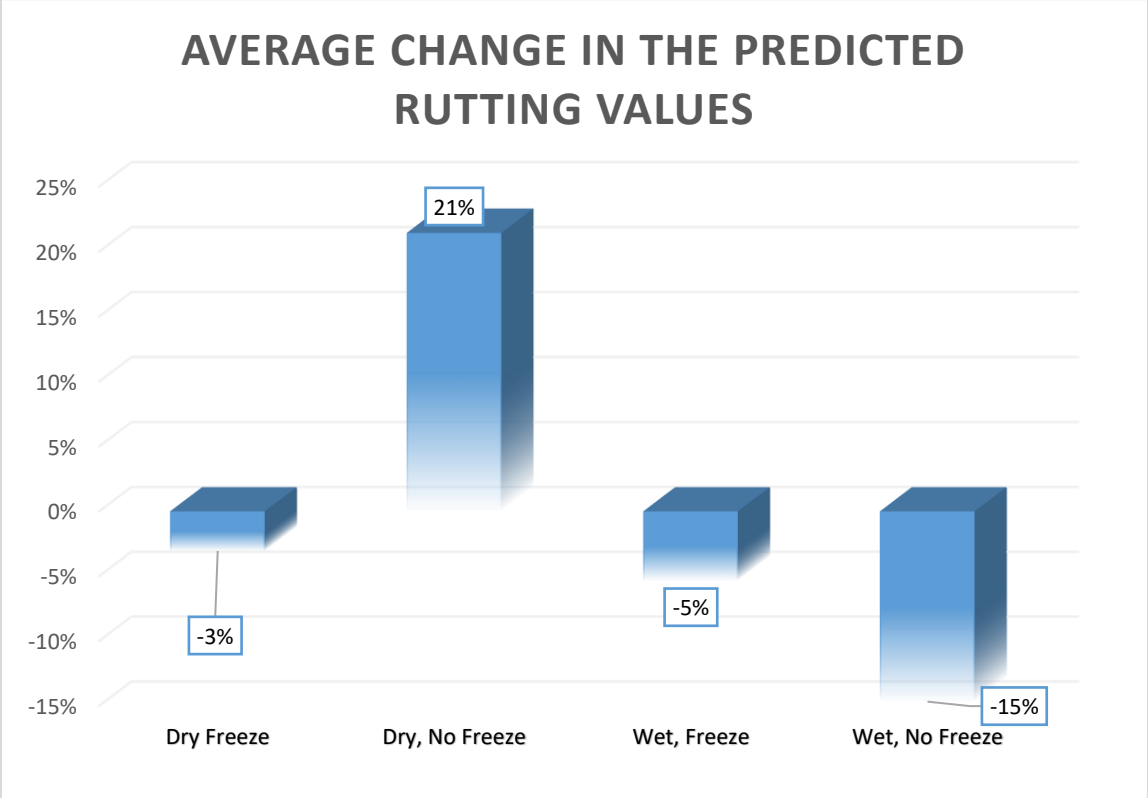


*Figure 83- Average Rutting Change*

Based on the variations of the Flow Number analyzed above, the results are expected in terms of predicted rutting values. As these values are only the average of the obtained values, and the percentages do depend on the number of sections in each region, one would expect these values to be higher, as the flow number values have greatly increased with the change in the mix design.

### 6.2.c Rutting Ranking Criteria

As discussed previously, when fitting a fitting based on a specific data, trying to input other values in the same model will cause it to become less accurate. When developing

such models, overfitting is most likely, and the accuracy of the model as well as reliability will decrease.

For the case of the predictive rutting model used in this study, it can be seen that is becomes less reliable for values greater than 0.6''. Nonetheless, it still predicted whether the mix design is going to exhibit a small or huge amount of permanent deformation.

As the Predictive Rutting Model used in this study is based on one major component, which is the Flow Number, it was possible to develop a set of ranking criteria to assess the quality of the pavement mixtures. The criteria Table 42 is found below:

*Table 42- Flow Number Criteria*

| | | |
|---|---|---|
| **FN Ranges** | Low | <400 |
| | Satisfactory | 400 - 600 |
| | Good | 600-800 |
| | Excellent | >800 |

Given the Flow Number for each mix design from both databases, the quality of the mix is assessed and recorded in the Table 43 below:

*Table 43- Ranking Table based on FN*

| State | City | Climatic Zone | FN (LTPP) | Rank | FN (U.S.) | Rank |
|---|---|---|---|---|---|---|
| **Arizona** | *Flagstaff* | *D, F* | 642 | G | 1206 | E |
| **Alaska** | *Anchorage* | | 332 | L | 1198 | E |
| **Colorado** | *Rio Blanco* | | 402 | S | 412 | S |
| **Colorado** | *El Paso* | | 353 | L | 170 | L |
| **Colorado** | *Yuma* | | 463 | S | 503 | S |
| **Washington** | *Spokane* | | 295 | L | 866 | E |
| **Arizona** | *Tucson* | *D, NF* | 424 | S | 154 | L |
| **Arizona** | *Phoenix* | | 214 | L | 190 | L |
| **Arizona** | *Kingman* | | 424 | S | 232 | L |
| **Indiana** | *La Porte* | *W, F* | 238 | L | 685 | G |
| **Indiana** | *Jackson* | | 360 | L | 587 | S |
| **Kansas** | *Cherokee* | | 306 | L | 460 | S |
| **Massachusetts** | *Boston* | | 306 | L | 431 | S |
| **Massachusetts** | *Springfield* | | 139 | L | 288 | L |
| **Michigan** | *Port Huron* | | 190 | L | 462 | S |
| **Michigan** | *Alpena* | | 309 | L | 493 | S |
| **Michigan** | *Marquette* | | 167 | L | 312 | L |
| **Michigan** | *Grand Rapids* | | 649 | G | 459 | S |
| **WV** | *Kanawha* | | 151 | L | 410 | S |
| **Alabama** | *Montgomery* | *W, NF* | 124 | L | 1086 | E |
| **Alabama** | *Tuscaloosa* | | 711 | G | 3916 | E |
| **Arkansas** | *Little Rock* | | 633 | G | 551 | S |
| **Indiana** | *Jefferson* | | 203 | G | 442 | S |
| **Kansas** | *Scott* | | 590 | Satisfactory | 251 | L |
| **SC** | *Columbia* | | 56 | Low | 266 | L |
| **Tennessee** | *Memphis* | | 159 | Low | 523 | S |
| **Washington** | *Seattle* | | 185 | Low | 822 | E |
| **WV** | *Charleston* | | 165 | Low | 218 | L |

Where E stands for Excellent, G for Good, S for Satisfactory and L for low.

For the Dry Freeze region, the mix designs have improved in terms of rutting. This can be explained by the increase in coarse aggregates and the use of a stiffer binder.

For the Dry, No Freeze region, the rutting behavior of the mixtures was low for all the previous mixtures and is still low. As the binder type used is softer, and the air void content is increased in addition to the increase in the asphalt content, softer behavior is to be expected. In terms of permanent deformation, stiffer behavior must be expected in order to resist permanent deformations, especially at higher temperatures or hot climates.

For the Wet, Freeze Region, the mix designs have improved rutting behavior. The binder types used in the recent dates are stiffer. However, the air void content has slightly increased, and the coarse aggregates' gradation has decreased. This explains why the pavement mixtures only slightly increased in terms of Flow Number, from to Satisfactory.

Finally, for the Wet Freeze Region, an improvement has also been noted. The binder type used is stiffer, and the air void content has decreased. Also, the aggregate gradation has been modified. Most of the pavement mixtures are not satisfactory as well, with only two potential "Excellent" in Alabama.

Based on the data gathered, a potential criterion for the volumetric properties has been set. Using the tables when having the input data at hand, the quality of the mix could be approximated at a first glance. The criteria are summarized in the Table 44 below:

*Table 44- Ranking Criteria by Volumetric Properties*

| | Dry, Freeze | | Dry, No Freeze | | Wet, Freeze | | Wet, No Freeze | |
|---|---|---|---|---|---|---|---|---|
| Poor Design | P200 (%) | 4-4.8 | P200 (%) | 3.7-4.2 | P200 (%) | 3-4.8 | P200 (%) | 3.8-5 |
| | R04 (%) | 39-45 | R04 (%) | 45-50 | R04 (%) | 25-40 | R04 (%) | 20-40 |
| | R34 (%) | 0-5 | R34 (%) | >9 | R34 (%) | 0 | R34 (%) | 0 |
| | Va (%) | 3.3-3.4 | Va (%) | >5 | Va (%) | >4 | Va (%) | >4 |
| | AC (%) | >5.5 | AC (%) | >5 | AC (%) | 5-5.5 | AC (%) | 4.3-5.8 |
| | | | | | | | | |
| Medium Design | P200 (%) | 4.8-6 | P200 (%) | 4.5-5 | P200 (%) | 5.5-7 | P200 (%) | 5-6. |
| | R04 (%) | 45-50 | R04 (%) | 45-50 | R04 (%) | 40-45 | R04 (%) | 40-55 |
| | R34 (%) | 0-5 | R34 (%) | 0-4 | R34 (%) | 0-4 | R34 (%) | 0-4 |
| | Va (%) | 3.5-4 | Va (%) | 3.9-4 | Va (%) | 4 | Va (%) | 4 |
| | AC (%) | 5.5-5.7 | AC (%) | 4.5-5 | AC (%) | 5.5-6 | AC (%) | 5.8-6.3 |
| | | | | | | | | |
| Excellent Design | P200 (%) | 5-6.8 | P200 (%) | 5-5.5 | P200 (%) | 10-Jul | P200 (%) | 6-9' |
| | R04 (%) | 50-55 | R04 (%) | 50-55 | R04 (%) | 45-60 | R04 (%) | 55-60 |
| | R34 (%) | 0-5 | R34 (%) | 0 | R34 (%) | 0-6 | R34 (%) | 0 |
| | Va (%) | 3.9-4.4 | Va (%) | 4-4.5 | Va (%) | 4 | Va (%) | 3.5-4 |
| | AC (%) | 4.6-5.5 | AC (%) | 4.5-5 | AC (%) | 5.5-6.5 | AC (%) | 5.9-6.6 |

The Excellent section in the table in the Dry, No Freeze region is simply because no excellent mix designs have been gathered in this region. Therefore, no accurate criteria could be developed. The proposed one is based on the supposed behavior trend observed from the evolution of the Poor and Medium designs.

## 6.3 Comparison of the Fatigue Behavior

### 6.3.a Comparison of the $N_f$

In this section, the fatigue behavior of the old and new databases will be assessed based on the developed number of cycles, $N_f$, defined in the previous chapter 3. As this number of cycles to failure defines when fatigue is prone to happen in the pavement, it is very beneficial to have a good indicator on the aspect of this distress.

The higher the number of cycles to failure, the longer it will take for the fatigue failure to happen. In this section, the $N_f$ values were calculated based on the pavement mixtures provided, and the difference will be studied. As the mixtures were shown to be different, certainly the fatigue behavior will be different. The fatigue failure is studied for the same strain level, which is 350 με. The values are tabulated below in Table 45:

*Table 45- Number of Cycles to Failure Comparison*

| State | City | Climatic Zone | Nf (LTPP Database) | Nf (US Database) |
|---|---|---|---|---|
| **Arizona** | *Flagstaff* | *Dry, Freeze* | 9435 | 14177 |
| **Alaska** | *Anchorage* | *Dry, Freeze* | 15257 | 30244 |
| **Colorado** | *Rio Blanco* | *Dry, Freeze* | 7734 | 14426 |
| **Colorado** | *El Paso* | *Dry, Freeze* | 7500 | 21303 |
| **Colorado** | *Yuma* | *Dry, Freeze* | 8234 | 18600 |
| **Washington** | *Spokane* | *Dry, Freeze* | 6262 | 16943 |
| **Arizona** | *Tucson* | *Dry, No Freeze* | 10887 | 11515 |
| **Arizona** | *Phoenix* | *Dry, No Freeze* | 13478 | 15898 |
| **Arizona** | *Kingman* | *Dry, No Freeze* | 12750 | 11304 |
| **Indiana** | *La Porte* | *Wet, Freeze* | 13055 | 15476 |
| **Indiana** | *Jackson* | *Wet, Freeze* | 13055 | 20482 |
| **Kansas** | *Cherokee* | *Wet, Freeze* | 8368 | 28278 |
| **Massachusetts** | *Boston* | *Wet, Freeze* | 4839 | 26026 |
| **Massachusetts** | *Springfield* | *Wet, Freeze* | 14058 | 21417 |
| **Michigan** | *Port Huron* | *Wet, Freeze* | 10066 | 27820 |
| **Michigan** | *Alpena* | *Wet, Freeze* | 7938 | 18941 |
| **Michigan** | *Marquette* | *Wet, Freeze* | 4646 | 20833 |
| **Michigan** | *Grand Rapids* | *Wet, Freeze* | 16032 | 22213 |
| **WV** | *Kanawha* | *Wet, Freeze* | 8100 | 13426 |
| **Alabama** | *Montgomery* | *Wet, No Freeze* | 7214 | 35166 |
| **Alabama** | *Tuscaloosa* | *Wet, No Freeze* | 8200 | 34172 |
| **Arkansas** | *Little Rock* | *Wet, No Freeze* | 12999 | 23761 |
| **Indiana** | *Jefferson* | *Wet, No Freeze* | 11617 | 18117 |
| **Kansas** | *Scott* | *Wet, No Freeze* | 16943 | 22622 |
| **SC** | *Columbia/Lexington* | *Wet, No Freeze* | 3136 | 27611 |
| **Tennessee** | *Memphis* | *Wet, No Freeze* | 6552 | 20581 |
| **Washington** | *Seattle* | *Wet, No Freeze* | 590 | 5562 |
| **WV** | *Charleston* | *Wet, No Freeze* | 5417 | 7250 |

The average change in the Nf has been computed, and the following Figure 84 has been generated:

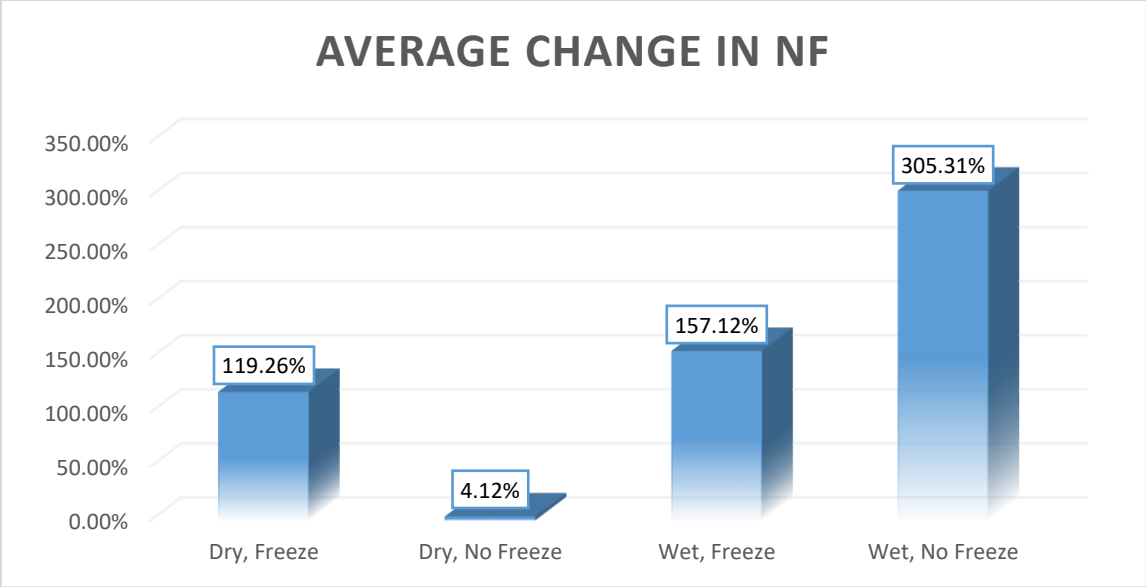


*Figure 84- Average Change in the Number of Cycles to Failure*

As mentioned in the first section and referring to the summarizing table of all the changes incurred to the mix designs in the recent dates, the behavior of the new pavement mixtures is suspected to go in favor of fatigue cracking.

For the Dry, Freeze region, a large increase in the asphalt content as well as the volume of effective binder content is noted. Also, the portion of coarse aggregates in the mix is decrease. This new mix design works in favor of the fatigue behavior of the mix, and this is shown by the obtained results.

For the Dry, No Freeze region, the air void content has been increased by 22%, whereas the $V_{beff}$ has not been very much increased. The behavior has still slightly increased, but not in a very high perspective.

For the Wet, Freeze region, the same positive increase in the number of cycles is being observed. The freeze regions are considering enhancing their mix designs in terms of fatigue life.

Finally, for the Wet No Freeze region, the mix designs are performing much better with the decrease in air void content (or decrease in permeability) and the increase in the $V_{beff}$.

So far, the new pavement mixtures are considering fatigue resistance in all the climatic regions.

### 6.3.b Fatigue Ranking Criteria

Based on the obtained results, as well as the measured fatigue behavior according to the LTPP, the fatigue model suggested has proven to be reliable. It is important to consider that the comparisons has been done for a certain strain level of 350 με, and that this strain level may and may not occur in the field. However, based on the measured data, a ranking criteria has been set in order to assess the quality of the pavement mixtures in terms of fatigue (Table 46)

*Table 46- Fatigue Design Criteria*

| | | |
|---|---|---|
| **Nf Ranges** | Low | <6,000 |
| | Satisfactory | 6,000-10,000 |
| | Good | 10,000-15,000 |
| | Excellent | >15,000 |

These ranges have been based on the observations made with respect to the LTPP Sections and the Predicted Number of cycles. The amount of alligator cracking and longitudinal cracking on the wheel-path determined the possible ranges mentioned in the Table 46 above.

Having a pavement mixture on hand with the required volumetric properties, it is possible to obtain the number of cycles to failure of this mix. Based on the ranking criteria, giving a certain quality of the mix in terms of fatigue would be possible.

The pavement mixtures on hand from the LTPP and US Databases were both ranked according to the criteria developed. The results are mentioned below in Table 47:

*Table 47- Ranking of the Mix Designs*

| State | City | Climatic Zone | Nf (LTPP) | Rank | Nf (US) | Rank |
|---|---|---|---|---|---|---|
| **Arizona** | *Flagstaff* | *Dry, Freeze* | 9435 | S | 14177 | G |
| **Alaska** | *Anchorage* | *Dry, Freeze* | 15257 | E | 30244 | E |
| **Colorado** | *Rio Blanco* | *Dry, Freeze* | 7734 | S | 14426 | G |
| **Colorado** | *El Paso* | *Dry, Freeze* | 7500 | S | 21303 | E |
| **Colorado** | *Yuma* | *Dry, Freeze* | 8234 | S | 18600 | E |
| **Washington** | *Spokane* | *Dry, Freeze* | 6262 | S | 16943 | E |
| **Arizona** | *Tucson* | *Dry, No Freeze* | 10887 | G | 11515 | G |
| **Arizona** | *Phoenix* | *Dry, No Freeze* | 13478 | G | 15898 | E |
| **Arizona** | *Kingman* | *Dry, No Freeze* | 12750 | G | 11304 | G |
| **Indiana** | *La Porte* | *Wet, Freeze* | 13055 | G | 15476 | E |
| **Indiana** | *Jackson* | *Wet, Freeze* | 13055 | G | 20482 | E |
| **Kansas** | *Cherokee* | *Wet, Freeze* | 8368 | S | 28278 | E |
| **Massachusetts** | *Boston* | *Wet, Freeze* | 4839 | L | 26026 | E |
| **Massachusetts** | *Springfield* | *Wet, Freeze* | 14058 | G | 21417 | E |
| **Michigan** | *Port Huron* | *Wet, Freeze* | 10066 | G | 27820 | E |
| **Michigan** | *Alpena* | *Wet, Freeze* | 7938 | S | 18941 | E |
| **Michigan** | *Marquette* | *Wet, Freeze* | 4646 | L | 20833 | E |
| **Michigan** | *Grand Rapids* | *Wet, Freeze* | 16032 | E | 22213 | E |
| **WV** | *Kanawha* | *Wet, Freeze* | 8100 | S | 13426 | G |
| **Alabama** | *Montgomery* | *Wet, No Freeze* | 7214 | S | 35166 | E |
| **Alabama** | *Tuscaloosa* | *Wet, No Freeze* | 8200 | S | 34172 | E |
| **Arkansas** | *Little Rock* | *Wet, No Freeze* | 12999 | G | 23761 | E |
| **Indiana** | *Jefferson* | *Wet, No Freeze* | 11617 | G | 18117 | E |
| **Kansas** | *Scott* | *Wet, No Freeze* | 16943 | E | 22622 | E |
| **SC** | *Columbia* | *Wet, No Freeze* | 3136 | L | 27611 | E |
| **Tennessee** | *Memphis* | *Wet, No Freeze* | 6552 | S | 20581 | E |
| **Washington** | *Seattle* | *Wet, No Freeze* | 590 | L | 5562 | L |
| **WV** | *Charleston* | *Wet, No Freeze* | 5417 | L | 7250 | S |

Where E stands for Excellent, G for Good, S for Satisfactory and L for Low.

Part of this effort included developing volumetric properties ranges, where as a combination of them would produce a specific fatigue behavior. Having the volumetric properties at hand and fitting them in the ranges below, the behavior of the pavement mixture in terms of fatigue can be forecasted. It is to be noted that these ranges are approximate with the sole purpose of giving an indication of the potential behavior.

Based on the data gathered, the following ranges were developed for the climate regions studied: (Table 48)

*Table 48- Possible Rating Criteria based on Volumetric Properties*

| | Dry, Freeze | | Dry, No Freeze | | Wet, Freeze | | Wet, No Freeze | |
|---|---|---|---|---|---|---|---|---|
| **Poor Design** | **VBE** | <8 | **VBE** | 8-10. | **VBE** | 8.4-8.9 | **VBE** | <8 |
| | **VFA** | <57 | **VFA** | <55 | **VFA** | <63 | **VFA** | 36-57 |
| | **Va** | <5.3 | **Va** | 5 | **Va** | <5.1 | **Va** | 5 |
| | **AC** | >5 | **AC** | >5 | **AC** | >5 | **AC** | >5 |
| | | | | | | | | |
| **Medium Design** | **VBE** | 8-10 | **VBE** | 10-11 | **VBE** | 9-11 | **VBE** | 8-10.5 |
| | **VFA** | 62-72 | **VFA** | 68-73 | **VFA** | 64-74 | **VFA** | 61-71 |
| | **Va** | 3.9-5.29 | **Va** | 3.9-4.6 | **Va** | 3.5-5 | **Va** | 4-3.5 |
| | **AC** | 4.8-5 | **AC** | 4.5-5 | **AC** | 4.8-5 | **AC** | 3.7-5 |
| | | | | | | | | |
| **Excellent Design** | **VBE** | 10-12. | **VBE** | 11-12.5 | **VBE** | 11 | **VBE** | 10.7-12.3 |
| | **VFA** | 72-80 | **VFA** | 75-80 | **VFA** | 74-84 | **VFA** | 72-80 |
| | **Va** | 3.5-4 | **Va** | 3.5-5 | **Va** | 2.3-3.5 | **Va** | 3-3.9 |
| | **AC** | 5.5-6.1 | **AC** | 4.8-5.5 | **AC** | 4.8-5 | **AC** | 5 |

## 6.4 Comparison the Thermal Cracking Behavior

### 6.4.a Comparison of the Thermal Cracking Input Parameters

In this section, the approximation of the thermal cracking behavior has been generated based on the calculation of the main input parameters of the TCMODEL. By predicting these values and comparing them to actual measured thermal cracks, the resistance to thermal cracking was assessed.

Even though no straight relationship defines tensile strength to thermal cracks directly, the tensile strength combined with creep compliance and fracture energy gives a possible trend for the thermal behavior.

The creep compliance, as well as the creep compliance fracture parameters, tensile strength and fracture energy were predicted for each mix design at hand. However, the limits of the fracture energy model were small, and the results were not very reliable as the model generated negative values. The positive values generated did make sense in terms of thermal cracks, as a high fracture energy means that more energy is required to initiate and propagate the crack. Also, the more the structure dissipates the energy, the higher is the likelihood of cracks happening. Once a crack happens, all the energy trapped inside is released.

In the Table 56 in Appendix A are summarized the results obtained for the LTPP Database, followed by the results obtained by the U.S. Database. Based on the predicted and measured stresses, a ranking criterion has been developed to assess the potential of cracking resistance of the mixtures.

In Table 73in appendix B are the results of the US Database.

Now comparing each parameter at a time:

For the creep compliance (Table 49)

*Table 49- Creep Compliance Comparison*

| State | City | Climate Zone | LTPP Database D(100) @ -10°C | US Database D(100) @ -10°C Database |
|---|---|---|---|---|
| **Arizona** | Flagstaff | Dry, Freeze | 1.12727E-06 | 2.396E-06 |
| **Alaska** | Anchorage | Dry, Freeze | 2.2525E-06 | 8.671E-06 |
| **Colorado** | Rio Blanco | Dry, Freeze | 1.79675E-06 | 3.977E-06 |
| **Colorado** | El Paso | Dry, Freeze | 1.0175E-06 | 2.875E-06 |
| **Colorado** | Yuma | Dry, Freeze | 9.09183E-07 | 2.585E-06 |
| **Washington** | Spokane | Dry, Freeze | 9.32245E-07 | 2.775E-06 |
| **Arizona** | Tuscon | Dry, No Freeze | 9.26867E-07 | 1.816E-06 |
| **Arizona** | Phoenix | Dry, No Freeze | 9.00447E-07 | 2.661E-06 |
| **Arizona** | Kingman | Dry, No Freeze | 9.16759E-07 | 1.712E-06 |
| **Indiana** | La Porte | Wet, Freeze | 1.36055E-06 | 2.497E-06 |
| **Indiana** | Jackson | Wet, Freeze | 8.25545E-07 | 2.455E-06 |
| **Kansas** | Cherokee | Wet, Freeze | 9.33395E-07 | 3.033E-06 |
| **Massachusetts** | Boston | Wet, Freeze | 9.14435E-07 | 3.310E-06 |
| **Massachusetts** | Springfield | Wet, Freeze | 7.13975E-07 | 3.093E-06 |
| **Michigan** | Port Huron | Wet, Freeze | 1.03577E-06 | 3.015E-06 |
| **Michigan** | Alpena | Wet, Freeze | 9.54255E-07 | 2.956E-06 |
| **Michigan** | Marquette | Wet, Freeze | 1.19158E-06 | 4.984E-06 |
| **Michigan** | Grand Rapids | Wet, Freeze | 1.52964E-06 | 2.768E-06 |
| **West Virginia** | Kanawha | Wet, Freeze | 9.25171E-07 | 2.579E-06 |
| **Alabama** | Montgomery | Wet, No Freeze | 8.04384E-07 | 2.637E-06 |
| **Alabama** | Tuscaloosa | Wet, No Freeze | 8.36473E-07 | 2.615E-06 |
| **Arkansas** | Little Rock | Wet, No Freeze | 6.91453E-07 | 2.641E-06 |
| **Indiana** | Jefferson | Wet, No Freeze | 1.16316E-06 | 2.343E-06 |
| **Kansas** | Scott | Wet, No Freeze | 9.77037E-07 | 2.788E-06 |
| **South Carolina** | Columbia/Lexington | Wet, No Freeze | 4.069E-07 | 3.012E-06 |
| **Tennessee** | Memphis | Wet, No Freeze | 8.37544E-07 | 3.147E-06 |
| **Washington** | Seattle | Wet, No Freeze | 3.6735E-07 | 1.856E-06 |
| **West Virginia** | Charleston | Wet, No Freeze | 7.30665E-07 | 1.831E-06 |

The average change in creep compliance have been reported in the Figure 85 below:

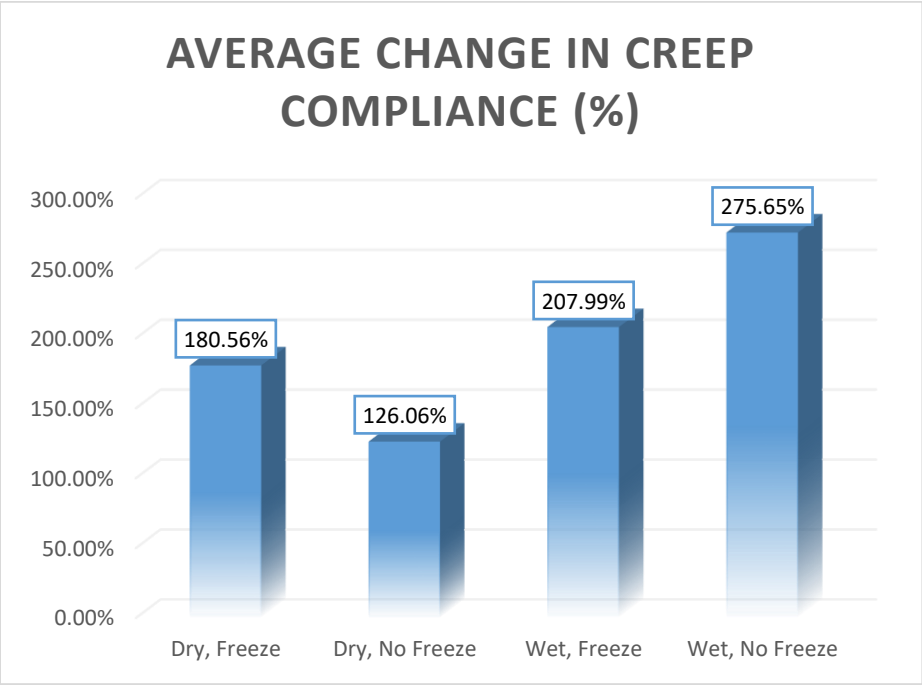


*Figure 85- Average Change in Creep Compliance (%)*

A huge increase in creep compliance is recorded for all the climatic region. Referring back to the table summarizing the changes in the mix design, all of the regions were expecting a softer behavior with the change in pavement mixtures. An increase in Asphalt content, as well as decrease of air voids will work for the benefit of the pavement mixtures (especially for the Wet, No Freeze Region). However, all in all, the changes have a positive impact on creep compliance behavior in all the regions.

In terms of tensile strength and fracture energy: (Table 50)

*Table 50- Comparison between Fracture Energy and Tensile Strength*

| | | | LTPP Database | | US Database | |
|---|---|---|---|---|---|---|
| **State** | **City** | **Climate Zone** | **FE (lb.in)** | **TS (14°F) in psi** | **FE (lb.in)** | **TS (14°F) in psi** |
| **Arizona** | Flagstaff | Dry, Freeze | -101.7 | 485.6 | 43.6 | 392.0 |
| **Alaska** | Anchorage | Dry, Freeze | -3109.3 | 551.1 | -156.1 | 582.6 |
| **Colorado** | Rio Blanco | Dry, Freeze | -1568.3 | 525.8 | -76.5 | 522.3 |
| **Colorado** | El Paso | Dry, Freeze | -118.4 | 546.1 | 136.0 | 424.1 |
| **Colorado** | Yuma | Dry, Freeze | 271.9 | 707.9 | -154.9 | 437.7 |
| **Washington** | Spokane | Dry, Freeze | 60.5 | 621.2 | 112.7 | 427.3 |
| **Arizona** | Tucson | Dry, No Freeze | -224.7 | 398.9 | 183.9 | 347.6 |
| **Arizona** | Phoenix | Dry, No Freeze | -260.2 | 377.1 | 14.5 | 418.2 |
| **Arizona** | Kingman | Dry, No Freeze | -281.7 | 388.6 | -19.6 | 347.7 |
| **Indiana** | La Porte | Wet, Freeze | 248.5 | 467.7 | 342.2 | 382.7 |
| **Indiana** | Jackson | Wet, Freeze | -574.2 | 450.7 | 186.6 | 383.6 |
| **Kansas** | Cherokee | Wet, Freeze | -56.9 | 487.1 | 334.5 | 408.9 |
| **Massachusetts** | Boston | Wet, Freeze | -13.7 | 557.6 | 573.9 | 401.2 |
| **Massachusetts** | Springfield | Wet, Freeze | -645.9 | 461.2 | 260.2 | 418.3 |
| **Michigan** | Port Huron | Wet, Freeze | -374.9 | 463.3 | 272.8 | 410.5 |
| **Michigan** | Alpena | Wet, Freeze | -729.8 | 477.5 | 63.5 | 431.0 |
| **Michigan** | Marquette | Wet, Freeze | -291.7 | 558.3 | -82.4 | 491.2 |
| **Michigan** | Grand Rapids | Wet, Freeze | -738.1 | 547.6 | -100.6 | 434.8 |
| **West Virginia** | Kanawha | Wet, Freeze | -97.9 | 498.6 | 144.4 | 395.4 |
| **Alabama** | Montgomery | Wet, No Freeze | 99.6 | 447.8 | 664.0 | 383.9 |
| **Alabama** | Tuscaloosa | Wet, No Freeze | 32.5 | 404.5 | 620.7 | 385.3 |
| **Arkansas** | Little Rock | Wet, No Freeze | -80.4 | 353.8 | -57.8 | 404.1 |
| **Indiana** | Jefferson | Wet, No Freeze | -34.9 | 445.2 | -10.0 | 397.0 |
| **Kansas** | Scott | Wet, No Freeze | -457.9 | 448.6 | -96.7 | 432.6 |
| **South Carolina** | Columbia | Wet, No Freeze | 353.1 | 845.4 | 448.8 | 366.9 |
| **Tennessee** | Memphis | Wet, No Freeze | 42.4 | 587.0 | -239.8 | 421.3 |
| **Washington** | Seattle | Wet, No Freeze | 518.9 | 1145.6 | -321.7 | 426.6 |
| **West Virginia** | Charleston | Wet, No Freeze | 224.9 | 682.0 | -758.0 | 487.7 |

The average changes for the tensile strength are summarized in the following Figure 86:

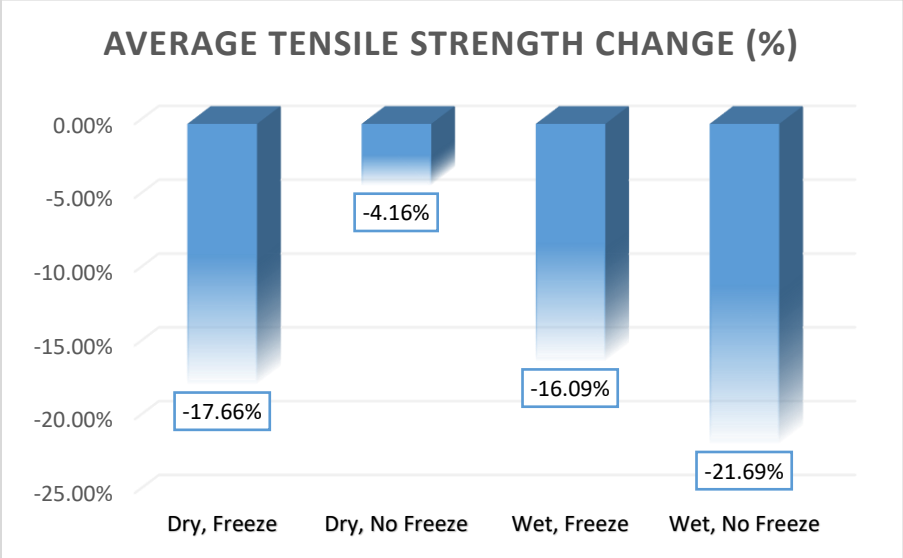


*Figure 86- Average Change in Tensile Strength*

With regards to the tensile strength, it is noticed to decrease slightly. As the model initially depends greatly on the Air Void Content (%) and the VFA (%), these parameters greatly affected the results obtained.

For the Dry Freeze Regions, the VFA increased and the Air void content decreased, which explains the decrease in tensile strength. The air void content has a great effect on the pavement performance. However, the model used in this study doesn't have the best accuracy. Therefore, in terms of modifications of the parameters, having a negative VFA will affect negatively the tensile strength

For the Dry, No Freeze region, the air void content is increasing and the VFA is decreasing however slightly. For this reason, the tensile strength is only varying very briefly (about 4%) which is not significant.

For the Wet Freeze and Wet No Freeze regions, the VFAs are increasing as well, leading to a decrease in the tensile strength. A greater increase in the VFA goes to the Wet, No Freeze region which is indicated by a great decrease of the tensile strength. Concerning the Fracture energy, as some values are in the negative portion, some of the values have been noticed to enter the limits of the model:

For the Dry Freeze Region, a great increase is noticed in terms of fracture energy. The asphalt content as well as the air void content and VFA greatly affect this prediction. When the asphalt content increases, the fracture energy increases. However, it all depends if the volumetric properties are within the boundaries of the model. For this reason, some behaviors are justified with an increase in fracture energy, while others switched from positive to negative fracture energies.

### 6.4.b Thermal Cracking Ranking Criteria

Having the measured and the predicted input parameters of the TCMODEL, or thermal cracking model, it was possible to come up with a certain criterion to determine the quality of the mix in terms of thermal resistance. Based on the data gathered by the LTPP considering the Measure transverse cracking as well as the measured longitudinal cracks on the non-wheel path, certain ranges were compared with the possible development of thermal cracks based on the predicted tensile strength, creep compliance and fracture energy (when available).

The following criteria is shown below in Table 51:

*Table 51- Ranking Criteria for Thermal Behavior*

| | Creep Compliance | Tensile Strength |
|---|---|---|
| **Low** | $< 9 * 10^{-7}$ | < 300 |
| **Satisfactory** | $6 * 10^{-7} - 9 * 10^{-7}$ | 300- 420 |
| **Good** | $9 * 10^{-7} - 2.6 * 10^{-6}$ | 420-500 |
| **Excellent** | $> 2.6 * 10^{-6}$ | > 500 |

Both Database's mix designs have been ranked based on the criteria above, and the results obtained are found in Table 74, Appendix C. The results also show the effect of the mix designs variation on the possible pavement performance.

The criteria developed for thermal cracking is a much more complex task. Therefore, these criteria are estimated based on the measured distresses from the LTPP. Measured data from the LTPP is not always accurate. For this reason, extensive research about thermal cracking on its own will need to be carried, as well as further testing.

However, this criterion helps in understanding the potential behavior with regards to thermal cracking based on all the United States' climatic regions.

A possible criterion was developed to obtain good results in terms of thermal behavior as per climatic regions: (Table 52)

*Table 52- Volumetric Criteria for Thermal Cracking in (%)*

| Dry, Freeze | | Dry, No Freeze | | Wet, Freeze | | Wet, No Freeze | |
|---|---|---|---|---|---|---|---|
| AC | 5-5.5 | AC | 5-5.5 | AC | 5-5. | AC | 5.2-5.5 |
| Va | 6.6-7.3 | Va | 4.5-5 | Va | 4-5 | Va | 7-8 |
| VMA | 14.5-15 | VMA | 16 | VMA | 14.5-15 | VMA | 14 |
| VFA | 55 | VFA | 65 | VFA | 60 | VFA | 50 |
| VBE | 9 | VBE | 10 | VBE | 10 | VBE | 6-7 |
| PEN 77 | 70 | PEN 77 | 40 | PEN 77 | 70 | PEN 77 | 50 |

## 6.5 Comparison of the Quality of the U.S. Mix Designs

Based on the criteria developed in all the previous sections an entire ranking for the new mix designs can be assessed. The assessment can give an indication on the possible behaviors concerning the pavement performance of the implemented mix designs. It is important to assess the quality of the pavement mixture in order to quantify and assess the need of introducing modifications to the mix design or add other components such as rubber or fibers in order to improve the durability and performance of the pavement.

In the Table 75 in Appendix C, the final assessments are the summarized based on the rankings developed in the previous sections for the new U.S. Mix designs.

The following Table 53 shows the count of the results:

*Table 53-Count of Final Quality Assessment*

| Quality Assessment | Count of Final Assessment |
|---|---|
| **Excellent Quality Mix** | 7 |
| **Good Quality Mix** | 17 |
| **Low Quality Mix** | 4 |
| **Satisfactory Quality Mix** | 20 |
| **Grand Total** | **48** |

## 6.6 Final Assessment Generation

As part of this effort, an excel sheet summarizing the generation of the three behaviors was created. A user-friendly interface was set in place to facilitate the prediction, as well as the assessment for the mixture in terms of Rutting, Fatigue and Thermal Cracking. In addition, a final quality check for the mixture overall will be provided.

In the first sheet, all in the input variables required are set into place, where the volumetric properties as well as climatic conditions and traffic volume are needed. (Refer to Figure 87 below)

| Volumetric Input Variables | | |
|---|---|---|
| PG- Binder Type | High | Low |
| Insert Corresponding Ai and VTSi | 64 | -22 |
| | 10.98 | -3.68 |
| Asphalt Content (%) | 3.9 | |
| Air Void Content (%) | 4 | |
| Voids in Mineral Aggregates (%) | 12.4 | |
| Effective Binder Content by Volume, Vbeff (%) | 8.4 | |
| Voids Filled with Asphalt (%) | 67.74193548 | |
| **Aggregate Gradation (%)** | | |
| Percent Retained on Sieve 3/4" (R34) | 35 | |
| Percent Retained on Sieve 3/8" (R38) | 55 | |
| Percent Retained on Sieve No. 4 (R04) | 67 | |
| Percent Passing on Sieve No. 200 (P200) | 3.9 | |
| **Climate Conditions** | | |
| Mean Annual Air Temperature (ºF) | 56 | |
| Windspeed (mph) | 4.283 | |
| Sunshine (%) | 48.2 | |
| Standard Deviation of the Mean Monthly Temperature | 15.121 | |
| Accumulated Rainfall Depth, in | 44.02 | |
| **Additional Input** | | |
| Deviator Stress, psi | 100 | |
| Confinement Level, psi | 20 | |
| Traffic Level, ESALs | 30000000 | |
| Asphalt Layer Thickness, in | 4 | |

| Ai and VTSi Input Variables | | | | | |
|---|---|---|---|---|---|
| Asphalt Binder Grade | Ai | VTSi | Asphalt Binder Grade | Ai | VTSi |
| PG 46-34 | 11.504 | -3.901 | PG 70-28 | 9.715 | -3.217 |
| PG 46-40 | 10.101 | -3.393 | PG 70-34 | 8.965 | -2.948 |
| PG 46-46 | 8.755 | -2.905 | PG 70-40 | 8.129 | -2.648 |
| PG 52-10 | 13.386 | -4.57 | PG 76-10 | 10.059 | -3.331 |
| PG 52-16 | 13.305 | -4.541 | PG 76-16 | 10.015 | -3.315 |
| PG 52-22 | 12.755 | -4.342 | PG 76-22 | 9.715 | -3.208 |
| PG 52-28 | 11.84 | -4.012 | PG 76-28 | 9.2 | -3.024 |
| PG 52-34 | 10.707 | -3.602 | PG 76-34 | 8.532 | -2.785 |
| PG 52-40 | 9.496 | -3.164 | PG 82-10 | 9.514 | -3.128 |
| PG 52-46 | 8.31 | -2.736 | PG 82-16 | 9.475 | -3.114 |
| PG 58-10 | 12.316 | -4.172 | PG 82-22 | 9.209 | -3.019 |
| PG 58-16 | 12.248 | -4.147 | PG 82-28 | 8.75 | -2.856 |
| PG 58-22 | 11.787 | -3.981 | PG 82-34 | 8.151 | -2.642 |
| PG 58-28 | 11.01 | -3.701 | AC-2,5 | 11.5167 | -3.89 |
| PG 58-34 | 10.035 | -3.35 | AC-5 | 11.2614 | -3.7914 |
| PG 58-40 | 8.976 | -2.968 | AC-10 | 11.0134 | -3.6454 |
| PG 64-10 | 11.432 | -3.842 | AC-20 | 10.7709 | -3.6017 |
| PG 64-16 | 11.375 | -3.822 | AC-3 | 10.6316 | -3.548 |
| PG 64-22 | 10.98 | -3.68 | AC-40 | 10.5338 | -3.5104 |
| PG 64-28 | 10.312 | -3.44 | PEN 40-50 | 10.5254 | -3.5047 |
| PG 64-34 | 9.461 | -3.134 | PEN 60-70 | 10.6508 | -3.5537 |
| PG 64-40 | 8.524 | -2.798 | PEN 85-100 | 11.8232 | -3.621 |
| PG 70-10 | 10.69 | -3.566 | PEN 120-150 | 11.0897 | -3.7252 |
| PG 70-16 | 10.641 | -3.548 | PEN 200-300 | 11.8107 | -4.0068 |
| PG 70-22 | 10.299 | -3.426 | - | - | - |

Variable cells highlighted in orange need to be inputted by the user.

*Figure 87- Overview of Sheet 1*

In the second sheet, the Flow Number, Rutting Depth, Number of Cycles to Fatigue Failure, Creep Compliance and Tensile Strength values are generated based on the input variables inserted in the first sheet. In addition, all the needed parameters such as Effective Temperatures, Viscosities, Dynamic Modulus of the Binder $|G^*_b|$, Phase Angle and Effective Total Energy are calculated to generate the key factors for the quality check. (Refer to Figure 88)

| | A | B | C |
|---|---|---|---|
| 1 | **Calculation Based on Input** | | |
| 2 | **Rutting/ Permanent Deformation** | | |
| 3 | Effective Rutting Temperature | | ºF |
| 4 | | | 109 |
| 5 | Frequency, Hz | | 18 |
| 6 | Pavement Depth from Surface, in | | 0.7 |
| 7 | Viscosity (Poise) at Effective Temperature | | 8.75E+04 |
| 8 | Normal Stress "p", psi | | 70 |
| 9 | Maximum Shear Stress "q", psi | | 50 |
| 10 | **Flow Number** | | 213 |
| 11 | **Rutting Depth, in** | | 1.253 |
| 12 | | | |
| 13 | **Fatigue Behavior** | | |
| 14 | Effective Fatigue Temperature | | ºC |
| 15 | | | 18 |
| 16 | Complex Shear Modulus for Binders, \|G*b\|, psi | | 13905983 |
| 17 | Phase Angle, δ | | 45.80 |
| 18 | Viscosity at Effective Fatigue Temperature and Frequency, cP | | 1.15E+09 |
| 19 | Binder Failure Envelope, FSC* | | 30.059 |
| 20 | Loading Frequency, Hz | | 10 |
| 21 | Strain Level, με | | 0.035 |
| 22 | **Number of Loading Cycles to Failure, Nf** | | 7250 |
| 23 | | | |
| 24 | **Thermal Cracking Behavior** | | |
| 25 | Penetration in 1/10 mm, at 77ºF | | 53.77 |
| 26 | D1, Fracture Parameter at -10ºC | | 2.73E-07 |
| 27 | m, Slope of Creep Compliance Curve at -10ºC | | 2.05E-01 |
| 28 | D, Creep Compliance 1/psi at 100 seconds | | 7.02E-07 |
| 29 | Tensile Strength, psi | | 471 |
| 30 | Fracture Energy, lb.in | | -758 |

*Figure 88-Overview of Sheet 2*

In the third and last sheet, an individual assessment in terms of each distress is generated as “Low”, “Satisfactory”, “Good” and “Excellent” based on the criteria developed in this study. Finally, a general and final assessment is generated for the entire pavement mixture, ranking it in the same scale. (Refer to Figure 89)

| | A | B | C | D |
|---|---|---|---|---|
| 1 | **Pavement Mixture Quality Assessment** | | | |
| 2 | Assessment in Terms of Rutting | | Low | |
| 3 | | | | |
| 4 | Assessment in Terms of Fatigue | | Satisfactory | |
| 5 | | | | |
| 6 | Assessment in Terms of Thermal Cracking | | Excellent | |
| 7 | | | | |
| 8 | **Final Assessment** | | Satisfactory | |
| 9 | | | | |

*Figure 89- Overview of Sheet 3*

# CHAPTER 7

# 7 SUMMARY, CONCLUSIONS AND RECOMMENDATIONS

## 7.1 Executive Summary

The main objective of this study was to outline a process to help assess the potential performance of HMA pavement structures in terms of rutting, fatigue and thermal cracking using only the asphalt mix design information and volumetric data. In this process, three predictive models were investigated, and their reliability was assessed based on existing pavement structures performance using LTPP (Long Term Pavement Performance) data. These models were also used to assess the quality of the asphalt mixtures for 48 current asphalt mixture designs collected from 25 States.

The comparison between the old and new asphalt mixtures data provided an interesting view on the change of the asphalt mixture design data over time, and efforts undertaken by the state agencies to respond to the pavement distresses known for each of them. Having fast and simple tools, such as the pavement performance models presented, assessing the quality of the asphalt mixtures was successful. This resulted in the criteria recommended for asphalt mixture performance as Poor, Satisfactory, Good or Excellent, in terms of the three most common pavement distresses.

While the MEPDG provides good predictions in terms of all three major distresses, it requires considerable data input and time. In this study, the proposed analysis for rutting was based on the Flow Number, and it is not included in the MEPDG. As for the Fatigue analysis, it is solely based on the properties of the binder correlated with the properties of the mixture. This approach is also new in terms of analysis and

does not depend on the damage accumulation within the pavement structure, but instead focuses on the main components and characteristics of the structure. Concerning the thermal cracking behavior, the issue at hand is still ambiguous as no real assessment is a 100% accurate. The interesting parameter introduced was certainly the Effective Fracture Energy. As this model did not provide good input to the criteria, thermal fracture energy is a great parameter that will certainly help in analyzing the effect and behavior of thermal cracks. In addition, the observed trend in terms of Creep Compliance and Tensile Strength was an interesting outcome, as the two parameters are not specifically related.

It is also to be noted that the distresses are much more complex in understanding, and that assessing the performance of the mixture doesn't solely depend on these developed criteria. However, having these new indications, can provide designers with the quality of the mix. In addition, it can provide the agency with the necessity of introducing new modifications to accommodate the distresses that need to be addressed. The modifications can be in terms of changes in the mix design itself, or by adding simple modifiers to the mixture, such as fibers, without major changes in the mix design. By having a satisfactory quality of the mix, the addition of fibers in terms of rutting for example could be very effective. On the other hand, having an excellent mix in terms of rutting will not necessitate the addition of these fibers.

## 7.2 Conclusions

Predicting pavement distresses in order to assess pavement performance is still both mechanistic and empirical task. Introducing useful tools to help in better understanding

the potential development of these distresses is of importance. Based on the effort presented in this thesis, the following can be concluded:

- The use of the rutting model gave a general idea about the rutting to be expected in the asphalt layer. As it is overfitted, the model is not very accurate. This model is based on the effective rutting temperature, at which the binder's viscosity was found. It is also largely depending on the flow number that is also predicted by the means of a new model introduced in this study. This model is based on the volumetric properties of the mix design, and assesses the number of cycles to reach failure, or tertiary flow. The rutting model also depends on two important factors, which are the ESAL, and the asphalt thickness. The data gathered from the LTPP was compared to the predicted values using the rutting model. A direct relationship could not be found. However, for values lower than 0.6'', the values were related. A ranking criterion was developed to rank the behavior of the pavement mixtures in terms of rutting,
- Concerning the fatigue model introduced, the approach tackled was new and accurate. Even though the model depends on a certain tensile strain to be exhibited by the pavement structure, the results were accurate and relatable to the measured distresses gathered from the LTPP. The fatigue model is based on the FSC*, which is the Fatigue Failure Envelope of the asphalt binder used. The results gathered were compared to the measured fatigue area and longitudinal cracks on the wheel path. A ranking criterion was developed based on the observed behaviors.

- The third model introduced into this study defines the thermal behavior of the pavement mixtures to be used. The values predicted was used to develop the TCMODEL, also used in the background of the MEPDG software. The main predicted values were the creep compliance at three testing temperatures, the tensile strength at -10$^{o}$C and the Total Fracture energy. The total fracture energy is a new concept that doesn't take part in the older versions of the MEPDG and is a great concept to consider. However, the limits of the model don't include all the possible mix design combinations. For this reason, the values generated for this model were not greatly considered for the future assessment of the mixtures. The tensile strength and creep compliance showed a great trend by increasing and decreasing simultaneously. As these two values are not officially related, it was a good conclusion to assess the reliability and accuracy of the models. The outputs obtained were compared to the measured thermal cracks and longitudinal cracks on the non-wheel paths of the LTPP sections during the first few years after construction. Thermal cracks are mostly susceptible to happen in the early stages of the pavement life, for this reason, only the early measurements were considered. Finally, a ranking criterion was developed as well as a limiting criterion for the total fracture energy.
- Finally, the quality of the proposed mixtures was assessed as Low, Satisfactory, Good or Excellent Quality Mix. The results are rather satisfactory, as out of the 48 proposed mixtures, the majority were between satisfactory and good pavement mixtures.

## 7.3 Recommendations

As further recommendations, it is important to consider the following:

- The introduced rutting model needs further refining, in order to reflect the measured data in the field. More testing needs to be done and included in order to broaden the existing database. Also, the model should fit the addition of RAP into the mixture. Any other modifier that does not require any conceptual changes to the existing pavement mixture could use the previous model. However, the addition of RAP/RAS, crumb rubber and others, require the development of a new model
- The fatigue model needs to reflect the actual tensile strain level in the field. This could be introduced by relating the traffic level to the tensile strain, which is then introduced into the model. Having this kind of modification will allow better reflection of the model's accuracy to the field. Also, the addition of the RAP/RAS, crumb rubber and other additives needs to be considered.
- Concerning the thermal cracking model implemented, the tensile strength prediction model has a low accuracy and needs to be modified by including more specimen testing. The values are a little bit far from the expectation. However, by combining the results with the creep compliance, the assessment is rather comprehensive and relatable. Concerning the total fracture energy, this model needs to be further modified to include a wider set of pavement mixtures, as a negative total fracture energy doesn't relate to any specific behavior.

- The developed assessments are depending on the data gathered and studied. It is important to enlarge the databases to include a broader analysis and therefore enhance the capabilities and accuracy of the assessment tool.

# REFERENCES


(1) Akili, W. (1975). Strength Behavior of Soil-Asphalt Mixtures in Compression. *The Journal of the Institution of Highway Engineers*,, Vol. 22, No 10, pp 9-13.

(2) J. Barry Barker et al. (2011) A Performance-Related Specification for Hot-Mixed Asphalt. Final 17 Report 704 NCHRP Project National Cooperative Highway Research Program Transportation 18 Research Board National Research Council.

(3) Fwa, T.F., Tan, S.A, Zhu, Y. Rutting Prediction of Asphalt Pavement Layer Using c-φ Model. *Journal of Transportation Engineering.* Volume 130, Issue 5, pp. 675-683, 2004.

(4) Brown, S.F., and C.A. Bell. The Prediction of Permanent Deformation in Asphalt Pavements, Proceedings, 77th Association of Asphalt Paving Technologists, Vol.48, 438-476, 1979.

(5) Francken, L. Pavement Deformation Law of Bituminous Road Mixes in Repeated Triaxial Compression. *Proceedings of the Fourth International Conference on the Structural Design of Asphalt Pavements, Volume I,* The University of Michigan, Ann Arbor, Michigan, August 1977.

(6) Biligiri, K., et al. Rational Modeling of Tertiary Flow for Asphalt Mixtures. *Transportation Research Record: Journal of the Transportation Research Board,* No. 2001, 2007, pp. 63-72.

(7) Khedr, S.A. Deformation Mechanism in Asphaltic Concrete, *Journal of Transportation Engineering*, American Society of Civil Engineers, Vol. 112, No. 1, 29-45, 1986.

(8) Witczak, M.W., and Kaloush, K.E. *Performance Evaluation of CitgoFlex Asphalt Modified Mixture using Advanced Material Characterization Tests*, Department of Civil Engineering, University of Maryland, College Park, Maryland, 1998.

(9) Zhou, Fujie., Scullion, Tom., and Sun, Lijun. Verification and Modeling of Three Stage Permanent Deformation Behavior of Asphalt Mixes. *Journal of Transportation Engineering*, ASCE, August 2004, pp 486-494.

(10) Kaloush, K.E. Simple Performance Test for Permanent Deformation of Asphalt Mixtures. Doctoral Dissertation, Department of Civil and Environmental Engineering, Arizona State University, Tempe, Arizona, 2001.

(11) Witczak, M. W. *Specification Criteria for Simple Performance Tests for Rutting NCHRP Report 580*. TRB, National Research Council, Washington, D. C, 2007.

(12) Kvanak et al. *Statistical development of a Flow Number predictive equation for the Mechanistic-Empirical Pavement Design Guide.* TRB Annual Meeting Paper 07-1000, 2007.

(13) Lee, H.-J., Daniel, J. S., & Kim, Y. R. (2000). Continuum Damage Mechanics-Based Fatigue Model of Asphalt Concrete. *Journal of Materials in Civil Engineering*, 12(2), 105–112. doi: 10.1061/(asce)0899-1561(2000)12:2(105)

(14) Lee, H., Kim, Y. R., & Lee, S. (2003). *Prediction of Asphalt Mix Fatigue Life with Viscoelastic Material Properties.* Transportation Research Record: Journal of the Transportation Research Board, 1832(1), 139–147. doi: 10.3141/1832-17

(15) Kim, Y. R., Lee, H. J., Kim, Y., and Little, D. N. (1997a). *''Mechanistic evaluation of fatigue damage growth and healing of asphalt concrete: Laboratory and field experiments.''* Proc., 8th Int. Conf. on Asphalt Pavements, Vol. II, International Society of Asphalt Pavements, 1089–1108.

(16) Kim, Y. R., Lee, H. J., and Little, D. N. (1997b). *''Fatigue characterization of asphalt concrete using viscoelasticity and continuum damage theory.''* J. Assn. of Asphalt Paving Technologists, 66, 520–569.

(17) Schapery, R. A. (1990). *''A theory of mechanical behavior of elastic media with growing damage and other changes in structure.*" J. Mech. Phys. Solids, 38, 215–253.

(18) Vanelstraete, A., Leonard, D. and Veys, J. (2000) "Structural design of roads with steel reinforcing nettings", Proceedings of the 4th International RILEM Conference–Reflective Cracking in Pavements, E & FN Spon, Ontario, Canada, pp 56–67.

(19) Al-Qadi, I. L., & Nassar, W. N. (2003). Fatigue Shift Factors to Predict HMA Performance. *International Journal of Pavement Engineering*, *4*(2), 69–76. doi: 10.1080/10298430310001593254

(20) Monismith, C.L. and Deacon, J.A., 1969. Fatigue of asphalt paving mixtures. *The Journal Transportation Engineering*, ASCE, Vol. 95, No. TE2.

(21) Pronk, A.C., 2006. Four-point dynamic bending test, *DWW-96-088*, Road and Hydraulic Division, the Netherlands pp. 23–27.

(22) *SHRP, 1994. Fatigue response of asphalt-aggregate mixes.* SHRP-A-404 Washington, DC: National Research Council.

(23) Monismith, C.L., et al., *1972.* Asphalt mixture behavior in repeated flexure. *Report No. TE70-5*, University of California, Berkeley: Institute of Transportation and Traffic Engineering.

(24) Roque, R., Hiltunen, D.R., and Buttlar, W.G. "Standard Test Method for Determining the Creep Compliance and Strength of Hot Mix Asphalt (HMA) Using the Indirect Tensile Test Device", Draft Test Protocol, AASHTO TP9-02, 2002

(25) Finn, F., et al., 1986. Development of pavement structural subsystems. N*CHRP Report 291*, Washington, DC: Transportation Research Board of the National Academies.

(26) Yoo, P., & Al-Qadi, I. (2010). A strain-controlled hot-mix asphalt fatigue model considering low and high cycles. *International Journal of Pavement Engineering*, 11(6), 565–574. doi: 10.1080/10298436.2010.488738

(27) Christensen, Jr., D. W., and N. Tran. Relationships between Mixture Fatigue Performance and Asphalt Binder Properties. *Journal of the Association of Asphalt Paving Technologists* (AAPT) (2019)

(28) Salim, R. (2019). *Asphalt Binder Parameters and their Relationship to the Linear Viscoelastic and Failure Properties of Asphalt Mixtures*. Arizona State University.

(29) LTPP Computed Parameter: Dynamic Modulus. (2015). *Federal Highway Administration—Office of Research, Development, and Technology: LTPP, FHWA-HRT-10-035*.

(30) American Association of State Highway and Transportation Officials. (2015). *Mechanistic-empirical pavement design guide: A manual of practice*. Washington, DC: American Association of State Highway and Transportation Officials

(31) Frost, L. (2020, January 26). What is Alligator Cracking?

(32) Zborowski, Aleksander. Development of a Modified Superpave Thermal Cracking Model for Asphalt Concrete Mixtures Based on the Fracture Energy Approach, Arizona State University, 2007.

(33) T.S. Vinson, V.C. Janoo, "R.C.G. Haas, "Low Temperature and Thermal Fatigue Cracking", *SHRP Summary Report No. A-003A*, 1989.

(34) Sugawara, T., and Mariyoshi, A., "Thermal Fracture of Bituminous Mixtures", Proc., Paving in Cold Areas Mini Workshop, 1984.

(35) Shahin, M.Y., and McCullough, B.F., "Damage Model for Predicting Temperature Cracking in Flexible Pavements", *Transportation Research Record No.521*, 1974.

(36) Mahboub, K., "Low Temperature Fracture Evaluation of Plasticized Sulfur Paving Mixtures", M.S. Thesis submitted to Texas A&M University, 1985.

(37) Little, D.N., and Mahboub, K., "Engineering Properties of First-Generation Plasticized Sulfur Binders and Low Temperature Fracture Evaluation of Plasticized Sulfur Paving Mixtures", *Transportation Research Record No.1034*, 1985.

(38) Majidzadeh, K., Buranrom, C., Karakomzian, M., "Application of Fracture Mechanics for Improved Design of Bituminous Concrete", *FHWA U.S. Department of Transportation Report No. 76-91,* 1976.

(39) Schmidt, R.J., Santucci, L.E., "*A* Practical Method for Determining the Glass Transition Temperature of Asphalt and Calculation of Their Low Temperature Viscosities", Proc., AAPT, Vol.35, 1966.

(40) Sugawara, T., and Mariyoshi, A., *"*Thermal Fracture of Bituminous Mixtures", Proc., Paving in Cold Areas Mini Workshop, 1984.

(41) H.L. Von Quintus, "Performance Prediction Models In the Superpave Mix Design System", *SHRP Report No. A-699.*

(42) Lytton, R.L., Uzan, J., Fernando, E.G., Roque, R., Hiltunen, D., Stoffels, S.M., "Development and Validation of Performance Prediction Models and Specifications for Asphalt Binders and Paving Mixes", *SHRP Report No. A-357,* Washington D.C., 1993

(43) Monismith, C.L., Secor, G.A., and Secor, K.E., *"*Temperature Induced Stresses and Deformations in Asphalt Concrete", Proc., AAPT, Vol.34, 1965.

(44) Zhiming Si, Little, D.N., and Lytton, P.E., "Characterization of Microdamage and Healing of Asphalt Concrete Mixtures", *Journal of Materials in Civil Engineering, December* 2002.

(45) Sotil, Andres. Use of the Dynamic E* Test as Permanent Deformation Performance Criteria for Asphalt Pavement Systems. Ph. D. Dissertation. Arizona State University, Tempe, AZ, May 2005.

(46) Rodezno, M. C., Kaloush, K. E., & Corrigan, M. R. (2010). Development of a Flow Number Predictive Model. *Transportation Research Record: Journal of the Transportation Research Board*, *2181*(1), 79–87. doi: 10.3141/2181-09

(47) El-Basyouny, M., Jeong, M. *Development of Probabilistic Performance Related Specifications Methodology based upon AASHTO MEPDG*, Accepted for Publication at the Transportation Research Board 88th Annual Meeting, Washington, D.C., January 2009

(48) Way, G., Sousa, J. and Kaloush, K., "Hot Mix Asphalt Design Prediction and Field Performance, An Arizona Study". 6th International RILEM Symposium on Performance Testing and Evaluation of Bituminous Materials, PTEBM'03, ISBN 2-912143-35-7, p.543-549, Zurich, Switzerland, April 2003.

(49) Carpenter, S.H., "Thermal Cracking in Asphalt Pavements: an Examination of Models and Input Parameters", USA CRREL, 1983.

(50) Dave, Eshan & Buttlar, William & Leon, Sofie & Behnia, Behzad & Paulino, Glaucio. (2013). IlliTC-Low Temperature Cracking Model for Asphalt Pavements. Road Materials and Pavement Design. 14. 10.1080/14680629.2013.812838.

# APPENDIX A

# DATA AND RESULTS FOR THE LTPP DATABASE

*Table 54-Collected LTPP Database*

| LOCATIONS | | | MEASURED DISTRESSES | | | | |
|---|---|---|---|---|---|---|---|
| **State** | **City** | **Section** | **Fatigue (ft2)** | **Transverse Cracks (count)** | **Long. NWP (ft)** | **Long. In the WP (ft)** | **Rutting (in)** |
| **Alabama** | *Montgomery* | 4125 | 825 | 80 | 0 | 0 | 0.55 |
| | *Tuscaloosa* | 6012 | 1352 | 57 | 314.63 | 14.11 | 0.35 |
| **Arizona** | *Tucson* | 6054 | 13 | 87 | 731.63 | 0.00 | 0.35 |
| | *Phoenix* | B961 | 498 | 4 | 0.00 | 0.00 | 0.24 |
| | *Flagstaff* | 669 | 0 | 97 | 239.50 | 0.00 | 0.24 |
| | *Kingman* | 1022 | 1294 | 0 | 32.81 | 0.00 | 0.43 |
| **Alaska** | *Anchorage* | 1004 | 22 | 0 | 141.08 | 0.00 | 0.98 |
| **Arkansas** | *Little Rock* | A606 | 656 | 0 | 16.40 | 0.00 | 0.16 |
| **Colorado** | *Rio Blanco* | 1053 | 926 | 14 | 61.68 | 0.00 | 0.63 |
| | *El Paso* | 7783 | 1199 | 12 | 75.46 | 0.00 | 0.79 |
| | *Yuma* | 502 | 812 | 5 | 397.64 | 108.3 | 0.20 |
| **Indiana** | *La Porte* | 5528 | 1424 | 75 | 1000.6 | 0.00 | 0.28 |
| | *Jackson* | A902 | 0 | 4 | 291.99 | 0.00 | 0.20 |
| | *Jefferson* | 18-1028 | 0 | 24 | 524.93 | 0.00 | 0.35 |
| **Kansas** | *Cherokee* | 1005 | 1663 | 58 | 619.75 | 4.59 | 0.20 |
| | *Scott* | 1006 | 358 | 37 | 119.75 | 0.00 | 0.08 |
| **Massachusetts** | *Boston* | 1003 | 1125 | 75 | 100.39 | 41.01 | 0.20 |
| | *Springfield* | 1002 | 2189 | 96 | 246.06 | 0.00 | 0.35 |
| **Michigan** | *Port Huron* | D330 | 0 | 56 | 772.64 | 8.20 | 0.00 |
| | *Alpena* | 6016 | 0 | 53 | 121.39 | 43.64 | 0.20 |
| | *Marquette* | 1004 | 24 | 40 | 505.25 | 0.00 | 0.12 |
| | *Grand Rapids* | 901 | 2955 | 7.4 | 941.60 | 0.00 | 0.20 |
| **South Carolina** | *Columbia* | 1024 | 243 | 0 | 9.84 | 0.00 | 0.16 |
| **Tennessee** | *Memphis* | 3109 | 237 | 0 | 0.00 | 0.00 | 0.24 |
| **Washington** | *Seattle* | 6049 | 0 | 2 | 130.58 | 130.58 | 0.00 |
| | *Spokane* | A320 | 14 | 29 | 649.61 | 2.95 | 0.75 |
| **West Virginia** | *Kanawha* | 1640 | 2778 | 0 | 374.02 | 0.00 | 0.12 |
| | *Charleston* | 7008 | 0 | 12 | 1000.9 | 0.00 | 0.24 |

| LOCATIONS | | DATA COLLECTED | | | | | | | | | | | |
|---|---|---|---|---|---|---|---|---|---|---|---|---|---|
| City | Section | $H_{HMA}$ (in) | PG | AC | $V_a$ | $P_{200}$ | $R_{04}$ | $R_{38}$ | $R_{34}$ | VMA | VFA | $V_{BE}$ | Meas ESAL |
| ***Montgomery*** | 4125 | 6 | 64-16 | 6 | 5.8 | 4.7 | 40 | 42 | 4 | 15 | 61 | 9 | 6.13E +06 |
| ***Tuscaloosa*** | 6012 | 5 | 64-16 | 6 | 5.2 | 4 | 63 | 12 | 4 | 15 | 65 | 10 | 2.86E +07 |
| ***Tucson*** | 6054 | 9 | 70-10 | 5 | 4.6 | 7.5 | 42 | 25 | 2 | 14.6 | 68 | 10 | 6.79E +06 |
| ***Phoenix*** | B961 | 10 | 76-10 | 5.3 | 4.5 | 3.8 | 50 | 35 | 9 | 14.6 | 69 | 10 | 5.46E +07 |
| ***Flagstaff*** | 669 | 6 | 58-28 | 4.6 | 4.9 | 4.7 | 52 | 39 | 5 | 14.6 | 66 | 10 | 5.48E +07 |
| ***Kingman*** | 1022 | 8.5 | 70-16 | 4.5 | 3.9 | 5.3 | 50 | 28 | 4 | 14.6 | 73 | 11 | 3.08E +07 |
| ***Anchorage*** | 1004 | 5.4 | 46-40 | 5.5 | 3.9 | 7.2 | 39 | 20 | 3 | 14 | 72 | 10 | 2.84E +06 |
| ***Little Rock*** | A606 | 5 | 64-16 | 5 | 3 | 9.4 | 60 | 39 | 15 | 15.3 | 80 | 12 | 2.04E +07 |
| ***Rio Blanco*** | 1053 | 6.8 | 46-34 | 4.8 | 4 | 9.1 | 48 | 19 | 0 | 14.3 | 72 | 10 | 2.14E +06 |
| ***El Paso*** | 7783 | 9.7 | 58-28 | 5 | 5.29 | 9.6 | 43 | 15 | 0 | 14 | 62 | 9 | 1.13E +07 |
| ***Yuma*** | 502 | 9.3 | 64-28 | 5 | 7.39 | 8.7 | 37 | 22 | 0 | 15 | 51 | 8 | 1.08E +07 |
| ***La Porte*** | 5528 | 7.2 | 58-28 | 4.8 | 6.18 | 5.9 | 40 | 33 | 0 | 16.6 | 63 | 10 | 5.97E +06 |
| ***Jackson*** | A902 | 6.8 | 58-28 | 5.4 | 2.7 | 5.8 | 46 | 35 | 0 | 14 | 81 | 11 | 8.23E +07 |
| ***Jefferson*** | 18-1028 | 18 | 58-28 | 3.7 | 4.303 | 3.1 | 59 | 35 | 0 | 15 | 71 | 11 | 1.84E +07 |
| ***Cherokee*** | 1005 | 12.7 | 64-22 | 6.5 | 5 | 9.5 | 21 | 14 | 0 | 14 | 64 | 9 | 1.07E +06 |
| ***Scott*** | 1006 | 14 | 64-28 | 5.8 | 3.2 | 8.2 | 39 | 19 | 0 | 14 | 77 | 11 | 1.17E +06 |
| ***Boston*** | 1003 | 6.6 | 58-22 | 5.6 | 5.6 | 5.4 | 46 | 18 | 0 | 14 | 60 | 8 | 6.55E +05 |
| ***Springfield*** | 1002 | 7.8 | 58-28 | 5 | 2.3 | 3.7 | 22 | 4 | 0 | 14 | 84 | 12 | 5.28E +06 |
| ***Port Huron*** | D330 | 2.2 | 58-28 | 5 | 4 | 6.2 | 14 | 9 | 0 | 14 | 71 | 10 | 1.67E +06 |
| ***Alpena*** | 6016 | 4.6 | 52-28 | 5 | 2.7 | 2.3 | 63 | 12 | 8 | 14 | 81 | 11 | 3.09E +06 |
| ***Marquette*** | 1004 | 4.2 | 52-28 | 5 | 5.12 | 6 | 30 | 13 | 7 | 14 | 63 | 9 | 1.33E +06 |
| ***Grand Rapids*** | 901 | 8.6 | 58-34 | 5 | 3.5 | 7 | 60 | 38 | 6 | 13.5 | 74 | 10 | 3.53E +07 |
| ***Columbia*** | 1024 | 1.6 | 64-16 | 5.2 | 7.9 | 3.7 | 30 | 8 | 0 | 14 | 44 | 6 | 2.60E +04 |
| ***Memphis*** | 3109 | 7 | 64-22 | 5.6 | 6 | 6 | 58 | 10 | 17 | 14 | 57 | 8 | 2.38E +06 |
| ***Seattle*** | 6049 | 10.6 | 52-16 | 5.5 | 8.9 | 5.2 | 42 | 23 | 2 | 14 | 36 | 5 | 6.54E +06 |

| | | | | | | | | | | | | | |
|---|---|---|---|---|---|---|---|---|---|---|---|---|---|
| ***Spokane*** | A320 | 2.7 | 58-28 | 5.6 | 6 | 5.6 | 41 | 16 | 5.6 | 14 | 57 | 8 | 9.57E +05 |
| ***Kanawha*** | 1640 | 2.5 | 64-22 | 6 | 5.14 | 2 | 35 | 6 | 0 | 14 | 63 | 9 | 1.52E +07 |
| ***Charleston*** | 7008 | 3.9 | 64-22 | 6 | 6.7 | 2.7 | 44 | 2 | 0 | 14 | 52 | 7 | 4.06E +07 |

*Table 55- Summary of the LTTP Database Thermal Input*

| State | City | Section | Climate Zone | D(100) @ -20°C | D(100) @ -10°C | D(100) @ 0°C | St (psi) | FE | Meas Transverse | Meas. Long. In the NWP |
|---|---|---|---|---|---|---|---|---|---|---|
| **Arizona** | *Flagstaff* | 669 | *DF* | 1.00E-06 | 2.25E-06 | 1.46E-05 | 551 | -3109.29 | 0 | 43 |
| **Alaska** | *Anchorage* | 1004 | | 4.92E-07 | 1.13E-06 | 3.19E-06 | 486 | -101.68 | 97 | 73 |
| **Colorado** | *Rio Blanco* | 1053 | | 8.13E-07 | 1.80E-06 | 8.67E-06 | 526 | -1568.32 | 14 | 18.8 |
| **Colorado** | *El Paso* | 7783 | | 4.17E-07 | 1.02E-06 | 2.98E-06 | 546 | -118.39 | 12 | 23 |
| **Colorado** | *Yuma* | 502 | | 3.19E-07 | 9.09E-07 | 2.71E-06 | 708 | 271.91 | 5 | 121.2 |
| **Washington** | *Spokane* | A320 | | 3.52E-07 | 9.32E-07 | 2.86E-06 | 621 | 60.49 | 29 | 198 |
| **Arizona** | *Tucson* | 6054 | *D, NF* | 4.26E-07 | 9.27E-07 | 2.02E-06 | 399 | -224.70 | 87 | 223 |
| **Arizona** | *Phoenix* | B961 | | 4.18E-07 | 9.00E-07 | 1.90E-06 | 377 | -260.23 | 4 | 0 |
| **Arizona** | *Kingman* | 1022 | | 4.47E-07 | 9.17E-07 | 1.98E-06 | 389 | -281.67 | 0 | 10 |
| **Indiana** | *La Porte* | 5528 | *W, F* | 5.65E-07 | 1.36E-06 | 3.99E-06 | 468 | 248.46 | 75 | 305 |
| **Indiana** | *Jackson* | A902 | | 4.30E-07 | 8.26E-07 | 2.07E-06 | 451 | -574.19 | 4 | 89 |
| **Kansas** | *Cherokee* | 1005 | | 4.03E-07 | 9.33E-07 | 2.29E-06 | 487 | -56.94 | 58 | 188.9 |
| **Massachusetts** | *Boston* | 1003 | | 3.64E-07 | 9.14E-07 | 2.52E-06 | 558 | -13.66 | 75 | 30.6 |
| **Massachusetts** | *Springfield* | 1002 | | 3.84E-07 | 7.14E-07 | 1.75E-06 | 461 | -645.89 | 96 | 75 |
| **Michigan** | *Port Huron* | D330 | | 4.83E-07 | 1.04E-06 | 2.80E-06 | 463 | -374.86 | 56 | 235.5 |
| **Michigan** | *Alpena* | 6016 | | 4.92E-07 | 9.54E-07 | 2.82E-06 | 478 | -729.83 | 53 | 37 |
| **Michigan** | *Marquette* | 1004 | | 4.91E-07 | 1.19E-06 | 4.06E-06 | 558 | -291.67 | 40 | 154 |
| **Michigan** | *Grand Rapids* | 901 | | 8.05E-07 | 1.53E-06 | 4.60E-06 | 548 | -738.12 | 7.4 | 287 |
| **West Virginia** | *Kanawha* | 1640 | | 3.93E-07 | 9.25E-07 | 2.29E-06 | 499 | -97.91 | 0 | 114 |
| **Alabama** | *Montgomery* | 4125 | *W, NF* | 3.15E-07 | 8.04E-07 | 1.98E-06 | 448 | 99.60 | 80 | 0 |
| **Alabama** | *Tuscaloosa* | 6012 | | 3.48E-07 | 8.36E-07 | 1.98E-06 | 405 | 32.49 | 57 | 95.9 |
| **Arkansas** | *Little Rock* | A606 | | 3.49E-07 | 6.91E-07 | 1.45E-06 | 354 | -80.44 | 0 | 5 |
| **Indiana** | *Jefferson* | 18-1028 | | 5.43E-07 | 1.16E-06 | 3.16E-06 | 445 | -34.87 | 24 | 160 |
| **Kansas** | *Scott* | 1006 | | 5.10E-07 | 9.77E-07 | 2.29E-06 | 449 | -457.88 | 37 | 36.5 |
| **South Carolina** | *Columbia* | 1024 | | 1.14E-07 | 4.07E-07 | 1.20E-06 | 845 | 353.10 | 0 | 3 |
| **Tennessee** | *Memphis* | 3109 | | 3.23E-07 | 8.38E-07 | 2.19E-06 | 587 | 42.37 | 0 | 0 |
| **Washington** | *Seattle* | 6049 | | 8.95E-08 | 3.67E-07 | 1.42E-06 | 1146 | 518.95 | 2 | 39.8 |
| **West Virginia** | *Charleston* | 7008 | | 2.58E-07 | 7.31E-07 | 2.01E-06 | 682 | 224.91 | 12 | 305.1 |

*Table 56-Thermal Cracking Behavior for LTPP Database*

| State | City | Climate Zone | D(100) @ -20°C | D(100) @ -10°C | D(100) @ 0°C | Tensile St (psi) | F. Energy (lb.in) | Meas. Trans. Cracks (count) | Meas. Long. In the NWP |
|---|---|---|---|---|---|---|---|---|---|
| **Arizona** | *Flagstaff* | *Dry, Freeze* | 4.92E-07 | 1.13E-06 | 3.19E-06 | 486 | -101.68 | 0 | 43 |
| **Alaska** | *Anchorage* | | 1.00E-06 | 2.25E-06 | 1.46E-05 | 551 | -3109.29 | 97 | 73 |
| **Colorado** | *Rio Blanco* | | 8.13E-07 | 1.80E-06 | 8.67E-06 | 526 | -1568.32 | 14 | 18.8 |
| **Colorado** | *El Paso* | | 4.17E-07 | 1.02E-06 | 2.98E-06 | 546 | -118.39 | 12 | 23 |
| **Colorado** | *Yuma* | | 3.19E-07 | 9.09E-07 | 2.71E-06 | 708 | 271.91 | 5 | 121.2 |
| **Washington** | *Spokane* | | 3.52E-07 | 9.32E-07 | 2.86E-06 | 621 | 60.49 | 29 | 198 |
| **Arizona** | *Tucson* | *Dry, No Freeze* | 4.26E-07 | 9.27E-07 | 2.02E-06 | 399 | -224.70 | 87 | 223 |
| **Arizona** | *Phoenix* | | 4.18E-07 | 9.00E-07 | 1.90E-06 | 377 | -260.23 | 4 | 0 |
| **Arizona** | *Kingman* | | 4.47E-07 | 9.17E-07 | 1.98E-06 | 389 | -281.67 | 0 | 10 |
| **Indiana** | *La Porte* | *Wet, Freeze* | 5.65E-07 | 1.36E-06 | 3.99E-06 | 468 | 248.46 | 75 | 305 |
| **Indiana** | *Jackson* | | 4.30E-07 | 8.26E-07 | 2.07E-06 | 451 | -574.19 | 4 | 89 |
| **Kansas** | *Cherokee* | | 4.03E-07 | 9.33E-07 | 2.29E-06 | 487 | -56.94 | 58 | 188.9 |
| **Massachusetts** | *Boston* | | 3.64E-07 | 9.14E-07 | 2.52E-06 | 558 | -13.66 | 75 | 30.6 |
| **Massachusetts** | *Springfield* | | 3.84E-07 | 7.14E-07 | 1.75E-06 | 461 | -645.89 | 96 | 75 |
| **Michigan** | *Port Huron* | | 4.83E-07 | 1.04E-06 | 2.80E-06 | 463 | -374.86 | 56 | 235.5 |
| **Michigan** | *Alpena* | | 4.92E-07 | 9.54E-07 | 2.82E-06 | 478 | -729.83 | 53 | 37 |
| **Michigan** | *Marquette* | | 4.91E-07 | 1.19E-06 | 4.06E-06 | 558 | -291.67 | 40 | 154 |
| **Michigan** | *Grand Rapids* | | 8.05E-07 | 1.53E-06 | 4.60E-06 | 548 | -738.12 | 7.4 | 287 |
| **West Virginia** | *Kanawha* | | 3.93E-07 | 9.25E-07 | 2.29E-06 | 499 | -97.91 | 0 | 114 |
| **Alabama** | *Montgomery* | *Wet, No Freeze* | 3.15E-07 | 8.04E-07 | 1.98E-06 | 448 | 99.60 | 80 | 0 |
| **Alabama** | *Tuscaloosa* | | 3.48E-07 | 8.36E-07 | 1.98E-06 | 405 | 32.49 | 57 | 95.9 |
| **Arkansas** | *Little Rock* | | 3.49E-07 | 6.91E-07 | 1.45E-06 | 354 | -80.44 | 0 | 5 |
| **Indiana** | *Jefferson* | | 5.43E-07 | 1.16E-06 | 3.16E-06 | 445 | -34.87 | 24 | 160 |
| **Kansas** | *Scott* | | 5.10E-07 | 9.77E-07 | 2.29E-06 | 449 | -457.88 | 37 | 36.5 |
| **SC** | *Columbia* | | 1.14E-07 | 4.07E-07 | 1.20E-06 | 845 | 353.10 | 0 | 3 |
| **Tennessee** | *Memphis* | | 3.23E-07 | 8.38E-07 | 2.19E-06 | 587 | 42.37 | 0 | 0 |
| **Washington** | *Seattle* | | 8.95E-08 | 3.67E-07 | 1.42E-06 | 1146 | 518.95 | 2 | 39.8 |
| **West Virginia** | *Charleston* | | 2.58E-07 | 7.31E-07 | 2.01E-06 | 682 | 224.91 | 12 | 305.1 |

# APPENDIX B

# RESULTS FOR THE U.S. DATABASE

*Table 57- New Pavement Mixtures Data from the US*

| State | | City | Climate Zone | NMAS | PG |
|---|---|---|---|---|---|
| **Alabama** | **AL** | *Montgomery* | *Wet, No Freeze* | ½'' | PG 76-22 |
| | | *Tuscaloosa* | *Wet, No Freeze* | ½'' | PG 76-22 |
| **Arizona** | **AZ** | *Flagstaff* | *Dry, Freeze* | ¾'' | PG 64-22 |
| | | *Kingman* | *Dry, No Freeze* | ¾'' | PG 70-10 |
| | | *Tucson* | *Dry, No Freeze* | ¾'' | PG 70-10 |
| | | *Phoenix* | *Dry, No Freeze* | ¾'' | PG 70-22 |
| **Alaska** | **AK** | *Anchorage* | *Dry, Freeze* | ½'' | PG 64-40 |
| | | *Fairbanks* | *Dry, Freeze* | ½'' | PG 58-34 |
| | | *Barrow* | *Dry, Freeze* | ½'' | PG 52-40 |
| **Arkansas** | **AR** | *Little Rock* | *Wet, No Freeze* | ¾'' | PG 76-22 |
| **Colorado** | **CO** | *Adams* | *Dry, Freeze* | ¾'' | PG 64-22 |
| | | *Rio Blanco* | *Dry, Freeze* | ¾'' | PG 58-34 |
| | | *El Paso* | *Dry, Freeze* | ½'' | PG 58-28 |
| | | *Yuma* | *Dry, Freeze* | ½'' | PG 64-28 |
| | | *El Rio Grande* | *Dry, Freeze* | ¾'' | PG 58-28 |
| **Indiana** | **IN** | *La Porte* | *Wet, Freeze* | 3/8'' | PG 64-22 |
| | | *Jackson* | *Wet, Freeze* | 3/8'' | PG 70-22 |
| | | *Jefferson* | *Wet, No Freeze* | 3/8'' | PG 70-22 |
| **Delaware** | **DE** | *Dover* | *Wet, No Freeze* | ¾'' | PG 64-22 |
| **Florida** | **FL** | *Tallahassee* | *Wet, No Freeze* | ½'' | PG 76-22 |
| **Hawaii** | **HI** | *Honolulu* | *Wet, No Freeze* | ½'' | PG 64-22 |
| **Iowa** | **IA** | *Harlan* | *Wet, Freeze* | ½'' | PG 58-28 |
| | | *Council Bluffs* | *Wet, Freeze* | ½'' | PG 58-28 |
| **Kansas** | **KS** | *Cherokee* | *Wet, Freeze* | ¾'' | PG 70-28 |
| | | *Scott* | *Wet, No Freeze* | ¾'' | PG 70-28 |
| **Maine** | **ME** | *Hermon* | *Wet, Freeze* | ½'' | PG 64-28 |
| | | *Sidney* | *Wet, Freeze* | 3/8'' | PG 64-28 |
| **Massachusetts** | **MA** | *Boston* | *Wet, Freeze* | ½'' | PG 64-28 |
| | | *Springfield* | *Wet, No Freeze* | 3/8'' | PG 64-28 |
| **Maryland** | **MD** | *Jessup* | *Wet, No Freeze* | 3/8'' | PG 76-22 |
| **Michigan** | **MI** | *Port Huron* | *Wet, Freeze* | ½'' | PG 70-28 |
| | | *Alpena* | *Wet, Freeze* | 3/8'' | PG 64-28 |
| | | *Marquette* | *Wet, Freeze* | 3/8'' | PG 58-34 |
| | | *Grand Rapids* | *Wet, Freeze* | 3/8'' | PG 70-28 |

| | | | | | |
|---|---|---|---|---|---|
| **Mississippi** | **MS** | *Jackson* | *Wet, No Freeze* | 3/8'' | PG 76-22 |
| **New Jersey** | **NJ** | *Newark* | *Wet, No Freeze* | ½'' | PG 64-22 |
| **North Carolina** | **NC** | *Greensboro* | *Wet, No Freeze* | 3/8'' | PG 58-28 |
| | | *Newark* | *Wet, No Freeze* | 3/8'' | PG 64-22 |
| **Ohio** | **OH** | *Columbus* | *Wet, Freeze* | ½'' | PG 76-22 |
| **South Carolina** | **SC** | *Columbia* | *Wet, No Freeze* | ½'' | PG 76-22 |
| **Tennessee** | **TN** | *Memphis* | *Wet, No Freeze* | ½'' | PG 76-22 |
| **Vermont** | **VT** | *Burlington* | *Wet, Freeze* | 3/8'' | PG 58-28 |
| **Washington** | **WA** | *Seattle* | *Wet, No Freeze* | ½'' | PG 58-22 |
| | | *Spokane* | *Dry, Freeze* | 3/8'' | PG 64-28 |
| **West Virginia** | **WV** | *Martinsburg* | *Wet, Freeze* | ¾'' | PG 64-22 |
| | | *Charleston* | *Wet, No Freeze* | 1'' | PG 64-22 |
| **Wisconsin** | **WI** | *Hayward* | *Wet, Freeze* | ½'' | PG 58-34 |
| | | *Madison* | *Wet, Freeze* | ½'' | PG 58-28 |

*Table 58- Effective Rutting Temperature for the US Database*

| State | City | MAAT (°F) | Effective Rutting Temp (°F) |
|---|---|---|---|
| **Alabama** | Montgomery | 65 | 120 |
| **Alabama** | Tuscaloosa | 65 | 103 |
| **Alaska** | Anchorage | 36 | 83 |
| **Alaska** | Fairbanks | 28 | 93 |
| **Alaska** | Barrow | 9 | 58 |
| **Arizona** | Flagstaff | 46 | 91 |
| **Arizona** | Kingman | 61 | 121 |
| **Arizona** | Tucson | 72 | 122 |
| **Arizona** | Phoenix | 75 | 129 |
| **Arkansas** | Little Rock | 63 | 121 |
| **Colorado** | Adams | 49 | 102 |
| **Colorado** | Rio Blanco | 47 | 96 |
| **Colorado** | El Paso | 76 | 112 |
| **Colorado** | Yuma | 51 | 104 |
| **Colorado** | El Rio Grande | 66 | 112 |
| **Delaware** | Dover | 57 | 111 |
| **Florida** | Tallahassee | 68 | 122 |
| **Hawaii** | Honolulu | 78 | 117 |
| **Indiana** | La Porte | 50 | 103 |
| **Indiana** | Jackson | 53 | 109 |
| **Indiana** | Jefferson | 56 | 111 |
| **Iowa** | Harlan | 48 | 109 |
| **Iowa** | Council Bluffs | 53 | 113 |
| **Kansas** | Cherokee | 57 | 115 |
| **Kansas** | Scott | 52 | 112 |
| **Maine** | Hermon | 60 | 100 |
| **Maine** | Sidney | 46 | 102 |
| **Maryland** | Jessup | 52 | 104 |
| **Massachusetts** | Boston | 51 | 107 |
| **Massachusetts** | Springfield | 51 | 111 |
| **Michigan** | Port Huron | 65 | 102 |
| **Michigan** | Alpena | 44 | 96 |
| **Michigan** | Marquette | 44 | 95 |
| **Michigan** | Grand Rapids | 49 | 101 |
| **Mississippi** | Jackson | 65 | 120 |
| **New Jersey** | Newark | 59 | 118 |

| | | | |
|---|---|---|---|
| **North Carolina** | Greensboro | 59 | 113 |
| **North Carolina** | Newark | 50 | 103 |
| **Ohio** | Columbus | 53 | 105 |
| **South Carolina** | Columbia | 64 | 120 |
| **Tennessee** | Memphis | 63 | 120 |
| **Vermont** | Burlington | 46 | 97 |
| **Washington** | Spokane | 48 | 94 |
| **Washington** | Seattle | 53 | 97 |
| **West Virginia** | Martinsburg | 53 | 108 |
| **West Virginia** | Charleston | 56 | 109 |
| **Wisconsin** | Hayward | 42 | 102 |
| **Wisconsin** | Madison | 46 | 103 |

*Table 59- Viscosities at Effective Rutting Temperature for the US Database*

| State | City | MAAT (°F) | Effective Rutting Temp (°F) | V1 (p) at Eff Temperature |
|---|---|---|---|---|
| **Alabama** | Montgomery | 65 | 120 | 1.29E+05 |
| **Alabama** | Tuscaloosa | 65 | 103 | 6.03E+05 |
| **Alaska** | Anchorage | 36 | 91 | 2.87E+05 |
| **Alaska** | Fairbanks | 28 | 121 | 1.10E+05 |
| **Alaska** | Barrow | 9 | 122 | 1.24E+06 |
| **Arizona** | Flagstaff | 46 | 129 | 6.57E+05 |
| **Arizona** | Kingman | 61 | 83 | 6.79E+04 |
| **Arizona** | Tucson | 72 | 93 | 6.10E+04 |
| **Arizona** | Phoenix | 75 | 58 | 2.78E+04 |
| **Arkansas** | Little Rock | 63 | 121 | 1.15E+05 |
| **Colorado** | Adams | 49 | 102 | 1.92E+05 |
| **Colorado** | Rio Blanco | 47 | 96 | 1.31E+05 |
| **Colorado** | El Paso | 76 | 112 | 1.88E+04 |
| **Colorado** | Yuma | 51 | 104 | 1.16E+05 |
| **Colorado** | El Rio Grande | 66 | 112 | 2.37E+04 |
| **Delaware** | Dover | 57 | 103 | 7.12E+04 |
| **Florida** | Tallahassee | 68 | 109 | 1.05E+05 |
| **Hawaii** | Honolulu | 78 | 111 | 4.02E+04 |
| **Indiana** | La Porte | 50 | 111 | 1.71E+05 |
| **Indiana** | Jackson | 53 | 117 | 1.83E+05 |
| **Indiana** | Jefferson | 56 | 109 | 1.52E+05 |
| **Iowa** | Harlan | 48 | 113 | 3.40E+04 |
| **Iowa** | Council Bluffs | 53 | 115 | 2.22E+04 |
| **Kansas** | Cherokee | 57 | 112 | 7.86E+04 |
| **Kansas** | Scott | 52 | 100 | 1.04E+05 |
| **Maine** | Hermon | 60 | 102 | 1.73E+05 |
| **Maine** | Sidney | 46 | 104 | 1.41E+05 |
| **Maryland** | Jessup | 52 | 107 | 5.59E+05 |
| **Massachusetts** | Boston | 51 | 111 | 8.33E+04 |
| **Massachusetts** | Springfield | 51 | 102 | 5.93E+04 |
| **Michigan** | Port Huron | 65 | 96 | 2.67E+05 |
| **Michigan** | Alpena | 44 | 95 | 2.60E+05 |
| **Michigan** | Marquette | 44 | 101 | 8.74E+04 |
| **Michigan** | Grand Rapids | 49 | 120 | 2.84E+05 |
| **Mississippi** | Jackson | 65 | 118 | 1.22E+05 |
| **New Jersey** | Newark | 59 | 113 | 3.49E+04 |
| **North Carolina** | Greensboro | 59 | 103 | 2.32E+04 |

| | | | | |
|---|---|---|---|---|
| **North Carolina** | Newark | 50 | 105 | 1.65E+05 |
| **Ohio** | Columbus | 53 | 120 | 5.26E+05 |
| **South Carolina** | Columbia | 64 | 120 | 1.23E+05 |
| **Tennessee** | Memphis | 63 | 97 | 1.27E+05 |
| **Vermont** | Burlington | 46 | 94 | 1.20E+05 |
| **Washington** | Spokane | 48 | 97 | 3.22E+05 |
| **Washington** | Seattle | 53 | 108 | 1.54E+05 |
| **West Virginia** | Martinsburg | 53 | 109 | 9.56E+04 |
| **West Virginia** | Charleston | 56 | 102 | 9.09E+04 |
| **Wisconsin** | Hayward | 42 | 103 | 4.89E+04 |
| **Wisconsin** | Madison | 46 | 103 | 6.33E+04 |

*Table 60- Predicted Flow Number for the U.S. Database*

| State | City | PG | FN |
|---|---|---|---|
| **AL** | Montgomery | PG 76-22 | 1086 |
| | Tuscaloosa | PG 76-22 | 3916 |
| **AK** | Anchorage | PG 64-40 | 1198 |
| | Fairbanks | PG 58-34 | 759 |
| | Barrow | PG 52-40 | 3366 |
| **AZ** | Flagstaff | PG 64-22 | 1206 |
| | Kingman | PG 70-10 | 232 |
| | Tucson | PG 70-10 | 154 |
| | Phoenix | PG 70-22 | 190 |
| **AR** | Little Rock | PG 76-22 | 551 |
| **CO** | Adams | PG 64-22 | 215 |
| | Rio Blanco | PG 58-34 | 412 |
| | El Paso | PG 58-28 | 170 |
| | Yuma | PG 64-28 | 503 |
| | El Rio Grande | PG 58-28 | 310 |
| **DE** | Dover | PG 64-22 | 398 |
| **FL** | Tallahassee | PG 76-22 | 293 |
| **HI** | Honolulu | PG 64-22 | 427 |
| **IN** | La Porte | PG 64-22 | 685 |
| | Jackson | PG 70-22 | 587 |
| | Jefferson | PG 70-22 | 442 |
| **IA** | Harlan | PG 58-28 | 167 |
| | Council Bluffs | PG 58-28 | 110 |
| **KS** | Cherokee | PG 70-28 | 460 |
| | Scott | PG 70-28 | 251 |
| **ME** | Hermon | PG 64-28 | 552 |
| | Sidney | PG 64-28 | 374 |
| **MD** | Jessup | PG 76-22 | 5020 |
| **MA** | Boston | PG 64-28 | 359 |
| | Springfield | PG 64-28 | 231 |
| **MI** | Port Huron | PG 70-28 | 462 |
| | Alpena | PG 64-28 | 493 |
| | Marquette | PG 58-34 | 312 |
| | Grand Rapids | PG 70-28 | 459 |
| **MS** | Jackson | PG 76-22 | 532 |
| **NJ** | Newark | PG 64-22 | 179 |
| **NC** | Greensboro | PG 58-28 | 248 |
| | Newark | PG 64-22 | 463 |
| **OH** | Columbus | PG 76-22 | 324 |

| | | | |
|---|---|---|---|
| **SC** | Columbia | PG 76-22 | 266 |
| **TN** | Memphis | PG 76-22 | 523 |
| **VT** | Burlington | PG 58-28 | 284 |
| **WA** | Spokane | PG 64-28 | 1079 |
| | Seattle | PG 58-22 | 641 |
| **WV** | Martinsburg | PG 64-22 | 410 |
| | Charleston | PG 64-22 | 218 |
| **WI** | Hayward | PG 58-34 | 741 |
| | Madison | PG 58-28 | 875 |

*Table 61- Rutting Depth Prediction for 2 levels of ESALs for the US Database*

| State | City | Climate Region | PG | FN | Rutting Depth for 4'' Asphalt Layer (in) | |
|---|---|---|---|---|---|---|
| | | | | | ESALs= 2 mil | ESALs = 30 mil |
| **Alaska** | Anchorage | *Dry, Freeze* | PG 64-40 | 1198 | 0.22 | 0.82 |
| **Alaska** | Fairbanks | *Dry, Freeze* | PG 58-34 | 759 | 0.25 | 0.92 |
| **Alaska** | Barrow | *Dry, Freeze* | PG 52-40 | 3366 | 0.17 | 0.64 |
| **Arizona** | Flagstaff | *Dry, Freeze* | PG 64-22 | 1206 | 0.22 | 0.82 |
| **Colorado** | Adams | *Dry, Freeze* | PG 64-22 | 215 | 0.34 | 1.25 |
| **Colorado** | Rio Blanco | *Dry, Freeze* | PG 58-34 | 412 | 0.29 | 1.07 |
| **Colorado** | El Paso | *Dry, Freeze* | PG 58-28 | 170 | 0.36 | 1.32 |
| **Colorado** | Yuma | *Dry, Freeze* | PG 64-28 | 503 | 0.28 | 1.02 |
| **Colorado** | El Rio Grande | *Dry, Freeze* | PG 58-28 | 310 | 0.31 | 1.14 |
| **Washington** | Spokane | *Dry, Freeze* | PG 64-28 | 1079 | 0.23 | 0.85 |
| **Arizona** | Kingman | *Dry, No Freeze* | PG 70-10 | 232 | 0.33 | 1.23 |
| **Arizona** | Tucson | *Dry, No Freeze* | PG 70-10 | 154 | 0.37 | 1.35 |
| **Arizona** | Phoenix | *Dry, No Freeze* | PG 70-22 | 190 | 0.35 | 1.29 |
| **Indiana** | La Porte | *Wet, Freeze* | PG 64-22 | 685 | 0.26 | 0.94 |
| **Indiana** | Jackson | *Wet, Freeze* | PG 70-22 | 587 | 0.27 | 0.98 |
| **Iowa** | Harlan | *Wet, Freeze* | PG 58-28 | 167 | 0.36 | 1.33 |
| **Iowa** | Council Bluffs | *Wet, Freeze* | PG 58-28 | 110 | 0.40 | 1.47 |
| **Kansas** | Cherokee | *Wet, Freeze* | PG 70-28 | 460 | 0.28 | 1.04 |
| **Maine** | Hermon | *Wet, Freeze* | PG 64-28 | 552 | 0.27 | 0.99 |
| **Maine** | Sidney | *Wet, Freeze* | PG 64-28 | 374 | 0.30 | 1.09 |
| **Massachusetts** | Boston | *Wet, Freeze* | PG 64-28 | 359 | 0.30 | 1.10 |
| **Michigan** | Port Huron | *Wet, Freeze* | PG 70-28 | 462 | 0.28 | 1.04 |
| **Michigan** | Alpena | *Wet, Freeze* | PG 64-28 | 493 | 0.28 | 1.02 |
| **Michigan** | Marquette | *Wet, Freeze* | PG 58-34 | 312 | 0.31 | 1.14 |
| **Michigan** | Grand Rapids | *Wet, Freeze* | PG 70-28 | 459 | 0.28 | 1.04 |
| **Ohio** | Columbus | *Wet, Freeze* | PG 76-22 | 324 | 0.31 | 1.13 |
| **Vermont** | Burlington | *Wet, Freeze* | PG 58-28 | 284 | 0.32 | 1.17 |
| **West Virginia** | Martinsburg | *Wet, Freeze* | PG 64-22 | 410 | 0.29 | 1.07 |
| **Wisconsin** | Hayward | *Wet, Freeze* | PG 58-34 | 741 | 0.25 | 0.93 |
| **Wisconsin** | Madison | *Wet, Freeze* | PG 58-28 | 875 | 0.24 | 0.89 |

| | | | | | | |
|---|---|---|---|---|---|---|
| **Alabama** | Montgomery | *Wet, No Freeze* | PG 76-22 | 1086 | 0.23 | 0.84 |
| **Alabama** | Tuscaloosa | *Wet, No Freeze* | PG 76-22 | 3916 | 0.17 | 0.62 |
| **Arkansas** | Little Rock | *Wet, No Freeze* | PG 76-22 | 551 | 0.27 | 1.00 |
| **Indiana** | Dover | *Wet, No Freeze* | PG 64-22 | 398 | 0.29 | 1.08 |
| **Delaware** | Tallahassee | *Wet, No Freeze* | PG 76-22 | 293 | 0.31 | 1.16 |
| **Florida** | Honolulu | *Wet, No Freeze* | PG 64-22 | 427 | 0.29 | 1.06 |
| **Hawaii** | Jefferson | *Wet, No Freeze* | PG 70-22 | 442 | 0.28 | 1.05 |
| **Kansas** | Scott | *Wet, No Freeze* | PG 70-28 | 251 | 0.33 | 1.20 |
| **Massachusetts** | Jessup | *Wet, No Freeze* | PG 76-22 | 5020 | 0.16 | 0.58 |
| **Maryland** | Springfield | *Wet, No Freeze* | PG 64-28 | 231 | 0.33 | 1.23 |
| **Mississippi** | Jackson | *Wet, No Freeze* | PG 76-22 | 532 | 0.27 | 1.00 |
| **New Jersey** | Newark | *Wet, No Freeze* | PG 64-22 | 179 | 0.35 | 1.31 |
| **North Carolina** | Greensboro | *Wet, No Freeze* | PG 58-28 | 248 | 0.33 | 1.21 |
| **North Carolina** | Newark | *Wet, No Freeze* | PG 64-22 | 463 | 0.28 | 1.04 |
| **South Carolina** | Columbia | *Wet, No Freeze* | PG 76-22 | 266 | 0.32 | 1.19 |
| **Tennessee** | Memphis | *Wet, No Freeze* | PG 76-22 | 523 | 0.27 | 1.01 |
| **Washington** | Seattle | *Wet, No Freeze* | PG 58-22 | 641 | 0.26 | 0.96 |
| **West Virginia** | Charleston | *Wet, No Freeze* | PG 64-22 | 218 | 0.34 | 1.25 |

*Table 62- Effective Fatigue Temperatures for the US Database*

| States | City | PG | Effective Fatigue Temperature (°F) |
|---|---|---|---|
| **AL** | *Montgomery* | PG 76-22 | 75.2 |
| | *Tuscaloosa* | PG 76-22 | 75.2 |
| **AZ** | *Flagstaff* | PG 64-22 | 64.4 |
| | *Kingman* | PG 70-10 | 80.6 |
| | *Tucson* | PG 70-10 | 80.6 |
| | *Phoenix* | PG 70-22 | 69.8 |
| **AK** | *Anchorage* | PG 64-40 | 48.2 |
| | *Fairbanks* | PG 58-34 | 48.2 |
| | *Barrow* | PG 52-40 | 37.4 |
| **AR** | *Little Rock* | PG 76-22 | 75.2 |
| **CO** | *Adams* | PG 64-22 | 64.4 |
| | *Rio Blanco* | PG 58-34 | 48.2 |
| | *El Paso* | PG 58-28 | 53.6 |
| | *Yuma* | PG 64-28 | 59 |
| | *El Rio Grande* | PG 58-28 | 53.6 |
| **IN** | *La Porte* | PG 64-22 | 64.4 |
| | *Jackson* | PG 70-22 | 69.8 |
| | *Jefferson* | PG 70-22 | 69.8 |
| **DE** | *Dover* | PG 64-22 | 64.4 |
| **FL** | *Tallahassee* | PG 76-22 | 75.2 |
| **HI** | *Honolulu* | PG 64-22 | 64.4 |
| **IA** | *Harlan* | PG 58-28 | 53.6 |
| | *Council Bluffs* | PG 58-28 | 53.6 |
| **KS** | *Cherokee* | PG 70-28 | 64.4 |
| | *Scott* | PG 70-28 | 64.4 |
| **ME** | *Hermon* | PG 64-28 | 59 |
| | *Sidney* | PG 64-28 | 59 |
| **MA** | *Boston* | PG 64-28 | 59 |
| | *Springfield* | PG 64-28 | 59 |
| **MD** | *Jessup* | PG 76-22 | 75.2 |
| **MI** | *Port Huron* | PG 70-28 | 64.4 |
| | *Alpena* | PG 64-28 | 59 |
| | *Marquette* | PG 58-34 | 48.2 |
| | *Grand Rapids* | PG 70-28 | 64.4 |
| **MS** | *Jackson* | PG 76-22 | 75.2 |
| **NJ** | *Newark* | PG 64-22 | 64.4 |

| | | | |
|---|---|---|---|
| **NC** | *Greensboro* | PG 58-28 | 53.6 |
| | *Newark* | PG 64-22 | 64.4 |
| **OH** | *Columbus* | PG 76-22 | 75.2 |
| **SC** | *Columbia* | PG 76-22 | 75.2 |
| **TN** | *Memphis* | PG 76-22 | 75.2 |
| **VT** | *Burlington* | PG 58-28 | 53.6 |
| **WA** | *Seattle* | PG 58-22 | 59 |
| | *Spokane* | PG 64-28 | 59 |
| **WV** | *Martinsburg* | PG 64-22 | 64.4 |
| | *Charleston* | PG 64-22 | 64.4 |
| **WI** | *Hayward* | PG 58-34 | 48.2 |
| | *Madison* | PG 58-28 | 53.6 |

*Table 63- Viscosity in (cP) at the Effective Fatigue Temperature for the US Database*

| States | City | PG | Effective Fatigue Temperature (°F) | μ (cP) |
|---|---|---|---|---|
| **AL** | *Montgomery* | PG 76-22 | 75.2 | 3.8E+08 |
| | *Tuscaloosa* | PG 76-22 | 75.2 | 3.8E+08 |
| **AZ** | *Flagstaff* | PG 64-22 | 64.4 | 1.15E+09 |
| | *Kingman* | PG 70-10 | 80.6 | 3.36E+08 |
| | *Tucson* | PG 70-10 | 80.6 | 3.36E+08 |
| | *Phoenix* | PG 70-22 | 69.8 | 6.25E+08 |
| **AK** | *Anchorage* | PG 64-40 | 48.2 | 1.4E+08 |
| | *Fairbanks* | PG 58-34 | 48.2 | 6.21E+08 |
| | *Barrow* | PG 52-40 | 37.4 | 3.61E+08 |
| **AR** | *Little Rock* | PG 76-22 | 75.2 | 3.8E+08 |
| **CO** | *Adams* | PG 64-22 | 64.4 | 1.15E+09 |
| | *Rio Blanco* | PG 58-34 | 48.2 | 3.11E+09 |
| | *El Paso* | PG 58-28 | 53.6 | 3.41E+08 |
| | *Yuma* | PG 64-28 | 59 | 7.88E+08 |
| | *El Rio Grande* | PG 58-28 | 53.6 | 1.52E+09 |
| **IN** | *La Porte* | PG 64-22 | 64.4 | 1.15E+09 |
| | *Jackson* | PG 70-22 | 69.8 | 6.25E+08 |
| | *Jefferson* | PG 70-22 | 69.8 | 6.25E+08 |
| **DE** | *Dover* | PG 64-22 | 64.4 | 1.15E+09 |
| **FL** | *Tallahassee* | PG 76-22 | 75.2 | 3.8E+08 |
| **HI** | *Honolulu* | PG 64-22 | 64.4 | 1.15E+09 |
| **IA** | *Harlan* | PG 58-28 | 53.6 | 1.52E+09 |
| | *Council Bluffs* | PG 58-28 | 53.6 | 1.52E+09 |
| **KS** | *Cherokee* | PG 70-28 | 64.4 | 4.43E+08 |
| | *Scott* | PG 70-28 | 64.4 | 4.43E+08 |
| **ME** | *Hermon* | PG 64-28 | 59 | 7.88E+08 |
| | *Sidney* | PG 64-28 | 59 | 7.88E+08 |
| **MA** | *Boston* | PG 64-28 | 59 | 7.88E+08 |
| | *Springfield* | PG 64-28 | 59 | 7.88E+08 |
| **MD** | *Jessup* | PG 76-22 | 75.2 | 3.8E+08 |
| **MI** | *Port Huron* | PG 70-28 | 64.4 | 4.43E+08 |
| | *Alpena* | PG 64-28 | 59 | 7.88E+08 |
| | *Marquette* | PG 58-34 | 48.2 | 6.21E+08 |
| | *Grand Rapids* | PG 70-28 | 64.4 | 4.43E+08 |
| **MS** | *Jackson* | PG 76-22 | 75.2 | 3.8E+08 |

| | | | | |
|---|---|---|---|---|
| **NJ** | *Newark* | PG 64-22 | 64.4 | 1.15E+09 |
| **NC** | *Greensboro* | PG 58-28 | 53.6 | 1.52E+09 |
| | *Newark* | PG 64-22 | 64.4 | 1.15E+09 |
| **OH** | *Columbus* | PG 76-22 | 75.2 | 3.8E+08 |
| **SC** | *Columbia* | PG 76-22 | 75.2 | 3.8E+08 |
| **TN** | *Memphis* | PG 76-22 | 75.2 | 3.8E+08 |
| **VT** | *Burlington* | PG 58-28 | 53.6 | 1.52E+09 |
| **WA** | *Seattle* | PG 58-22 | 59 | 2.43E+09 |
| | *Spokane* | PG 64-28 | 59 | 7.88E+08 |
| **WV** | *Martinsburg* | PG 64-22 | 64.4 | 1.15E+09 |
| | *Charleston* | PG 64-22 | 64.4 | 1.15E+09 |
| **WI** | *Hayward* | PG 58-34 | 48.2 | 6.21E+08 |
| | *Madison* | PG 58-28 | 53.6 | 1.52E+09 |

*Table 64- Phase Angle for the US Database*

| States | City | PG | Effective Fatigue Temperature (°F) | μ (cP) | δ |
|---|---|---|---|---|---|
| **AL** | *Montgomery* | PG 76-22 | 75.2 | 3.8E+08 | 47.7 |
| | *Tuscaloosa* | PG 76-22 | 75.2 | 3.8E+08 | 47.7 |
| **AZ** | *Flagstaff* | PG 64-22 | 64.4 | 1.15E+09 | 45.8 |
| | *Kingman* | PG 70-10 | 80.6 | 3.36E+08 | 50.2 |
| | *Tucson* | PG 70-10 | 80.6 | 3.36E+08 | 50.2 |
| | *Phoenix* | PG 70-22 | 69.8 | 6.25E+08 | 47.0 |
| **AK** | *Anchorage* | PG 64-40 | 48.2 | 1.4E+08 | 49.0 |
| | *Fairbanks* | PG 58-34 | 48.2 | 6.21E+08 | 46.6 |
| | *Barrow* | PG 52-40 | 37.4 | 3.61E+08 | 47.7 |
| **AR** | *Little Rock* | PG 76-22 | 75.2 | 3.8E+08 | 47.7 |
| **CO** | *Adams* | PG 64-22 | 64.4 | 1.15E+09 | 45.8 |
| | *Rio Blanco* | PG 58-34 | 48.2 | 3.11E+09 | 41.6 |
| | *El Paso* | PG 58-28 | 53.6 | 3.41E+08 | 48.9 |
| | *Yuma* | PG 64-28 | 59 | 7.88E+08 | 46.2 |
| | *El Rio Grande* | PG 58-28 | 53.6 | 1.52E+09 | 44.7 |
| **IN** | *La Porte* | PG 64-22 | 64.4 | 1.15E+09 | 45.8 |
| | *Jackson* | PG 70-22 | 69.8 | 6.25E+08 | 47.0 |
| | *Jefferson* | PG 70-22 | 69.8 | 6.25E+08 | 47.0 |
| **DE** | *Dover* | PG 64-22 | 64.4 | 1.15E+09 | 45.8 |
| **FL** | *Tallahassee* | PG 76-22 | 75.2 | 3.8E+08 | 47.7 |
| **HI** | *Honolulu* | PG 64-22 | 64.4 | 1.15E+09 | 45.8 |
| **IA** | *Harlan* | PG 58-28 | 53.6 | 1.52E+09 | 44.7 |
| | *Council Bluffs* | PG 58-28 | 53.6 | 1.52E+09 | 44.7 |
| **KS** | *Cherokee* | PG 70-28 | 64.4 | 4.43E+08 | 47.2 |
| | *Scott* | PG 70-28 | 64.4 | 4.43E+08 | 47.2 |
| **ME** | *Hermon* | PG 64-28 | 59 | 7.88E+08 | 46.2 |
| | *Sidney* | PG 64-28 | 59 | 7.88E+08 | 46.2 |
| **MA** | *Boston* | PG 64-28 | 59 | 7.88E+08 | 46.2 |
| **MD** | *Springfield* | PG 64-28 | 59 | 7.88E+08 | 46.2 |
| | *Jessup* | PG 76-22 | 75.2 | 3.8E+08 | 47.7 |
| **MI** | *Port Huron* | PG 70-28 | 64.4 | 4.43E+08 | 47.2 |
| | *Alpena* | PG 64-28 | 59 | 7.88E+08 | 46.2 |
| | *Marquette* | PG 58-34 | 48.2 | 6.21E+08 | 46.6 |
| | *Grand Rapids* | PG 70-28 | 64.4 | 4.43E+08 | 47.2 |
| **MS** | *Jackson* | PG 76-22 | 75.2 | 3.8E+08 | 47.7 |

| | | | | | |
|---|---|---|---|---|---|
| **NJ** | *Newark* | PG 64-22 | 64.4 | 1.15E+09 | 45.8 |
| **NC** | *Greensboro* | PG 58-28 | 53.6 | 1.52E+09 | 44.7 |
| | *Newark* | PG 64-22 | 64.4 | 1.15E+09 | 45.8 |
| **OH** | *Columbus* | PG 76-22 | 75.2 | 3.8E+08 | 47.7 |
| **SC** | *Columbia* | PG 76-22 | 75.2 | 3.8E+08 | 47.7 |
| **TN** | *Memphis* | PG 76-22 | 75.2 | 3.8E+08 | 47.7 |
| **VT** | *Burlington* | PG 58-28 | 53.6 | 1.52E+09 | 44.7 |
| **WA** | *Seattle* | PG 58-22 | 59 | 2.43E+09 | 44.0 |
| | *Spokane* | PG 64-28 | 59 | 7.88E+08 | 46.2 |
| **WV** | *Martinsburg* | PG 64-22 | 64.4 | 1.15E+09 | 45.8 |
| | *Charleston* | PG 64-22 | 64.4 | 1.15E+09 | 45.8 |
| **WI** | *Hayward* | PG 58-34 | 48.2 | 6.21E+08 | 46.6 |
| | *Madison* | PG 58-28 | 53.6 | 1.52E+09 | 44.7 |

*Table 65- G*b Calculations for the US Database*

| States | City | PG | Effective Fatigue Temperature (°F) | δ | G* Pa |
|---|---|---|---|---|---|
| **AL** | *Montgomery* | PG 76-22 | 75.2 | 47.7 | 5.26E+06 |
| | *Tuscaloosa* | PG 76-22 | 75.2 | 47.7 | 5.26E+06 |
| **AZ** | *Flagstaff* | PG 64-22 | 64.4 | 45.8 | 1.39E+07 |
| | *Kingman* | PG 70-10 | 80.6 | 50.2 | 5.45E+06 |
| | *Tucson* | PG 70-10 | 80.6 | 50.2 | 5.45E+06 |
| | *Phoenix* | PG 70-22 | 69.8 | 47.0 | 8.21E+06 |
| **AK** | *Anchorage* | PG 64-40 | 48.2 | 49.0 | 2.11E+06 |
| | *Fairbanks* | PG 58-34 | 48.2 | 46.6 | 7.94E+06 |
| | *Barrow* | PG 52-40 | 37.4 | 47.7 | 4.97E+06 |
| **AR** | *Little Rock* | PG 76-22 | 75.2 | 47.7 | 5.26E+06 |
| **CO** | *Adams* | PG 64-22 | 64.4 | 45.8 | 1.39E+07 |
| | *Rio Blanco* | PG 58-34 | 48.2 | 41.6 | 2.70E+07 |
| | *El Paso* | PG 58-28 | 53.6 | 48.9 | 5.11E+06 |
| | *Yuma* | PG 64-28 | 59 | 46.2 | 9.75E+06 |
| | *El Rio Grande* | PG 58-28 | 53.6 | 44.7 | 1.70E+07 |
| **IN** | *La Porte* | PG 64-22 | 64.4 | 45.8 | 1.39E+07 |
| | *Jackson* | PG 70-22 | 69.8 | 47.0 | 8.21E+06 |
| | *Jefferson* | PG 70-22 | 69.8 | 47.0 | 8.21E+06 |
| **DE** | *Dover* | PG 64-22 | 64.4 | 45.8 | 1.39E+07 |
| **FL** | *Tallahassee* | PG 76-22 | 75.2 | 47.7 | 5.26E+06 |
| **HI** | *Honolulu* | PG 64-22 | 64.4 | 45.8 | 1.39E+07 |
| **IA** | *Harlan* | PG 58-28 | 53.6 | 44.7 | 1.70E+07 |
| | *Council Bluffs* | PG 58-28 | 53.6 | 44.7 | 1.70E+07 |
| **KS** | *Cherokee* | PG 70-28 | 64.4 | 47.2 | 5.91E+06 |
| | *Scott* | PG 70-28 | 64.4 | 47.2 | 5.91E+06 |
| **ME** | *Hermon* | PG 64-28 | 59 | 46.2 | 9.75E+06 |
| | *Sidney* | PG 64-28 | 59 | 46.2 | 9.75E+06 |
| **MA** | *Boston* | PG 64-28 | 59 | 46.2 | 9.75E+06 |
| | *Springfield* | PG 64-28 | 59 | 46.2 | 9.75E+06 |
| **MD** | *Jessup* | PG 76-22 | 75.2 | 47.7 | 5.26E+06 |
| **MI** | *Port Huron* | PG 70-28 | 64.4 | 47.2 | 5.91E+06 |
| | *Alpena* | PG 64-28 | 59 | 46.2 | 9.75E+06 |
| | *Marquette* | PG 58-34 | 48.2 | 46.6 | 7.94E+06 |
| | *Grand Rapids* | PG 70-28 | 64.4 | 47.2 | 5.91E+06 |
| **MS** | *Jackson* | PG 76-22 | 75.2 | 47.7 | 5.26E+06 |

| | | | | | |
|---|---|---|---|---|---|
| **NJ** | *Newark* | PG 64-22 | 64.4 | 45.8 | 1.39E+07 |
| **NC** | *Greensboro* | PG 58-28 | 53.6 | 44.7 | 1.70E+07 |
| | *Newark* | PG 64-22 | 64.4 | 45.8 | 1.39E+07 |
| **OH** | *Columbus* | PG 76-22 | 75.2 | 47.7 | 5.26E+06 |
| **SC** | *Columbia* | PG 76-22 | 75.2 | 47.7 | 5.26E+06 |
| **TN** | *Memphis* | PG 76-22 | 75.2 | 47.7 | 5.26E+06 |
| **VT** | *Burlington* | PG 58-28 | 53.6 | 44.7 | 1.70E+07 |
| **WA** | *Seattle* | PG 58-22 | 59 | 44.0 | 2.55E+07 |
| | *Spokane* | PG 64-28 | 59 | 46.2 | 9.75E+06 |
| **WV** | *Martinsburg* | PG 64-22 | 64.4 | 45.8 | 1.39E+07 |
| | *Charleston* | PG 64-22 | 64.4 | 45.8 | 1.39E+07 |
| **WI** | *Hayward* | PG 58-34 | 48.2 | 46.6 | 7.94E+06 |
| | *Madison* | PG 58-28 | 53.6 | 44.7 | 1.70E+07 |

*Table 66- FSC* Calculation for the US Database*

| States | City | PG | Effective Fatigue Temperature (°F) | \|G*b\| Pa | FSC* |
|---|---|---|---|---|---|
| **AL** | Montgomery | PG 76-22 | 75.2 | 5.26E+06 | 47.76 |
| | Tuscaloosa | PG 76-22 | 75.2 | 5.26E+06 | 47.76 |
| **AZ** | Flagstaff | PG 64-22 | 64.4 | 1.39E+07 | 30.06 |
| | Kingman | PG 70-10 | 80.6 | 5.45E+06 | 47.14 |
| | Tucson | PG 70-10 | 80.6 | 5.45E+06 | 47.14 |
| | Phoenix | PG 70-22 | 69.8 | 8.21E+06 | 39.66 |
| **AK** | Anchorage | PG 64-40 | 48.2 | 2.11E+06 | 62.18 |
| | Fairbanks | PG 58-34 | 48.2 | 7.94E+06 | 40.27 |
| | Barrow | PG 52-40 | 37.4 | 4.97E+06 | 48.76 |
| **AR** | Little Rock | PG 76-22 | 75.2 | 5.26E+06 | 47.76 |
| **CO** | Adams | PG 64-22 | 64.4 | 1.39E+07 | 30.06 |
| | Rio Blanco | PG 58-34 | 48.2 | 2.70E+07 | 19.46 |
| | El Paso | PG 58-28 | 53.6 | 5.11E+06 | 48.28 |
| | Yuma | PG 64-28 | 59 | 9.75E+06 | 36.49 |
| | El Rio Grande | PG 58-28 | 53.6 | 1.70E+07 | 26.66 |
| **IN** | La Porte | PG 64-22 | 64.4 | 1.39E+07 | 30.06 |
| | Jackson | PG 70-22 | 69.8 | 8.21E+06 | 39.66 |
| | Jefferson | PG 70-22 | 69.8 | 8.21E+06 | 39.66 |
| **DE** | Dover | PG 64-22 | 64.4 | 1.39E+07 | 30.06 |
| **FL** | Talhassee | PG 76-22 | 75.2 | 5.26E+06 | 47.76 |
| **HI** | Honolulu | PG 64-22 | 64.4 | 1.39E+07 | 30.06 |
| **IA** | Harlan | PG 58-28 | 53.6 | 1.70E+07 | 26.66 |
| | Council Bluffs | PG 58-28 | 53.6 | 1.70E+07 | 26.66 |
| **KS** | Cherokee | PG 70-28 | 64.4 | 5.91E+06 | 45.68 |
| | Scott | PG 70-28 | 64.4 | 5.91E+06 | 45.68 |
| **ME** | Hermon | PG 64-28 | 59 | 9.75E+06 | 36.49 |
| | Sidney | PG 64-28 | 59 | 9.75E+06 | 36.49 |
| **MA** | Boston | PG 64-28 | 59 | 9.75E+06 | 36.49 |
| | Springfield | PG 64-28 | 59 | 9.75E+06 | 36.49 |
| **MD** | Jessup | PG 76-22 | 75.2 | 5.26E+06 | 47.76 |
| **MI** | Port Huron | PG 70-28 | 64.4 | 5.91E+06 | 45.68 |
| | Alpena | PG 64-28 | 59 | 9.75E+06 | 36.49 |
| | Marquette | PG 58-34 | 48.2 | 7.94E+06 | 40.27 |
| | Grand Rapids | PG 70-28 | 64.4 | 5.91E+06 | 45.68 |
| **MS** | Jackson | PG 76-22 | 75.2 | 5.26E+06 | 47.76 |

| | | | | | |
|---|---|---|---|---|---|
| **NJ** | Newark | PG 64-22 | 64.4 | 1.39E+07 | 30.06 |
| **NC** | Greensboro | PG 58-28 | 53.6 | 1.70E+07 | 26.66 |
| | Newark | PG 64-22 | 64.4 | 1.39E+07 | 30.06 |
| **OH** | Columbus | PG 76-22 | 75.2 | 5.26E+06 | 47.76 |
| **SC** | Columbia | PG 76-22 | 75.2 | 5.26E+06 | 47.76 |
| **TN** | Memphis | PG 76-22 | 75.2 | 5.26E+06 | 47.76 |
| **VT** | Burlington | PG 58-28 | 53.6 | 1.70E+07 | 26.66 |
| **WA** | Seattle | PG 58-22 | 59 | 2.55E+07 | 20.27 |
| | Spokane | PG 64-28 | 59 | 9.75E+06 | 36.49 |
| **WV** | Martinsburg | PG 64-22 | 64.4 | 1.39E+07 | 30.06 |
| | Charleston | PG 64-22 | 64.4 | 1.39E+07 | 30.06 |
| **WI** | Hayward | PG 58-34 | 48.2 | 7.94E+06 | 40.27 |
| | Madison | PG 58-28 | 53.6 | 1.70E+07 | 26.66 |

*Table 67- Number of Cycles to Failure Nf for the US Database*

| States | City | PG | Eff Fatigue T(°F) | μ (cP) | δ | \|G*b\| Pa | FSC* | Nf |
|---|---|---|---|---|---|---|---|---|
| **AL** | Montgomery | PG 76-22 | 75.2 | 3.8E+08 | 47.74 | 5.26E+06 | 47.76 | 35166 |
| | Tuscaloosa | PG 76-22 | 75.2 | 3.8E+08 | 47.74 | 5.26E+06 | 47.76 | 34172 |
| **AZ** | Flagstaff | PG 64-22 | 64.4 | 1.15E+09 | 45.79 | 1.39E+07 | 30.06 | 14177 |
| | Kingman | PG 70-10 | 80.6 | 3.36E+08 | 50.18 | 5.45E+06 | 47.14 | 11304 |
| | Tucson | PG 70-10 | 80.6 | 3.36E+08 | 50.18 | 5.45E+06 | 47.14 | 11515 |
| | Phoenix | PG 70-22 | 69.8 | 6.25E+08 | 47.00 | 8.21E+06 | 39.66 | 15898 |
| **AK** | Anchorage | PG 64-40 | 48.2 | 1.4E+08 | 48.97 | 2.11E+06 | 62.18 | 30244 |
| | Fairbanks | PG 58-34 | 48.2 | 6.21E+08 | 46.63 | 7.94E+06 | 40.27 | 24458 |
| | Barrow | PG 52-40 | 37.4 | 3.61E+08 | 47.69 | 4.97E+06 | 48.76 | 25848 |
| **AR** | Little Rock | PG 76-22 | 75.2 | 3.8E+08 | 47.74 | 5.26E+06 | 47.76 | 23761 |
| **CO** | Adams | PG 64-22 | 64.4 | 1.15E+09 | 45.79 | 1.39E+07 | 30.06 | 11300 |
| | Rio Blanco | PG 58-34 | 48.2 | 3.11E+09 | 41.64 | 2.70E+07 | 19.46 | 14426 |
| | El Paso | PG 58-28 | 53.6 | 3.41E+08 | 48.93 | 5.11E+06 | 48.28 | 21303 |
| | Yuma | PG 64-28 | 59 | 7.88E+08 | 46.15 | 9.75E+06 | 36.49 | 18600 |
| | El Rio Grande | PG 58-28 | 53.6 | 1.52E+09 | 44.72 | 1.70E+07 | 26.66 | 15100 |
| **IN** | La Porte | PG 64-22 | 64.4 | 1.15E+09 | 45.79 | 1.39E+07 | 30.06 | 15476 |
| | Jackson | PG 70-22 | 69.8 | 6.25E+08 | 47.00 | 8.21E+06 | 39.66 | 20482 |
| | Jefferson | PG 70-22 | 69.8 | 6.25E+08 | 47.00 | 8.21E+06 | 39.66 | 18117 |
| **DE** | Dover | PG 64-22 | 64.4 | 1.15E+09 | 45.79 | 1.39E+07 | 30.06 | 15211 |
| **FL** | Tallahassee | PG 76-22 | 75.2 | 3.8E+08 | 47.74 | 5.26E+06 | 47.76 | 18345 |
| **HI** | Honolulu | PG 64-22 | 64.4 | 1.15E+09 | 45.79 | 1.39E+07 | 30.06 | 6552 |
| **IA** | Harlan | PG 58-28 | 53.6 | 1.52E+09 | 44.72 | 1.70E+07 | 26.66 | 12091 |
| | Council Bluffs | PG 58-28 | 53.6 | 1.52E+09 | 44.72 | 1.70E+07 | 26.66 | 9435 |
| **KS** | Cherokee | PG 70-28 | 64.4 | 4.43E+08 | 47.21 | 5.91E+06 | 45.68 | 28278 |
| | Scott | PG 70-28 | 64.4 | 4.43E+08 | 47.21 | 5.91E+06 | 45.68 | 22622 |
| **ME** | Hermon | PG 64-28 | 59 | 7.88E+08 | 46.15 | 9.75E+06 | 36.49 | 33350 |
| | Sidney | PG 64-28 | 59 | 7.88E+08 | 46.15418 | 9.75E+06 | 36.49 | 21054 |
| **MA** | Boston | PG 64-28 | 59 | 7.88E+08 | 46.15 | 9.75E+06 | 36.49 | 26026 |
| | Springfield | PG 64-28 | 59 | 7.88E+08 | 46.15 | 9.75E+06 | 36.49 | 21417 |
| **MD** | Jessup | PG 76-22 | 75.2 | 3.8E+08 | 47.74 | 5.26E+06 | 47.76 | 37713 |
| **MI** | Port Huron | PG 70-28 | 64.4 | 4.43E+08 | 47.21 | 5.91E+06 | 45.68 | 27820 |

| | | | | | | | | |
|---|---|---|---|---|---|---|---|---|
| | Alpena | PG 64-28 | 59 | 7.88E+08 | 46.15 | 9.75E+06 | 36.49 | 18941 |
| | Marquette | PG 58-34 | 48.2 | 6.21E+08 | 46.63 | 7.94E+06 | 40.27 | 20833 |
| | Grand Rapids | PG 70-28 | 64.4 | 4.43E+08 | 47.21 | 5.91E+06 | 45.68 | 22213 |
| **MS** | Jackson | PG 76-22 | 75.2 | 3.8E+08 | 47.74 | 5.26E+06 | 47.76 | 35166 |
| **NJ** | Newark | PG 64-22 | 64.4 | 1.15E+09 | 45.79 | 1.39E+07 | 30.06 | 21897 |
| **NC** | Greensboro | PG 58-28 | 53.6 | 1.52E+09 | 44.72 | 1.70E+07 | 26.66 | 14835 |
| | Newark | PG 64-22 | 64.4 | 1.15E+09 | 45.79708 | 1.39E+07 | 30.06 | 15211 |
| **OH** | Columbus | PG 76-22 | 75.2 | 3.8E+08 | 47.74081 | 5.26E+06 | 47.76 | 34172 |
| **SC** | Columbia | PG 76-22 | 75.2 | 3.8E+08 | 47.74081 | 5.26E+06 | 47.76 | 27611 |
| **TN** | Memphis | PG 76-22 | 75.2 | 3.8E+08 | 47.74081 | 5.26E+06 | 47.76 | 20581 |
| **VT** | Burlington | PG 58-28 | 53.6 | 1.52E+09 | 44.72593 | 1.70E+07 | 26.66 | 16458 |
| **WA** | Seattle | PG 58-22 | 59 | 2.43E+09 | 43.98211 | 2.55E+07 | 20.27 | 5562 |
| | Spokane | PG 64-28 | 59 | 7.88E+08 | 46.15418 | 9.75E+06 | 36.49 | 16943 |
| **WV** | Martinsburg | PG 64-22 | 64.4 | 1.15E+09 | 45.79708 | 1.39E+07 | 30.06 | 13426 |
| | Charleston | PG 64-22 | 64.4 | 1.15E+09 | 45.79708 | 1.39E+07 | 30.06 | 7250 |
| **WI** | Hayward | PG 58-34 | 48.2 | 6.21E+08 | 46.6316 | 7.94E+06 | 40.27 | 18056 |
| | Madison | PG 58-28 | 53.6 | 1.52E+09 | 44.72593 | 1.70E+07 | 26.66 | 11394 |

*Table 68- D1 Fracture Parameter Calculation for the US Database*

| State | City | Climate Zone | Va | Vbe | D1 (-20°C) | D1(-10°C) | D1 (0°C) |
|---|---|---|---|---|---|---|---|
| AK | *Anchorage* | *Dry, Freeze* | 3.96 | 11.6 | 3.12E-07 | 4.14E-07 | 5.19E-07 |
| AK | *Fairbanks* | *Dry, Freeze* | 5.2 | 10.2 | 1.89E-07 | 3.07E-07 | 4.11E-07 |
| AK | *Barrow* | *Dry, Freeze* | 5.6 | 10.3 | 1.91E-07 | 3.18E-07 | 4.3E-07 |
| AZ | *Flagstaff* | *Dry, Freeze* | 5 | 10.5 | 3.26E-07 | 4.65E-07 | 6.08E-07 |
| CO | *Adams* | *Dry, Freeze* | 3.3 | 10.4 | 2.56E-07 | 3.35E-07 | 4.16E-07 |
| CO | *Rio Blanco* | *Dry, Freeze* | 3.5 | 11.9 | 3.11E-07 | 3.98E-07 | 4.98E-07 |
| CO | *El Paso* | *Dry, Freeze* | 3.5 | 12.2 | 2.97E-07 | 3.83E-07 | 4.71E-07 |
| CO | *Yuma* | *Dry, Freeze* | 3.5 | 11.3 | 3.23E-07 | 4.09E-07 | 5.06E-07 |
| CO | *El Rio Grande* | *Dry, Freeze* | 3.4 | 12.1 | 2.9E-07 | 3.72E-07 | 4.57E-07 |
| WA | *Spokane* | *Dry, Freeze* | 4.4 | 9.3 | 1.62E-07 | 2.57E-07 | 3.41E-07 |
| AZ | *Kingman* | *Dry, No Freeze* | 4 | 11.4 | 7.11E-07 | 7.96E-07 | 9.8E-07 |
| AZ | *Tucson* | *Dry, No Freeze* | 4 | 12.3 | 4.16E-07 | 5.22E-07 | 6.46E-07 |
| AZ | *Phoenix* | *Dry, No Freeze* | 3.3 | 11.7 | 4.45E-07 | 5.16E-07 | 6.26E-07 |
| IN | *La Porte* | *Wet, Freeze* | 4 | 12 | 3.25E-07 | 4.3E-07 | 5.37E-07 |
| IN | *Jackson* | *Wet, Freeze* | 4 | 10.1 | 3.73E-07 | 4.79E-07 | 6.07E-07 |
| IA | *Harlan* | *Wet, Freeze* | 4 | 10.9 | 2.77E-07 | 3.8E-07 | 4.81E-07 |
| IA | *Council Bluffs* | *Wet, Freeze* | 4 | 9.7 | 2.39E-07 | 3.39E-07 | 4.36E-07 |
| KS | *Cherokee* | *Wet, Freeze* | 4 | -318.119 | 4.75E-07 | 5.79E-07 | 7.14E-07 |
| ME | *Hermon* | *Wet, Freeze* | 4 | 11 | 3.3E-07 | 4.35E-07 | 5.48E-07 |

| | | | | | | | |
|---|---|---|---|---|---|---|---|
| ME | *Sidney* | *Wet, Freeze* | 4 | 12 | 3.65E-07 | 4.71E-07 | 5.86E-07 |
| MA | *Boston* | *Wet, Freeze* | 4 | -244.102 | 3.68E-07 | 4.74E-07 | 5.9E-07 |
| MI | *Port Huron* | *Wet, Freeze* | 4 | -256.546 | 4.71E-07 | 5.75E-07 | 7.1E-07 |
| MI | *Alpena* | *Wet, Freeze* | 4 | -48.0668 | 3.44E-07 | 4.5E-07 | 5.64E-07 |
| MI | *Marquette* | *Wet, Freeze* | 4 | 97.79787 | 3.81E-07 | 4.87E-07 | 6.09E-07 |
| MI | *Grand Rapids* | *Wet, Freeze* | 4 | 115.5697 | 4.14E-07 | 5.21E-07 | 6.52E-07 |
| OH | *Columbus* | *Wet, Freeze* | 4 | -608.434 | 5.32E-07 | 6.32E-07 | 7.7E-07 |
| VT | *Burlington* | *Wet, Freeze* | 4 | 12.6 | 3E-07 | 4.04E-07 | 5.02E-07 |
| WV | *Martinsburg* | *Wet, Freeze* | 4.4 | 11.3 | 3.12E-07 | 4.3E-07 | 5.48E-07 |
| WI | *Hayward* | *Wet, Freeze* | 4.4 | 201.7701 | 3.58E-07 | 4.8E-07 | 6.13E-07 |
| WI | *Madison* | *Wet, Freeze* | 4.4 | 89.18414 | 2.52E-07 | 3.63E-07 | 4.68E-07 |
| AL | *Montgomery* | *Wet, No Freeze* | 3.5 | 14 | 5E-07 | 5.76E-07 | 6.91E-07 |
| AL | *Tuscaloosa* | *Wet, No Freeze* | 3.5 | 13.8 | 4.93E-07 | 5.7E-07 | 6.85E-07 |
| AR | *Little Rock* | *Wet, No Freeze* | 4 | 11.5 | 4.36E-07 | 5.42E-07 | 6.75E-07 |
| DE | *Dover* | *Wet, No Freeze* | 4 | -326.054 | 3.28E-07 | 4.33E-07 | 5.4E-07 |
| FL | *Talhassee* | *Wet, No Freeze* | 4 | -170.723 | 3.63E-07 | 4.69E-07 | 5.85E-07 |
| HI | *Honolulu* | *Wet, No Freeze* | 4 | 25.20235 | 3.39E-07 | 4.44E-07 | 5.58E-07 |
| IN | *Jefferson* | *Wet, No Freeze* | 4 | 8 | 1.91E-07 | 2.85E-07 | 3.77E-07 |
| KS | *Scott* | *Wet, No Freeze* | 4 | 111.7861 | 4.19E-07 | 5.25E-07 | 6.56E-07 |
| MD | *Jessup* | *Wet, No Freeze* | 4 | -556.613 | 4.08E-07 | 5.14E-07 | 6.31E-07 |

| | | | | | | | |
|---|---|---|---|---|---|---|---|
| MA | *Springfield* | *Wet, No Freeze* | 3.5 | 14.5 | 5.16E-07 | 5.9E-07 | 7.06E-07 |
| MS | *Jackson* | *Wet, No Freeze* | 4 | 14 | 5.4E-07 | 6.4E-07 | 7.77E-07 |
| NJ | *Newark* | *Wet, No Freeze* | 4 | 14.3 | 3.91E-07 | 4.96E-07 | 6.07E-07 |
| NC | *Greensboro* | *Wet, No Freeze* | 4 | -159.268 | 3.1E-07 | 4.14E-07 | 5.18E-07 |
| NC | *Newark* | *Wet, No Freeze* | 4 | -250.293 | 3.25E-07 | 4.3E-07 | 5.37E-07 |
| SC | *Columbia* | *Wet, No Freeze* | 5.8 | 12.4 | 5.24E-07 | 7.08E-07 | 9.16E-07 |
| TN | *Memphis* | *Wet, No Freeze* | 4 | 10.7 | 4.01E-07 | 5.07E-07 | 6.37E-07 |
| WA | *Seattle* | *Wet, No Freeze* | 4.4 | 10.8 | 3.31E-07 | 4.51E-07 | 5.76E-07 |
| WV | *Charleston* | *Wet, No Freeze* | 4 | 8.4 | 2.06E-07 | 3.01E-07 | 3.96E-07 |

*Table 69- Penetration Calculation for the US Database*

| State | City | Climate Region | PG | PEN 1/10mm (77°F) |
|---|---|---|---|---|
| **Arizona** | *Flagstaff* | *Dry, Freeze* | PG 64-22 | 53.77 |
| **Colorado** | *Adams* | *Dry, Freeze* | PG 64-22 | 53.77 |
| **Colorado** | *Rio Blanco* | *Dry, Freeze* | PG 58-34 | 126.23 |
| **Colorado** | *El Paso* | *Dry, Freeze* | PG 58-28 | 92.06 |
| **Colorado** | *Yuma* | *Dry, Freeze* | PG 64-28 | 69.55 |
| **Colorado** | *El Rio Grande* | *Dry, Freeze* | PG 58-28 | 92.06 |
| **Alaska** | *Anchorage* | *Dry, Freeze* | PG 64-40 | 136.27 |
| **Alaska** | *Fairbanks* | *Dry, Freeze* | PG 58-34 | 126.23 |
| **Alaska** | *Barrow* | *Dry, Freeze* | PG 52-40 | 219.70 |
| **Washington** | *Spokane* | *Dry, Freeze* | PG 64-28 | 69.55 |
| **Arizona** | *Kingman* | *Dry, No Freeze* | PG 70-10 | 34.60 |
| **Arizona** | *Tucson* | *Dry, No Freeze* | PG 70-10 | 34.60 |
| **Arizona** | *Phoenix* | *Dry, No Freeze* | PG 70-22 | 41.69 |
| **Iowa** | *Harlan* | *Wet, Freeze* | PG 58-28 | 92.06 |
| **Iowa** | *Council Bluffs* | *Wet, Freeze* | PG 58-28 | 92.06 |
| **Kansas** | *Cherokee* | *Wet, Freeze* | PG 70-28 | 43.15 |
| **Maine** | *Hermon* | *Wet, Freeze* | PG 64-28 | 69.55 |
| **Maine** | *Sidney* | *Wet, Freeze* | PG 64-28 | 69.55 |
| **Michigan** | *Port Huron* | *Wet, Freeze* | PG 70-28 | 43.15 |
| **Michigan** | *Alpena* | *Wet, Freeze* | PG 64-28 | 69.55 |
| **Michigan** | *Marquette* | *Wet, Freeze* | PG 58-34 | 126.23 |
| **Michigan** | *Grand Rapids* | *Wet, Freeze* | PG 70-28 | 43.15 |
| **Ohio** | *Columbus* | *Wet, Freeze* | PG 76-22 | 32.99 |
| **Vermont** | *Burlington* | *Wet, Freeze* | PG 58-28 | 92.06 |
| **West Virginia** | *Martinsburg* | *Wet, Freeze* | PG 64-22 | 53.77 |
| **West Virginia** | *Hayward* | *Wet, Freeze* | PG 58-34 | 126.23 |
| **Wisconsin** | *Madison* | *Wet, Freeze* | PG 58-28 | 92.06 |
| **Indiana** | *La Porte* | *Wet, Freeze* | PG 64-22 | 53.77 |
| **Indiana** | *Jackson* | *Wet, Freeze* | PG 70-22 | 41.69 |
| **Massachusetts** | *Boston* | *Wet, Freeze* | PG 64-28 | 69.55 |
| **Washington** | *Seattle* | *Wet, No Freeze* | PG 58-22 | 72.03 |
| **Delaware** | *Dover* | *Wet, No Freeze* | PG 64-22 | 53.77 |
| **Florida** | *Tallahassee* | *Wet, No Freeze* | PG 76-22 | 32.99 |
| **Massachusetts** | *Springfield* | *Wet, No Freeze* | PG 64-28 | 69.55 |
| **Alabama** | *Montgomery* | *Wet, No Freeze* | PG 76-22 | 32.99 |
| **Alabama** | *Tuscaloosa* | *Wet, No Freeze* | PG 76-22 | 32.99 |

| | | | | |
|---|---|---|---|---|
| **Arkansas** | *Little Rock* | *Wet, No Freeze* | PG 76-22 | 32.99 |
| **Indiana** | *Jefferson* | *Wet, No Freeze* | PG 70-22 | 41.69 |
| **Hawaii** | *Honolulu* | *Wet, No Freeze* | PG 64-22 | 53.77 |
| **Kansas** | *Scott* | *Wet, No Freeze* | PG 70-28 | 43.15 |
| **Maryland** | *Jessup* | *Wet, No Freeze* | PG 76-22 | 32.99 |
| **Indiana** | *Jackson* | *Wet, No Freeze* | PG 76-22 | 32.99 |
| **New Jersey** | *Newark* | *Wet, No Freeze* | PG 64-22 | 53.77 |
| **North Carolina** | *Greensboro* | *Wet, No Freeze* | PG 58-28 | 92.06 |
| **North Carolina** | *Newark* | *Wet, No Freeze* | PG 64-22 | 53.77 |
| **South Carolina** | *Columbia* | *Wet, No Freeze* | PG 76-22 | 32.99 |
| **Tennessee** | *Memphis* | *Wet, No Freeze* | PG 76-22 | 32.99 |
| **West Virginia** | *Charleston* | *Wet, No Freeze* | PG 64-22 | 53.77 |

*Table 70- Variation of the "m" parameter for the U.S. Database*

| State | City | Climate Zone | m (-20°C) | m (-10°C) | m (0°C) |
|---|---|---|---|---|---|
| **Arizona** | *Flagstaff* | *Dry, Freeze* | 0.11 | 0.20 | 0.33 |
| **Colorado** | *Adams* | *Dry, Freeze* | 0.11 | 0.20 | 0.32 |
| **Colorado** | *Rio Blanco* | *Dry, Freeze* | 0.16 | 0.26 | 0.45 |
| **Colorado** | *El Paso* | *Dry, Freeze* | 0.14 | 0.23 | 0.39 |
| **Colorado** | *Yuma* | *Dry, Freeze* | 0.12 | 0.21 | 0.35 |
| **Colorado** | *El Rio Grande* | *Dry, Freeze* | 0.14 | 0.23 | 0.39 |
| **Alaska** | *Anchorage* | *Dry, Freeze* | 0.18 | 0.27 | 0.47 |
| **Alaska** | *Fairbanks* | *Dry, Freeze* | 0.17 | 0.26 | 0.46 |
| **Alaska** | *Barrow* | *Dry, Freeze* | 0.23 | 0.33 | 0.61 |
| **Washington** | *Spokane* | *Dry, Freeze* | 0.13 | 0.22 | 0.36 |
| **Arizona** | *Kingman* | *Dry, No Freeze* | 0.11 | 0.20 | 0.31 |
| **Arizona** | *Tucson* | *Dry, No Freeze* | 0.11 | 0.20 | 0.31 |
| **Arizona** | *Phoenix* | *Dry, No Freeze* | 0.11 | 0.20 | 0.32 |
| **Iowa** | *Harlan* | *Wet, Freeze* | 0.14 | 0.24 | 0.40 |
| **Iowa** | *Council Bluffs* | *Wet, Freeze* | 0.14 | 0.24 | 0.40 |
| **Kansas** | *Cherokee* | *Wet, Freeze* | 0.11 | 0.20 | 0.31 |
| **Maine** | *Hermon* | *Wet, Freeze* | 0.13 | 0.22 | 0.36 |
| **Maine** | *Sidney* | *Wet, Freeze* | 0.13 | 0.22 | 0.36 |
| **Michigan** | *Port Huron* | *Wet, Freeze* | 0.11 | 0.20 | 0.31 |
| **Michigan** | *Alpena* | *Wet, Freeze* | 0.13 | 0.22 | 0.36 |
| **Michigan** | *Marquette* | *Wet, Freeze* | 0.17 | 0.26 | 0.46 |
| **Michigan** | *Grand Rapids* | *Wet, Freeze* | 0.11 | 0.20 | 0.31 |
| **Ohio** | *Columbus* | *Wet, Freeze* | 0.10 | 0.19 | 0.30 |
| **Vermont** | *Burlington* | *Wet, Freeze* | 0.14 | 0.24 | 0.40 |
| **West Virginia** | *Martinsburg* | *Wet, Freeze* | 0.12 | 0.21 | 0.34 |
| **West Virginia** | *Hayward* | *Wet, Freeze* | 0.17 | 0.27 | 0.46 |
| **Wisconsin** | *Madison* | *Wet, Freeze* | 0.15 | 0.24 | 0.40 |
| **Indiana** | *La Porte* | *Wet, Freeze* | 0.12 | 0.20 | 0.33 |
| **Indiana** | *Jackson* | *Wet, Freeze* | 0.11 | 0.19 | 0.31 |
| **Massachusetts** | *Boston* | *Wet, Freeze* | 0.13 | 0.22 | 0.36 |

| | | | | | |
|---|---|---|---|---|---|
| **Washington** | *Seattle* | *Wet, No Freeze* | 0.13 | 0.22 | 0.37 |
| **Delaware** | *Dover* | *Wet, No Freeze* | 0.12 | 0.20 | 0.33 |
| **Florida** | *Tallahassee* | *Wet, No Freeze* | 0.10 | 0.19 | 0.30 |
| **Massachusetts** | *Springfield* | *Wet, No Freeze* | 0.13 | 0.22 | 0.36 |
| **Alabama** | *Montgomery* | *Wet, No Freeze* | 0.09 | 0.18 | 0.29 |
| **Alabama** | *Tuscaloosa* | *Wet, No Freeze* | 0.09 | 0.18 | 0.29 |
| **Arkansas** | *Little Rock* | *Wet, No Freeze* | 0.10 | 0.19 | 0.30 |
| **Indiana** | *Jefferson* | *Wet, No Freeze* | 0.11 | 0.19 | 0.31 |
| **Hawaii** | *Honolulu* | *Wet, No Freeze* | 0.12 | 0.20 | 0.33 |
| **Kansas** | *Scott* | *Wet, No Freeze* | 0.11 | 0.20 | 0.31 |
| **Maryland** | *Jessup* | *Wet, No Freeze* | 0.09 | 0.18 | 0.29 |
| **Indiana** | *Jackson* | *Wet, No Freeze* | 0.10 | 0.19 | 0.30 |
| **New Jersey** | *Newark* | *Wet, No Freeze* | 0.12 | 0.20 | 0.33 |
| **North Carolina** | *Greensboro* | *Wet, No Freeze* | 0.14 | 0.24 | 0.40 |
| **North Carolina** | *Newark* | *Wet, No Freeze* | 0.12 | 0.20 | 0.33 |
| **South Carolina** | *Columbia* | *Wet, No Freeze* | 0.11 | 0.20 | 0.31 |
| **Tennessee** | *Memphis* | *Wet, No Freeze* | 0.10 | 0.19 | 0.30 |
| **West Virginia** | *Charleston* | *Wet, No Freeze* | 0.12 | 0.20 | 0.33 |

*Table 71- Creep Compliance Generation for the US Database*

| State | City | Climate Zone | D(100) -20°C | D(100) -10°C | D(100) 0°C |
|---|---|---|---|---|---|
| **Arizona** | *Flagstaff* | *Dry, Freeze* | 5.284E-07 | 1.063E-06 | 2.396E-06 |
| **Colorado** | *Adams* | *Dry, Freeze* | 4.210E-07 | 8.358E-07 | 1.857E-06 |
| **Colorado** | *Rio Blanco* | *Dry, Freeze* | 6.635E-07 | 1.314E-06 | 3.977E-06 |
| **Colorado** | *El Paso* | *Dry, Freeze* | 5.630E-07 | 1.114E-06 | 2.875E-06 |
| **Colorado** | *Yuma* | *Dry, Freeze* | 5.664E-07 | 1.094E-06 | 2.585E-06 |
| **Colorado** | *El Rio Grande* | *Dry, Freeze* | 5.472E-07 | 1.078E-06 | 2.775E-06 |
| **Alaska** | *Anchorage* | *Dry, Freeze* | 1.606E-06 | 2.782E-06 | 8.671E-06 |
| **Alaska** | *Fairbanks* | *Dry, Freeze* | 9.083E-07 | 1.758E-06 | 5.289E-06 |
| **Alaska** | *Barrow* | *Dry, Freeze* | 1.289E-06 | 2.379E-06 | 1.019E-05 |
| **Washington** | *Spokane* | *Dry, Freeze* | 6.038E-07 | 1.245E-06 | 3.074E-06 |
| **Arizona** | *Kingman* | *Dry, No Freeze* | 3.138E-07 | 7.607E-07 | 1.712E-06 |
| **Arizona** | *Tucson* | *Dry, No Freeze* | 3.219E-07 | 7.963E-07 | 1.816E-06 |
| **Arizona** | *Phoenix* | *Dry, No Freeze* | 5.514E-07 | 1.178E-06 | 2.661E-06 |
| **Iowa** | *Harlan* | *Wet, Freeze* | 5.379E-07 | 1.126E-06 | 3.010E-06 |
| **Iowa** | *Council Bluffs* | *Wet, Freeze* | 4.644E-07 | 1.004E-06 | 2.730E-06 |
| **Kansas** | *Cherokee* | *Wet, Freeze* | 7.779E-07 | 1.429E-06 | 3.033E-06 |
| **Maine** | *Hermon* | *Wet, Freeze* | 5.923E-07 | 1.187E-06 | 2.874E-06 |
| **Maine** | *Sidney* | *Wet, Freeze* | 6.553E-07 | 1.284E-06 | 3.074E-06 |
| **Michigan** | *Port Huron* | *Wet, Freeze* | 7.710E-07 | 1.419E-06 | 3.015E-06 |
| **Michigan** | *Alpena* | *Wet, Freeze* | 6.179E-07 | 1.226E-06 | 2.956E-06 |
| **Michigan** | *Marquette* | *Wet, Freeze* | 8.306E-07 | 1.640E-06 | 4.984E-06 |
| **Michigan** | *Grand Rapids* | *Wet, Freeze* | 6.779E-07 | 1.284E-06 | 2.768E-06 |
| **Ohio** | *Columbus* | *Wet, Freeze* | 8.399E-07 | 1.500E-06 | 3.012E-06 |
| **Vermont** | *Burlington* | *Wet, Freeze* | 5.824E-07 | 1.197E-06 | 3.147E-06 |
| **West Virginia** | *Martinsburg* | *Wet, Freeze* | 5.392E-07 | 1.120E-06 | 2.579E-06 |
| **West Virginia** | *Hayward* | *Wet, Freeze* | 7.945E-07 | 1.638E-06 | 5.110E-06 |
| **Wisconsin** | *Madison* | *Wet, Freeze* | 4.962E-07 | 1.092E-06 | 2.988E-06 |
| **Indiana** | *La Porte* | *Wet, Freeze* | 5.573E-07 | 1.112E-06 | 2.497E-06 |
| **Indiana** | *Jackson* | *Wet, Freeze* | 5.917E-07 | 1.151E-06 | 2.455E-06 |
| **Massachusetts** | *Boston* | *Wet, Freeze* | 7.325E-07 | 1.400E-06 | 3.310E-06 |
| **Washington** | *Seattle* | *Wet, No Freeze* | 2.979E-07 | 7.176E-07 | 1.856E-06 |
| **Delaware** | *Dover* | *Wet, No Freeze* | 5.522E-07 | 1.104E-06 | 2.482E-06 |
| **Florida** | *Tallahassee* | *Wet, No Freeze* | 5.884E-07 | 1.137E-06 | 2.377E-06 |
| **Massachusetts** | *Springfield* | *Wet, No Freeze* | 6.615E-07 | 1.293E-06 | 3.093E-06 |
| **Alabama** | *Montgomery* | *Wet, No Freeze* | 7.715E-07 | 1.340E-06 | 2.637E-06 |
| **Alabama** | *Tuscaloosa* | *Wet, No Freeze* | 7.616E-07 | 1.327E-06 | 2.615E-06 |
| **Arkansas** | *Little Rock* | *Wet, No Freeze* | 6.892E-07 | 1.286E-06 | 2.641E-06 |

| | | | | | |
|---|---|---|---|---|---|
| **Indiana** | *Jefferson* | *Wet, No Freeze* | 5.516E-07 | 1.090E-06 | 2.343E-06 |
| **Hawaii** | *Honolulu* | *Wet, No Freeze* | 3.251E-07 | 7.309E-07 | 1.745E-06 |
| **Kansas** | *Scott* | *Wet, No Freeze* | 6.853E-07 | 1.295E-06 | 2.788E-06 |
| **Maryland** | *Jessup* | *Wet, No Freeze* | 7.959E-07 | 1.373E-06 | 2.693E-06 |
| **Indiana** | *Jackson* | *Wet, No Freeze* | 8.521E-07 | 1.517E-06 | 3.041E-06 |
| **New Jersey** | *Newark* | *Wet, No Freeze* | 6.642E-07 | 1.274E-06 | 2.806E-06 |
| **North Carolina** | *Greensboro* | *Wet, No Freeze* | 6.017E-07 | 1.229E-06 | 3.243E-06 |
| **North Carolina** | *Newark* | *Wet, No Freeze* | 5.522E-07 | 1.104E-06 | 2.482E-06 |
| **South Carolina** | *Columbia* | *Wet, No Freeze* | 8.814E-07 | 1.772E-06 | 3.846E-06 |
| **Tennessee** | *Memphis* | *Wet, No Freeze* | 6.324E-07 | 1.203E-06 | 2.494E-06 |
| **West Virginia** | *Charleston* | *Wet, No Freeze* | 3.493E-07 | 7.730E-07 | 1.831E-06 |

*Table 72- Fracture Energy for the U.S Database*

| State | City | Climate Zone | Fracture Energy (lb.in) |
|---|---|---|---|
| **Arizona** | *Flagstaff* | *Dry, Freeze* | 43.6 |
| **Colorado** | *Adams* | *Dry, Freeze* | -623.9 |
| **Colorado** | *Rio Blanco* | *Dry, Freeze* | -76.5 |
| **Colorado** | *El Paso* | *Dry, Freeze* | 136.0 |
| **Colorado** | *Yuma* | *Dry, Freeze* | -154.9 |
| **Colorado** | *El Rio Grande* | *Dry, Freeze* | 112.7 |
| **Alaska** | *Anchorage* | *Dry, Freeze* | -156.1 |
| **Alaska** | *Fairbanks* | *Dry, Freeze* | 179.2 |
| **Alaska** | *Barrow* | *Dry, Freeze* | -1189.4 |
| **Washington** | *Spokane* | *Dry, Freeze* | 62.7 |
| **Arizona** | *Kingman* | *Dry, No Freeze* | -19.6 |
| **Arizona** | *Tucson* | *Dry, No Freeze* | 183.9 |
| **Arizona** | *Phoenix* | *Dry, No Freeze* | 14.5 |
| **Iowa** | *Harlan* | *Wet, Freeze* | -126.0 |
| **Iowa** | *Council Bluffs* | *Wet, Freeze* | -452.9 |
| **Kansas** | *Cherokee* | *Wet, Freeze* | 334.5 |
| **Maine** | *Hermon* | *Wet, Freeze* | -73.8 |
| **Maine** | *Sidney* | *Wet, Freeze* | 292.2 |
| **Michigan** | *Port Huron* | *Wet, Freeze* | 272.8 |
| **Michigan** | *Alpena* | *Wet, Freeze* | 63.5 |
| **Michigan** | *Marquette* | *Wet, Freeze* | -82.4 |
| **Michigan** | *Grand Rapids* | *Wet, Freeze* | -100.6 |
| **Ohio** | *Columbus* | *Wet, Freeze* | 626.2 |
| **Vermont** | *Burlington* | *Wet, Freeze* | 377.8 |
| **West Virginia** | *Martinsburg* | *Wet, Freeze* | 144.4 |
| **West Virginia** | *Hayward* | *Wet, Freeze* | -186.8 |
| **Wisconsin** | *Madison* | *Wet, Freeze* | -74.2 |
| **Indiana** | *La Porte* | *Wet, Freeze* | 342.2 |
| **Indiana** | *Jackson* | *Wet, Freeze* | 186.6 |
| **Massachusetts** | *Boston* | *Wet, Freeze* | 573.9 |
| **Washington** | *Seattle* | *Wet, No Freeze* | -321.7 |
| **Delaware** | *Dover* | *Wet, No Freeze* | 163.2 |
| **Florida** | *Tallahassee* | *Wet, No Freeze* | -416.8 |
| **Massachusetts** | *Springfield* | *Wet, No Freeze* | 260.2 |
| **Alabama** | *Montgomery* | *Wet, No Freeze* | 664.0 |

| | | | |
|---|---|---|---|
| **Alabama** | *Tuscaloosa* | *Wet, No Freeze* | 620.7 |
| **Arkansas** | *Little Rock* | *Wet, No Freeze* | -57.8 |
| **Indiana** | *Jefferson* | *Wet, No Freeze* | -10.0 |
| **Hawaii** | *Honolulu* | *Wet, No Freeze* | -876.4 |
| **Kansas** | *Scott* | *Wet, No Freeze* | -96.7 |
| **Maryland** | *Jessup* | *Wet, No Freeze* | 927.7 |
| **Indiana** | *Jackson* | *Wet, No Freeze* | 700.4 |
| **New Jersey** | *Newark* | *Wet, No Freeze* | 996.4 |
| **North Carolina** | *Greensboro* | *Wet, No Freeze* | 175.3 |
| **North Carolina** | *Newark* | *Wet, No Freeze* | 266.3 |
| **South Carolina** | *Columbia* | *Wet, No Freeze* | 448.8 |
| **Tennessee** | *Memphis* | *Wet, No Freeze* | -239.8 |
| **West Virginia** | *Charleston* | *Wet, No Freeze* | -758.0 |

*Table 73- Summary Table for TCMODEL input variables for the US Database*

| State | City | Zone | D(100) -20°C | D(100) -10°C | D(100) 0°C | FE (lb.in) | TS (psi) |
|---|---|---|---|---|---|---|---|
| **AZ** | *Flagstaff* | *D, F* | 5.284E-07 | 1.063E-06 | 2.396E-06 | 43.6 | 392 |
| **CO** | *Adams* | | 4.210E-07 | 8.358E-07 | 1.857E-06 | -623.9 | 419 |
| **CO** | *Rio Blanco* | | 6.635E-07 | 1.314E-06 | 3.977E-06 | -76.5 | 522 |
| **CO** | *El Paso* | | 5.630E-07 | 1.114E-06 | 2.875E-06 | 136.0 | 424 |
| **CO** | *Yuma* | | 5.664E-07 | 1.094E-06 | 2.585E-06 | -154.9 | 438 |
| **CO** | *El Rio Grande* | | 5.472E-07 | 1.078E-06 | 2.775E-06 | 112.7 | 427 |
| **AK** | *Anchorage* | | 1.606E-06 | 2.782E-06 | 8.671E-06 | -156.1 | 583 |
| **AK** | *Fairbanks* | | 9.083E-07 | 1.758E-06 | 5.289E-06 | 179.2 | 475 |
| **AK** | *Barrow* | | 1.289E-06 | 2.379E-06 | 1.019E-05 | -1189.4 | 566 |
| **WA** | *Spokane* | | 6.038E-07 | 1.245E-06 | 3.074E-06 | 62.7 | 444 |
| **AZ** | *Kingman* | *D, NF* | 3.138E-07 | 7.607E-07 | 1.712E-06 | -19.6 | 348 |
| **AZ** | *Tucson* | | 3.219E-07 | 7.963E-07 | 1.816E-06 | 183.9 | 348 |
| **AZ** | *Phoenix* | | 5.514E-07 | 1.178E-06 | 2.661E-06 | 14.5 | 418 |
| **IO** | *Harlan* | *W, F* | 5.379E-07 | 1.126E-06 | 3.010E-06 | -126.0 | 440 |
| **IO** | *Council Bluffs* | | 4.644E-07 | 1.004E-06 | 2.730E-06 | -452.9 | 472 |
| **KS** | *Cherokee* | | 7.779E-07 | 1.429E-06 | 3.033E-06 | 334.5 | 409 |
| **ME** | *Hermon* | | 5.923E-07 | 1.187E-06 | 2.874E-06 | -73.8 | 439 |
| **ME** | *Sidney* | | 6.553E-07 | 1.284E-06 | 3.074E-06 | 292.2 | 420 |
| **MI** | *Port Huron* | | 7.710E-07 | 1.419E-06 | 3.015E-06 | 272.8 | 410 |
| **MI** | *Alpena* | | 6.179E-07 | 1.226E-06 | 2.956E-06 | 63.5 | 431 |
| **MI** | *Marquette* | | 8.306E-07 | 1.640E-06 | 4.984E-06 | -82.4 | 491 |
| **MI** | *Grand Rapids* | | 6.779E-07 | 1.284E-06 | 2.768E-06 | -100.6 | 435 |
| **OH** | *Columbus* | | 8.399E-07 | 1.500E-06 | 3.012E-06 | 626.2 | 371 |
| **VT** | *Burlington* | | 5.824E-07 | 1.197E-06 | 3.147E-06 | 377.8 | 397 |
| **WV** | *Martinsburg* | | 5.392E-07 | 1.120E-06 | 2.579E-06 | 144.4 | 395 |
| **WV** | *Hayward* | | 7.945E-07 | 1.638E-06 | 5.110E-06 | -186.8 | 509 |
| **WI** | *Madison* | | 4.962E-07 | 1.092E-06 | 2.988E-06 | -74.2 | 436 |
| **IN** | *La Porte* | | 5.573E-07 | 1.112E-06 | 2.497E-06 | 342.2 | 383 |
| **IN** | *Jackson* | | 5.917E-07 | 1.151E-06 | 2.455E-06 | 186.6 | 384 |
| **MS** | *Boston* | | 7.325E-07 | 1.400E-06 | 3.310E-06 | 573.9 | 401 |
| **WA** | *Seattle* | *W, NF* | 2.979E-07 | 7.176E-07 | 1.856E-06 | -321.7 | 427 |
| **DE** | *Dover* | | 5.522E-07 | 1.104E-06 | 2.482E-06 | 163.2 | 384 |
| **FL** | *Tallahassee* | | 5.884E-07 | 1.137E-06 | 2.377E-06 | -416.8 | 437 |
| **MS** | *Springfield* | | 6.615E-07 | 1.293E-06 | 3.093E-06 | 260.2 | 418 |

| | | | | | | | |
|---|---|---|---|---|---|---|---|
| **AL** | *Montgomery* | | 7.715E-07 | 1.340E-06 | 2.637E-06 | 664.0 | 384 |
| **AK** | *Tuscaloosa* | | 7.616E-07 | 1.327E-06 | 2.615E-06 | 620.7 | 385 |
| **AR** | *Little Rock* | | 6.892E-07 | 1.286E-06 | 2.641E-06 | -57.8 | 404 |
| **IN** | *Jefferson* | *W, NF* | 5.516E-07 | 1.090E-06 | 2.343E-06 | -10.0 | 397 |
| **HI** | *Honolulu* | | 3.251E-07 | 7.309E-07 | 1.745E-06 | -876.4 | 507 |
| **KS** | *Scott* | | 6.853E-07 | 1.295E-06 | 2.788E-06 | -96.7 | 433 |
| **MD** | *Jessup* | | 7.959E-07 | 1.373E-06 | 2.693E-06 | 927.7 | 381 |
| **IN** | *Jackson* | | 8.521E-07 | 1.517E-06 | 3.041E-06 | 700.4 | 368 |
| **NJ** | *Newark* | | 6.642E-07 | 1.274E-06 | 2.806E-06 | 996.4 | 355 |
| **NC** | *Greensboro* | | 6.017E-07 | 1.229E-06 | 3.243E-06 | 175.3 | 419 |
| **NC** | *Newark* | | 5.522E-07 | 1.104E-06 | 2.482E-06 | 266.3 | 384 |
| **SC** | *Columbia* | | 8.814E-07 | 1.772E-06 | 3.846E-06 | 448.8 | 367 |
| **TN** | *Memphis* | | 6.324E-07 | 1.203E-06 | 2.494E-06 | -239.8 | 421 |
| **WV** | *Charleston* | | 3.493E-07 | 7.730E-07 | 1.831E-06 | -758.0 | 488 |

# APPENDIX C

## RESULTS FOR FINAL CRITERIA

*Table 74- Ranking Criteria for Thermal Properties*

| | | LTPP Database | | | U.S. Database | | |
|---|---|---|---|---|---|---|---|
| **City** | **Climate Zone** | **Tensile St.** | **LTPP Database D(100) -10°C** | **Rank** | **TS (14°F) in psi** | **US Database D(100) -10°C** | **Rank** |
| **Yuma** | Dry, Freeze | 707.9 | 9.0918E-07 | G | 437.7 | 2.585E-06 | G |
| **Spokane** | Dry, Freeze | 621.2 | 9.3225E-07 | G | 427.3 | 2.775E-06 | G |
| **El Paso** | Dry, Freeze | 546.1 | 1.0175E-06 | E | 424.1 | 2.875E-06 | G |
| **Flagstaff** | Dry, Freeze | 485.6 | 1.1273E-06 | G | 392.0 | 2.396E-06 | S |
| **Rio Blanco** | Dry, Freeze | 525.8 | 1.7968E-06 | E | 522.3 | 3.977E-06 | E |
| **Anchorage** | Dry, Freeze | 551.1 | 2.2525E-06 | E | 582.6 | 8.671E-06 | E |
| **Phoenix** | Dry, No Freeze | 377.1 | 9.0045E-07 | S | 418.2 | 2.661E-06 | S |
| **Kingman** | Dry, No Freeze | 388.6 | 9.1676E-07 | S | 347.7 | 1.712E-06 | S |
| **Tucson** | Dry, No Freeze | 398.9 | 9.2687E-07 | S | 347.6 | 1.816E-06 | S |
| **Springfield** | Wet, Freeze | 461.2 | 7.1398E-07 | G | 418.3 | 3.093E-06 | S |
| **Jackson** | Wet, Freeze | 450.7 | 8.2554E-07 | G | 383.6 | 2.455E-06 | S |
| **Boston** | Wet, Freeze | 557.6 | 9.1444E-07 | G | 401.2 | 3.310E-06 | G |
| **Kanawha** | Wet, Freeze | 498.6 | 9.2517E-07 | G | 395.4 | 2.579E-06 | G |
| **Cherokee** | Wet, Freeze | 487.1 | 9.3339E-07 | G | 408.9 | 3.033E-06 | G |
| **Alpena** | Wet, Freeze | 477.5 | 9.5425E-07 | G | 431.0 | 2.956E-06 | G |
| **Port Huron** | Wet, Freeze | 463.3 | 1.0358E-06 | G | 410.5 | 3.015E-06 | S |
| **Marquette** | Wet, Freeze | 558.3 | 1.1916E-06 | G | 491.2 | 4.984E-06 | G |
| **La Porte** | Wet, Freeze | 467.7 | 1.3605E-06 | G | 382.7 | 2.497E-06 | S |
| **Grand Rapids** | Wet, Freeze | 547.6 | 1.5296E-06 | E | 434.8 | 2.768E-06 | G |
| **Seattle** | Wet, No Freeze | 1145.6 | 3.6735E-07 | S | 426.6 | 1.856E-06 | G |
| **Columbia** | Wet, No Freeze | 845.4 | 4.069E-07 | S | 366.9 | 3.012E-06 | S |
| **Little Rock** | Wet, No Freeze | 353.8 | 6.9145E-07 | S | 404.1 | 2.641E-06 | S |

| | | | | | | | |
|---|---|---|---|---|---|---|---|
| **Charleston** | Wet, No Freeze | 682.0 | 7.3066E-07 | S | 487.7 | 1.831E-06 | G |
| **Montgomery** | Wet, No Freeze | 447.8 | 8.0438E-07 | G | 383.9 | 2.637E-06 | G |
| **Tuscaloosa** | Wet, No Freeze | 404.5 | 8.3647E-07 | G | 385.3 | 2.615E-06 | S |
| **Memphis** | Wet, No Freeze | 587.0 | 8.3754E-07 | G | 421.3 | 3.147E-06 | G |
| **Scott** | Wet, No Freeze | 448.6 | 9.7704E-07 | G | 432.6 | 2.788E-06 | G |
| **Jefferson** | Wet, No Freeze | 445.2 | 1.1632E-06 | G | 397.0 | 2.343E-06 | S |

*Table 75- Final Assessment of the US Mix Designs*

| State | City | Climate Zone | Rutting Criteria | Fatigue Criteria | Thermal Cracking Criteria | Final Assessment |
|---|---|---|---|---|---|---|
| **AL** | Montgomery | Wet, No Freeze | Excellent | Excellent | Goof | Excellent Quality Mix |
| | Tuscaloosa | Wet, No Freeze | Excellent | Excellent | Satisfactory | Good Quality Mix |
| **AZ** | Flagstaff | Dry, Freeze | Excellent | Good | Satisfactory | Good Quality Mix |
| | Kingman | Dry, Freeze | Low | Good | Satisfactory | Satisfactory Quality Mix |
| | Tucson | Dry, Freeze | Low | Good | Satisfactory | Satisfactory Quality Mix |
| | Phoenix | Dry, Freeze | Low | Excellent | Satisfactory | Satisfactory Quality Mix |
| **AK** | Anchorage | Dry, No Freeze | Excellent | Excellent | Excellent | Excellent Quality Mix |
| | Fairbanks | Dry, No Freeze | Good | Excellent | Good | Good Quality Mix |
| | Barrow | Dry, No Freeze | Excellent | Excellent | Excellent | Excellent Quality Mix |
| **AR** | Little Rock | Wet, No Freeze | Satisfactory | Excellent | Satisfactory | Satisfactory Quality Mix |
| **CO** | Adams | Dry, Freeze | Low | Good | Satisfactory | Satisfactory Quality Mix |
| | Rio Blanco | Dry, Freeze | Satisfactory | Good | Excellent | Excellent Quality Mix |
| | El Paso | Dry, Freeze | Low | Excellent | Good | Good Quality Mix |
| | Yuma | Dry, Freeze | Satisfactory | Excellent | Good | Good Quality Mix |
| | El Rio Grande | Dry, Freeze | Low | Excellent | Good | Good Quality Mix |
| **IN** | La Porte | Wet, No Freeze | Good | Excellent | Satisfactory | Good Quality Mix |
| | Jackson | Wet, No Freeze | Satisfactory | Excellent | Satisfactory | Satisfactory Quality Mix |
| | Jefferson | Wet, No Freeze | Satisfactory | Excellent | Satisfactory | Satisfactory Quality Mix |

| | | | | | | |
|---|---|---|---|---|---|---|
| **DE** | Dover | Wet, Freeze | Low | Excellent | Satisfactory | Satisfactory Quality Mix |
| **FL** | Tallahassee | Wet, Freeze | Low | Excellent | Good | Good Quality Mix |
| **HI** | Honolulu | Wet, No Freeze | Satisfactory | Satisfactory | Good | Satisfactory Quality Mix |
| **IA** | Harlan | Wet, Freeze | Low | Good | Good | Satisfactory Quality Mix |
| | Council Bluffs | Wet, Freeze | Low | Satisfactory | Good | Satisfactory Quality Mix |
| **KS** | Cherokee | Wet, Freeze | Satisfactory | Excellent | Good | Good Quality Mix |
| | Scott | Wet, No Freeze | Low | Excellent | Good | Satisfactory Quality Mix |
| **ME** | Hermon | Wet, Freeze | Satisfactory | Excellent | Good | Good Quality Mix |
| | Sidney | Wet, Freeze | Low | Excellent | Good | Satisfactory Quality Mix |
| **MA** | Boston | Wet, No Freeze | Satisfactory | Excellent | Satisfactory | Satisfactory Quality Mix |
| | Springfield | Wet, Freeze | Low | Excellent | Good | Good Quality Mix |
| **MD** | Jessup | Wet, No Freeze | Excellent | Excellent | Satisfactory | Excellent Quality Mix |
| **MI** | Port Huron | Wet, Freeze | Satisfactory | Excellent | Satisfactory | Good Quality Mix |
| | Alpena | Wet, Freeze | Satisfactory | Excellent | Good | Good Quality Mix |
| | Marquette | Wet, Freeze | Low | Excellent | Good | Good Quality Mix |
| | Grand Rapids | Wet, Freeze | Satisfactory | Excellent | Good | Good Quality Mix |
| **MS** | Jackson | Wet, No Freeze | Satisfactory | Excellent | Satisfactory | Satisfactory Quality Mix |
| **NJ** | Newark | Wet, No Freeze | Low | Excellent | Satisfactory | Low Quality Mix |
| **NC** | Greensboro | Wet, No Freeze | Low | Good | Good | Satisfactory Quality Mix |
| | Newark | Wet, No Freeze | Satisfactory | Excellent | Satisfactory | Satisfactory Quality Mix |

| | | | | | | |
|---|---|---|---|---|---|---|
| **OH** | Columbus | Wet, Freeze | Low | Excellent | Satisfactory | Low Quality Mix |
| **SC** | Columbia | Wet, No Freeze | Low | Excellent | Satisfactory | Low Quality Mix |
| **TN** | Memphis | Wet, No Freeze | Satisfactory | Excellent | Good | Good Quality Mix |
| **VT** | Burlington | Wet, Freeze | Low | Excellent | Satisfactory | Low Quality Mix |
| **WA** | Seattle | Dry, Freeze | Excellent | Low | Good | Satisfactory Quality Mix |
| | Spokane | Wet, No Freeze | Excellent | Excellent | Good | Excellent Quality Mix |
| **WV** | Martinsburg | Wet, Freeze | Satisfactory | Good | Satisfactory | Satisfactory Quality Mix |
| | Charleston | Wet, No Freeze | Low | Satisfactory | Excellent | Satisfactory Quality Mix |
| **WI** | Hayward | Wet, Freeze | Good | Excellent | Excellent | Excellent Quality Mix |
| | Madison | Wet, Freeze | Excellent | Good | Good | Good Quality Mix |